Defining roles for *Pax6* in fetal mouse development: Investigations of the developmental potential of cells deficient for *Pax6* using small eye homozygous mutants and aggregation chimaeras.

Jane Catherine Quinn

Ph. D.

University of Edinburgh

1996

Declaration

The experiments described in this thesis were the unaided work of the author except where acknowledgement is made by reference. No part of this work has previously been accepted for any other degree nor is any part of it being submitted concurrently in candidature for another degree.

Jane Quinn

September 1996

Acknowledgements

There are a great many people who have helped me over the past three years to whom I owe a huge debt of thanks .

First and foremost, a big thank you to my supervisors John West and Bob Hill. With their contrasting and complementing styles of supervision, that is, John's attention to detail and Bob's laid back 'we'll see what happens' approach, they have encouraged and invited experimental initiative whilst keeping me from straying too far from the right path. Their exacting standards and endless quests for "the right word" have taught me both the importance of written expression and the fastidious nature of scientific publishing. They also both have an innate understanding of when to become involved and when to stand back and watch which has allowed me to develop ideas on my own initiative which, for me, has been the most rewarding aspect of the past three years. I can safely say that, in the end, two has certainly been better than one!

My next huge thank you goes to Jean and Margaret, without whom I should not have survived my studentship at all! They have selflessly imparted their skills and knowledge, fixing my mistakes and keeping me under control in the lab. They have been supportive when things were going badly and enthusiastic when things were going well and have had a smile and a laugh for every occasion. They have been both the best friends and workmates I could have asked for and have made my time at the CRB the best I could have hoped for. Within the lab, I must also thank Clare, Pin Chi for chinese biscuits and a cheerful smile and Sam for his help with the 1-D analysis. I also owe a great deal to Annemarie who, although no longer with us, was a great source of inspiration to me over the first two years of my PhD by being the life and soul of every party and a wonderful person to know.

As with all things, there have been a host of people working quietly behind the scenes without whom I would have achieved nothing at all. Thank you to Maureen, Jim, Jimmy and Dennis in the animal house and Vince over at the Western for taking care of my mice. (I guess I had better thank all my mice too, although I don't suppose they thank me very much!) Tom and Ted in graphics deserve a big thank you for the wonderful photographs and posters they have put so much time and effort into on my behalf, as well as keeping me laughing with their jokes and banter! Also, a big thank you to Vicky, Morag and Carol in the office for their endless supply of stationary and smiles.

I have been lucky enough to be involved in several collaborations during the time I have been with John and Bob which have been both productive and enjoyable. It has been a real pleasure to have worked with Matt Kaufman, his willingness to impart his extensive knowledge of mouse anatomy being a great source of learning for me. I must also thank Nigel Brooks and Anne Aitkenhead at the CRB (good luck for your PhD too, Anne) as well as Duncan Davidson, Richard Baldock and Margaret Stark at the MRC HGU for letting me loose on their fantastic computer equipment!

My family have been tirelessly supportive and endlessly entertaining over the past three years. They have rejoiced at my successes, commiserated with my failures and generally kept my mind off the bad bits with their all their exploits and news. I guess I also should touch my cap to The British Army who have kindly provided me an alternative source of trials and tribulations to keep me from dwelling over the problems of my PhD!

Finally, my biggest thank you goes to my husband, Cameron, without who's love and support I would not have been able to have undertaken this PhD or to have achieved so much over the past three years.

Thank you all!

Abstract

Pax6 is a developmentally important, highly conserved transcription factor. *Pax6* mutations in mouse, man and *Drosophila* cause eye abnormalities. *Pax6* mutations in the mouse cause the small eye phenotype. Several small eye alleles have been identified, including *Sey* and Sey^{Neu}. The heterozygous small eye mouse (*Sey/+*) exhibits micropthalmia and anterior segment abnormalities similar to the human conditions of aniridia and Peter's anomaly. The homozygous small eye mouse (*Sey/Sey*) exhibits anopthalmia, absence of nasal tissues, severe brain defects and cranio-facial abnormalities and is an early post-natal lethal.

It is difficult to determine from the small eye homozygous phenotype alone the developmental potential of cells deficient in *Pax6* during eye and nasal development as the eyes and nasal tissues are completely absent. Therefore, to investigate roles for *Pax6* in eye and nasal development, cells deficient for *Pax6* were incorporated with wild-type cells within aggregation chimaeras. This strategy attempts to rescue *Pax6* deficient cells into lens and nasal tissue formation. Production of E12.5 Sey^{Neu}/Sey ↔+/+ aggregation chimaeras showed that Sey^{Neu}/Sey cells were unable to contribute to the lens and nasal epithelium, thus defining a cell autonomous role for *Pax6* in these tissues. Severe abnormalities of optic cup development were also observed in Sey^{Neu}/Sey ↔+/+ chimaeras. Optic cup phenotypes indicated requirements for *Pax6* in cell-to-cell interaction in the optic cup due to marked segregation between Sey^{Neu}/Sey cells and wild-type cells. Also, Sey^{Neu}/Sey cells were found to be excluded from the retinal pigment epithelium (RPE) which indicated a possible cell autonomous role for *Pax6* in RPE differentiation.

Inability of Sey^{Neu}/Sey cells to contribute to RPE could be due to a failure of mutant cells to be recruited to this differentiation pathway or incomplete or retarded

differentiation of *Sey*^{Neu}*/Sey* cells relative to wild-type cells within the chimaeric eye. These possibilities were explored by analysis of expression of *Pax6* and an early RPE marker, *Trp2,* in E12.5 and E14.5 *Sey*^{Neu}*/Sey* ↔+/+ chimaeras. These experiments confirmed a role for *Pax6* in the development of the RPE and indicated that although *Sey*^{Neu}*/Sey* cells were able to be specified as RPE, they were unable to differentiate at the stages examined.

A preliminary investigation into luteinising hormone-releasing hormone neuron migration showed absence of these neurons in the *Sey*^{Neu}*/Sey*^{Neu} homozygote fetus but no overt abnormality of migration in the *Sey*^{Neu}/+ heterozygote. Finally, a study investigating small eye homozygous (*Sey/Sey*, *Sey*^{Neu}*/Sey* and *Sey*^{Neu}*/Sey*^{Neu}) phenotypes showed effects of genetic background on fronto-nasal facial phenotypes, and identified a novel phenotype involving ectopic cartilage growth in the nasal region.

Contents

Appendices

pages 274-324

Previously published work

Abbreviations

AP	Alkaline phosphatase
d	days
DAB	diaminobenzadine tetrahydrochloride
DNA	deoxyribonucleic acid
d.p.c.	days post coitum
E	Embryonic day
ENU	Ethylnitrosourea
GPI	Glucose phosphate isomerase
HRP	Horseradish peroxidase
mRNA	messenger ribonucleic acid
Pax1	paired box homeotic gene 1
Pax2	paired box homeotic gene 2
Pax3	paired box homeotic gene 3
Pax4	paired box homeotic gene 4
Pax5	paired box homeotic gene 5
Pax6	paired box homeotic gene 6
Pax7	paired box homeotic gene 7

Pax8	paired box homeotic gene 8
Pax9	paired box homeotic gene 9
PCR	polymerase chain reaction
RNA	ribonucleic acid
RPE	retinal pigment epithelium
TBE	Tris-borate/EDTA
TE	Tris/EDTA
TESPA	3-aminopropyltriethoxysilane
TEMED	N,N,N',N'-tetramethylethylenediamine
tRNA	transfer ribonucleic acid
Trp1	Tyrosinase-related protein 1
Trp2	Tyrosinase-related protein 2
Sey	$Pax6^{Sey}$
Sey^{Neu}	$Pax6^{Sey\text{-}Neu}$
Sey^{Dey}	$Pax6^{Sey\text{-}Dey}$
Sey^{H}	$Pax6^{Sey\text{-}H}$
Tg	β-globin transgene

Chapter 1
Introduction

1.1. The small eye mutant

Small eye (*Sey*) is a semidominant mutation characterised in the heterozygous (*Sey/+*) animal by microphthalmia and anterior segment disorders and likened to the human conditions of aniridia and Peter's anomaly (Jordan *et al.*, 1992; Hanson *et al.*, 1994). Eyes and nasal tissues fail to form in the *Sey/Sey* homozygous fetus, which die shortly after birth. In addition to eye and nasal phenotypes, the homozygous small eye mutant exhibits severe brain abnormalities including hypoplasia of the frontal lobes and complete absence of the olfactory lobes. Nomenclature of the different small eye alleles has recently been changed as it is now known that they are *Pax6* mutants, (see *Mouse Genome* (1996) **94**:332). For clarity and ease of reference the new nomenclature will be abbreviated as follows: $Pax6^{Sey}$ to *Sey*; $Pax6^{Sey\text{-}Dey}$ to Sey^{Dey}; $Pax6^{Sey\text{-}H}$ to Sey^{H} and $Pax6^{Sey\text{-}Neu}$ to Sey^{Neu}.

The small eye mutation arose spontaneously in a mouse colony in Edinburgh and was first characterised as a novel semidominant mouse mutant by Roberts in 1967 (Roberts, 1967). Clayton *et al.* (1968) investigated the phenotype of the heterozygous small eye (*Sey/+*) animal, finding degenerative changes in the retina, retinal pigment epithelium and lenses containing swollen, disorganised cells.

Embryological analysis was undertaken by Hogan *et al.* (1986; 1988). Hogan showed that the small eye homozygous phenotype appeared to be caused by a failure of the presumptive lens and nasal placodes. Hogan noted that homozygous embryos could be unambiguously identified on histological examination at E10.5 due to the complete absence of nasal pits and the formation of optic vesicle structures that contained no

lenses. Hogan noted the presence of mesodermal cells lying between the optic vesicle and the overlying ectoderm at E10.5 in the *Sey/Sey* homozygous fetus but was unable to conclude whether this was a cause or effect of the lack of contact between surface ectoderm and optic vesicle (Hogan *et al.*, 1988). By mapping a radiation induced small eye deletion mutation, Sey^{H}, Hogan and colleagues were able to position the small eye mutation on mouse chromosome 2 (Hogan *et al.*, 1986).

The small eye heterozygous (*Sey/+*) animal can be visually identified during late gestation as the developing eye is smaller than that of normal wild type littermates. The small eye heterozygous fetus is viable and easily characterised at weaning by the reduced size of the eyes in which cataracts have developed. Variable phenotypic severity (variable expressivity) can be observed among these micropthalmic eyes, ranging from animals whose eyes are of small size but appear otherwise normal to those whose cataracts are very severe or lids are fused. Unilateral effects can be observed, with differences in severity of eye abnormality between the left and right eyes of an individual (Clayton *et al.*, 1968; Pritchard, 1973). The small eye heterozygous phenotype has been likened to the human disorders aniridia and Peters' anomaly (Hanson *et al.*, 1993; 1994; Glaser *et al.*, 1994).

A detailed histological analysis of *Sey/Sey* homozygous fetuses undertaken by Grindley *et al.* (1995) noted absence of the earliest morphological determinant of lens development, the lens placode (Grindley *et al.*, 1995). Instead, at E10.0, a region of dense tissue was observed adjacent to the distal optic vesicle which Grindley *et al.* suggested to be a condensation of mesenchymal cells under the undifferentiated surface ectoderm.

The optic vesicle of the *Sey/Sey* homozygote appeared distorted towards the distal end and broader than in wild type littermates. Further analysis of *Sey/Sey* optic vesicles by

transmission electron microscopy from E9.5 onwards showed that the mutant optic vesicle was able to make contact with the overlying surface ectoderm but that this contact was progressively lost as mesenchymal cells intervened between the two tissues (Grindley *et al.*, 1995). The *Sey/Sey* optic stalk retained its lumen with no evidence of optic nerve formation at E15.5. Grindley *et al.* also noted the complete absence of nasal epithelium in the *Sey/Sey* homozygous mutant. In contrast, development of the nasal tissues, lens, neural retina and retinal pigment epithelium (RPE) was seen to be normal in small eye heterozygous *Sey/+* fetuses.

The brain abnormalities associated with the homozygous small eye mutant phenotype have been comprehensively classified by Schmahl *et al.* (1993). In a detailed analysis of homozygous Sey^{Neu}/Sey^{Neu} fetuses, Schmahl reports impairment of axonal growth and differentiation with neurons of the cortical plate ceasing to differentiate at approximately E16.0. Degeneration of axons, glial cells and glial fibres was also noted. These cumulative abnormalities resulted in a severe impairment of neuronal migration within the developing forebrain, resulting in a severe hypoplasia of the whole forebrain region. The ventricular zone was found to be greatly enlarged within the forebrain and hindbrain of homozygous fetuses. No abnormalities of the thalamic or hypothalamic regions were noted in small eye homozygous fetus and pituitary development was found to be normal.

Although brain abnormalities in the small eye heterozygous $Sey^{Neu}/+$ fetus had not been investigated by previous studies, Schmahl *et al.* (1993) noted an increased diameter of the ventricular and sub-ventricular zones of the telencephalon and a dense clustering of migrating cells within the intermediate zone at E18.0. This finding is of particular interest as, to date, no brain abnormalities have been associated with the human ocular disorders homologous to the small eye heterozygous phenotype.

In addition to mouse small eye mutants, the rat small eye mutant, *rSey,* has also been characterised and exhibits a similar microphthalmic heterozygous phenotype to its murine counterpart (Mastuo *et al.*, 1993; Fujiwara *et al.*, 1994). The homozygous *rSey/rSey* fetus also fails to develop eyes and nasal tissues although an incidence of bilateral facial clefting is also reported. Matsuo *et al.* investigated neural crest cell migration in the rat mutant and found that midbrain neural crest failed to migrate into the nasal region. Therefore, combined data from studies of the rat and mouse small eye homozygous brain phenotypes appears to indicate a causal relationship between the small eye genotype and abnormalities of neural cell migration. The mechanisms resulting in this abnormal migration have not yet been elucidated.

1.1.1. *Pax6*, small eye mutations and human ocular disorders

Hogan *et al.* (1986) mapped the small eye (*Sey*) mutation to mouse chromosome 2. Meer de Jong *et al.* (1990) further defined this localisation to a region of mouse chromosome 2 syntenic with the region containing the aniridia-2 (AN2) gene on human chromosome 11p13. Hill *et al.* (1991) identified that mutations within a mouse paired box and homeobox containing gene, designated *Pax6* by Walther and Gruss (1991), were the cause of the small eye phenotype. Concurrently, Ton *et al.* (1991) cloned a candidate cDNA from the human aniridia locus, also later characterising the mouse small eye gene (Ton *et al.*, 1992). They found the two genes showed a high level of homology (<92%) in nucleotide sequence and virtual identity at an amino acid level. Therefore mutations within both mouse and human *Pax6* genes were found to cause developmental eye abnormalities.

Since this discovery, a number of human eye abnormalities distinct from classical aniridia; congenital cataracts, Peters' anomaly, dominant autosomal keratinitis and foveal hypoplasia, have all been identified as being caused by mutations within the

human *PAX6* gene (Jordan *et al.*, 1992; Hanson *et al.*, 1993; Glaser *et al.*, 1994; Hanson *et al.*, 1994; Fantes *et al.*, 1995; Mirzayans *et al.*, 1995; Fukushima *et al.*, 1995; Azuma *et al.*, 1995; 1996, Hanson and van Heyningen, 1995). A few cases of putative human aniridia homozygous fetuses have been identified (Hodgson and Saunders, 1980; Edwards *et al.*, 1984; Margo, 1983), In a recent report, a human fetus born lacking both eyes and a nose, was found to be compound heterozygous for mutations within the *PAX6* gene (Glaser *et al.*, 1994).

1.1.2. *Pax6* and the *Pax* gene family

Pax6 is a member of a developmentally important family of transcription factors, the paired homeobox-containing genes or *Pax* genes. Most *Pax* genes contain a characteristic DNA binding motif; the paired domain. The first paired domain genes isolated were three *Drosophila* segmentation genes identified by virtue of conservation of the paired DNA binding domains to other identified binding motifs (Bopp *et al.*, 1986). The first paired domain containing gene was isolated in the mouse by sequence homology to the *Drosophila* paired box probe and named *Pax1* (Deutsch *et al.*, 1988). Subsequently, a further eight *Pax* genes were identified: *Pax2* (Dressler *et al.*, 1990; Nornes *et al.*, 1990), *Pax3*, (Goulding *et al.*, 1991); *Pax4*, *Pax5* and *Pax6*, (Walther *et al.*, 1991); *Pax7*, (Jostes *et al.*, 1990); *Pax8*, (Plachov *et al.*, 1990) and *PAX9*, (Stapleton *et al.*, 1993) (for review see Mansouri *et al.*, 1994). These *Pax* genes constitute six distinct classes (Walther *et al.*, 1991; Chalepakis *et al.*, 1992, for review see Stuart *et al.*, 1994), defined by presence or absence of the homeobox, serine/threonine-rich and octapeptide regions.

Pax6 homologues have been identified and characterised in the mouse (Jong *et al.* , 1990; Hill *et al.*, 1991; Ton *et al.*, 1992;), human (Ton *et al.*, 1991), rat (Matsuo *et*

al., 1993; Fujiwara *et al.*, 1994), chick (Li *et al.*, 1994), quail (Martin *et al.*, 1992; Plaza *et al.*, 1993; Dozier *et al.*, 1993), zebrafish (Krauss *et al.*, 1991; Puschel *et al.*, 1992), *Drosophila melanogaster* (Quiring *et al.*, 1994), *Caenorhabditis elegans*, (Zhang and Emmons, 1995), cephalopod molluscs (Tomarev *et al.*, 1996) and sea urchins (Czerny and Busslinger, 1995).

Mutations in *Pax* genes other than *Pax6* in both mouse and man are known to cause mutant phenotypes. Mutations in *Pax1* cause the mouse mutant undulated (*un*) (Balling *et al.*, 1988) characterised by severe vertebral malformations along the entire vertebral axis (Grunberg, 1954). Mutations with the *Pax3* cause the mouse Splotch *(Sp)* mutant (Epstein et al., 1991). Mutations within the human *PAX3* gene give rise to Wardenburg's Syndrome Type 1 which is characterised by hearing and pigmentation defects (Tassabehji *et al.*, 1992; Chalepakis *et al.*, 1994).

The *Pax* gene paired domain contains three α-helices, one residing in the animo terminal of the paired domain, the other two are located in the carboxy region, the α-helix of the animo terminal being more highly conserved than those of the carboxy region (Bopp *et al.*, 1991; Treisman *et al.*, 1991, Walther *et al.*, 1991). It is the second of these three α-helices which is reported to be involved in specific DNA recognition (Treisman *et al.*, 1989). In addition to the paired box and homeobox domains found in most *Pax* genes, a conserved octapeptide sequence of unknown function is also found to be present in some, but not in *Pax6* or *Pax4*.

As a transcription factor, PAX6 is thought to act via the DNA binding property of the paired domain, this DNA binding property being highly conserved between species (Chalepakis *et al.*, 1991; Treisman *et al.*, 1991; Adams *et al.*, 1992; Kozmik *et al.*, 1993; Czerny and Busslinger; 1995). Another potent region for transcriptional activation has been shown to be the C-terminal region of the *PAX6* protein (Glaser *et*

al., 1994), this region being absent in both the *Sey* and Sey^{Neu} translation products (Hill *et al.*, 1991). The *PAX6* homeodomain is also likely to be involved in DNA binding and/or transcriptional regulation, as is the case in the homeobox genes, but has not been investigated thoroughly to date.

Despite detailed knowledge of the genomic and mRNA structure of the *Pax6* gene in the mouse, relatively little is known about the protein product. Early binding studies with the quail *Pax6* homologue, Pax-QNR (Dozier *et al.*, 1993) showed the presence of alternative splicing events, both at the 5' end and middle of the mRNA transcript. In addition, Pax-QNR protein was able to initiate transcription *in vitro*. Pax-QNR was found to bind to a promoter upstream of the *Drosophila even-skipped* gene (Dozier *et al.*, 1993) and has also been shown to contain neuroretina-specific enhancer elements (Plaza *et al.*, 1995). Plaza (1995) showed that *PAX6* was capable of self regulation by binding and transactivation of its own promoter. *Pax6* has also shown to be transcribed by at least two promotors indicating the possibility of multiple activation/repression interactions in different cell types in both fetal and adult tissues (Plaza *et al.*, 1993).

PAX6 binding activity is conferred by regions within the paired and homeodomain regions and the C-terminus can activate transcription. This suggests that PAX6 is involved in multiple protein and/or DNA interactions (for review see Cvekl and Piatigorsky, 1996). PAX6 has also been shown to bind *in vitro* to the neural cell adhesion molecule L1 (Chalepakis *et al.*, 1994) and studies in the chick (Cvekl *et al.*, 1994; 1995a), mouse (Cvekl *et al.*, 1995b) and guinea pig (Richardson *et al.*, 1995) have reported PAX6 to be associated with the activation of five different crystallin genes. Although no PAX6 inducers have been reported to date, several genes have been shown to down regulate expression of *Pax6* , including activin A (Pituello *et al.*, 1995) and *sonic hedgehog* (Macdonald *et al.*, 1995; Ekker *et al.*, 1995). It appears

from the work of Macdonald *et al.* (1995) studies that down regulation of *Pax6* by *sonic hedgehog* and reciprocal expression of *Pax2* may be instrumental in defining the boundaries between optic cup and optic stalk.

Czerny and Busslinger (1995) identified that specific differences at the animo acid level conferred the different binding properties of PAX6 and PAX5, this binding specificity being lost or changed when these specific binding sequences were altered. A number of splice variants of the murine PAX6 protein have been identified which may possess different physiological properties *in vivo* (Sperbeck *et al.*, 1996). Therefore, by induction of multiple promoter regions, transcription of products containing multiple DNA binding domains and the additional translational complexity of multiple splice forms, *Pax6* has the functional capacity to assume many complex and interactive roles during fetal development and adult life.

1.1.3. *Pax6* genotypes and phenotypes

Several different non-complementing alleles of small eye have been identified to date, two spontaneously-arising alleles *Sey* (Roberts, 1967) and Sey^{Dey} (Theiler *et al.*, 1978; 1980), a radiation-induced variant Sey^{H} (Hogan *et al.*, 1986) and an ethylnitrosourea-induced mutation Sey^{Neu} (Favor *et al.*, 1988; Hill *et al.*, 1991). All of these mutations produce a characteristic microphthalmic heterozygous phenotype. Mutations in *Pax6* genes in the rat, *Drosophila* and *C.elegans* have now also been identified and shown to cause eye or sense organ abnormalities (Mastuo *et al.*, 1993; Quiring *et al.*, 1994; Chisholm and Horvitz, 1995).

Studies to date suggest that the human aniridia (AN) and mouse small eye are null mutations (Hill *et al.*, 1991; Jordan *et al.*, 1992; Glaser *et al.*, 1992; 1994, Mirzayans *et al.*, 1995). In addition, the semidominant nature of known *Sey* alleles indicates that

the function of the PAX6 protein is dosage dependant. Ton *et al.* (1991) suggested that the phenotypes observed in human aniridia patients and the mouse small eye mutant might be due to the affected tissues of the eye being sensitive to a morphogenetic gradient, similar to the *bicoid* gradient morphogen in *Drosophila*, (Struhl *et al.*, 1989). This hypothesis suggests that fields specified by homeotic genes could be highly dependent on certain gene products at precise times and locations. Thus, inadequate gene dosage, due either to genomic deletion or loss of physiological properties of the protein product, could have severe effects on morphogenesis of the dependent tissue.

The complexity of *Pax6* gene dosage effects during eye morphogenesis has been investigated by Schedl *et al.* (1996). By generation of mice containing a *PAX6*-YAC construct, Schedl (1996) was able to show that expression of a single copy of the human *PAX6* gene could restore a wild type phenotype to the small eye heterozygous animal. However, expression of multiple copies of the human *PAX6* gene on a wild type backgound resulted in mice exhibiting severe eye defects including severe microphthalmia. It is interesting to note that only eye tissues were affected in these animals. This indicated that development of the eye is supremely sensitive to abnormal dosage of *Pax6* product as overexpression and loss of expression were observed to result in similar phenotypes (Schedl *et al.*, 1996). It is possible that overexpression of *PAX6* in these animals created an autoregulatory feedback loop which resulted in abnormal induction, maintenance or loss of expression of *Pax6* in specific *Pax6*-sensitive cell types during development, resulting in the abnormal phenotypes observed.

A hypothesis of a sensitivity of eye development to *Pax6* gene dosage is supported when the phenotypes of the different human *PAX6* mutations are considered. Both sporadic and familial cases of aniridia have been shown to be caused by a wide variety

of genetic lesions within the *PAX6* gene resulting from genomic insertions or deletions (Glaser *et al.*, 1992; Jordon *et al.*, 1992), nonsense mutations (Glaser *et al.*, 1992; 1994; Hanson *et al.*, 1993; Martha *et al.*, 1994) and splice mutations (Glaser *et al.*, 1992; Jordon *et al.*, 1992; Hanson *et al.*, 1993, Epstein *et al.*, 1994; for review see Hanson and van Heyningen, 1995). In all cases, bar one, these *PAX6* mutations resulted in premature termination of translation the PAX6 protein, assuming transcription of a functional RNA transcript. Only two missense mutations have been identified to date, both resulting in milder eye phentoypes than other aniridia *PAX6* mutations, possibly due to a reduction in protein binding efficacy or efficiency rather than a 50% reduction in functional protein product (Epstein *et al.*, 1994; Glaser *et al.*, 1994).

However, although there are phenotypic differences between the anterior segment disorders caused by mutations within the *PAX6* gene, the severity of genetic lesion does not appear be related to the severity of eye phenotype (Hanson and van Heyningen, 1995). Individuals with minor genomic changes to those with deletions of the entire *PAX6* gene can manifest with similar clinical symptoms. This suggests that most *PAX6* mutations result in a complete loss of PAX6 function, this haploinsufficency resulting in the abnormal eye phenotypes observed in these patients.

Within the small eye mutations, there is also a diversity of genomic lesions that create a variety of translation products, from loss of most of the transcriptional domain to single base pairs changes creating nonsense or deleted sequences in the translated protein (Hogan *et al.*, 1986; Hill *et al.*, 1991; Matsuo *et al.*, 1993). For example, both the Sey^{Neu} and *rSey* mRNA products contain mutations affecting only the serine/threonine rich region at the carboxy terminus of the PAX6 protein whilst the *Sey* mutation truncates the product prior to the homeodomain (Hill *et al.*, 1991; Matsuo *et al.*, 1993). The radiation induced small eye allele, Sey^{H}, in the homozygous

state is an early embryonic lethal. The severity of phenotype is reflected at a genomic level as this mutation was found to be a large deletion that spans all of the *Pax6* open reading frame and possibly other important genes in its flanking regions (Hogan *et al.*, 1986; R. Hill, personal communication).

For the purposes of this study, two small eye alleles, *Sey* and Sey^{Neu}, will be considered in some detail. The overt phenotypes observed in animals heterozygous or homozygous for either *Sey* or Sey^{Neu} allele are the result of single base pair changes within the *Pax6* gene (Hill *et al.*, 1991). The *Sey* mutation results from a single base pair change 5' to the *Pax6* homeobox region. Sequence analysis of this region shows a single base pair change at codon 194 of the protein that resulted in a wild-type G:C to T:A transversion. The *Sey* mutation converts a wild-type GGA triplet to a TGA stop codon resulting in translation terminating prior to the homeobox. A novel DdeI restriction enzyme site is encoded by this single base pair change at the genomic level and can be used for identification of the presence of the *Sey* mutation site. The product of the *Sey* gene contains the paired box region of the wild type *PAX6* protein which has been shown to confer both binding specificity and trans-activation properties (Treisman *et al.*, 1991; Czerny *et al.*, 1993; Epstein *et al.*, 1994; Czerny and Busslinger, 1995).

The Sey^{Neu} allele, produced by chemical mutation (Favor *et al.*, 1988), has been shown by genetic crosses to be a semidominant mutation similar to the spontaneously derived small eye (*Sey*) (Roberts, 1967; Hogan *et al.*, 1986). On investigation, Hill *et al.* (1991) detected an increased length of mRNA transcript in the Sey^{Neu}/Sey^{Neu} homozygous embryo relative to wild-type. Sizing of Sey^{Neu} mRNA fragments showed this extension to be an extra 116 nucleotides 3' to the homeodomain. On sequencing of genomic DNA from Sey^{Neu}/Sey^{Neu} homozygous embryos, both wild type and Sey^{Neu} introns proved to be of identical length but the Sey^{Neu} intron

contained single base pair transversion, a mutant T replacing a wild type G at a predicted splice site. This single base pair change abolishes splicing at this site, producing an extended cDNA product which, in turn, contained an intron-encoded stop codon which truncates the protein 115 amino acids from the C terminus. Thus, the Sey^{Neu} product contained an nonsense sequence insert and lacked part of the serine threonine rich region which has been suggested to be involved in transcriptional activation (Glaser *et al.*, 1994). The Sey^{Neu} product does, however, contain both the paired domain and homeodomain regions (Hill *et al.*, 1991). Similar to the *Sey* mutation, the Sey^{Neu} mutation single genomic base pair change was found to encode a novel HindII restriction enzyme site, diagnostic for presence of the Sey^{Neu} mutation.

1.2. *Pax6* expression during fetal development

Pax6 expression during mouse fetal development has been extensively characterised (Walther and Gruss, 1991; Grindley *et al.*, 1995, see also Figure 1.1.). The wild type expression pattern of *Pax6* proved to be somewhat divergent from that of the other documented *Pax* genes, as unlike *Pax1*, *Pax3*, *Pax7* and *Pax9*, it was not found to be expressed in segmented mesodermal structures (Deutsch *et al.*, 1988; Dietrich *et al.*, 1993; Goulding *et al.*, 1991; Wallin *et al.*, 1994; Williams and Ordahl, 1994; Jostes *et al.*, 1994).

Walther and Gruss (1991) observed *Pax6* expression in the developing brain, olfactory epithelium and eye of the developing mouse fetus. Transcripts were first detected at E8.0 in the developing fore and hindbrain and, at E8.5, in the spinal cord on closure of the neural tube. In the forebrain, expression continued until E18.5, with highest levels noted in the cerebellum and olfactory bulbs. In the forebrain, the domain of *Pax6* expression extended up to a sharp border which delineated the boundaries between the diencephalon and mesencephalon.

Figure 1.1. Expression domains of *Pax6* during mouse development.

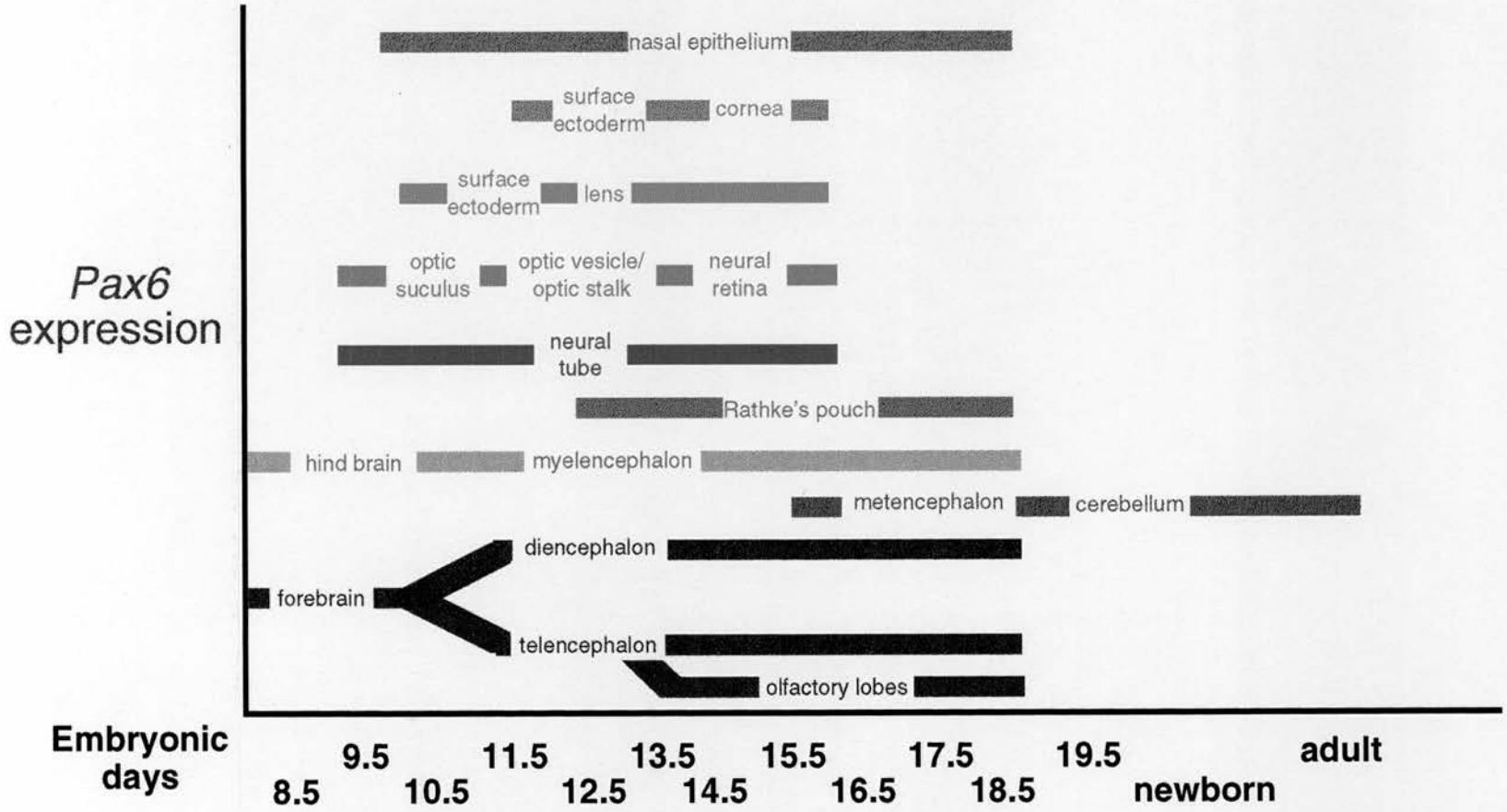

Pax6 expression in the eye was first noted at E8.5 in the optic succulus and the presumptive optic vesicle; the invaginating base of the forebrain. By E9.5, this invagination has formed the optic vesicle and *Pax6* transcripts were detected in the epithelial layer of the optic vesicle and the optic stalk. Concurrently, the lens placode developing from the overlying surface ectoderm was seen to strongly express *Pax6.* The surface ectoderm expressed *Pax6* both prior to and during formation of this early lens structure. As the lens placode invaginated to form the lens vesicle, *Pax6* expression was observed in both the inner and outer layers of the developing optic cup underlying the developing lens. Strong expression was still observed in the overlying surface ectoderm at this stage.

As differentiation of the eye progresses, expression of *Pax6* was restricted to the anterior epithelium of the cornea and the lens, although transcripts were higher in the anterior lens epithelium than in the body of lens fibres. By E12.5, expression in the optic cup was observed to restrict to the inner layer with down regulation in the developing retinal pigment epithelium. At this stage, strongest expression is to be found only in the most dorsal part of the optic cup, the area closest to the lens body itself.

By E15.5, most of the adult structures of the eye are formed. *Pax6* expression was found to be restricted to the inner layer of the neural retina and the anterior cornea and lens. As the neural retina develops, equal levels of expression are observed in the inner and outer neural retinal layers. The inner layer contains mostly post-mitotic ganglion cells and the outer layer densely packed, mitotically active cells (Walther and Gruss, 1991). *Pax6* expression was also observed in the developing nasal epithelium although, overall, expression was seen to be at a lower level to that observed in the eye.

From analysis of expression and by virtue of the DNA binding motifs located in the paired-box and homeobox domains, Walther and Gruss postulated that *Pax6* is a developmentally important transcription factor involved in morphogenesis of the eye and nasal structures.

Grindley *et al.* (1995) added resolution to the *Pax6* expression pattern reported by Walther and Gruss (1991), making particular reference to *Pax6* expression during lens development. They reported expression to be restricted by E9.5 in the surface ectoderm to the region of the developing lens placode, this domain diminishing further until only the surface ectoderm of the eye region was seen to be expressing *Pax6*. Although a connecting domain of surface ectoderm expression was observed between the lens and nasal placodes, this domain was also restricted until the nasal and lens placodes were separated. Grindley *et al.* suggest that this restriction of *Pax6* expression in the surface ectoderm of the developing head correlates to specified areas of lens and nasal competence. At the latest developmental stage examined by Grindley *et al.*, E15.5, *Pax6* transcripts were still observed in surface ectoderm-derived tissues of the eye.

Grindley *et al.* (1995) also reported *Pax6* expression in the neural ectoderm with expression first noted at E8.5 shortly before closure of the head folds. In the optic vesicle, expression was seen to be polarised distally from E9.5, with the strongest expression observed around the rim of the developing optic cup, with weaker expression seen in the back of the optic cup and developing optic stalk. By E14.5, expression is lost from the outer layer of the optic cup with expression seen to be restricted to the inner layer. Grindley investigated the pattern of *Pax6* expression of the neural retina and pigmented epithelium, confirming the pattern reported by Walther

and Gruss, but in addition, noting that the most anterior pigmented retinal epithelium, the future iris, was observed to be expressing *Pax6* at E15.5.

Cell specific requirements for *Pax6* in the developing neural retina have been implicated. Hitchcock *et al.* (1996) show expression of *Pax6* in mature amacrine and some ganglion cells in the adult teleost retina with strong labelling also seen in the constantly regenerating neuronal progenitors cells found at the retinal margin.

Ton *et al.* (1991) investigated the expression pattern of *PAX6* in the developing human fetus and found it to mimic that reported in the mouse. *PAX6* expression was noted in the neural retina, rim of the optic cup and neuroctodermal components of the iris and ciliary body. Strong *PAX6* expression was also observed in the lens and presumptive cornea and conjunctiva. In the developing human brain, transcripts were detected in the cerebellum and pons with a lower level of expression in the temporal lobes, midbrain, medulla oblongata and choroid plexus. Transcripts were also detected in the human olfactory bulbs (Ton *et al.*, 1991).

Characterisation of Pax6 expression has also been achieved in the chick embryo. Li *et al.* report a comprehensive study of early Pax6 expression in the developing chick (Li *et al.*, 1994). They showed Pax6 to be expressed in the neural epithelium, optic vesicles and invaginating surface ectoderm and subsequent lens tissues, but found this expression to occur at a substantially earlier stage than had previously been documented in the mouse (Li *et al.*, 1994). Li also reports Pax6 expression in the region of presumptive lens and corneal ectoderm prior to formation of the optic vesicle. They showed late gastrula stage embryos to be expressing Pax6, although the pattern was diffuse and localised generally around the anterior aspect of the embryo. As development progresses, Pax6 expression was observed to be confined to a specific band of prospective ectoderm cells near the anterior margin of the neural plate.

It is interesting to note that Li was not able to show Pax6 expression in the nasal placodes of the chick, although expression in the nasal placode had been reported in the mouse by Walter and Gruss (1991) and Grindley *et al.* (1995).

Li (1994) noted strong expression of Pax6 covering the whole region of the developing forebrain at the neural plate stage in the chick, with this extensive domain only being seen to restrict by stage 9 when the optic vesicles had begun to develop. Experimental manipulations also showed expression of Pax6 in the surface ectoderm to be independent of the optic vesicle after the neural plate stage, as ablation of anterior neural plate did not affect expression of Pax6 in the overlying surface ectoderm. Indeed, the overlying surface ectoderm was observed to strongly express Pax6 even when the optic vesicles were completely absent. This surface ectoderm expression pattern was repeated in cases where the optic vesicle had been moved ventrally or dorsally to its normal position. This indicated an independence of Pax6 expression in the surface ectoderm to developing neural structures.

Expression studies in both *Drosophila* (Quiring *et al.*, 1995) and *C. elegans* (Chisholm and Horvitz, 1995; Zhang and Emmons, 1995) show *Pax6* homologue expression in anterior head regions. In *Drosophila*, expression is observed in the developing neural and ocular systems and in *C. elegans*, Pax6 is observed to define sense-organ identity.

1.2.1. *Pax6* expression in *Sey/Sey* mice

Grindley *et al.* (1995) performed extensive *Pax6* expression studies by mRNA *in situ* hybridisation on homozygous small eye (*Sey/Sey*) fetuses. They observed that from E8.0 to E8.5, *Sey/Sey* embryos exhibited a wild-type *Pax6* expression pattern in the developing brain and optic outgrowths. However, at E9.5, no surface ectoderm

expression was seen anywhere in the head region of the *Sey/Sey* embryos, including the presumptive lens regions. *Pax6* expression in the abnormal *Sey/Sey* optic cup was observed to follow a similar pattern to that of wild-type and heterozygous littermates. Where a distinction was able to be made between optic cup and optic stalk, it was only the optic cup-like structures that showed *Pax6* expression. By E15.5, the abnormal optic cup structures observed in the homozygous mutants fetuses had approximated an inner layer/outer layer structure, both of these layers were seen to express *Pax6*.

Grindley (1995) observed a regulated restriction of *Pax6* expression in the surface ectoderm of wild-type fetuses and suggested that *Pax6* expression is governed by autoregulatory mechanisms in the surface ectoderm of the head. Activation and binding studies support this hypothesis as studies by Plaza *et al.* (1993) have shown that the quail *Pax6* protein, PAX-QNR, was able to bind and trans-activate its own promoter. This indicated that the mutant phenotype of the small eye homozygous mutant resulting in loss of lens and nasal placode formation might be caused by either a complete loss of *Pax6* expression, or a failure to maintain its own expression in the surface ectoderm of the head. This could be caused by a loss of autoregulatory function of the mutant *Pax6* product.

1.3. Lens development

The process of lens development has been extensively studied, both in terms of its histological morphogenesis and the genes involved in this process. For a diagramatic representation of eye morphogenesis in the mouse, see Figure 1.2.

Lens development begins in lens-specified surface ectoderm at approximately E9.5 in the mouse fetus. Surface ectoderm within the region of head overlying the developing optic vesicle thickens to form a lens placode. This placode region is characterised by

Figure 1.2.

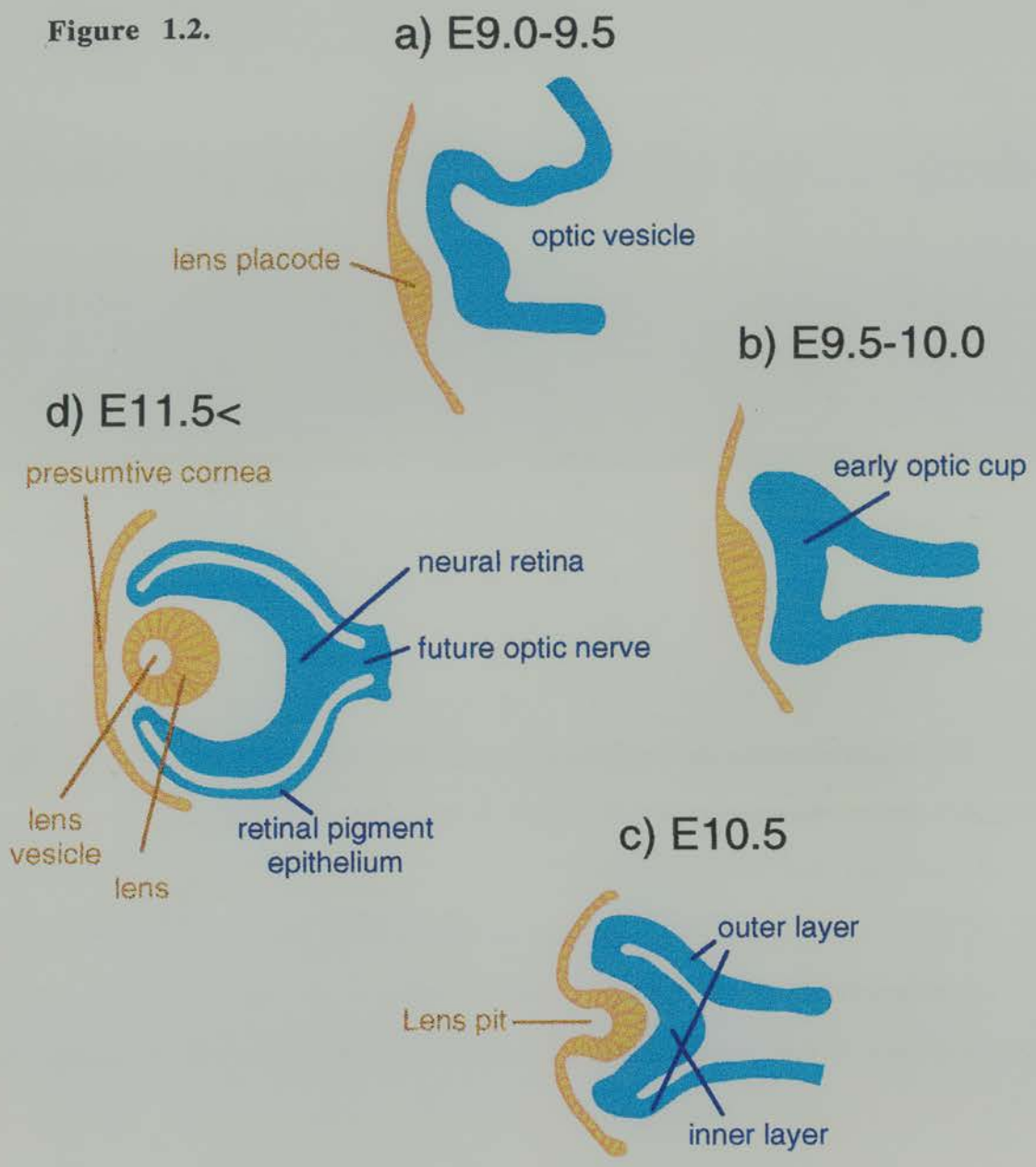

Figure 1.2. Schematic diagram of fetal eye development in the mouse. **a)** At embryonic day 9-9.5, the optic vesicle is forming as an outgrowth of the ventral forebrain. The overlying surface ectoderm thickens to form the lens placode. **b)** By E9.5-10, the optic vesicle makes contact with the lens placode. **c)** At approximately E10.5, the lens placode invaginates to form the lens pit and the optic vesicle invaginates to form the optic cup. **d)** By E11.5, the lens has separated from the presumptive cornea and contains two distinct cell populations; the primary lens fibre cells and the anterior cuboidal epithelial cells. The optic cup is now composed of two layers; the outer retinal pigment epithelium and the inner neural retina. As eye development progresses, the lens vesicle will be lost and the inner layer of the optic cup will differentiate to give rise to all of the layers of the neural retina.

an increase in surface ectodermal cell length and cell condensation to give the placode a thickened, disk-like shape. The event of placode formation is the earliest identifiable morphogenetic step towards lens development in all animal species. The lens placode is also the first developmental stage of lens morphogenesis to express lens antigens (Langman, 1959a; 1959b; Maisel and Langman, 1961; Barabanov and Fedstova, 1982).

It is at the placode stage that the developing lens first comes into physical contact with the developing optic vesicle. This contact is maintained throughout development of the eye to ensure a functional and physical relationship between the lens and the neurally derived optic structures of the eye.

The lens placode invaginates to form the lens vesicle before constricting at its anterior surface to detach from the surface ectoderm at approximately E10.5 to become a separate entity - the early lens. The lens at this stage is immature, consisting of a layer of lens epithelial cells at its anterior margin, an open lens vacuole and the main body of posterior lens cells which will differentiate to form the lens fibres. However, by detachment of the lens from the surface ectoderm, the lens is a complete unit, containing all precursor cells necessary for its development. Differentiation of lens cells continues throughout fetal life.

1.3.1. Lens induction

Embryonic formation of the eye involves a series of complex inductive processes. The eye is composed of a variety of complex tissues and cell types, including both neurally derived and ectodermally derived structures. The inductive processes defining the development of these structures must be highly co-ordinated to achieve an eye that is functionally and positionally correct. One such inductive interaction is that of the

development of lens tissue from surface ectoderm and the positional relationship of the developing lens to the optic vesicle.

Initially, it was hypothesised that localised thickening and invagination of the surface ectoderm of the head and the subsequent formation of a lens placode was induced by the proximity of the optic vesicle. Studies by Lewis (1904) demonstrated the appearance of a lens in association with optic vesicles that had been transplanted to more posterior regions of the body. The interpretation of these experiments was that optic vesicle could induce lens formation in surface ectoderm of virtually any region of the fetus.

However, the results of subsequent investigations by Spemann (1912a; 1919; 1938) and others (Rabl, 1898; Lehmann, 1933) were not consistent with a hypothesis of autonomy of the optic vesicle on lens development. The most comprehensive of these early studies on the role of the optic vesicle in lens development were carried out by Spemann (1912a; 1919; 1938) and still bear relevance today. In contrast to the developmental scenario postulated by Lewis (1904), Spemann hypothesised independence of optic cup development from lens formation from transplant and ablation experiments carried out in amphibians (Spemann, 1938). The fundamental hypothesis of Lewis' early experiments (1904) was that the mechanism by which lens formation was induced was totally reliant on presence of the optic vesicle. However, Spemann performed studies in which lens formation was both lost and maintained after removal of the primitive optic rudiments (Spemann, 1938). Spemann's final conclusion was that lens formation in different genera reacted differently to removal of optic rudiments and that this difference reflected a variable importance of the optic vesicle on lens formation.

Spemann also elucidated from ectoderm transplant experiments that lens forming capacity in the surface ectoderm of the fetus was spatially restricted. He showed that ectoderm transplanted from the trunk region of the animal to overlie the optic vesicle was unable to from lens tissue whilst ectoderm from the head surrounding the eye was able to develop into lens (Spemann, 1912b). Spemann was the first to identify the thickening of the surface ectoderm as the earliest morphological determinant of lens formation.

More recently, the idea of regional specificity has been reviewed and suggestions made that surface ectoderm must have a regional competence to respond to the optic vesicle in order that lens formation may be initiated (Jacobson, 1966.) Reinvestigation of the early transplantation experiments using cell markers (Henry and Grainger, 1987) elucidated that original results may have been obtained because lens-specified ectoderm was transplanted along with optic vesicle tissue, rather than by induction of host ectoderm. The validity of the ablation experiments was also questioned when it was found that in many species lenses could still form after ablation of retinal tissue at the neural plate stage. In the new lens morphogenesis pathway, lens was said to be specified in the head ectoderm, this process beginning in the gastrula and early neurula, being complete by the time predetermined ectoderm made contact with the optic vesicle (Grainger, 1992).

Barabanov and Fedstova (1982) showed that the inducing lens ability of the early optic vesicle of *Xenopus laevis* was enhanced when optic vesicle tissue was co-cultured with dorsolateral mesoderm. However, Barabanov and Fedstova could not induce lens formation from dorsolateral endoderm or mesoderm alone, which had been suggested to be early inducers of lens competence by Jacobson (1958; 1966). However, these models of lens induction still relied on the presence of optic vesicle for lens formation to occur *in-vivo*.

It had also been concluded that the optic vesicle was not sufficient, in itself, to induce lens competence and formation from surface ectoderm. (Saha *et al.*, 1989). Most early ablation experiments had been done in amphibians (Spemann, 1938) but more recently studies have been carried out in the chick by Li *et al.*, (1994). Li's ablation experiments showed that presence of an optic vesicle was not sufficient in isolation to induce lens competence in overlying ectoderm. Li removed anterior neural plate tissue at stage 7 from one side of the chick embryo. The ablated side failed to produce a lens whilst the unoperated side developed normally.

It has now been suggested that lens induction has four phases; competence, bias, specification and differentiation (Grainger, 1992). 'Competence' can been described as the ability of a tissue to respond to an inducing signal. The competence of a tissue may differ at different developmental stages, suggesting that competence is a temporally regulated state. Once a tissue has become competent to undertake a particular developmental pathway, additional signals 'bias' the tissue towards following that pathway above others. Once the tissue has reached this stage, the number of cells competent to become a particular tissue becomes tightly restricted and the tissue forming area can be said to be 'specified'. Specification defines those cells that will differentiate to form the tissue proper and may require exogenous spatial signals from interacting tissues. Once specification has been achieved, tissue 'differentiation' can occur.

Lens competence in *Xenopus* has been shown to appear and disappear from cultured tissues *in vitro* (Servetnick and Grainger, 1991), suggesting lens competence is under the control of a developmental timer that is independent of tissue interaction. Experiments using *Xenopus* have also shown that the strong lens-inducing signal present at gastrulation is the result of a planar signal present throughout the sheet of

surface ectoderm. This signal originates from the presumptive neural plate, possibly from the region of the presumptive optic cup itself (Henry and Grainger 1990). The signal results in 'lens forming bias' throughout the head ectoderm. It has been shown by studies in the chick that 'bias' is sufficiently strong to cause the differentiation of surface ectoderm into small lentoid structures if tissues are resected and grown *in vitro*. (Barabanov and Fedstova, 1982).

By the time that the optic vesicle has reached the surface ectoderm, the region of lens competence has been assigned and surface ectoderm will develop into lentoid structures if removed and cultured *in vitro* (Henry and Grainger, 1990; Li, 1994). It therefore might be assumed that the optic vesicle plays a late role in lens formation and may function purely to indicate the location of the developing lens within the head ectoderm. As lens competence is realised in the lens placode, conversely, lens competence must be lost from the surrounding surface ectoderm. An early study postulated that this spatial regulation was achieved by the physical presence of neural crest cells migrating around the optic vesicle after closure of the neural tube, physically separating the influence of the optic vesicle from adjacent surface ectoderm (von Woellwarth, 1969). However, this does not comply with a theory of optic vesicle-independent lens specification. The exact mechanisms by which lens competence is 'turned off' in the surrounding ectoderm is likely to be controlled at a molecular level rather than by physical processes.

Although the early stages of lens induction may occur independently of interaction with the optic vesicle, after lens formation has begun the lens and optic cup tissues develop in close communication. It has been shown that once lens and retina have been specified, mutual interactions are necessary for maintenance of the individual tissues as a diminution or enlargement of one tissue produces a concomitant size change in the other. This has been experimentally demonstrated in ablation studies

using diphtheria toxin gene linked to the α-crystallin promoter (Kaur *et al.*, 1989; Harrington *et al.*, 1992). A loss of lens tissue by ablation of lens fibre cells after initial lens formation resulted in a concomitant size reduction in the optic cup. As α-crystallin is expressed in differentiated lens cells, retinal development has already begun by the time lens ablation occurs, thus indicating a mutual co-ordination of growth between the developing lens and retina. Early work to identify a role for the lens in retinal differentiation of amphibians shows that the arrangement of the retinal layers, with respect to their orientation to the lens, is not determined until the onset of optic cup differentiation (Eakin, 1947), indicating a fundamental role for the lens in this process.

1.3.2. Roles for *Pax6* in lens development

As has already been described, expression studies of *Pax6* in the mouse have identified strong expression in all of the tissues of the head involved in lens morphogenesis, the surface ectoderm, lens placode and then the developing lens itself (Walter and Gruss, 1991; Grindley *et al.*, 1995). Expression and ablation experiments in the chick (Li *et al.*, 1994) first elucidated a causal link between *Pax6* expression and lens competence in the surface ectoderm of the head, although *Pax6* expression was observed in the surface ectoderm of the chick head at stages prior to that reported in the mouse.

By ablation of increasing areas of neural tissue, Li *et al.* (1994) showed that expression of *Pax6* in the surface ectoderm was independent of presence of an optic vesicle, optic vesicles abnormally orientated or completely absent having no effect on regionalisation of *Pax6* expression. That is, *Pax6* expression was maintained in the surface ectoderm of the head overlying the normal position of the optic vesicle even if the vesicle was absent. However, they do not report if the areas of surface ectoderm seen to be expressing *Pax6* were subsequently able to form lens placodes. In addition,

Li identifies *Pax6* expression in the surface ectoderm at a stage prior to lens placode formation. Taken together, Li's results indicate that *Pax6* is involved in lens competence prior to lens placode formation or any inductive signal from the optic vesicle. Conversely, these experiments indicated that regions of head ectoderm capable of induction to lens formation are those that are *Pax6* expressing.

These recent experiments support data examining lens competence in fish and amphibians, showing that substantial morphological lens development could occur in these animals in the absence of neural-ectodermal structures (Saha *et al.*, 1989; Henry and Grainger, 1990; Grainger, 1992). These studies suggest an early role for *Pax6* in lens development.

Transdifferentiation studies further define roles for *Pax6* during lens morphogenesis (Adler *et al.*, 1994). By examining *Pax6* expression in lens cells derived from cell types other than surface ectoderm, Adler show that retinal glial cells were able to transdifferentiate to form *Pax6* expressing lentoid bodies in culture. *Pax6* expression was observed in these cell cultures prior to and during transdifferentiation of recognisable lens cell clusters. This pattern of expression was seen to mimic that occurring during normal lens induction and development, confirming a role for *Pax6* in both competence to become lens and lens development *in vitro*.

The hypothesis that *Pax6* is required for lens competence is supported by morphological examination of the small eye homozygous fetus. Hogan *et al.* (1986) suggested that the anopthalmic phenotype observed in the small eye homozygous mutant fetus might arise from a failure of lens placode formation. They noted that although optic vesicle formation appeared to be progressing well at E10.5 in the small eye homozygous fetus, no evidence of epithelial thickening occurred in the surface ectoderm juxtaposed to the developing optic vesicle. They also reported that optic

vesicles in the small eye mutants did not appear to make contact with the overlying surface ectoderm of the head. Therefore, Hogan *et al.* suggested that the primary defect resulting in absence of lens tissue in the mutant embryos was one of growth and differentiation of the lens placode.

The hypothesis that placode formation failed in the small eye homozygous fetus was also supported by the recent study of *Pax6* expression in the small eye homozygous mutant (Grindley *et al.*, 1995). Although the small eye homozygous mutant produced no functional *PAX6* protein, *Pax6* mRNA was still detectable by *in situ* hybridisation. Although Grindley *et al.* could detect *Pax6* expression in the surface ectoderm of the homozygous mutant at E8.5, this expression was lost by E9.5. (In a wild type embryo at this stage *Pax6* expression would be restricting to the lens and nasal placode regions). However, transcripts of mutant mRNA could, however, be detected in the developing optic vesicles at this stage. This suggested a primary role for *Pax6* in formation of the lens and nasal placodes and indicated a causal link between failure of lens and nasal tissue formation and *Pax6* mutations in the homozygous small eye fetus.

A study by Fujiwara *et al.* (1994) investigated the competence of homozygous *rSey/Sey* cells to form lens by tissue recombination experiments using the rat small eye (*rSey*) mutant. Fujiwara showed that surface ectoderm from homozygous *rSey/rSey* fetuses was unable to form lens tissue when cultured in-vitro with *rSey/+* or +/+ optic vesicle. Conversely, +/+ surface ectoderm could be induced to form lens when co-cultured with +/+, *rSey/+* or *rSey/rSey* optic vesicle. Fujiwara concluded from these results that the failure of *rSey/rSey* surface ectoderm to differentiate lens tissue was due to defects in an unspecified early signal emanating from the neural plate or underlying head mesenchyme.

However, these conclusions are open to question as if mutations within the rat *Pax6* gene cause a phenotype similar to that observed in the mouse small eye mutant, the areas of surface ectoderm tissue resected for Fujiwara's tissue recombination experiments were inherently unable to form a lens placode. Indeed, one criteria for recognition of *rSey/rSey* embryos for tissue resection was that of abnormal eye rudiment development, suggesting that effects of loss of *Pax6* function were already apparent in the developing eye tissue at the time of dissection. As with the early tissue recombination experiments, true isolation of the different tissue types was unlikely and attached mesenchyme from both surface ectoderm and optic vesicle tissue may be affecting the experimental results. In addition, identification of surface ectoderm from the lens-forming region by orientation to a developing optic vesicle indicates that lens competence will already have been achieved in this tissue, biasing results towards lens formation. Therefore, although this Fujiwara *et al.*(1994) suggest the small eye defect to be one of early lens competence or specification, they could not conclusively resolve this issue.

The complete failure of lens morphogenesis in the small eye homozygous (*Sey/Sey*) fetus provides the most direct evidence for a requirement for *Pax6* during eye morphogenesis. In addition, *Pax6* has also been shown to be involved in eye morphogenesis in invertebrates. Quiring *et al.* (1994) identified the *Drosophila eyeless* gene as the homologue of the human aniridia (AN) and mouse small eye (*Pax6*) genes. *Eyeless* is a homeobox and paired box-containing gene expressed during *Drosophila* eye morphogenesis. Quiring's work suggested that the mechanisms of eye morphogenesis that produced the radically different eye structures observed in mammals and insects were controlled by similar genetic mechanisms. In support of this hypothesis, Halder *et al.* (1995) carried out an elegant series of experiments in which formation of compound eyes was induced in *Drosophila* by ectopic expression of both the *Drosophila eyeless* and murine *Pax6* genes in the imaginal discs of the

head and thorax. Identical results have also been recently reported by ectopic expression of the squid *Pax6* homologue in *Drosophila* (Tomarev *et al.*, 1996). These experiments confirmed *Pax6* genes are homologous across species.

Halder's studies also indicated that *Pax6* plays a role in morphogenesis of the neural components of the eye as, in addition to compound lenses being formed at ectopic sites, associated neural retinal tissues were present including photoreceptor and pigment cells (Halder *et al.*, 1995). In effect, a full eye structure was generated although these ectopic eyes had no contact with the central nervous system. This indicated that the degree of evolutionary conservation observed between *Pax6* genes of different species was mirrored at a functional level in terms of putative downstream target genes.

1.4. Development of the optic cup and retinal differentiation

The optic cups originate as outgrowths from the ventrolateral aspects of the developing forebrain at approximately E8.0 in the mouse. By E9.5, these outgrowths have assumed a tubular structure which invaginates to form the optic vesicle, achieving physical contact with the surface ectoderm of the head at its most anterior aspects by E10.5. The optic vesicle then further invaginates to form a recognisable cup structure, comprising inner and outer layers. The outer layer of the optic cup will develop to form the retinal pigment epithelium (RPE) and the inner layer, the neural retina, iris and ciliary structures. It is important to note that both the inner and outer layers of the optic cup are derived from a contiguous sheet of neural ectoderm. Therefore, this neural ectoderm must be multipotent to form RPE, all retinal cell types and other neural-derived eye structures such as the iris and ciliary bodies (see Figure 1.2. for diagramatic representation of eye development in the mouse).

Early experimental evidence for this multipotency was achieved by transplantation experiments (Stroeva, 1960). Optic vesicle tissue transplanted into the anterior chamber of the optic cup became neural retina in the absence of mesenchyme but developed as retinal pigment epithelium if contacted by mesenchymal cells, usually iris. This early work indicated that the early optic vesicle was potentially able to form both layers of the optic cup and also that environmental factors were involved in this developmental decision. In addition, early optic cup tissue was found to be able to produce all retinal cell types when cultured from explants in-vitro (Sparrow and Barnstable, 1986).

Later studies have attempted to determine the processes of retinal cell specification more precisely. Host and donor marking and the use of specific cell markers have been critical in determining retinal differentiation. Turner *et al.* (1990) demonstrated, using retroviral cell markers, that a single cell precursor was able to produce all the retinal cells. Similarly, inhibition experiments in *Xenopus* were also able to make the same conclusion (Harris, 1991). When cell division and DNA synthesis were blocked in early gastrula stage embryos, eye development continued normally. Although the retina was seen to form fewer but larger cells, most retinal cell types differentiated appropriately (Harris, 1991). Both of these studies showed that cell fate in the retina is not strictly temporally defined as cells can be specified, or re-specified by changes of cell-to-cell interaction. However, a definite hierarchy of photoreceptor cell differentiation is observed within the developing neural retina, beginning with ganglion and horizontal cells and ending with rod photoreceptors (Altshuler, 1992; 1993) indicating some degree of temporal regulation of this process.

Retinal cell culture experiments have also indicated an independent side to retinal cell development. Transdifferentiation experiments have shown that the inner layer and outer layer of the neural retina are able to survive and proliferate in isolation from each

other in culture. However, if the inner layer is damaged or removed, outer layer cells can reconstitute the inner layer indicating critical interactive roles within the inner and outer layers during development (Pittack *et al.*, 1991). Turner and Cepko identified that retinal progenitors were present throughout development of the eye and can generate the diverse retinal cell types late in eye development (Turner and Cepko, 1987)

Therefore, in *précis*, the inner layer of the optic cup arises from a multipotential indented disc of cells and is capable of forming all the layers of the retina proper. It is in close connection with the developing outer layer which both requires, and is required for the normal development of the optic cup. The neural retina has a close interactive relationship with the developing lens and although, in itself, does not initiate lens development contact is required for lens fibre differentiation. Constant interaction between the developing neural retina and the lens confers size regulation to the developing eye to ensure maintenance of a functional eye structure.

1.4.1. Genes involved in development of the inner layer of the optic cup

A number of genes have been identified that are involved in specification or differentiation of the inner layer of the optic cup during mammalian eye development. Although a great deal of work has been done in this area, our understanding of the genetic mechanisms by which the complex and highly specified cell types of the adult retina develop from the undifferentiated inner layer of the optic cup is still primitive.

Retinal ganglion cells in the chick have been shown to be selected from a pool of competent progenitor cells by the action of the neurogenic gene *Notch* (Austin *et al.*, 1995). A complex variety of transcription factors, homeobox genes and other

developmentally important genes have been found to be expressed during various stages of retinal differentiation. Several homeobox genes, including *Dlx1*, *Msx1* and *Msx2* have been identified and found to be expressed during mouse retinal development (Monaghan *et al.*, 1991; Dolle *et al.*, 1992). *Chx10*, a homeodomain containing gene, has also been found to be expressed during retinal development, becoming restricted to the inner nuclear layer of the adult retina (Lui *et al.*, 1994). The *Chx10* mouse mutant complements the known expression pattern with an abnormal phenotype of impaired retinal progenitor cell proliferation (Burmeister *et al.*, 1996). Other compounds, such as the ribosome related protein p40 (Rabacchi *et al.*, 1990) and an isoform of aldehyde dehydrogenase (McCaffery *et al.*, 1991) have also been shown to be localised to the dorsal region of the developing retina at the early optic cup stage.

Pax-2 has been shown to be localised in the ventral half of the developing optic cup and the optic stalk (Nornes *et al.*, 1990). Recent work by MacDonald *et al.* (1995) showed that ectopic expression of Sonic hedgehog (*shh*) resulted in a down regulation of *Pax6* expression with a concurrent up-regulation of *Pax2* expression. Although these two genes demarcate proximal/distal boundaries within the developing eye, this study suggests that *shh* is involved in the regulatory processes partitioning the optic primordia into optic cup and optic stalk.

A number of cell adhesion molecules have been found to be expressed in the retina and are found to be involved in retinal cell adhesion during development (Hoffman and Edelman, 1983; Daniloff *et al.*, 1986; Hoffman *et al.*, 1986; Matsunaga *et al.*, 1988). It appears that cell adhesion molecules may be playing a role in cell sorting and lamination in the neural retina and optic stalk. However, our understanding of the complex interactions by which this ever enlarging pool of genes controls development of the neural retina is still in its infancy.

1.4.2. Roles for *Pax6* in optic cup and retinal development

Perhaps by virtue of the extensive expression studies undertaken in the mouse embryo by Walther and Gruss (1991) and Grindley *et al.* (1995), in addition to the medical importance of *Pax6* in eye disorders, recent studies of *Pax6* expression have attempted to determine the specific role for this gene during development of the retina. Differential splicing of the *Pax6* gene product has been identified and suggests that different splice forms might have differing roles in the lens and retina during eye morphogenesis (Epstein *et al.*, 1994; Sperbeck *et al.*, 1996).

A detailed study undertaken in the goldfish by Hitchcock *et al.*, (1996) identified *Pax6* protein expression in the nuclei of mature amacrine and ganglion cells. As the retina of teleosts is constantly growing throughout adult life it conceptually contains cells in both adult and fetal states of development. At the differentiating retinal margin, Hitchock *et al.* showed neuronal progenitors and newly post mitotic neurons to express *Pax6*. These recent experiments have indicated a role for *Pax6* in amacrine and ganglion cell development and, importantly, in differentiation of mature cell types from undifferentiated progenitors in the retina. This hypothesis is also supported by the study by Halder *et al.* discussed previously, as both lens and neural retinal tissues were induced by ectopic expression of *Drosophila* and mouse *Pax6* genes.

Until recently, no retinal defects had been reported in association with the anterior segment disorders associated with mutations in the human *PAX6* gene. However, a recent report has identified a retinal defect, foveal hypoplasia, in a family containing a missense mutation in the C-terminus region of *PAX6* (Azuma *et al.*, 1995; 1996). Although foveal hypoplasia is commonly associated with aniridia, a number of family members exhibiting foveal hypoplasia showed no abnormalities of the anterior

segment of the eye. This data appears to separate anterior segment and retinal phenotypes in patients with different *PAX6* mutations indicating multiple physiological roles for *PAX6* during eye development.

1.4.3. The retinal pigment epithelium

The retinal pigment epithelium (RPE) is a highly specialised simple cuboidal epithelium located in close association to the outer layers of the neural retina. It serves several important functions including absorption of light passing through the retina and restores photosensitivity to visual pigments dissociated in response to light stimulus. The RPE also plays an important role in homeostasis of the neural retina by controlling phagocytosis and disposal of membranous materials from the retinal photoreceptor layer and acting as part of the blood/retina barrier (Peyman and Bok, 1972; Bok, 1985; Bosch *et al.*, 1993). Once the adult retina is fully formed, most cells of the RPE do not divide and therefore must stay functional throughout the adult life of the animal. Overall, maintenance of a functional RPE is vital for normal retinal development, growth and homeostasis.

The neural retina and RPE are both derived from the same multipotent neurectodermal sheet that formed the optic vesicle. At the earliest stage of eye development, the relationship between cells destined to from the inner layer of the optic cup, and those destined to become the outer layer, is purely spatial. Despite this uniformity, the optic vesicle is able to appropriately form an inner and outer layer but the processes by which this delicate specification is achieved are, as yet, undetermined. Attention has been focused on experimentally inducing RPE to neural retina transformation, with this phenomenon having been extensively described *in vitro* (Coulombre and Coulombre, 1965; 1970; Okada, 1980; Vollmer *et al.*, 1984; Layer and Wilbold,

1989; Buse and de Groot, 1991). However, the processes involved in determination of RPE from early optic tissue has been less well characterised.

A complex but elegant experiment by Buse *et al.* (1993) has helped to develop our understanding of RPE determination from the primitive optic vesicle in the mouse embryo. Culture of optic vesicle in an *in vitro* environment produced both inner layer and outer layer isolates indicating maintenance of normal inductive interactions in the culture conditions. However, when early eye primordia were cultured with the presumptive inner layer selectively removed, ability to form RPE was almost completely lost from the cultured isolates. These experiments indicate that determination of RPE is dependant upon signals from both surrounding mesenchyme and the presumptive neural retina.

As in the normal adult the RPE does not divide, it is surprising that RPE is able to transdifferentiate to reconstitute all of the layers of the neural retina after mechanical insult or injury (Layer and Willbold, 1989; Okada, 1984; Buse and de Groot, 1991). Conversely, experiments by Raymond and Jackson (1995) using transgenic mice containing a differentially expressed diphtheria toxin gene construct driven by the *Trp1* promoter show that if the RPE is ablated at the stage of inner layer/outer layer determination the whole process of eye formation is lost. However, if ablation of RPE cells occurs after formation of the optic cup, eye development can be maintained although the retinal layers become disorganised. Therefore, there appear to be a vital reciprocal interaction between the developing RPE and neural retina and that presence of both layers is crucial to both initiate and maintain normal optic cup development.

1.4.4. The RPE and pigment formation

The differentiated RPE produces pigment in the form of melanin granules. Melanin production is controlled by expression of tyrosinase and the tyrosinase-related proteins. Two tyrosinase-related proteins have been identified in the mouse to date, *Trp1* and *Trp2*, both of which are involved in the regulation of melanin production (Kobayashi *et al.*, 1994; Winder *et al.*, 1994). Tyrosinase is the product of the *albino* locus, mutations within which cause reduction or loss of pigmentation (Silvers, 1979; Jackson and Bennett, 1990). The tyrosinase related proteins, *Trp1* and *Trp2* show approximately 40% similarity at the amino acid level. In the mouse, TRP1 is the product of the *brown* locus and TRP2 the product of the *slaty* locus (Jackson, 1988; Jackson *et al.*., 1992) with mutations in *Trp1* and *Trp2* affecting pigment quality.

Steel *et al.* (1992) performed expression studies in the mouse for tyrosinase and the two tyrosinase-related proteins. *Trp1* and *Trp2* are both expressed in the RPE prior to visual formation of pigment. *Trp2* is expressed earliest in mouse development with transcripts first detected at E9.5, in the optic vesicle prior to its invagination. *Trp2* expression was seen to restrict to the outer layer of the optic cup, to the developing RPE prior to pigment formation. *Trp2* expression is also noted in cells that will form the iris. Steel (1992) suggests that *Trp2* labels undifferentiated melanoblasts in the developing eye. Expression of *Trp2* in migratory melanocytes in the skin, pinnae and inner ear of the developing fetus supports this hypothesis. *Trp1* and tyrosinase are also reported to share a similar expression pattern. *Trp1* expression was noted at E11.5 and tyrosinase at E13.5, however, it is highly likely that tyrosinase is expressed prior to this stage. Tyrosinase and the tyrosinase-related proteins are therefore the earliest reported markers of RPE development.

Another gene family which is involved in formation of the RPE is that of the micropthalmia (*mi*) complex. The first *mi* gene was identified as a semidominant allele originating from the descendants of an irradiated male (Hertwig, 1942). The homozygous *mi/mi* mouse lacks pigmentation of the eyes, skin and inner ear and is microphthlamic and deaf (Gruneberg, 1953; Silvers, 1979). A number of *mi* alleles have been identified (Grunberg, 1953; Wolf and Coleman, 1964; Hollander, 1968) all of which manifest, with varying severity, disorders of pigmentation, ear or eye development (Stelzner, 1964, 1966; Southard, 1974; Lerner, 1986; Lamoreux *et al.*, 1992). The *mi* gene has been identified to encode novel basic-helix-loop-helix-zipper protein, a novel transcription factor expressed the developing eye ear and skin (Hodgkinson *et al.*, 1993).

1.4.5. Roles for *Pax6* in RPE formation

Transdifferentiation experiments by Adler *et al.* (1994) previously discussed with reference to *Pax6* in lens formation, also report an interesting phenomenon which may provide insight into the mechanisms of specification of the RPE from undetermined optic vesicle. Alder (1994) noted that, in addition to lentoid body formation occurring from *Pax6* expressing transdifferentiated glial cell cultures, retinal pigment epithelial-like cell formation was also observed. Although the details are scant, this may indicate that expression of *Pax6* is also a prerequisite for RPE development. Although speculative at present, it would be interesting to determine as, to date, *Pax6* has not been suggested to play a role in development of the RPE. However, as *Pax6* is expressed strongly in both the inner and outer layers of the primitive optic vesicle and expression of *Pax6* is down regulated as RPE differentiation occurs, this might indicate that the down regulation of *Pax6* expression might be part of the RPE determination process.

1.5. Development of the olfactory system

In comparison to the eye, little is known about development of the olfactory system. The olfactory system is composed of the nasal epithelium, the olfactory lobes and their integral interconnecting axons. The nasal epithelium consists of paired cavities lined with columnar epithelium, separated by the nasal septum. The olfactory epithelium lines the most posterior and dorsal regions of the nasal cavity with the rest of the lining being composed of respiratory epithelium (Kahle, 1986). Odour recognition is achieved by activation of sensory receptors within the external layers of the olfactory epithelium (Buck and Axel, 1991). Individual odours activate specific and unique groups of receptors, this stimulus being transferred to the olfactory lobes via a network of sensory axons for neural processing and odour recognition (Allison, 1953).

A study of the development of the olfactory epithelium in the mouse was reported by Cusheri and Bannister (1975). The nasal epithelium develops from invagination of the nasal placodes. Similar to the lens, the nasal placodes can be identified as a thickened area of surface ectoderm and constitute the first morphological determinant of nasal development. Nasal development begins prior to lens placode morphogenesis, with nasal placodes being well developed by E9.5 in the mouse. The nasal placodes then invaginate to form the nasal pits, which in turn, develop to give rise to the convoluted nasal epithelium. By E12.5 in the mouse, the nasal epithelium comprises a large tissue area within the fronto-nasal mass and is beginning to show formation of the complex convolutions that will form the adult conchae of the nose.

Similar to the eye, the nasal epithelium is closely innervated both to and from the brain and this neural contact is required for continued development of both the nasal tissues and the olfactory lobes. Olfactory axons begin to arrive at the margins of the forebrain

at approximately E11.5 in the mouse embryo (Cushieri and Bannister, 1975). As the presumptive olfactory lobes are indivisible from the forebrain mass at this stage, it has been suggested that this nervous connection between nasal epithelium and neural tissue induces their formation (Gong and Shipley, 1995). It is therefore difficult to determine if loss of olfactory lobes in the small eye homozygous fetus is a primary effect of loss of *Pax6* function within the developing forebrain, or if the phenotype is caused by loss of olfactory lobe induction due to absence of developing nasal epithelial tissues.

1.5.1. Induction of olfactory tissues

The mechanisms of induction of the nasal placodes and associated forebrain structure have not been well defined. Early ablation and grafting experiments in amphibians by Bell (1906; 1907) indicated that nasal tissues could form independently of the olfactory lobes. However, ablation of forebrain tissue may have been carried out after specification of nasal tissues had been achieved and their developmental pathway well underway. Conversely, Zwilling (1934) induced ectopic nasal tissue formation from general surface ectoderm by transplantation of large areas of early forebrain tissue. These experiments in the frog, and similar experiments in the chick (Waddington and Cohen, 1936) have highlighted the interactive nature of nasal system induction and showed that once induction has been achieved, development of the nasal tissues and olfactory lobes progresses independently of one another.

1.5.2. Genes expressed in the developing olfactory system

A number of genes have been found to be expressed during nasal development including the mouse homeobox-containing genes, *Msx1* and *Msx2* (Mackenzie *et al.*, 1991; 1992). Neural cell adhesion molecules have also been shown to be expressed in

the developing mouse olfactory system (Miragall *et al.*, 1989). N-CAM has been shown to be slightly expressed in the nasal placode at day E9.0 in the mouse with stronger expression in the underlying mesenchyme. N-CAM and L1, another neural cell adhesion molecule, were both found to be expressed in the developing nasal epithelium from E10.5 onwards. It is interestingly that N-CAM and L1 were not found to be expressed in the developing respiratory epithelium. The embryonic form of N-CAM (E-N-CAM) was found to mirror N-CAM expression during fetal development but was restricted to a small number of sensory bodies and axons by the early postnatal period. L1 remained prominently expressed on axonal processes throughout development. Both N-CAM and L1 were also found to be expressed in the developing olfactory bulb (Chung *et al.*, 1991), highlighting the possibility that both molecules play an integral role in the development of neuronal connections between the developing nasal epithelium and the olfactory bulb.

1.5.3. A role for *Pax6* in nasal development

The observation that the small eye homozygous fetus does not develop nasal tissues or olfactory lobes has prompted only the suggestion that failure of placode regions causes eye, brain and nasal phenotypes. However, it is apparent that eye and nasal tissues are extremely different in development, function, innervation and morphology. Therefore, it has not been adequately explained how the loss of a single gene product, *Pax6*, can affect two such radically different organ systems. Little work, has been done to try to elucidate the complex interactive events involved in olfactory system development at a molecular level.

Grindley *et al.* (1995) attempted to address this issue by examining the role of *Msx1* during nasal development in the small eye homozygous fetus. In +/+ and *Sey*/+ fetuses, Grindley *et al.* (1995) noted *Msx1* expression in the surface epithelium

constituting the lateral nasal placode, with no expression observed in the medial nasal placode or underlying mesenchyme. This expression continued throughout development of the placode regions although expression was not examined later in development. Grindley *et al.* (1995) showed that *Msx1* was not expressed in the small eye homozygous fetus. However, it is not clear whether loss of *Msx1* expression was due to a failure of *Msx1* activation or because the cells found to express *Msx1* in +/+ and *Sey*/+ littermates, the cells of the developing lateral nasal placode, were absent in the small eye homozygous fetus.

Expression of neural cell adhesion molecules appears to play a role both in development of the nasal tissues and olfactory lobes, as well as in the axonal connections between them (Miragall *et al.*, 1989). Although, Schmahl *et al.* (1993) showed severe defects of neuronal cell migration within the developing brain in the small eye homozygous fetus, expression of the neural cell molecules during development of the small eye homozygote has not been examined. It is relevant to the brain pathologies observed in the small eye homozygous fetus that *Pax6* has recently been shown to bind and activate the L1 promoter (Chalepakis *et al.*, 1994). Similarly, N-CAM has been shown to be activated in-vitro by a number of homeobox-containing genes (Jones *et al.*, 1993; Goomer *et al.*, 1994; Chalepakis *et al.*, 1994) and by *Pax8* (Holst *et al.*, 1994). If loss of *Pax6* expression in the small eye homozygous fetus were affecting downstream expression of other developmentally important homeotic genes, expression of both these neural cell adhesion molecules might be affected, possibly determining phenotype in the olfactory lobes. However, these issues have yet to be addressed.

1.6. The chimaera as an experimental tool

A chimaera is an organism which has been derived from more than one fertilised egg. This can be achieved either by aggregation of two separate fertilised embryos, (first achieved by Tarkowski in 1961 and simplified by Mintz, 1962), or by injection of individual cells from the early embryo or pluripotent embryonic carcinoma or embryonic stem cells into the cavity of blastocyst stage embryos (Gardner, 1968; Mintz and Illmensee, 1975; Papaioannou *et al.*, 1978; Fujii *et al.*, 1980; Evans and Kaufman, 1981; Martin, 1981, Bradley *et al.*, 1984). In addition, embryonic carcinoma or embryonic stem cells have been aggregated to early embryos to produce chimaeras (Stewart, 1980; Fujii and Martin, 1980; Wood *et al.*, 1993).

Chimaeras have been used as a powerful tool to analyse tissue growth and follow cell fates during embryogenesis (Gardner and Papaioannou, 1975, Mintz, 1967; 1971; Moore and Mintz, 1972; Sanyal and Zeilmaker, 1977; West, 1978; Kusakabe *et al.*, 1988; Williams and Goldwitz, 1992; Boland and Gosden, 1994; West and Flockhart, 1994) or to analyse gene function or examine mutants where loss of a gene product or chromosomal abnormality is known to cause severe developmental abnormalities (Harrison and Astle, 1976; Lavail and Mullen, 1976; Stephenson, 1985; Muggleton-Harris *et al.*, 1987; Palmer and Burgoyne, 1991a; 1991b) or embryonic lethality (Papaioannou and Gardner, 1979; Rashbass *et al.*, 1991).

Using chimaeras, a gene product can be identified as having either a non-autonomous or autonomous effect. A non-autonomous effect is indicated where loss of the gene product can be overcome developmentally by the presence of wild type cells. Conversely, an autonomous effect describes the situation where cells unable to produce the specific product cannot survive or interact normally even given a wild-

type environment in which to do so. The term "rescue" has been coined with particular reference to chimaera strategies to describe this inclusion or survival of cells in an environment to which they were previously unable to contribute. "Rescue" denotes an affect at a cellular level, the consequences of which can be observed at both a micro- and macro-morphological level in the fetal and adult chimaera.

1.6.1. Use of aggregation chimeras for the study of ocular defects

A number of mouse mutants have been used to study morphogenesis of the developing eye (LaVail and Mullen, 1976a; 1976b; Zwaan and Webster, 1984; 1985). The production of aggregation chimeras has been used to attempt "rescue" of mouse mutants with lens abnormalities (Muggleton-Harris *et al.*, 1984; Yoshiki *et al.*, 1991).

An early chimaera experiment by LaVail and Sidman (1971) examined the effect of the *rd* mutation on postnatal retinal development in *rd/rd*↔+/+ mouse aggregation chimaeras. They found that the mutant *rd/rd* retinal phenotype was not completely "rescued" by the presence of wild type cells in chimaeric retinas, as areas of both degenerating and abnormal photoreceptors were observed (LaVail and Sidman, 1971).

LaVail and Mullen (1976b) investigated further the role of the *rd* gene using rat chimaeras. By aggregation of embryos of a pigmented wild type strain to un-pigmented *rdy/rdy* embryos they were anble to show an autonomous effect for the retinal dystrophy (*rdy*) gene in the RPE. They found patches of abnormal and degenerating photoreceptors were only located opposite areas of mutant *rdy/rdy* RPE, thus indicating that the retinal dystrophy gene was acting directly and cell autonomously on cells of the photoreceptor layer. However, some "rescue" of the degenerating photoreceptor cells was achieved when wild type cells at the periphery of the mutant inner layer patches were in contact with the degenerating cell layer (LaVail

and Mullen, 1976b) indicating that cell-to-cell interaction between the RPE and photoreceptor layer was necessary for the *rdy* gene to perturb photoreceptor development.

Muggleton-Harris used the congenital cataractous mutant mouse (CAT) to show that "rescue" of eye abnormalities could be achieved by aggregation of mutant and normal embryos (Muggleton-Harris *et al.*, 1984). The CAT mutant eye has been shown to exhibit similar histological finding to that of some human cataractous eyes, with vacuolation and degeneration of the cortical lens fibres and anterior lens fibre cells exhibiting abnormal mitotic activity. Abnormalities of lens morphogenesis were detected in mutant fetuses E15.0 days. Therefore, the CAT mutations affects late lens development with affected animals exhibiting full cataracts by the time the eyes opens. By aggregating mutant embryos to a non-cataractous mouse strain, Muggleton-Harris *et al.* were able to produce live young that showed no lens abnormalities. Using glucose phosphate isomerase-1 (GPI1) allozymes as strain markers, they were able to show that the animals with normal eye phenotypes contained a higher proportion of wild type cells than CAT cells. They also observed that these normal lenses could contain a high proportion of CAT mutant cells whilst exhibiting no histological abnormality. Muggleton-Harris therefore suggested that the mechanism for rescue of lens development in these chimaeras was via cell-cell interaction, thus defining the action of the CAT gene as non-autonomous.

An elegant study by Yoshiki *et al.* (1991) used similar techniques to attempt "rescue" of another mouse mutant with abnormal lens development. The eye lens obsolescence (*Elo*) mutant exhibits morphological abnormalities of the nuclei of lens fibre cells, resulting in deficient elongation of lens fibres and posterior rupture of the lens capsule. Although lens fibres were seen to be morphologically abnormal at E13.0 days, the

number of lens fibre cells showed no significant reduction until E15.0. By the late fetal stage lenses in this mutant strain were observed to be small and deformed.

To investigate whether the *Elo* phenotype was caused by genotype or cellular environment, Yoshiki *et al.* aggregated C3H-*Elo* mice to BALB/c embryos to create aggregation chimeras. However, in this case "rescue" was not achieved as even those embryos with a low C3H-*Elo* contribution were found to have opacities of the lens, although the lenses formed were normal in shape and rupture had not occurred. C3H-*Elo* dominant chimeras were found to have a morphology similar to that of *Elo* littermates. Using immunohistochemical staining with a anti-C3H antibody, Yoshiki was able to identify C3H-*Elo* cells within the developing lens and demonstrated that abnormal lens fibres were solely of C3H-*Elo* derivation. This result defined the action of the *Elo* gene product as cell autonomous (Yoshiki *et al.*, 1991).

Aggregation chimaeras have proved to be a powerful tool for examining the roles of developmentally important genes during embryogenesis, fetal, and adult development. Therefore, this strategy was adopted to attempt to determine roles for *Pax6* during fetal eye and nasal development using the small eye mouse mutant as an experimental model.

1.6.2. Cell selection in chimaera experiments

Preferential selection or allocation of cells into different tissues or cell lineages has been reported in chimaera experiments (Mintz and Palm, 1969; Mullen and Whitten, 1971; Garner and McLaren, 1972; Barnes *et al.*, 1974; McLaren, 1976; West, 1977; Everett and West, 1996). In particular, aggregation chimeras have been used to study the developmental potential of lethal parthenogenetic cell populations during fetal development. Chimaera studies have shown that parthenogenetic cells make a variable

contribution to fetal and adult tissues. Aggregation of parthenogenetic to wild type cells in chimaeras showed that parthenogenetic cells were preferentially selected to the primitive ectoderm, (Surani *et al.*, 1988; Thomson and Solter, 1988, Fundele *et al.*, 1990) whilst androgenetic cells were lost from primitive ectoderm-derived tissues (Surani *et al.*, 1988, Thomson and Solter, 1989).

Nagy *et al.* (1989) showed that parthenogenetic cells made a varied contribution to the fetus and adult but certain tissues contained a higher contribution of parthenogenetic cells than others. The largest contribution of parthenogenetic cells was to be found in the brain, heart and coat pigment cells, whilst cells were systematically excluded from skeletal muscle, liver, adrenals, blood, bladder and salivary glands. It was suggested that this selection may vary according to the method of renewal of these tissues, as tissues with a low rate of cells division or clonally renewing cell populations showed the highest proportion of parthenogenetic cells. However, tissues where parthenogenetic cells were at a very low or sporadic concentration are more difficult to explain as it is unsure whether cells failed to contribute to the developing tissues or were actively excluded from them.

1.6.3. Use of cell markers in experimental chimaeras

The fundamental concept embracing chimaera experiments is the interaction of two differentially-derived cell populations at a cellular level. Therefore, maximum analytical data can only be achieved if the two cell populations can be distinguished within the tissues of the chimaera. Cell markers have been used to determine both proportion of cell contribution and spatial determination of cell identity within experimental chimaeras.

Various types of cell markers have been used to identify cell strains in aggregation chimeras. A commonly used method for analysis of proportion of cell contribution in chimaeras is coat colour (Tarkowski, 1964; Mintz, 1967; 1971; Mullen and Whitten, 1971; West and McLaren, 1976; Muggleton-Harris *et al.*, 1987; Nagy *et al.*, 1989; Fundele *et al.*, 1989; Yoshiki *et al.,* 1991). By aggregating embryos from two strains differing in coat colour, the percentage contribution could be assessed by the proportion of pigmented to non-pigmented patches in adult chimaeric animals. The disadvantage of this approach is that it can only be used once chimaeras have reached term and may also give imprecise proportions as the nature of melanocyte colonisation in hair fibres can produce variegation of pigmentation.

One of the most widely used biochemical markers for estimation of cell contribution in chimaeric fetuses is that of the enzyme glucose phosphate isomerase (GPI). GPI is a dimeric molecule for which several different monomers have been identified including GPI1A, GPI1B and GPI1C (Carter and Parr, 1967; De Lorenzo and Ruddle, 1969; Padua *et al.*, 1978; Conrad *et al.*, 1987). GPI dimers can be separated and their allozyme type identified by virtue of different electrophoretic mobilities (Chapman *et al.*, 1971). Although current electrophoretic methodologies allow determination of allozyme activity to as little as 3% in tissue homogenates, the nature of the sampling methodology does not provide spatial information of cell contribution. Also, as a tissue mass must be taken to provide homogenate for activity reactions, the value obtained for each allozyme type is only an average for the tissue assessed.

Pigmentation in the retinal pigment epithelium in the developing eye can be used as a cellular marker of chimaerism in the developing fetus. Pigment formation in the RPE is complete by E12.5 and can be used as a marker of chimaerism in mid-gestation fetuses, prior to development of pigment in the choriod. The proportion of pigmented verses non-pigmented cells contributing to the RPE can, in turn, be used as an

indication of percentage contribution of the two cell types to the chimaeric fetus as a whole. In recent study by West *et al.* (1996), composition of chimaeric fetuses, as estimated using the cellular marker glucose phosphate isomerase 1 (GPI1), was found to be positively correlated to a subjective estimate of pigment in the eye. In a further study by West *et al.*, (unpublished data, 1996), the correlation between cell contribution by GPI1 analysis and percentage eye pigment was shown to hold true even when the proportion of pigment in the RPE was determined from a single histological section. These studies indicate that assessment of pigment contribution to the fetal RPE gives a good approximation of percentage cell contribution to other tissues of the chimaera.

In order to be able to identify the different strains contributing to a chimaera at a cellular level, histochemical techniques have been used. Chimaera experiments have utilised strain specific enzymatic markers (Condamine *et al.*, 1971; West, 1976; Gardner, 1984; West, 1984) and more recently, strain specific antibodies have been used for identification of cells derived from different mouse embryos (Kusakabe *et al.*, 1988). More recently, elegant cell markers have been created by means of transgenic technologies which allow foreign marker genes to be inserted in the genomic DNA of specific strains. Identification of marked cells can be achieved by DNA-DNA in situ hybridisation.

The first DNA in-situ cell marker system was described by Rossant *et al.* (1983). Similar to strain specific antibody approaches, DNA satellite probes were used to detect cells derived from either *Mus musculus* or *Mus caroli* in *Mus musculus* ↔ *Mus caroli* chimaeras. This experiment was the first to use a DNA marker that could be detected on histological sections to allow the spatial distribution of cells to be analysed. Palmer and Burgoyne also used this approach, identifying cell lineage in their XX↔XY and sex-reversal chimaera experiments by hybridisation to Y

chromosome sequences (Burgoyne *et al.*, 1988; Palmer and Burgoyne, 1991a; 1991b).

The mouse strain 83 has been extensively used for cell lineage and chimaera experiments. Strain 83 was created by Lo in 1986 and contains 1,000 copies of the mouse β-major globin gene (TgN(Hbb-b1)83Lo) incorporated into a single site on chromosome 3 (Lo, 1986). The β-major globin transgene can be detected by DNA-DNA in-situ hybridisation and visualised using digoxygenin labelled probes (Lo, 1986; Lo *et al.*, 1987; Keighren and West; 1993). This cell marker fulfils most of the criteria required for a use in developmental lineage studies (Thomson and Solter, 1988b) that is, it is cell autonomous and is ubiquitously present in all tissues of the animal. Such ubiquitous presence of a large exogenous transgene might be expected to have a developmentally detrimental effect on rapidly dividing tissues due to the size of the insert. However, a recent study by Keighren and West (1996) has shown this cell marker to be developmentally neutral, at least in the hemizygous state. As presence of the transgene does not retard cell growth or division in a marked strain compared to an unmarked strain, this makes this a good cellular marker for use in chimaera experiments.

1.7. Experimental Aims

The aims of the studies reported in this thesis are to elucidate roles for the murine paired-box and homeobox containing gene *Pax6* during mouse fetal development, with particular reference to formation of the eyes, nasal tissues, brain and fronto-facial region. The mouse small eye mutant will be used to investigate the role of *Pax6* during fetal eye development by virtue of its well described genotype and phenotype. Although the small eye phenotype is known to be caused by mutations within the *Pax6* gene, the severity of the homozygous phenotype, that is, the complete absence of eye and nasal tissues makes it difficult to elucidate primary roles for *Pax6* during development of these tissues. However, the small eye mouse model can be used to analyse the developmental potential of cells unable to produce a functional *Pax6* product by incorporation with +/+ cells in fetal mouse aggregation chimaeras.

This thesis will be divided into two parts. Part 1 (chapters 2-4) will address results obtained from studies investigating roles for *Pax6* in eye and nasal development using two small eye alleles, Sey^{Neu} and *Sey*, to create $Sey^{Neu}/Sey \leftrightarrow +/+$ aggregation chimaeras. Aggregation chimaeras were produced to attempt to determine the developmental potential of cells unable to express functional *Pax6* and test if these cells were supported by wild type cells in an *in vivo* environment. The use of cell markers allows accurate Sey^{Neu}/Sey-cell contribution and spatial analysis *in vivo* to determine the potential of these cells during eye and nasal morphogenesis. *Pax6* and *Trp2* expression is examined by mRNA *in situ* hybridisation in mid-gestation $Sey^{Neu}/Sey \leftrightarrow +/+$ aggregation chimaeras to attempt to determine developmental the status of Sey^{Neu}/Sey cells during formation of the optic cup and to identify a role for *Pax6* in formation of the RPE.

Part 2 reports a preliminary study which attempts to identify effects of loss of *Pax6* on migration of a specific subset of neurons (the LHRH-neurons) in the brains of homozygous and heterozygous small eye fetuses (chapter 5). Finally, a study defining abnormal phenotypes in the small eye homozygous mutant fetus will be described (chapter 6). This study attempts to determine the effects both of allele type and genetic background on development of the small eye homozygous fetus by histological analysis of the small eye fronto-facial phenotypes.

PART ONE

Chapter 2

Analysis of E12.5 *Sey^{Neu}/Sey*↔+/+ chimaeras - Effects of *Pax6* in lens and nasal development

2.1. Introduction

Mouse embryos homozygous for the small eye (*Sey/Sey*) mutation die shortly after birth with severe cranio-frontofacial abnormalities, including a complete absence of the eyes and nasal tissues (Roberts, 1967; Hogan *et al.*, 1986; 1988). The small eye phenotype is caused by mutations within the *Pax6* gene (Hill *et al.*, 1991). Previous work has indicated that initial contact between the optic vesicle and surface ectoderm occurs in the small eye homozygous fetus, but that this contact is then lost, with subsequent degeneration of optic cup tissue (Hogan *et al.*, 1986; 1988; Fujiwara *et al.*, 1894; Grindley *et al.*, 1995). The initial stages of lens and nasal epithelium formation; that of differentiation of a placode region from surface ectoderm, appears to be absent in the homozygous mutant, although the primary defect which causes failure of the placode regions has not been identified to date.

As formation of a placode is the primary developmental step in both lens and nasal epithelium formation, it has been suggested that the causal defect resulting in loss of these tissues in the small eye homozygote fetus is one of placode formation rather than subsequent secondary tissue degeneration. This hypothesis is supported by the *Pax6* expression pattern as *Pax6* is seen to localise from a broad domain in the surface ectoderm of the head to be restricted to the developing placodes (Li *et al.*, 1994; Grindley *et al.*, 1995). As no eye or nasal tissue formation occurs in the homozygous *Sey/Sey* fetus and the development of the eye and nasal tissues in the *Sey/+* heterozygote is grossly normal, (albeit the eye is small and the lens opaque), neither

the *Sey/Sey* or *Sey/+* fetus provides much insight as to the primary role that *Pax6* plays during development of these very different and complex tissues.

In order to examine the role of *Pax6* in the development of the eye and nasal epithelium, [the tissues with overt phenotypes in the small eye homozygous *(Sey/Sey)* mutant], a strategy was needed to attempt to rescue *Pax6*-deficient cells by integrating them into a wild type environment. Although this can be achieved using tissue culture techniques, to examine the highly complex interactions necessary for complete tissue formation of the eye and nasal epithelium, it was necessary to allow normal tissue interactions to occur *in vivo*. This could be achieved by using aggregation chimaeras comprising a mixture of mutant and wild type cells.

To elucidate roles for *Pax6* in developmental processes using aggregation chimaeras, it is necessary firstly, to be able to establish the genotype combination of each chimaera, secondly, to be able to accurately determine the percentage contribution within the fetus of cells from each of the two embryos aggregated, and thirdly, to determine the spatial distribution of cells from of the two genotypes within chimaeric tissues. Several methodologies were utilised to fulfil these requirements and allow maximal analysis of the aggregation chimaeras produced in this study.

2.1.1. Identification of chimaeric fetuses

Easy identification of chimaeric fetuses was achieved at dissection as the parents used to produce mutant embryos for aggregation were pigmented. When these embryos were aggregated to +/+ embryos from an albino strain, chimaeras could be identified at dissection by the variegated pattern of pigmentation in the eye. This is a classic methodology for identification of mid-gestation chimaeric fetuses (e.g. Tarkowski, 1964; Muggleton-Harris *et al.*, 1987; Yoshiki *et al.*, 1991).

The polymorphic enzyme glucose phosphate isomerase (GPI) has been used in many previous chimaera experiments to identify percentage contribution in chimaeric fetuses (Chapman *et al.*, 1972; Gardner and Papaioannou, 1976; Gearhart *et al.*, 1981; Rashbass *et al.*, 1991; Keighren and West, 1993; Konyukhov *et al.*, 1994; James *et al.*, 1995; West *et al*, 1996). By using small eye and wild type strains differing at their *Gpi1* locus it was possible to accurately identify percentage chimaerism by cellulose acetate electrophoresis and scanning densitometry of the different GPI1 bands.

Finally, for the analysis of spatial distribution of cells derived from the heterozygous small eye parental cross, the *Sey* strain used in this study was homozygous for a β-globin transgenic cell marker which could be visualised on histological sections using DNA-DNA in-situ hybridisation (Lo, 1986; 1987; Keighren and West, 1993). Consequently, all mutant embryos were hemizygous for this transgene which was visualised as a single hybridisation signal in the cell nucleus. Using a nuclear cellular marker allowed accuracy of position to be specified at a single cell level. The same nuclear cell marker had been used with success in a number of previous chimaera experiments (Boland and Gosden, 1994; James *et al*; 1995; Everett and West, 1995; West *et al*; 1996).

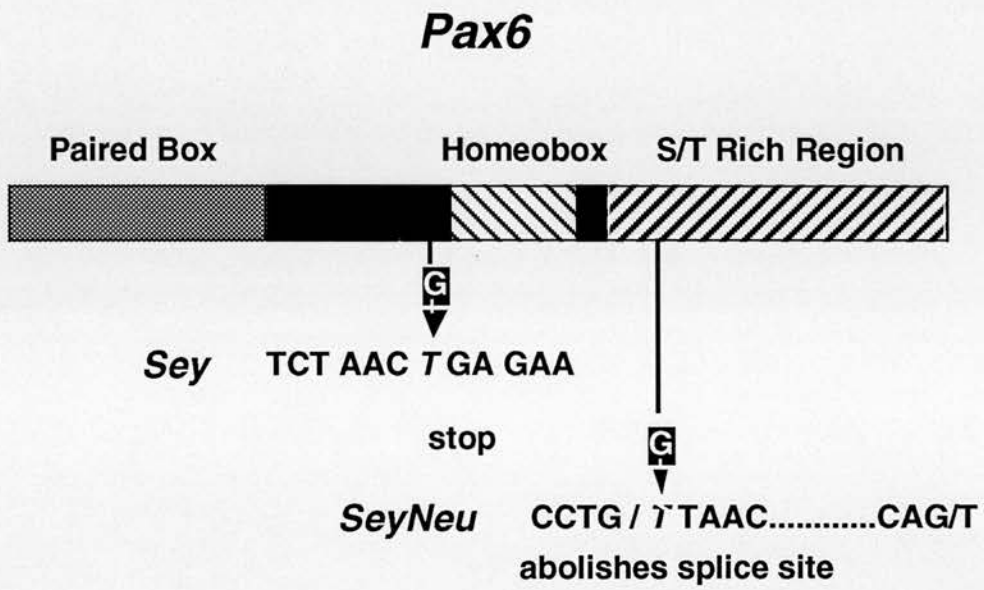

Figure 2.1. Diagram showing approximate position of single base-pair mutation sites within the mouse *Pax6* gene encoding the *Sey* and Sey^{Neu} mutations. The *Sey* mutation terminates translation prior to the homeobox region resulting in a truncated protein product. The Sey^{Neu} mutation abolishes a splice site resulting in an insertion of nonsense message sequence, which in turn contains a novel stop codon, truncating this mutant product within the serine/threonine-rich region. Both mutations result in a non-functional protein product.

2.1.2. Distinction of chimaeric genotypes

In order to be able to distinguish between chimaeras containing cells heterozygous or homozygous for small eye mutations; two alleles of small eye, *Sey* and Sey^{Neu} were utilised. Both alleles have been characterised and are genetically distinct at the genomic level (Hill *et al*; 1991) [see Figure 2.1.].

The production of Sey^{Neu}/Sey compound heterozygous embryos for aggregation is hampered by early post-natal lethality of small eye homozygous offspring. In order to overcome this, embryos were produced by crossing heterozygous $Sey^{Neu}/+$ female x *Sey/+* male parents and the genotype of the embryos diagnosed retrospectively by analysis of genomic DNA. This allows accurate identification of chimaeras containing compound heterozygous Sey^{Neu}/Sey cells which are unable to produce a functional *Pax6* product due to presence of both small eye mutations.

2.2. Mice

2.2.1. Testing for complementation between of *Sey* and Sey^{Neu} alleles

Although the *Sey/Sey* mutant has been extensively characterised (Roberts *et al.*, 1967; Clayton *et al.*, 1968, Hogan *et al.*, 1986; 1988; Grindley *et al.*, 1995; Kaufman *et al.*, 1995), the eye and nasal phenotypes of the Sey^{Neu}/Sey^{Neu} mutant has been less fully characterised and the Sey^{Neu}/Sey compound heterozygous fetus has not been examined. In order to determine if the *Sey* and Sey^{Neu} alleles were non-complementing, a number of $Sey^{Neu}/+$ x *Sey/+* timed matings were set up. Embryos were examined both at a macro- and micro-morphological level to compare the phenotypes of *Sey/Sey*, Sey^{Neu}/Sey^{Neu} homozygous fetuses and Sey^{Neu}/Sey

compound heterozygous fetuses. No eye or nasal tissue was present in any of the homozygous or compound heterozygous fetuses. All three genotypes exhibited gross external features of a domed appearance to the head, foreshortened upper jaw with protruding tongue and absence of eyes. Therefore, both the *Sey* and Sey^{Neu} mutations belong to the same complementation group and are non-complementing alleles of the *Pax6* locus.

2.2.2. Production of *Sey/+, Tg/Tg* (SEYTG) stock

To enable visualisation of the position of *Sey/+* x $Sey^{Neu}/+$ cells within the aggregation chimaeras, a *Sey/+* stock (SEYTG) carrying a β-globin transgene was created by inter-crossing stocks CBA/Ca-*Sey/+* and "TGB". The TGB stock was derived from transgenic strain 83 (Lo *et al*, 1986; 1987), which carries the reiterated TgN(Hbb-b1)83Clo β-globin transgene [abbreviated to *Tg*] (West *et al*; 1995). The TGB stock is homozygous for the transgene (*Tg/Tg)* and contains a mixed C57BL/Ola x CBA/Ca background (Keighren and West, 1994). Recent comparisons of *Tg/-* ↔ *-/-* and *-/-* ↔ *-/-* chimaeras showed that cells hemizygous for the transgene were not at a selective disadvantage (West *et al.*, 1996). This transgene is therefore viable as a ubiquitous, neutral cell marker for chimaera experiments.

The SEYTG stock was created and maintained at the Centre for Reproductive Biology, Edinburgh. First generation crosses between CBA/Ca-*Sey/+* and TGB parents were set up and *Sey/+* offspring identified by their micropthalmic phenotype. A blood smear was taken from the tail vein of each mouse at weaning for DNA-DNA in-situ hybridisation to the β-globin transgene (see Appendix III). Using this technique it is possible to identify animals carrying one (*Tg/-*) or two (*Tg/Tg*) copies of the β-globin transgene. Offspring were selected as both *Sey/+* and homozygous (*Tg/Tg*) for the β-globin transgene. Founder offspring were then random bred to TGB animals for four

generations prior to males being used as studs for chimaera experiments. The SEYTG stock was also selected to be homozygous for the glucose phosphate isomerase *Gpi1*^{b} allele.

2.2.3. The *Sey*^{Neu}/+ stock

Sey^{Neu}/+ animals originally donated by Dr J. Favor from a colony at the Institut fur Saugetiergenetik, Neuherberg, Germany, were crossed onto a CBA/Ca background and maintained at the Biomedical Research Facility at the Western General Hospital, Edinburgh. Females were selected at weaning for *Sey*^{Neu}/+ microphthlamic phenotype. Females were superovulated for chimaera production at 5-7 weeks of age. *Sey*^{Neu}/+ females were also homozygous for the glucose phosphate isomerase *Gpi1*^{b} allele.

2.2.4. *Sey*^{Neu}/+ x *Sey*/+ matings

To distinguish between the different classes of chimaeras, crosses between female *Sey*^{Neu}/+ and male *Sey*/+ mice were used. Both strains were pigmented *(C/C)* and homozygous for the glucose phosphate isomerase *Gpi1*^{b} allele. The *Sey*/+ males were homozygous *(Tg/Tg)* for the reiterated TgN(Hbb-b1)83Clo β-globin transgene (Lo 1986, Lo *et al.,* 1987; West *et al.,* 1995). All embryos obtained from this *Sey*^{Neu}/+ x *Sey*/+ cross were *Gpi-1*$^{b/b}$, heterozygous for the β-globin transgene (*Tg*/-) and pigmented (*C/C*) [see Appendix I].

Embryos from *Sey*^{Neu} x *Sey*/+ matings were aggregated to BALB/c/Eumm embryos which were unpigmented *(c/c)* and homozygous for the glucose phosphate isomerase *Gpi1*^{a} allele. These BALB/c embryos were always +/+ at the small eye locus and did

not carry the β-globin transgene. BALB/c females were purchased from the Department of Medical Microbiology at the University of Edinburgh.

Pseudo-pregnant female F_1 recipients (CF_1) were produced from crosses between C57BL-*Gpi1*^{c}/Ws females and BALB/c-*Gpi1*^{c}/Ws males. These females were homozygous for the *Gpi1*^{c} allele and albino (*c/c*). A summary of the genotypes of the mouse stocks used is shown in Table 2.1. (see also Appendix I).

Table 2.1.

Strain	**Genotype at *Pax6* locus**	**Genotype at *Gpi1* locus**	**Genotype at albino locus (*C*)**	**Copies of Transgene (*Tg*)**
SEYTG	*Sey/+*	*b/b*	*C/C*	*Tg/Tg*
CBA/Ca-*Sey*^{Neu}	*Sey*^{Neu}*/+*	*b/b*	*C/C*	*-/-*
BALB/c	*+/+*	*a/a*	*c/c*	*-/-*
CF_1	*+/+*	*c/c*	*c/c*	*-/-*

Table 2.1. Genotype of strains used for chimaera production showing copies of β-globin transgene and genotype at *Pax6*, *Gpi1* and albino loci.

2.3. Methods

2.3.1. Production of aggregation chimaera

Eight cell embryos were obtained from two crosses. CBA/Ca-*Sey*^{Neu}/+ (*Sey*^{Neu}/+, -/-, *Gpi1*$^{b/b}$) females were mated to SEYTG (*Sey*/+, *Tg*/*Tg*, *Gpi1*$^{b/b}$) males to produce embryos of four possible genotypes; *Sey*^{Neu}/*Sey*, *Sey*^{Neu}/+ , *Sey*/+ and +/+ embryos, all of which were homozygous for *Gpi1*^{b}, pigmented (*C*/*C*) and hemizygous for the β-globin transgene (*Tg*/-). BALB/c females were mated to BALB/c stud males to produce embryos homozygous for *Gpi1*^{a} , non-pigmented (*c*/*c*) and wild-type (+/+) at the small eye locus (see Table 2.2) [see Appendix VII]..

Embryos were aggregated, allowed to grow overnight before transfer to recipient CF_1 females (see Apendix VIII). At the designated date, the recipient mothers were killed by cervical dislocation and embryos dissected from the uterus. Conceptuses were carefully removed from the uterus for further dissection using a Wild dissecting microscope. A schematic representation of the entire experimental protocol can be seen in Figure 2.2.

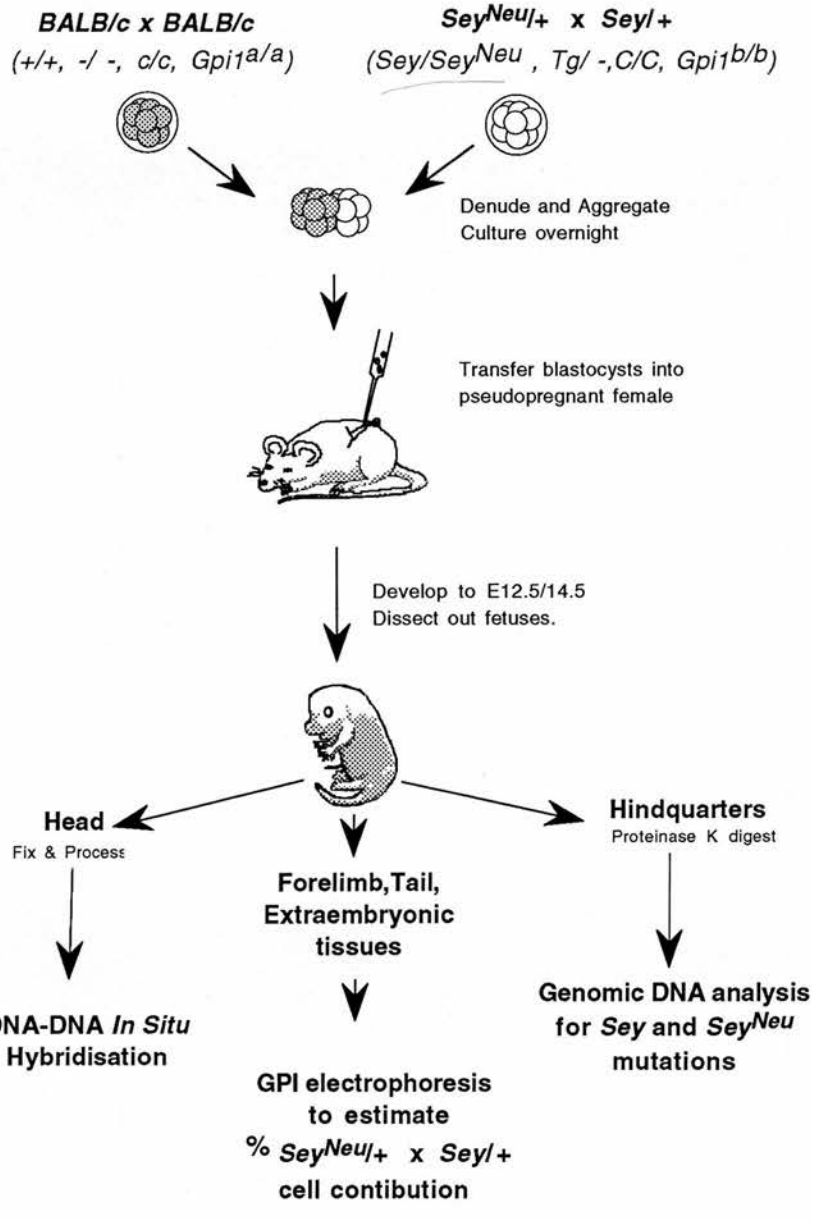

Figure 2.2. Schematic representation of the experimental design to investigate the role of *Pax6* in development of the mouse eye and nasal epithelium using aggregation chimaeras. Two small eye mutant alleles, *Sey* and Sey^{Neu}, are crossed to produce eight cell stage embryos that were pigmented (*C/C*), homozygous $Gpi1^{b/b}$ and hemizygous for the β-globin transgene (*Tg/-*), differing at the small eye locus (+/+, *Sey/+*, $Sey^{Neu}/+$ or Sey/Sey^{Neu}). These were aggregated to BALB/c strain embryos and cultured overnight to blastocyst before transfer into a recipient pseudopregnant CF_1 female. Embryos were allowed to develop in-utero to E12.5 or E14.5. Contribution from the $Sey^{Neu}/+$ x *Sey/+* derived embryo was quantified by DNA-DNA in situ hybridisation to the reiterated β-globin transgene and GPI1 electrophoresis of the tail, forelimb, amnion, whole yolk sac and placenta from each fetus.

Four possible genotypes of chimaeras were produced from the host and donor embryo aggregations. The possible genotypes for small eye, with GPI1 and transgene phenotypes were as follows:

Table 2.2.

Parental crosses:	**BALB/c x BALB/c**	↔	***Sey^{Neu}/+ x SEYTG***
Genotype	+/+	↔	+/+
			Sey/+
			Sey^{Neu}/+
			Sey^{Neu}/Sey
GPI1 phenotype	A	↔	B
Pigmented/albino	albino	↔	pigmented
Copies of transgene	-/-	↔	*Tg/-*

2.3.2. Fetal measurements and estimation of fetal age

Measurement of various fetal parameters were performed at dissection in order to assess age and stage of fetal development. The crown-rump length was measured using a calibrated eyepiece graticule and weight of the conceptus, fetus and placenta was recorded. A general description of the macromorphology of each fetus was also recorded, with particular reference to phenotype of the facial region.

Figure 2.3. (Following page) Photograph of a plate stained for visualisation of GPI1 bands after electrophoresis at 200 volts for 60 minutes. Lanes 1-3 show bands from embryos of genotypes *Gpi1^{a}/Gpi1^{a}* , *Gpi1^{b}/Gpi1^{b}* and a chimaeric embryo of genotype *Gpi1^{a}/Gpi1^{a}* ↔*Gpi1^{b}/Gpi1^{b}*. Lane 4 shows a placental sample from a *Gpi1^{a}/Gpi1^{a}* ↔*Gpi1^{b}/Gpi1^{b}* chimaeric embryo, the *Gpi1^{c}/Gpi1^{c}* band is from the maternal (CF_1) component of the placenta.

Figure 2.3.

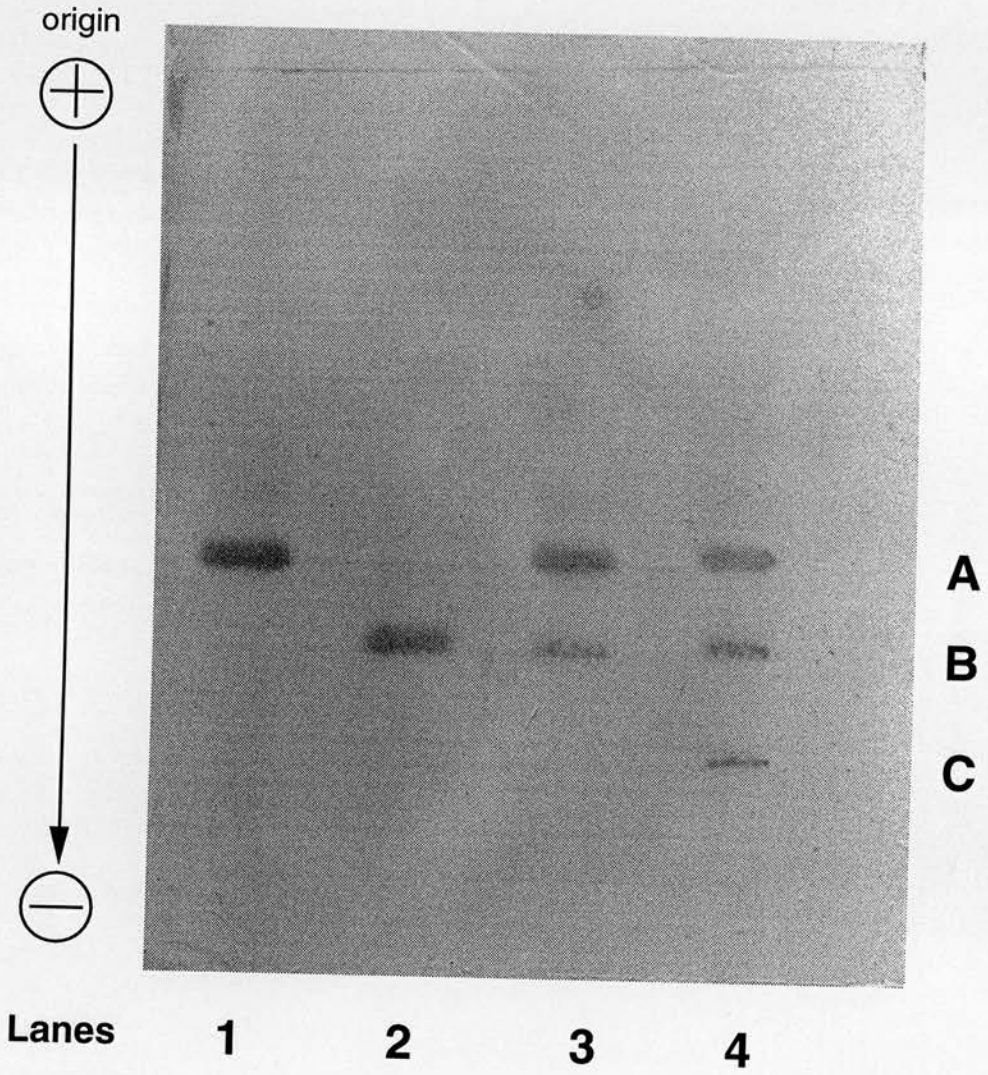

To determine approximate fetal age, the developmental stage of the left hind limb of each fetus was noted at dissection. It has been shown that the hind limb can give a relatively accurate, estimate of stage of fetal development. At mid gestation, the limbs are developing rapidly and can be staged to fetal age by their maturity (McLaren and Buehr, 1990; Palmer and Burgoyne, 1991).

2.3.3. Estimation of percentage eye pigment

At dissection, an estimation of the percentage of pigment in each eye of all embryos was recorded. By E12.5, production of pigmentation in the retinal pigment epithelium (RPE) is complete and provides a simple methodology for estimation of percentage chimaerism between pigmented and albino strain embryos. At E12.5, estimation of eye pigment can be used as an early marker for chimaerism in the RPE as formation of the choroid layer has not yet taken place. Later in gestation, development of the choroid masks non-pigmented patches in the RPE. Although eye pigment estimation is somewhat subjective, it can still be used as a quick and easy marker for both eye development and approximate percentage chimaerism in a fetus.

A more detailed 1-D histological analysis was also performed to more accurately estimate percentage eye pigment in those chimaeras subjected to detailed histological analysis. The protocol and results will be discussed in detail in Chapter 3.

2.3.4. Estimation of $Sey^{Neu}/+$ x $Sey/+$ cell contribution by GPI1 allozyme electrophoresis and scanning densitometry

GPI1 allozyme electrophoresis and scanning densitometry were used for easy and accurate assessment of percentage cell contribution from the different embryonic lineages in chimaeras. The left fore limb and tail, as well as amnion, yolk sac and placenta, were resected from each fetus at dissection and stored in a glycerol : water

50:50 solution for GPI electrophoresis and scanning densitometry (see Figure 2.3.) [see Appendix IX].

The proportion of the two cell populations in the chimaeric fetus was taken as the percentage of GPI1A and GPI1B allozymes on scanning. An average was taken from fetal left forelimb and tail samples which will be defined as the mean percentage (%) fetal GPI1B for each fetus. This percentage is the estimate of the contribution of cells derived from the *Sey*^{Neu}/+ x *Sey*/+ embryo. Previous experiments in our laboratory have shown that the GPI electrophoresis, staining and scanning densitometry methodologies used in this study are capable of detecting proportions of GPI1 dimers as low as 3% in a heterogenous tissue sample (Kelley, 1995).

The percentage contribution for placental samples, where maternal GPI1C bands were present, was taken as A/(A+B) or B/(A+B). Where heteropolymer was present, the percentage contribution was calculated as (A+$^1/_2$AB)/(A+AB+B) or (B+$^1/_2$AB)/(A+AB+B). As aggregated embryos were transferred into pseudopregnant CF_1 females homozygous for the *Gpi-1*^{c} allele, any possible maternal contamination of fetal samples would be identified by the presence of a GPI1C band. No maternal contamination was observed in any of the fetal samples scanned.

2.3.5. Genotyping of chimaeras

To identify the presence of the *Sey* and *Sey*^{Neu} mutations, genomic DNA was isolated from the trunk region of each fetus and segments of the *Pax6* gene were amplified using PCR for subsequent restriction enzyme digest analysis. A negative control containing no DNA template was included in each PCR run, for each set of primers to identify any exogenous contamination. After cycling, fragments were visualised on 1.2% agarose gel containing ethidium bromide and photographed on viewing under UV light (see Figure 2.4a).

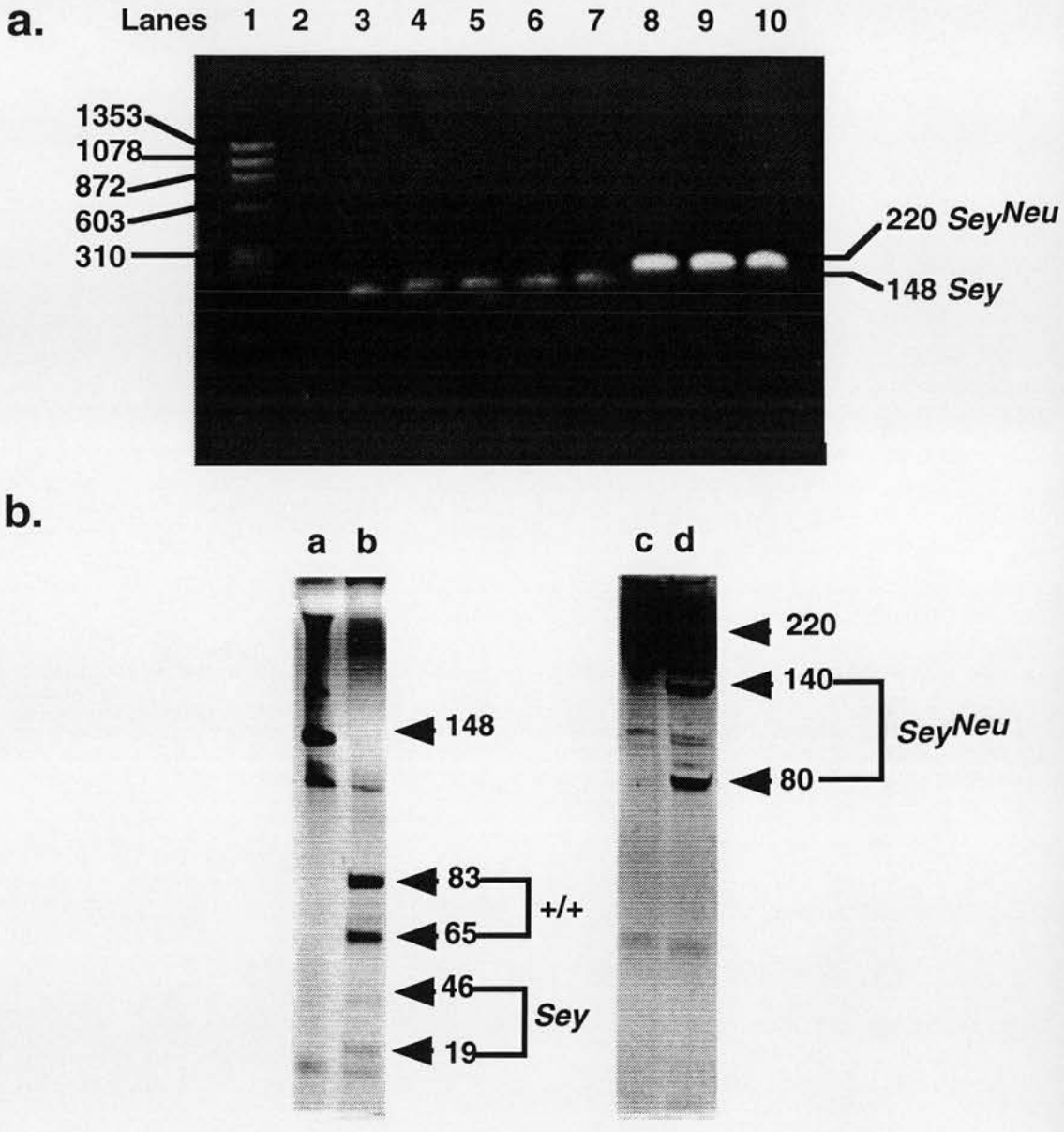

Figure 2.4.a) 1.2% agarose gel showing 220 and 148bp PCR products for identification of *Sey* and *Sey*^{Neu} mutations. Lane 1, size markers; lane 2, no template control; lanes 3-7, G459 + B509 148bp *Sey* fragment; lanes 7-10, Hax5 + G15 220bp *Sey*^{Neu} fragment. **b)** 15% bis:polyacrylamide 1:19 gel silverstained to show restriction frgament lengths for DdeI restriction enzyme digest for presence of *Sey* mutation and HindII restriction enzyme digest for presence of *Sey*^{Neu} mutation. DdeI digests shows 83 and 65bp bands present in wildtype sequence and 46 and 19bp bands indicating presence of *Sey* mutation. HindII digest shows uncut wild-type 220bp band and mutant 140 and 80bp bands indictaing presence of *Sey*^{Neu} mutation. a, uncut G459 + B509 fragment, b, G459 + B509 fragment cut with DdeI, c, Hax5 + G15 uncut fragment, Hax5 + G15 fragment cut with HindII.

Restriction digest analysis for the *Sey*^{Neu} mutation was carried out by digestion with HindII, and for the *Sey* mutation with DdeI (see Appendix X). Digested and undigested control samples for each fetus were loaded onto a 15% polyacrylamide gel and visualised after electrophoresis by silver staining of polyacrylamide gels (see Appendix XI). After staining, gels were transferred to distilled water and photographed immediately.

Presence of the *Sey* allele was identified as digestion of a 148bp PCR fragment into four fragments of 83, 65, 46 and 19 base pairs in length, the 83 and 65bp fragments being always present for both *Sey* and wild type sequence. The 46bp fragment from the *Sey* DdeI digest was found to be highly labile and could often only be seen as an area of differential staining on immediate viewing of the gels after staining, the subtlety of which was often lost on photography. Therefore, the 19bp fragment only (or with the 46bp fragment where visible) was used primarily as the diagnostic marker for presence of the *Sey* mutation. The *Sey*^{Neu} mutation was visualised as the presence of two bands of 140 and 80 base pairs in length, these digestion products being only present in the mutant sequence, in the wild-type sequence the 220 base pair PCR fragment remained undigested (see Figure 2.4b).

Figure 2.5. (Following page) Polyacrylamide gels silver stained for visualisation of 'nested' PCR restriction fragment lengths after restriction enzyme digest for presence of **a**) *Sey*^{Neu} and **b**) *Sey* mutations in genomic DNA samples from *Sey*^{Neu}*/Sey* ↔+/+ chimaeras. A gradation of intensity of staining of *Sey*^{Neu} 140bp and 80bp diagnostic fragments and *Sey* 19bp diagnostic fragments can be observed in proportion to the percentage of mutant sequence present as expected from percentage mean fetal GPI1B. Lanes a) *Sey* fragments, uncut. b) cut with DdeI. Lanes c) *Sey*^{Neu} fragments, uncut, d) cut with HindII. *JC46 is *Sey*^{Neu}/+↔+/+ genotype and so has no *Sey* band in (b).Other chimaera smaples are all *Sey*^{Neu}*/Sey* ↔+/+.

Figure 2.5.

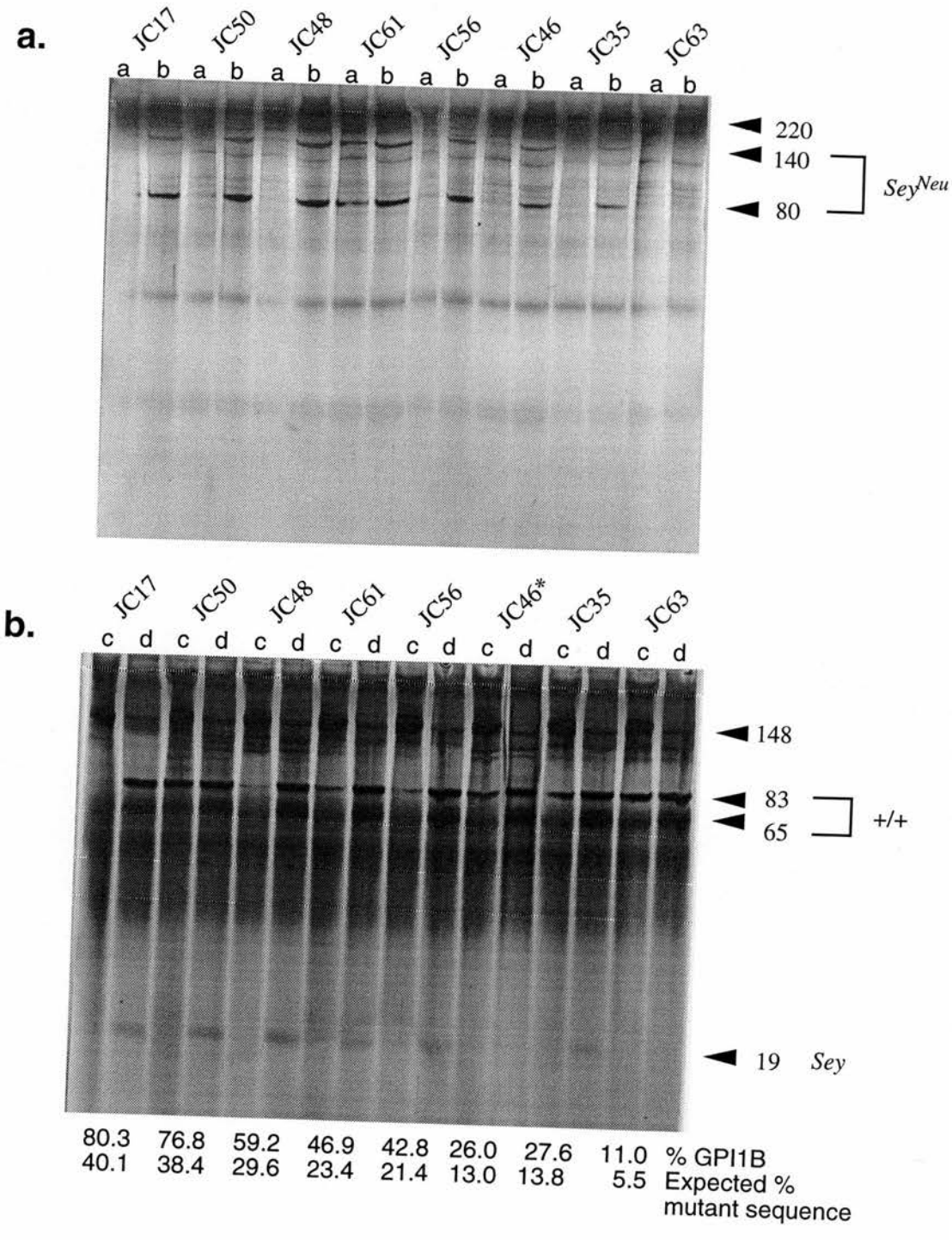
a.
JC17
JC50
JC48
JC61
JC56
JC46
JC35
JC63
a b a b a b a b a b a b a b a b
220
140
80
Sey^Neu
b.
JC17
JC50
JC48
JC61
JC56
JC46*
JC35
JC63
c d c d c d c d c d c d c d c d
148
83
65
+/+
19 Sey
80.3 76.8 59.2 46.9 42.8 26.0 27.6 11.0 % GPI1B
40.1 38.4 29.6 23.4 21.4 13.0 13.8 5.5 Expected % mutant sequence

In order to evaluate the efficiency of detection for low levels of mutant sequence, a second 'nested' PCR reaction was devised. This strategy reduced the level of non-specific background sequence detected using the original sets of PCR primers, *G459* and *MC130*, *G15* and *Hax5* for the *Sey* and Sey^{Neu} fragments respectively (see Appendix X). First round primers were used that lay outside the original PCR primers but still within the *Pax6* coding region. PCR products were visualised on 1.2% agarose gels, digested and subjected to polyacrylamide gel electrophoresis and silver staining as described previously.

Using this second 'nested' protocol, it was possible to show that as little as 5% mutant sequence could be detected using the original PCR protocol. Although PCR methodology was not used in a quantitative fashion for the purposes of this experiment, staining intensity of mutant allele bands was seen to be broadly in proportion to the percentage contribution of mutant sequence as predicted by GPI1 electrophoresis and scanning densitometry (see Figure 2.5.).

2.3.6. DNA-DNA in-situ hybridisation for visualisation of the β-globin transgenic cell marker

The head of each fetus was resected at dissection and fixed in 3:1 ethanol : acetic acid for 6 hours and then transferred to 70% ethanol for storage until processing. Samples were then automatically processed to paraffin wax blocks and sectioned in the transverse plane at 7μm onto TESPA (3-aminopropyltriethoxysilane, Sigma) coated slides. Slides were baked at 37°C overnight before being subjected to DNA-DNA in-situ hybridisation for visualisation of the β-globin transgenic cell marker according to the protocol of Keighren and West (1993), [see Appendix III].

In each *in-situ* run, sections from *Tg/-* and *-/-* fetuses were included as positive and negative controls respectively. Control slides were used to check efficacy of the *in-situ* run and estimate levels of non-specific background hybridisation.

2.3.7. Analysis of tissue sections after *in-situ* hybridisation to the β-globin transgenic cell marker

After DNA-DNA *in-situ* hybridisation, the percentage of $Sey^{Neu}/+$ x *Sey/+* cells (i.e. those cells positive for the transgenic cell marker) was estimated in tissues from each chimaera by counting numbers of nuclei verses numbers of hybridisation signals under phase contrast light microscopy. The composition of primitive ectoderm-derivatives, (including the entire fetus), tend to be similar within a chimaera (McLaren, 1976). Therefore, unless the presence of mutant cells affects the composition of a specific tissue, the hybridisation index should be positively correlated to the estimate of % GPI1B in the fetal tissues. Both are estimates of the $(Sey^{Neu}/+ \; x \; Sey/+)$ cell contribution to the chimaera, as designated by GPI1 electrophoresis and scanning densitometry.

The contribution of $Sey^{Neu}/+$ x *Sey/+* derived cells from each tissue was estimated from counts taken of Tg+ve nuclei from three widely spaced sections. In the case of the eye, these were the mid-section and the two sections half way between the mid-section and the last dorsal or ventral section. The hybridisation indices for head and brain tissues were estimated from three widely spaced sections from within the whole head region.

An eyepiece grid was used and a standard sampling protocol designed for each individual tissue. 150-1000 cells were classified, dependent on the size of the tissue examined. Every cell of the lens, retinal pigment epithelium (RPE) and surface

ectoderm, both general and overlying the eye, was classified on a single section. For morphologically normal RPE, where an identifiable single cuboidal layer of cells was present, cells were identified as pigmented and/or positive for the transgene signal.

A set grid sampling method using an eyepiece grid was used for tissues covering larger areas; for example, the nasal epithelium, mesenchyme of the head, inner layer of the optic cup, optic stalk and hindbrain. In the case of the head mesenchyme, hindbrain and nasal epithelium, alternate grid sections were classified from three randomly sampled areas on each of the three sections examined. For the optic cup, the whole area of this tissue was classified on each section examined with counts taken from alternate grid segments. Tissues where the cells were densely packed, for example the nasal epithelium and the inner layer of the optic cup, where individual cells might not be identified with their signal were classified as the total number of cells and the total number of hybridisation signals within the given counting area.

The primary counts for hybridisation signal-positive cells (Tg+ve) per total cell number in a given tissue were corrected to allow for the failure to detect a hybridisation signal in a proportion of $Sey^{Neu}/+$ x *Sey/+* cells due to sectioning artefact. Tissue specific correction factors were derived by performing the tissue specific counting protocols on two E12.5 embryos known to be hemizygous for the β-globin transgene *(Tg/-)*. Original counting results were adjusted using tissue specific correction factors with the corrected value for each individual tissue designated as the 'hybridisation index' for that tissue. Tissue specific correction factors were as follows: nasal epithelium, 105.5%; lens, 83.3%; inner and outer layer of the optic cup, 84.5%; surface ectoderm overlying the eye; 64.5%, general head ectoderm, 56.8%; hindbrain, 89.1%; head mesoderm, 88.5%; hindbrain, 89.1%.

Most tissue specific correction factors were below 100% as sectioning artefact means that a proportion of nuclei within a given tissue section will fail to include a hybridisation signal. However, in densely packed tissues, such as the nasal epithelium, this correction factor was over 100%. This is due to a loss of definition of individual nuclei due to dense cell packing. Also, the final corrected cell hybridisation index for densely packed tissues may exceed 100% if the percentage of cells positive for the transgene in a given tissue was close to 100% in the original count and the correction factor overcompensates for this.

Table 2.3. (Following page) Estimation of lens size by Chalkey Grid measurement for E12.5 fetal *Sey*^{Neu}*/Sey* ↔+/+ aggregation chimaeras. Using Spearman's Rank Correlation test, the mean % fetal GPI1B is positively correlated to degree of morphological abnormality in the optic cup (r_S= 0.933; P = 0.0001) and lens and nasal epithelia size were also positively correlated (r_S= 0.736; P = 0.0008). Lens size was negatively correlated to mean % fetal GPI1B (r_S= -0.789; P = 0.0004).

[a] %GPI1B is the mean %GPI1B from a tail and forelimb sample from each fetus.

[b] Area was estimated by using a modified Chalkley Grid, as described in section 1.12 (see also Figure 2.13. for plotted data.)

[c] +; normal morphology with normal outer RPE layer and inner layer of neural retina. ++; slightly abnormal, small areas of ectopic growth in the outer layer. +++; more abnormal tissue but double-layer structure of optic cup maintained. ++++; abnormal distortion of double layer structure with lens still present. +++++; grossly abnormal convoluted structure with loss of double layer integrity, lens absent.

Table 2.3.

Chimaera	Side	%GPI1B in fetus[a]	Area in section ($\mu m^2 \times 10^4$)[b]		Optic cup[c] dysmorphology
			lens	nasal epithelium	
JC63	left	11.0	4.5	14.7	+
JC63	right	11.0	5.7	15.9	+
JC35	left	27.5	5.5	9.8	+
JC35	right	27.5	4.7	13.5	+
JC56	left	42.8	3.9	7.4	+++
JC56	right	42.8	5.7	11.0	+
JC61	left	46.9	2.1	1.2	++
JC61	right	46.9	6.1	2.5	++++
JC48	left	59.2	2.6	4.9	+++++
JC48	right	59.2	0	2.5	+++++
JC50	left	76.8	0	0	+++++
JC50	right	76.8	0	0	+++++
JC17	left	80.3	0	2.5	+++++
JC17	right	80.3	0	0	+++++

2.3.8. Morphological grading of eye abnormality

The eyes of all *Sey*^{Neu}/*Sey*↔+/+ chimaeras were graded according to the severity of morphological abnormality observed (see Table 2.3.). The lowest grade (+) defined a normal eye with normal size and maturity of lens development with both inner and outer layers of the optic cup showing no abnormality. Grades (++) and (+++) indicate increasing levels of morphological abnormality with ectopic areas of optic cup tissue observed whilst overall maintenance of the bi-layered optic cup structure and presence of a morphologically normal lens was preserved. Grade (++++) shows the highest level of optic cup abnormality whilst still maintaining lens development. Eyes of this grade showed severe distortion of the bi-layered optic cup structure. The highest grade (+++++) indicates a loss of integrity of the bi-layered optic cup structure with overgrowth of optic cup tissue and no identifiable lens formation (see Table 2.1. for results).

2.3.9. Analysis of lens and nasal epithelial tissue size

The size of the lens or nasal epithelium was estimated using a modified 20 point Chalkley grid (Graticules Ltd., Kent). The area of tissue was estimated in a single section on which the tissue area was deemed to be maximal. In the case of the lens, this section was taken as the mid-section of the tissue by counting the number of section and selecting the median. Four individual readings were taken using the Chalkley grid, rotating the grid 90^{o} in the field of vision before each new reading was taken. All readings were taken at x10 magnification using a Leica Diaplan light microscope. The mean number of spots falling within a given tissue area was converted to an area (μm^2) by multiplication of single spot area derived from the total area of the Chalkley grid at x10 magnification (Curtis; 1960) [see Table 2.3. for results].

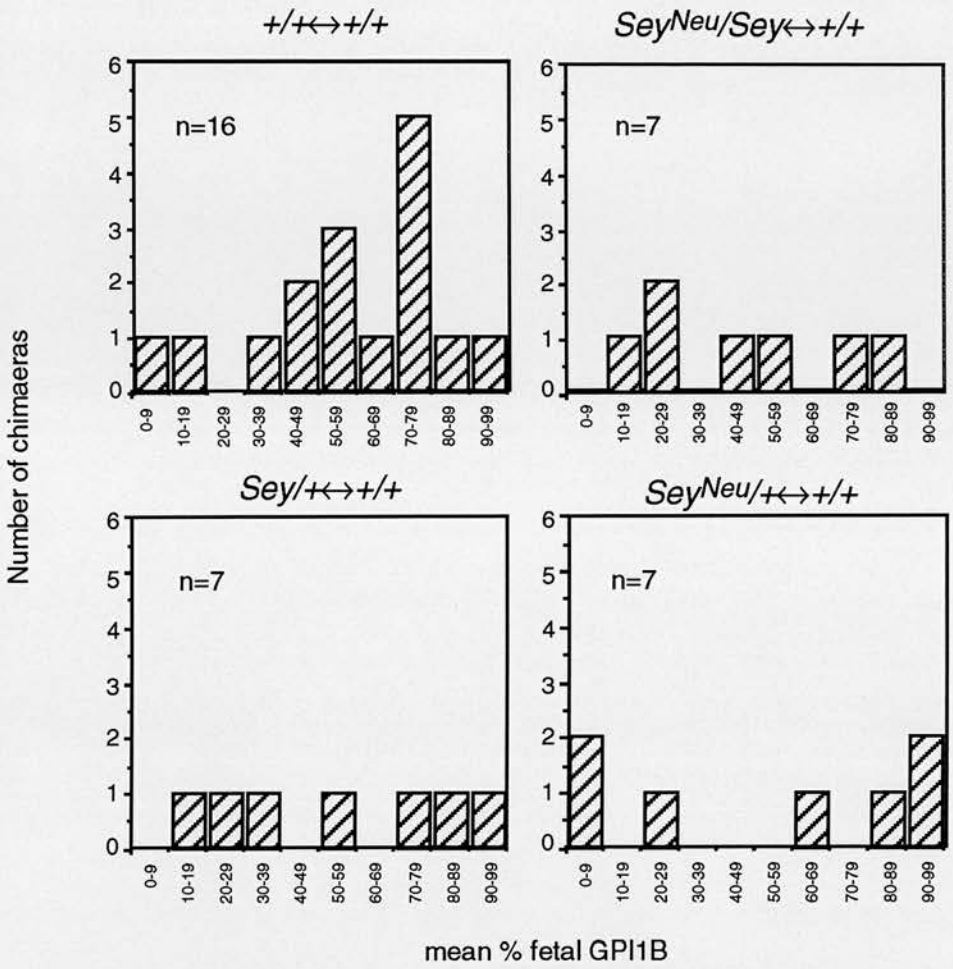

Figure 2.6. Histograms showing percentage of *Sey*/+ x *Sey*^{Neu}/+ cells for each of the chimaera groups examined estimated as the mean percentage fetal GPI1B. Fetal GPI1B was calculated as the mean the left forelimb and tail for each fetus. +/+↔+/+ histograms show that 11 of 16 fetuses produced have a mean percentage fetal GPI1B of greater than 50%.

2.4. Results - Analysis of E12.5 chimaeric fetuses

2.4.1. GPI1 analysis

The composition of any series of chimaeras tends not to follow a normal distibution. In "unbalanced" strain chimaeras (Mullen and Whitten, 1972) one genotype predominates. Even in more balanced strain combinations the distribution tends to be flat with significant numbers of individuals of a single genotype (Falconer and Avery, 1978). In this respect, BALB/c embryos tend to make a poor contribution to chimaeric fetuses (Mullen and Whitten, 1972, West *et al.*, 1975). Selection of BALB/c embryos as the donor strain in this study was deliberate to ensure that *Sey*^{Neu}*/Sey* cells were at a maximum advantage to contribute to chimaeric fetuses without negative selective pressure from a donor embryo of vigorous genotype.

A total of 65 fetuses were dissected at E12.5. Of these 65 fetuses, 37 were identified as chimaeras by GPI1 allozyme electrophoresis. These 37 chimaeric fetuses were identified as being of the following genotypes: 7 Sey^{Neu}*/Sey*↔+/+; 7 Sey^{Neu}/+↔+/+; 7+/*Sey*↔+/+ and 16+/+↔+/+ chimaeras. Despite appearances, this 7:7:7:16 ratio was not statistically significantly different from the expected 1:1:1:1 ratio (χ^2=6.57; P=0.05).

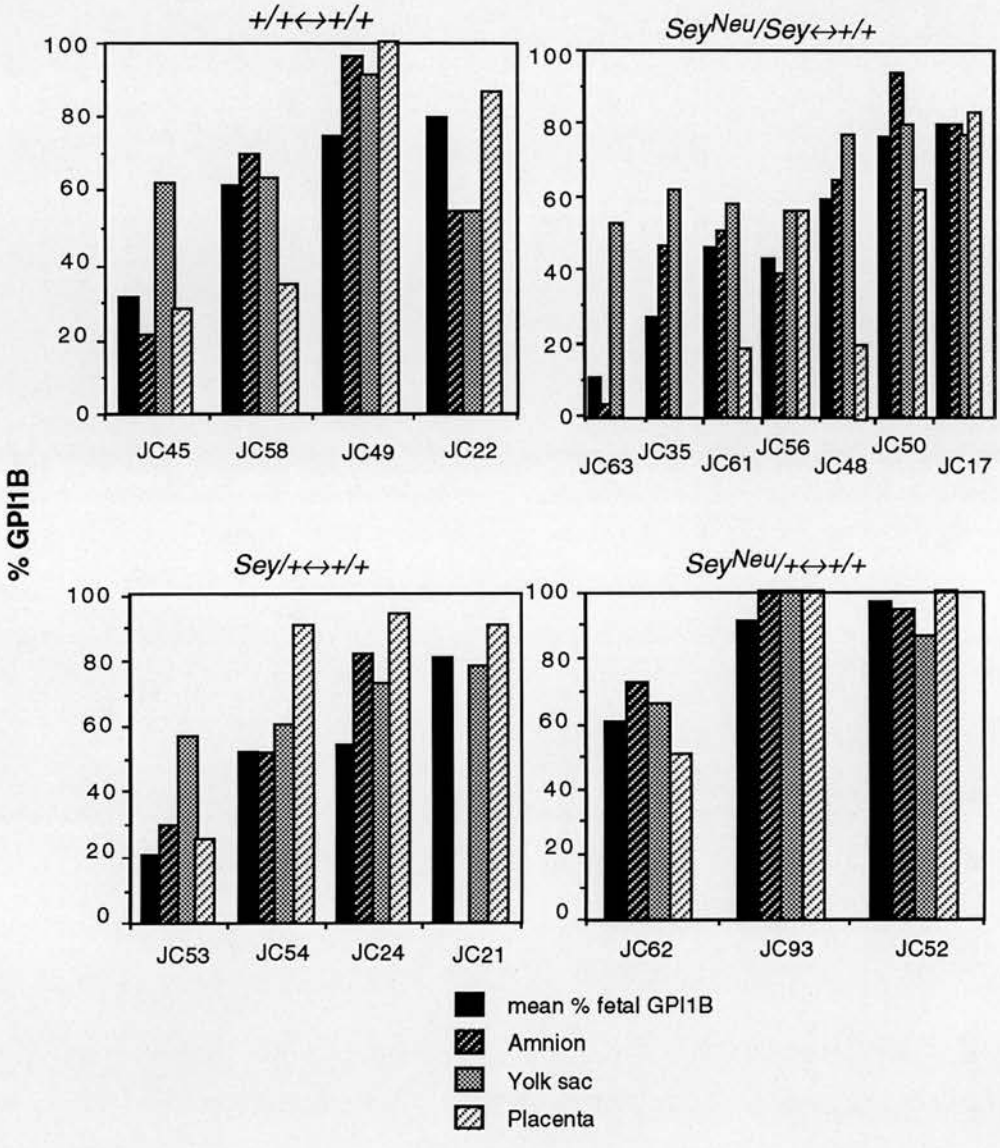

Figure 2.7. Histograms showing % fetal GPI1B for all tissues from the 16 chimaeras examined from the four genotype groups. The percentage mean fetal GPI1B was calculated as the mean of the left forelimb and tail samples. Results for all other tissues are derived from scanning of a single sample. No amnion sample was available from chimaera JC21.

The chimaeras produced in this study show the BALB/c genotype making a relatively poor contribution to chimaeric fetuses, best demonstrated in the +/+↔+/+ group where 11 of the 16 chimaeric fetuses produced were of 50% or above GPI1B i.e. cells from the *Sey*^{Neu}/+ x *Sey*/+ parental cross (see Figure 2.6.). However, the numbers in the heterozygous *Sey*/+↔+/+, *Sey*^{Neu}/+↔+/+ and *Sey*^{Neu}/*Sey*↔+/+ are too small to allow full statistical comparison.

Figure 2.7 shows that the fetus and various extraembryonic memebranes tested (amnion, yolk sac and placenta) were mixtures of GPI1A and GPI1B in most of the chimaeras studied. Presence of the GPI1B allozyme indicates a contribution from the (*Sey*^{Neu}/+ x *Sey*/+) embryo. The results for the *Sey*^{Neu}/*Sey*↔+/+ chimaeras shows that *Sey*^{Neu}/*Sey* cells are able to make significant contributions to the amnion, yolk sac and placenta as well as the fetus.

Although GPI1 allozyme electrophoresis confirmed all of the 37 embryos as chimaeric, embryos retrospectively genotyped as *Sey*^{Neu}/*Sey*↔+/+ did not exhibit eye pigment (see Figure 2.8.). On further investigation, absence of pigment in this genotype group was not attributable to retarded development of these fetuses. Statistical analysis of fetal weight and crown rump length, and fetal developmental stage by as determined by hindlimb morphology, revealed no significant difference between the genotype groups.

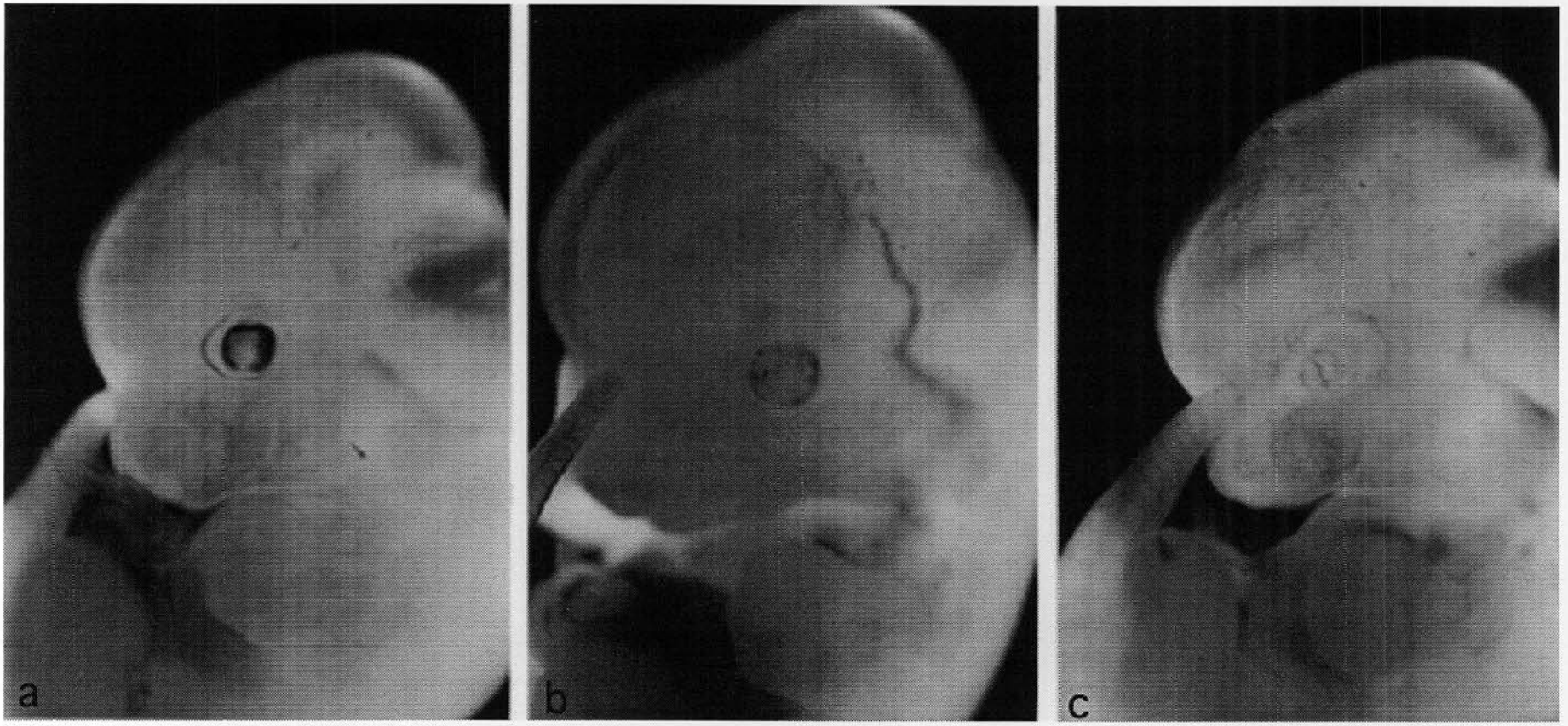

+/+ ↔ +/+
70.2 % GPI1B

+/+ ↔+/+
48.8 % GPI1B

Sey/Neu *Sey*↔+/+
72.8 % GPI1B

Figure 2.8. E12.5 chimaeras and mean % fetal GPI1B as determined by scanning densitometry. Note variegated pattern of eye pigmentation in +/+ ↔+/+ chimaeras a) and b) whilst *Sey*^{Neu}/*Sey* ↔+/+ chimaera c) posesses no eye pigmentation comparable to the high proportion of *Sey*/+ x *Sey*^{Neu}/+ cells present in this chimaera by % GPI1B.

Chimaeras in the *Sey*/+↔+/+, *Sey*^{Neu}/+↔+/+ and +/+↔+/+ genotype groups exhibited variegated patterns of non-pigmented and pigmented cells in the RPE. The percentage of pigmented cells in the RPE of these fetuses was positively correlated to percentage *Sey*^{Neu}/+ x *Sey*/+ cell contribution by GPI1 electrophoresis using Kendall's rank correlation test in those chimaeras sectioned and analysed (left eye pigment; τ= 0.8545, P=0.0003, right eye pigment; τ= 0.8182, P=0.0005), [see Chapter 3 for full method, data and discussion].

2.4.2. Eye morphology of *Sey*^{Neu}*/Sey*↔+/+ chimaeras

On dissection, the external morphology of the eyes of all chimaeras was examined for any overt morphological abnormalities. *Sey*^{Neu}*/Sey*↔+/+ chimaeras revealed no striking abnormalities in those chimaeras with a mean fetal % GPI1B of less than 50% (JC63, mean fetal GPI1B 11.0%; JC35, mean fetal GPI1B 27.5%; JC56, mean fetal GPI1B 42.8% and JC61, mean fetal GPI1B 46.9%). The only anomaly observed in this group after retrospective GPI analysis and genotyping was the lack of eye pigmentation (see Figure 2.8.).

Sey^{Neu}*/Sey*↔+/+ chimaeras with a mean fetal % GPI1B of greater than 50% (JC48, mean fetal GPI1B 59.2%; JC50, mean fetal GPI1B 76.8% and JC17; mean fetal GPI1B 80.3%) exhibited macromorphological abnormalities of the eye, where externally an eye could be identified. Chimaera JC48 showed gross extension of the presumptive corneal surface of the right eye, well beyond the normal margin of the head, with convoluted retinal structures visible through the semi-opaque covering (see Figure 2.9.). The left eye of this chimaera appeared normal in size with no observable external abnormalities (detailed histological analysis will be described in section 2.4.3.) Those chimaeras with the highest mean fetal % GPI1B, JC50 and JC17,

exhibited eye anomalies identical to those observed in the *Sey*^{Neu}*/Sey* compound heterozygote fetus. These fetuses were anophthalmic with no externally visible eye development although lid structures were identifiable.

Similarly, the facial region of those *Sey*^{Neu}*/Sey* ↔+/+ chimaeras with a low *Sey*^{Neu}*/Sey* cell contribution revealed no striking abnormalities, the fronto-facial region of these chimaeras appearing to be normal in size and development. In chimaeras JC50 and JC17, the fronto-facial region resembled that of the *Sey*^{Neu}*/Sey* compound heterozygote with abnormally foreshortened upper jaw, protruding tongue and domed head. No abnormalities of the caudal head region, limbs or trunk was observed in the *Sey*^{Neu}*/Sey* ↔+/+ fetuses. No craniofacial abnormalities were noted in chimaeras of the other genotype groups.

2.4.3. General histological analysis of *Sey*^{Neu}*/Sey*↔+/+ chimaeras

A detailed histological analysis was undertaken of four +/+ ↔+/+, four *Sey*/+ ↔+/+, three *Sey*^{Neu}/+ ↔+/+ and seven *Sey*^{Neu}*/Sey*↔+/+ chimaeras. Histological analysis revealed striking morphological abnormalities in the *Sey*^{Neu}*/Sey*↔+/+ group, with no abnormalities evident in the other genotype groups.

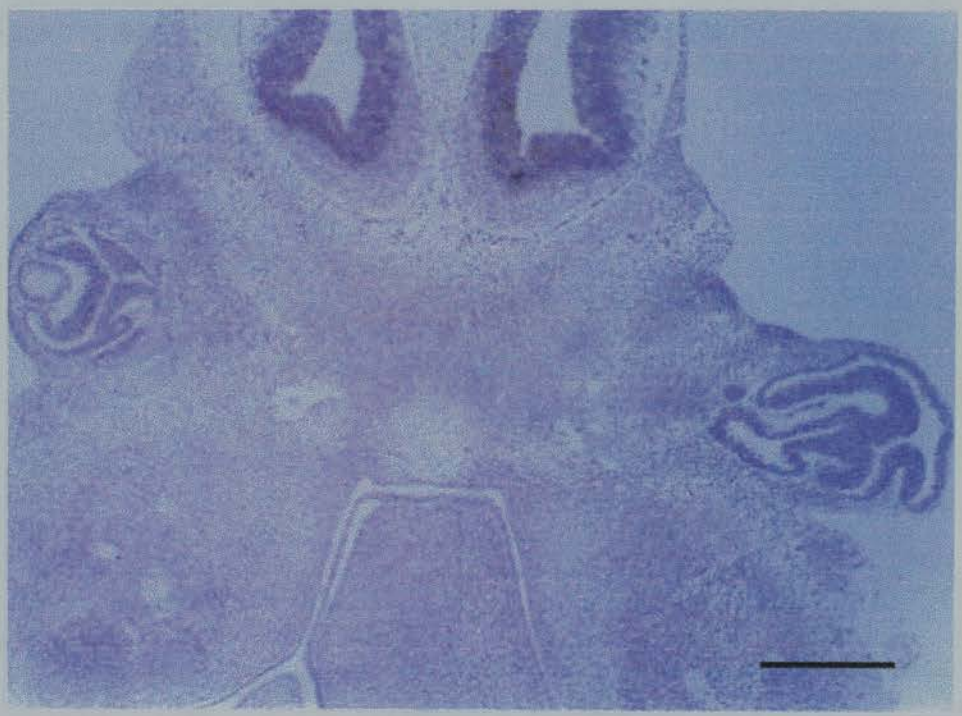

Figure 2.9. (Following page) Low power photograph of a transverse histological section through the head of *Sey*^{Neu}*/Sey* ↔+/+ chimaera JC48. The right eye has no lens whereas a small lens is observed in the left eye. (Scale bar - 500μm).

Figure 2.10. (Following page) **a)** Histological section of the left eye of +/+ ↔+/+ chimaera JC49 with a contribution of 75% *Sey*^{Neu}/+ x *Sey*/+ derived (Tg+ve) cells. Patches of albino and pigmented cells are observed in the retinal pigment epithelium and strong contribution of Tg+ve cells can be seen in the lens, inner layer of the optic cup and the surrounding mesenchyme of the head. The transgene signal is visulaised as small dark dots in the cell nucleus. **b)** Histological section of the left eye of *Sey*^{Neu}/*Sey* ↔+/+ chimaera JC48. There is complete absence of *Sey*^{Neu}/+ x *Sey*/+ derived (Tg+ve) cells in the lens and areas of the optic cup. The optic cup shows areas of ectopic growth in the outer layer. (L) lens, (IL) inner layer of the optic cup, (OL) outer layer of the optic cup, (HP) hyaloid plexus, (M) mesenchyme.
[In 2.10a) (OL) = retinal pigment epithelium]. (Scale bar - 200μm).

Figure 2.11. (Following page but one) **a)** Histological section through the head of +/+ ↔+/+ chimaera JC49 showing strong presence of *Sey*^{Neu}/+ x *Sey*/+ derived (Tg+ve) cells in both the nasal epithelium and surrounding mesenchyme.
b) Histological section through the head of *Sey*^{Neu}/*Sey*↔+/+ chimaera JC61 showing presence of *Sey*^{Neu}/+ x *Sey*/+ derived (Tg+ve) cells in the mesenchyme but complete absence of these cells in the nasal epithelium. (NE) nasal epithelium, (M) mesenchyme of the head. (Scale bar - 80μm).

Figure 2.10.

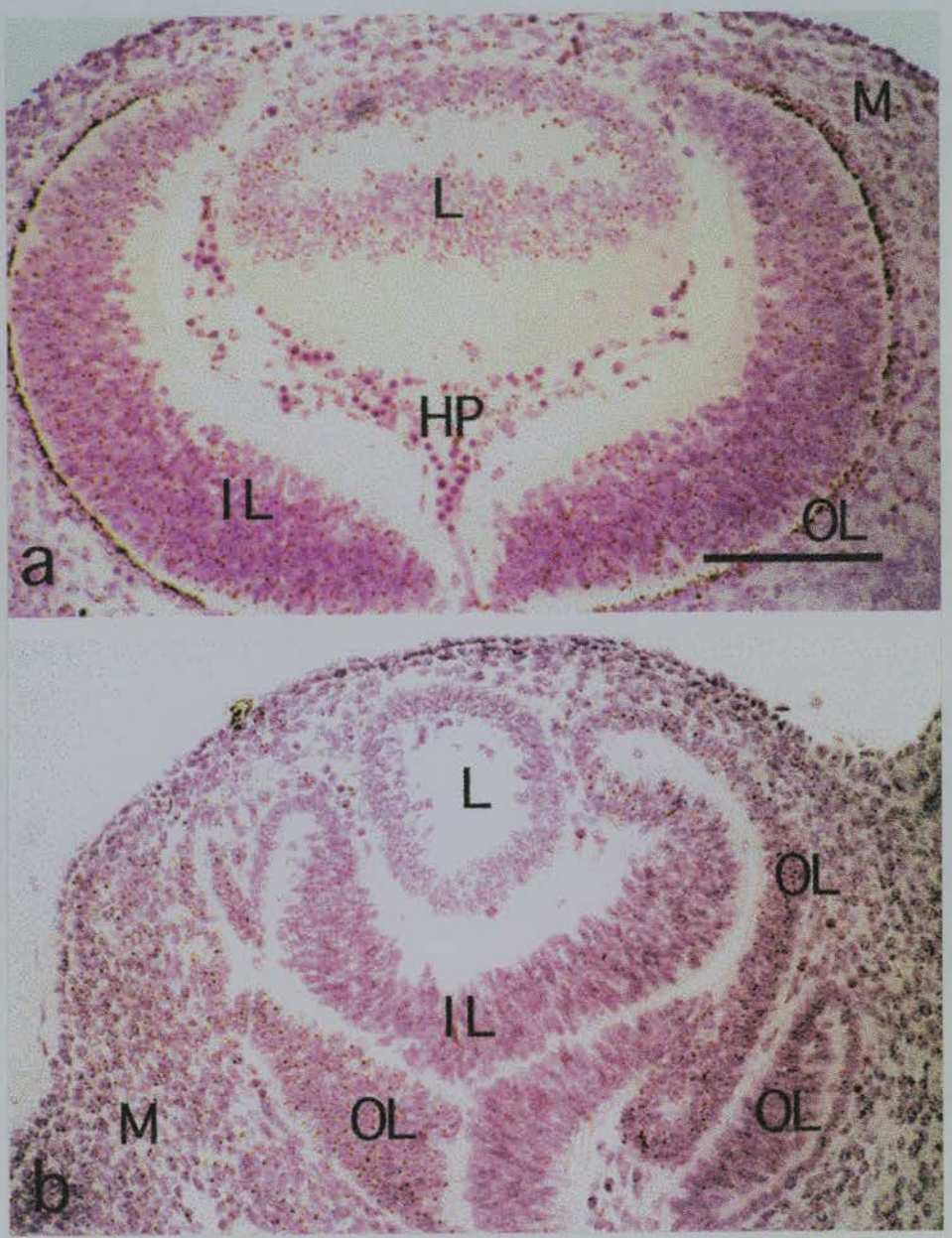

Figure 2.11.

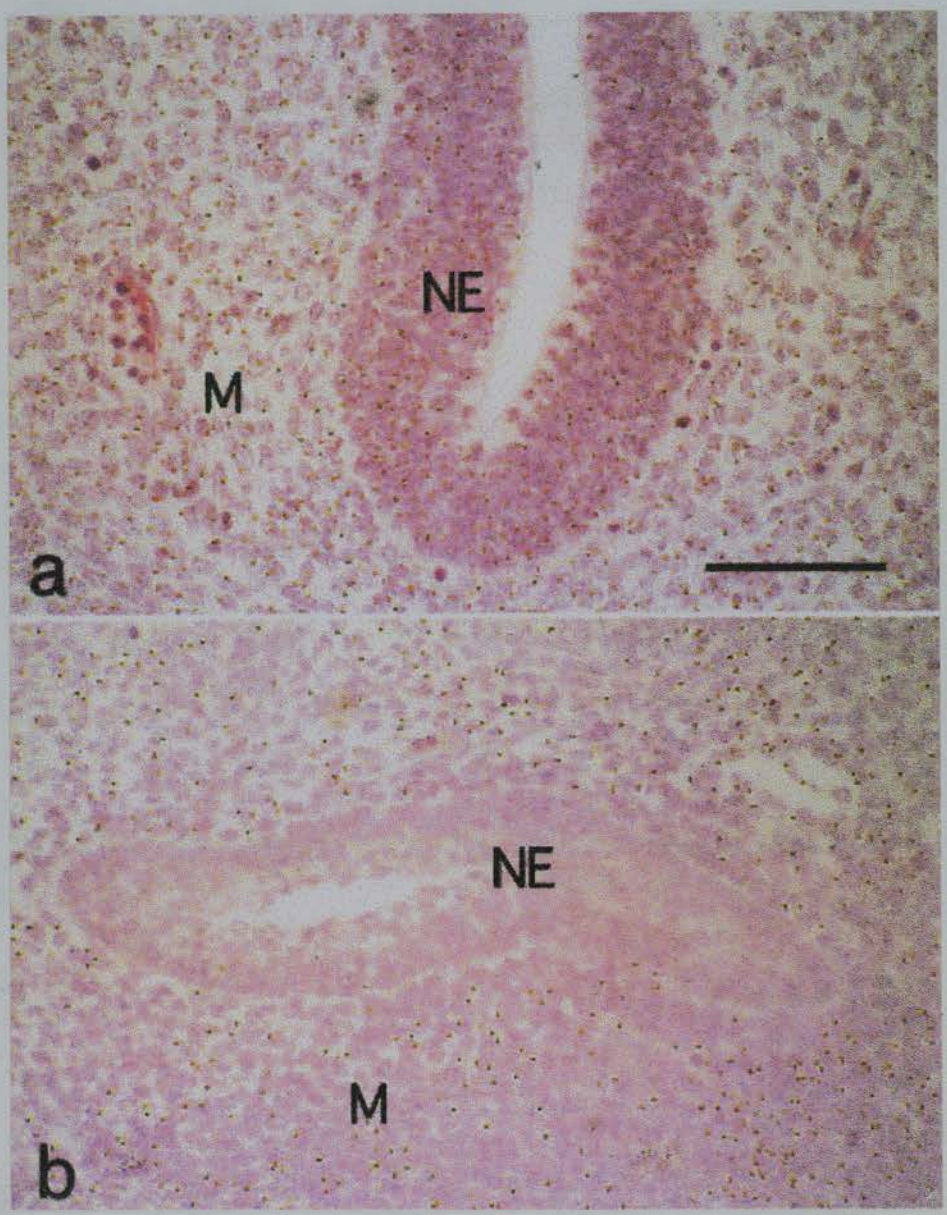

Three of the seven *Sey^{Neu}/Sey*↔+/+ chimaeras failed to form lenses; both eyes were affected in chimaeras JC17 and JC50 and one eye in chimaera JC48. Highly abnormal over-proliferation of optic cup tissue was observed in these lensless eyes (see Figure 2.9.). Although areas of morphologically normal RPE were identifiable by their simple cuboidal epithelial morphology, no pigmentation was observed. The normal inner and outer layer identity of the optic cup could not be defined due to the convoluted nature of these abnormal optic cup structures. However, areas of 'normal' inner layer with associated non-pigmented RPE could be observed albeit often in abnormal orientation. This will be discussed further in chapter 3.

The left eye of JC48 contained a lens but this appeared to be smaller and slightly retarded in development with a small lens vesicle. The lens cells present were disorganised and did not form a central 'bow' (see Figure 2.10.b). In the left eye of JC56, a lens was present but appeared smaller than normal, whilst the right lens of this chimaera was of normal size. The lenses in the remaining chimaeras, JC35, JC61 and JC63, appeared normal in size, morphology and development.

Nasal epithelium was found to be present in all *Sey^{Neu}/Sey*↔+/+ chimaeras except JC50. However, only a very small area of nasal epithelium was observed on the right side in the fronto-facial region of chimaera JC17. This tissue exhibited only a tiny lumen and no branching structures. Chimaeras JC48 and JC61 showed formation of nasal epithelium, albeit of smaller size and less convoluted than in a wild-type fetus of comparable age (see Figure 2.11.b) Size and development of nasal tissues of the remaining *Sey^{Neu}/Sey*↔+/+ chimaeras examined (JC63, JC35 and JC56) appeared normal with regard to tissue size and maturity.

2.4.4. Estimation of size of lens and nasal epithelial tissue

Estimation of lens and nasal epithelium tissue size for all seven *Sey*^{Neu}*/Sey*↔+/+ chimaeras revealed a negative correlation between tissue size and mean % fetal GPI1B (i.e. *Sey*^{Neu}*/Sey* cell contribution). No such correlation was observed in any of the other genotype groups (see Figure 2.12.). Statistical analysis of data using Spearman's Rank Correlation defined a significant positive correlation between the size of the lens and nasal epithelium (r_s = 0.736; P = 0.008) in these chimaeras, and identified a significant negative correlation between mean % fetal GPI1B and lens size (r_s= -0.789, P = 0.004), [see Table 2.3.].

These data suggest that the size of the lens and nasal epithelial tissue in the *Sey*^{Neu}*/Sey*↔+/+ chimaeras is inversely correlated with the percentage of *Sey*^{Neu}*/Sey* cells contributing to the fetus. Those chimaeras with a high contribution of compound heterozygous cells are unable to form lens and nasal epithelial tissue. Chimaeras with lower percentages of *Sey*^{Neu}*/Sey* cell contribution were able to initiate formation of lens and nasal epithelial tissue although the overall size of the tissues was directly related to the percentage of +/+ cells in the fetus. No relationship between tissue size and *Sey*^{Neu}/+ x *Sey*/+ derived cell contribution was observed in chimaeras of any other genotype group.

The nature of the relationship between size of lens and nasal epithelial tissue and contribution of *Sey*^{Neu}*/Sey* cells in the *Sey*^{Neu}*/Sey*↔+/+ chimaeras appears to be different between lens and nasal epithelium tissues (see Figure 2.12.).

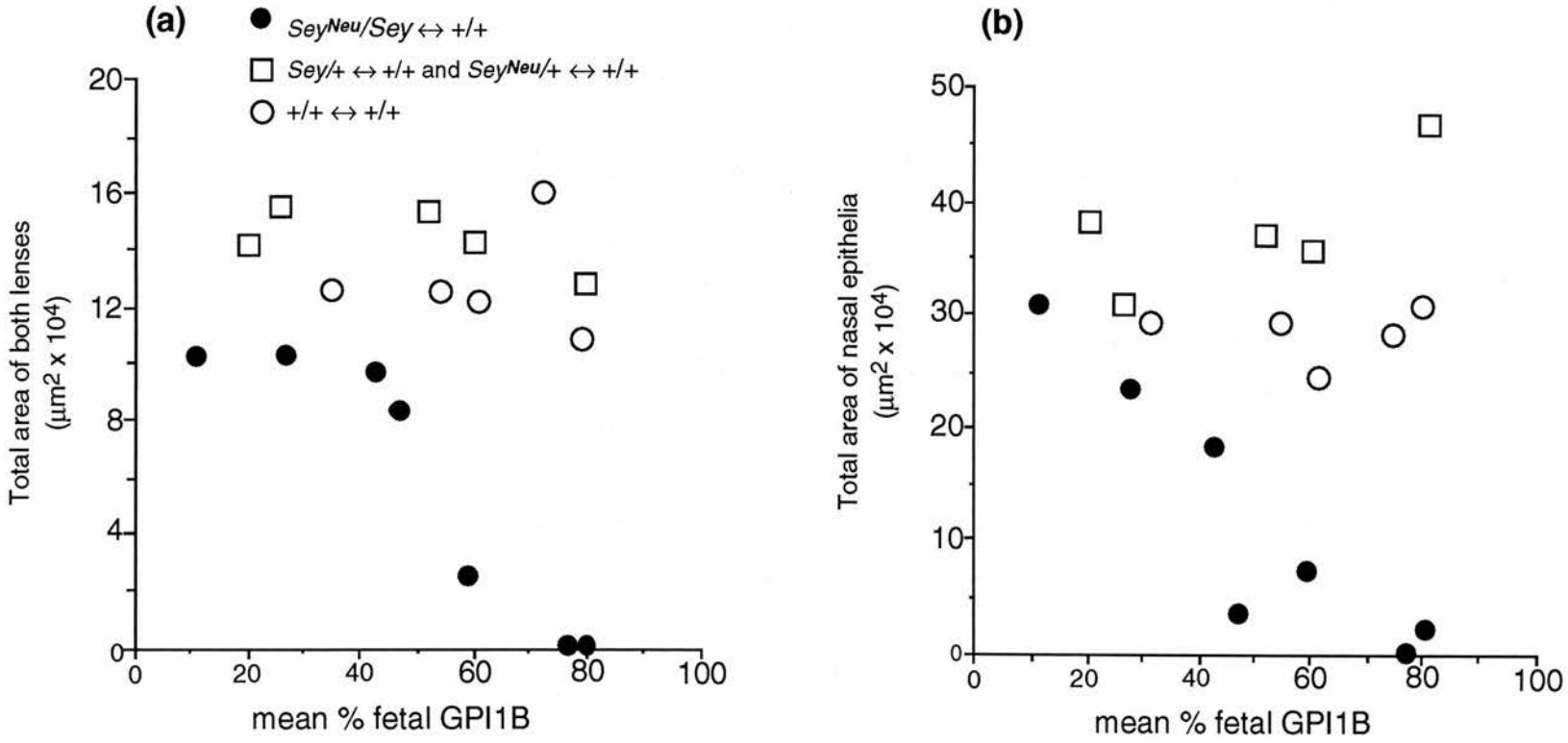

Figure 2.12. Relationship between the % fetal GPI1B and the estimated mean size of both (a) lenses or (b) nasal epithelia f
+/+ ↔+/+, *Sey*/+ ↔+/+, *Sey*^{Neu}/+↔+/+and *Sey*^{Neu}/*Sey*↔+/+chimaeras.

Development of lens tissue appears to be more sensitive to a high percentage of compound heterozygous *Sey^{Neu}/Sey* cells than the nasal epithelium. Table 2.3. indicates that lens formation appeared to be perturbed at a *Sey^{Neu}/Sey* cell contribution of approximately 50-70% in these chimaeras (right eye of chimaera JC48), whilst a small area of nasal epithelial tissue was still observed in chimaera JC17 containing 80.3% *Sey^{Neu}/Sey* cells. Chimaeras approaching the critical threshold of approximately 50% *Sey^{Neu}/Sey* cells, namely JC48 and JC61, are able to form a lens but this tissue is proportionately smaller than normal.

The curves of scattergrams 2.12.a) and b) appear to differ in their shape. The size of the lens appears to follow a sigmoidal curve whilst the relationship between nasal epithelia size and compound heterozygous cell contribution (as determined by GPI1 analysis) seems more linear. However, it does appear that a critical percentage of wild-type cells is required before initiation of both lens and nasal tissue formation can occur in the *Sey^{Neu}/Sey*↔+/+ chimaeras.

2.4.5. Analysis of *Sey^{Neu}*/+ x *Sey*/+ cell contribution to tissues of the head by DNA-DNA *in-situ* hybridisation to the β-globin transgene

In total, 16 chimaeric fetuses of the four genotype groups were systematically analysed for presence of *Sey^{Neu}*/+ x *Sey*/+ cells in tissues of the head. The results of this analysis are shown in Figure 2.13.

Figure 2.13. Histograms showing contribution of *Sey*^{Neu}/+ x *Sey*/+ cells to tissues of the 16 chimaeric fetuses examined. Overall contribution to the fetus is described as mean percentage fetal GPI1B, derived as a mean average from scanning densitometry results from left forelimb and tail samples. The contribution of cells to the retinal pigment epithelium, where present, was estimated as the percentage of pigmented cells. The contribution to other tissues was estimated as the corrected hybridisation index score from three widely spaced histological sections. For tissues of the eye, hybridisation index score was estimated from the mid-section and two sections mid-way to the lateral surfaces of the eye. Results for the neural retina and retinal pigment epithelium are presented together as the optic cup value, as in some *Sey*^{Neu}/*Sey*↔+/+ chimaeras these tissues could not be classified individually due to morphological abnormality. (*) Chimaera JC48 had no lens in its right eye. (**) Chimaera JC17 had no lens in either eye. † Tissues from the left side of the head were not analysed from chimaera JC93.

Figure 2.13.

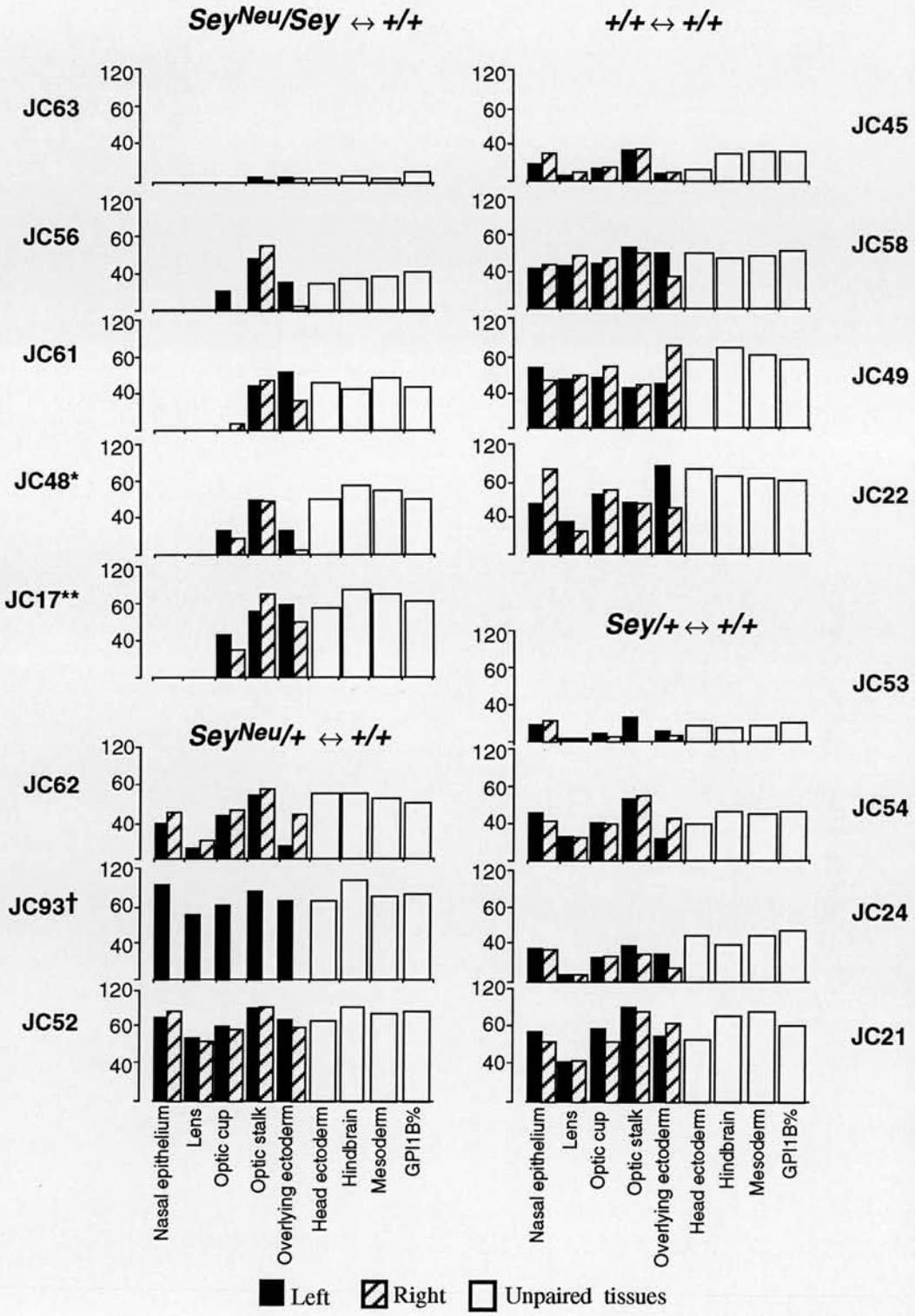
Sey^Neu/Sey ↔ +/+
+/+ ↔ +/+
JC63
JC45
JC56
JC58
JC61
JC49
JC48*
JC22
JC17**
Sey/+ ↔ +/+
JC53
Sey^Neu/+ ↔ +/+
JC62
JC54
JC93†
JC24
JC52
JC21
120
60
40
Nasal epithelium
Lens
Optic cup
Optic stalk
Overlying ectoderm
Head ectoderm
Hindbrain
Mesoderm
GPI1B%
Left
Right
Unpaired tissues

Statistical analysis of the control *Sey*^{Neu}/+ ↔+/+; +/*Sey* ↔+/+ and +/+↔+/+ chimaera groups by Spearman's Rank correlation showed positive correlations between mean % fetal GPI1B and hybridisation index score for most tissues: left nasal epithelium, right nasal epithelium, left lens, right lens, left optic cup inner layer, right optic cup inner layer, left RPE, right RPE, left total optic cup, right total optic cup, left optic stalk, surface ectoderm overlying left eye, surface ectoderm overlying right eye, general head ectoderm, hindbrain and general head mesoderm (see Appendix XII, section XII.I.I.).

Similarly, the five *Sey*^{Neu}/*Sey*↔+/+ chimaeras showed significant positive correlations between mean % fetal GPI1B and hybridisation index score for right total optic cup, right outer layer of the optic cup, left optic stalk, surface ectoderm overlying the right eye, general head ectoderm, hindbrain and general head mesoderm. However, no correlation was observed between % mean fetal GPI1B and hybridisation index score for the left total optic cup, left outer layer of the optic cup, the right optic stalk and surface ectoderm of the head overlying the left eye (see Appendix XII, section XII.I.I.). These differences may be related to local variations in *Sey*^{Neu}/*Sey* cell populations within the tissues of the head as indicated by the variability in severity of ocular phenotypes observed in these chimaeras.

Presence of hybridisation signal was analysed in each designated tissue from three separate sections of the head in chimaeras from each genotype group. No hybridisation signal was observed in any of the cells counted in the right or left lens or nasal epithelium in any chimaeras of the *Sey*^{Neu}/*Sey* ↔+/+ genotype group (see Figure 2.13.). Further analysis of every available section of lens tissue in chimaeras of the *Sey*^{Neu}/*Sey*↔+/+ genotype group, (13-25 sections per chimaeric lens), showed complete absence of signal from all lens tissue. Similarly, a detailed analysis of every

available section of nasal epithelia (10-32 section per chimaera), only 2-14 scattered signals per left or right total tissue area were identified in the 5 *Sey*^{Neu}*/Sey* ↔+/+ chimaeras. This low level of transgene signal is consistent with a low level of false positive signals observed in other chimaera studies using this nuclear transgenic marker (Everett and West; 1996).

Analysis of the surface ectoderm overlying the eye and the general surface ectoderm of the head in *Sey*^{Neu}*/Sey*↔+/+ chimaeras shows that *Sey*^{Neu}*/Sey* cells are able to contribute to surface ectoderm. This indicates that the loss of *Sey*^{Neu}*/Sey* cells from the lens and nasal epithelium of *Sey*^{Neu}*/Sey*↔+/+ chimaeras is not due to an inability of *Sey*^{Neu}*/Sey* cells to contribute to general ectoderm of the head region. Therefore, an early selective effect against *Sey*^{Neu}*/Sey* cells can be suggested as a mechanism producing the exclusively wild-type lens and nasal epithelial tissues in these chimaeras.

Thus, the data shows that presence of wild-type cells cannot rescue *Sey*^{Neu}*/Sey* cells into the lens or nasal epithelium in *Sey*^{Neu}*/Sey*↔+/+ chimaeras, even though *Sey*^{Neu}*/Sey* cells are able to contribute to other tissues of the head including the surface ectoderm. This defines the role of *Pax6* in lens and nasal epithelial development as cell autonomous .

2.5. Discussion

2.5.1. A cell autonomous effect for *Pax6* in the transition from surface ectoderm to lens and nasal placode

As the results of this study show, cells unable to produce a functional *Pax6* product (*Sey*^{Neu}*/Sey* cells) are unable to contribute to lens and nasal epithelium. The role of *Pax6* in development of the lens and nasal epithelium can therefore be defined as cell autonomous. As *Pax6* is a putative transcription factor, a cell autonomous action might have been predicted but to date had remained unproven.

The expression pattern of *Pax6* in the developing embryo, with high expression in the surface ectoderm both prior to, during and after lens placode formation, identifies three vital developmental stages of lens development during which *Pax6* may play a crucial, primary role. These stages are firstly, prior to specification of the lens placode, secondly, at the stage of placode formation from surface ectoderm and thirdly, at the stage of early lens vesicle development. A loss of *Pax6* function at any of these stages might produce the phenotype observed in the *Sey*^{Neu}*/Sey*↔+/+ chimaeras with cells that are unable to produce functional *Pax6* being excluded from the developing lens. The possible cellular effects of loss of *Pax6* function at these early stages of lens development are schematically represented in Figure 2.14.

Figure 2.14. (Following page) Schematic representation of the possible relationships between induction of surface ectoderm, response to induction and differentiation of the lens in the eyes of $Sey^{Neu}/Sey \leftrightarrow +/+$ chimaeras. There are three possible mechanisms that could results in lenses containing only +/+ derived cells in the $Sey^{Neu}/Sey \leftrightarrow +/+$ chimaeras; **1)** that only +/+ cells are present in the lens forming region and are therefore able to undergo the differentiation process, **2)** that both +/+ and Sey^{Neu}/Sey cells are present in the lens forming region and are able to respond to lens inducing signals, only +/+ cells are maintained during lens development with the Sey^{Neu}/Sey cells being progressively lost from the tissue, or **3)** that both +/+ and Sey^{Neu}/Sey cells are present in the lens forming region but only +/+ cells are able to respond to lens induction and therefore constitute the entire lens tissue. Data from this study and other experiments regarding spatial and temporal expression of *Pax6* in the developing eye indicates that the primary defect resulting in absence of Sey^{Neu}/Sey cells from the lens in $Sey^{Neu}/Sey \leftrightarrow +/+$ chimaeras is that of 3) an inability of Sey^{Neu}/Sey cells to undergo transition from surface ectoderm to lens placode.

Figure 2.14.

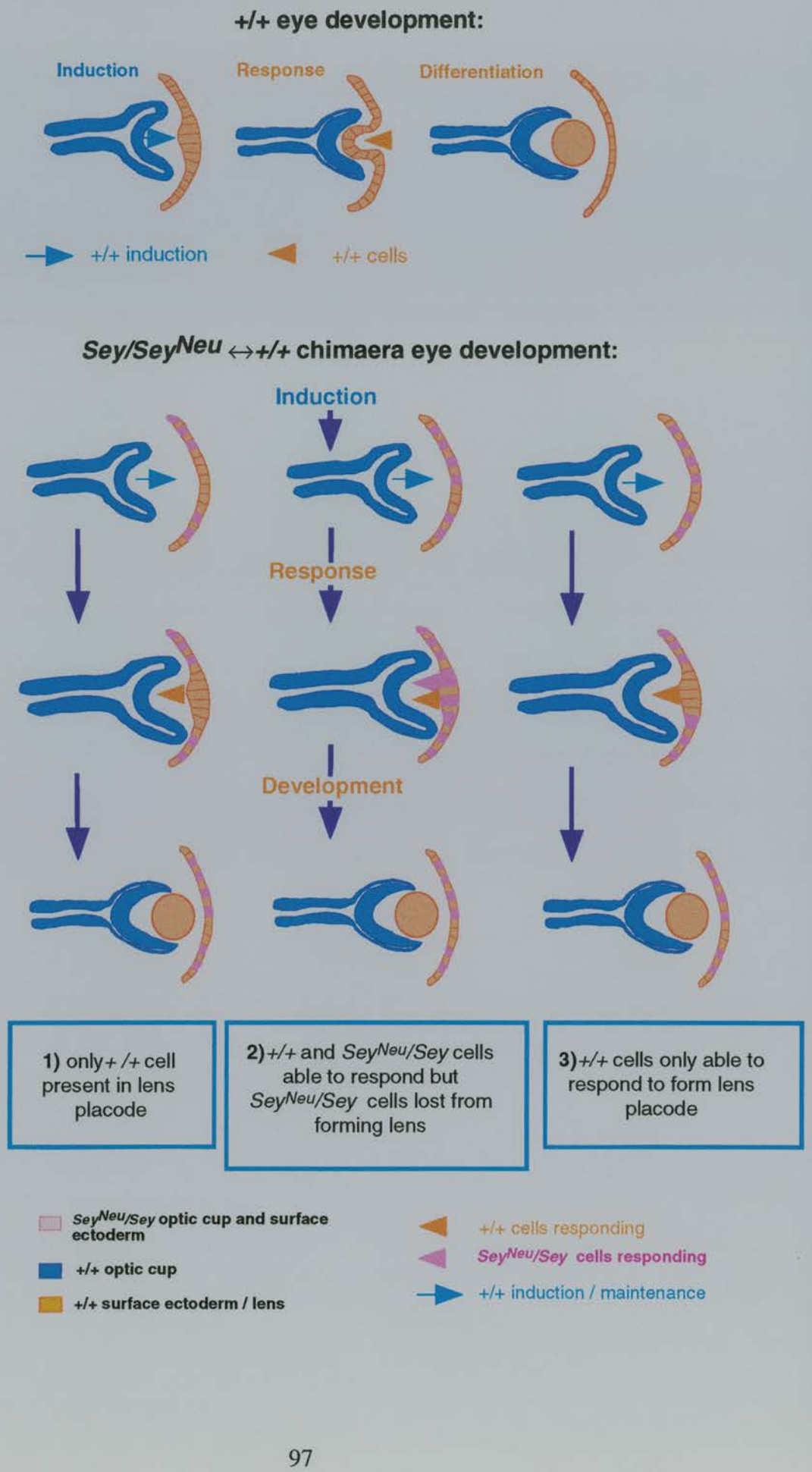
+/+ eye development:
Induction
Response
Differentiation
+/+ induction
+/+ cells
Sey/SeyNeu ↔+/+ chimaera eye development:
Induction
Response
Development
1) only+ /+ cell present in lens placode
2)+/+ and SeyNeu/Sey cells able to respond but SeyNeu/Sey cells lost from forming lens
3)+/+ cells only able to respond to form lens placode
SeyNeu/Sey optic cup and surface ectoderm
+/+ optic cup
+/+ surface ectoderm / lens
+/+ cells responding
SeyNeu/Sey cells responding
+/+ induction / maintenance

If the critical role for *Pax6* were prior to the earliest morphological determination of lens development, cells unable to express *Pax6* might be excluded from areas of surface ectoderm destined to become the lens placode. Alternatively, cells might be excluded from, or unable to contribute to the developing lens placode itself. If the crucial role for *Pax6* were later in lens development, that is, at or after formation of the lens vesicle, it is also possible to hypothesise scenarios that might result in the complete exclusion of Sey^{Neu}/Sey cells from the lenses of $Sey^{Neu}/Sey \leftrightarrow +/+$ chimaeras. Sey^{Neu}/Sey cells could be recruited into early lens development, in that they were able to make the transition from surface ectoderm to lens placode and then development to lens vesicle, but then subsequently lost from the lens tissue.

Although the results of this study define the critical period for expression of *Pax6* in lens and nasal epithelial development as prior to E12.5, when taken in isolation these results do not identify its role in formation of the lens and nasal epithelium. Therefore, in order to define the role of *Pax6* in these developmental processes, it is necessary to reconsider what is already known about the small eye homozygous mutant phenotype and *Pax6* expression.

Studies by Hogan *et al.* (1986; 1988) and Grindley *et al.* (1995) showed that not only do the lens and nasal epithelial cavities fail to form in the small eye homozygote fetus, but that no evidence of lens or nasal placode formation is observed. The formation of lens and nasal placodes from surface ectoderm is the earliest identifiable morphogenetic step in lens and nasal epithelial development in the embryo, occurring at approximately E9.5 in the mouse. With relation to this, *Pax6* expression in the surface ectoderm is dynamic and seen to restrict to the presumptive lens and nasal placode regions prior to their morphological development (Grindley *et al*; 1995). Therefore, it has been suggested that failure of placode formation is the primary defect

resulting in complete loss of eye and nasal tissue formation in the small eye mouse (Hogan *et al*; 1986 and Grindley *et al*; 1995).

Tissue culture experiments support a hypothesis of placode failure as being the cause of the small eye homozygous mutant phenotype. Fujiwara *et al.*, (1994) intimated a cell autonomous effect for *Pax6* in differentiation of lens placode from surface ectoderm using co-culture techniques as *rSey/rSey* lens ectoderm cultured with either +/+ , *rSey/+* or *rSey/rSey* optic vesicle was unable to induce lens fibre formation. However, when +/+ lens ectoderm was cultured with either +/+ , *rSey/+* or *rSey/rSey* optic vesicle, lentoid body formation was seen to occur. Therefore, Fujiwara *et al.* suggested from this study that failure of lens formation in the *rSey/rSey* mutant was an early effect, that is, affecting lens morphogenesis prior to contact between optic cup and surface ectoderm.

If the exclusion of Sey^{Neu}/Sey cells from lens and nasal epithelial tissues shown in $Sey^{Neu}/Sey \leftrightarrow +/+$ aggregation chimaeras is considered in conjunction with the known expression pattern of *Pax6* and aetiology of the small eye homozygous phenotype, this data supports a role for *Pax6* at the earliest stages of tissue formation, that of the transition of surface ectoderm to lens or nasal tissue-forming placode.

A cell autonomous effect for *Pax6* is also concomitant with a general requirement, that is, an action that is not tissue-type specific but one involved in a morphogenetic process. As the results of this study show that Sey^{Neu}/Sey cells are able to contribute to the surface ectoderm of the head (see Figure 2.13.) and *Pax6* is expressed in the surface ectoderm of the head prior to differentiation of the lens and nasal placodes (Walther and Gruss, 1991; Li *et al*; 1994), this supports the hypothesis that functional *Pax6* is required for the transition of surface ectoderm to 'placode' in the anterior head region.

There are several mechanisms by which the cell exclusion from the developing lens and nasal placodes might be achieved in *Sey*^{Neu}*/Sey*↔+/+ chimaeras. One possible mechanism is by apoptosis. Apoptotic mechanisms would allow a very rapid cell clearing, such that no evidence of *Sey*^{Neu}*/Sey* cell contribution would be apparent at E12.5 days. It is possible that *Sey*^{Neu}*/Sey* cells recruited into lens development, which then subsequently exhibited a loss of developmental potential, could be rapidly cleared from the forming tissues by this mechanism.

It is also possible that an undefined sorting mechanism requiring functional *Pax6* excludes *Sey*^{Neu}*/Sey* cells from the presumptive lens and nasal epithelium placode regions of head surface ectoderm (see Figure 2.14.). In this alternative hypothesis, *Sey*^{Neu}*/Sey* cells would be excluded from the lens and nasal epithelium at an early stage prior to placode development, thus defining a role for *Pax6* at the earliest onset of its expression in the mouse embryo. If this were the case, only patches of surface ectoderm with a high density of wild-type cells would be able to undergo lens formation. An early role for *Pax6* in specification of "placode" per say, could result in both the severe aplasic phenotypes of the small eye homozygous mutant and the extreme cell exclusion observed in *Sey*^{Neu}*/Sey*↔+/+ chimaeras.

Although *Pax6* plays an important role in specification of the anterior regions of the developing head (Chisholm *et al.*, 1995; Macdonald *et al.*, 1995; Zhang *et al.*, 1995), it is unlikely that lens or nasal placode identity is determined by expression of *Pax6* alone as the fates of these cells are very different. Similarly, if *Pax6* had a general role in placode formation, other placode-derived tissues of the head (such as the otic and pharyngeal regions) might be expected to be affected in the small eye homozygous fetus which is not the case. Also, as this study shows that *Sey*^{Neu}*/Sey* cells are able to make a good contribution to the surface ectoderm overlying the region of the eye, as

well as the general ectoderm of the head in *Sey*^{Neu}*/Sey*↔+/+ chimaeras, this supports a role for *Pax6* in transition of the lens and nasal placode regions.

As previous work has shown (Hogan *et al.*, 1988; Fujiwara *et al.* 1994), cells unable to express *Pax6* are not capable of forming lens placode, either in the homozygous small eye fetus or in tissue co-culture experiments. This supports a hypothesis that only +/+ cells present in the surface ectoderm of the presumptive placode regions of *Sey*^{Neu}*/Sey*↔+/+ chimaeras are able to respond to signals inducing placode formation (be it lens or nasal), whilst their *Sey*^{Neu}*/Sey* cell neighbours are not. This would result both in the complete exclusion of *Sey*^{Neu}*/Sey* cells from the lens and nasal tissues and also a concomitant reduction in tissue size coincident with the number of +/+ cells present in the placode region able to undertake this developmental step.

Therefore, the hypothesis that *Pax6* plays a cell autonomous role at the crucial transitional step from surface ectoderm to lens placode during early lens and nasal epithelial development is best supported by known experimental and morphological data of the small eye homozygous fetus and is coincident with a cell autonomous effect for *Pax6* by virtue that *Sey*^{Neu}*/Sey* cells are unable to contribute to the lens and nasal tissues in *Sey*^{Neu}*/Sey*↔+/+ chimaeras.

2.5.2. Size of lens and nasal epithelium in *Sey*^{Neu}*/Sey*↔+/+ chimaeras, a role for *Pax6* in placode competence

As Figure 2.12. shows, development of lens and nasal epithelial tissues in *Sey*^{Neu}*/Sey*↔+/+ chimaeras is inversely correlated to the contribution of *Sey*^{Neu}*/Sey* cells within the chimaera. This suggests that the size of the lens and nasal epithelia in *Sey*^{Neu}*/Sey*+/+ chimaeras is dependent on the number of wild-type cells recruited into this developmental process. This relationship is schematically represented in Figure

2.15. A relationship is also observed between the severity of optic cup dysmorphology and presence or absence of a lens, although this is secondary to loss or reduction in lens tissue.

Definition of a cell autonomous role for *Pax6* in lens and nasal epithelium, in conjunction with a loss of placode formation in the small eye homozygous fetus, allows us to suggest a critical period for expression during lens and nasal placode formation as discussed previously in this chapter. The proportional nature of lens and nasal epithelia size observed in the $Sey^{Neu}/Sey \leftrightarrow +/+$ chimaeras also indirectly supports the hypothesis that only cells able to express functional *Pax6* are able to undergo the transition from surface ectoderm to placode and therefore contribute to lens and nasal tissues.

Figure 2.15. (Following page) Schematic representation of the relationship between % Sey^{Neu}/Sey cell contribution in the $Sey^{Neu}/Sey \leftrightarrow +/+$ chimaeras and the induction of lens formation. In chimaeras with a Sey^{Neu}/Sey cell contribution of less than 60%, the critical threshold of cells competent to undergo transition from surface ectoderm to lens placode is achieved and lens formation can occur. The size of the lens is directly related to the initial number of cells within the lens forming region of the surface ectoderm that are competent to undergo this process. In chimaeras with a Sey^{Neu}/Sey cell contribution of more than 60%, the transition of surface ectoderm to lens placode is perturbed by the number of Sey^{Neu}/Sey cells contributing to the lens forming region and no lens formation can be initiated. (The threshold of 60% is approximate).

Figure 2.15.

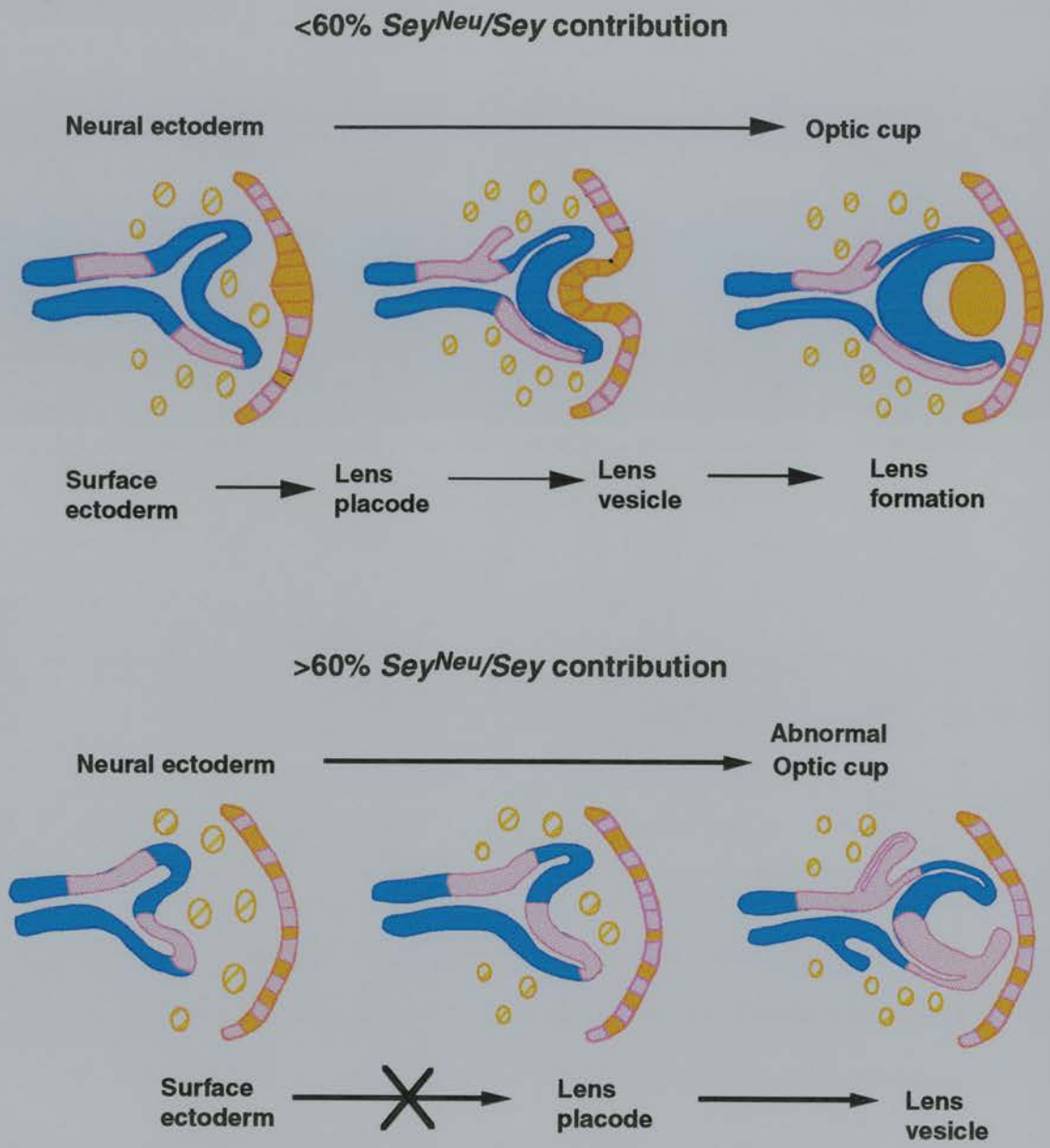
<60% *Sey*^{Neu}/*Sey* contribution
Neural ectoderm
Optic cup
Surface ectoderm
Lens placode
Lens vesicle
Lens formation
>60% *Sey*^{Neu}/*Sey* contribution
Neural ectoderm
Abnormal Optic cup
Surface ectoderm
Lens placode
Lens vesicle
Sey^{Neu}/*Sey* optic cup and surface ectoderm
+/+ optic cup
+/+ surface ectoderm

Therefore, the phenotypic effect of loss of *Pax6* function is on lens tissue size and relates to the number of cells situated within the lens placode region able to undergo induction to lens formation. However, it cannot be ruled out that the final lens size could also be influenced by the severity of optic cup dysmorphology as in both chimaeras JC61 and JC56, the smaller lens is associated with a more dysmorphic optic cup structure. It is possible that presence of Sey^{Neu}/Sey cells in these optic cups are actively inhibiting lens growth and/or differentiation later in lens development. However, if this is the case, the relationship between optic cup dysmorphology and final lens size is undoubtedly reciprocal (see Table 2.3.), as loss of lens formation, (as seen in chimaeras JC50 and JC17), appears to induce marked over-proliferation of optic cup tissue (see Chapter 3). In conclusion, if severity of optic cup dysmorphology is affecting lens size, this is a related but secondary effect on lens development.

Data shown in Figure 2.12. and Table 2.3. predicts that the size of lens or nasal epithelial tissue is defined solely by the number of wild type cells within the presumptive placode region able to undertake tissue induction. Unilateral effects were observed in the $Sey^{Neu}/Sey{\leftrightarrow}+/+$ chimaeras, with the right lens of chimaeras JC56 and JC61 being larger than the left. This indirectly suggests a difference in the number of cells able to undergo transformation from surface ectoderm to lens placode on the left side compared to right side of the head. Unilateral effects were also observed in the nasal epithelium of $Sey^{Neu}/Sey{\leftrightarrow}+/+$ chimaeras. Chimaera JC17 has formed a small area of nasal epithelium on the right side of the head with no tissue formation on the left. The similarity of unilateral effects observed indicates a similarity in the role of *Pax6* between these two very different tissues.

The direct correlation observed between lens and nasal tissue size and overall contribution of *Sey^{Neu}/Sey* cells to the fetus also indicates that no compensatory growth mechanisms are affecting final tissue size.

Correlation between competence of the placode forming regions and expression of *Pax6* has been determined using tissue culture experiments (Li, 1994). As lens forming competence in the surface ectoderm is independent of interaction with the optic vesicle (Barabanov and Fedstova, 1982; Henry and Grainger, 1990; Li, 1994), this competence precludes actual placode development, concurrent with earliest *Pax6* expression. Additionally, transdifferentiation experiments have shown that differentiated retinal glial cells re-express *Pax6* prior to formation of lentoid structure (Adler *et al*; 1995), also predating *Pax6* expression to lens development and indicating a role in lens competence.

If the data from these experiments is considered in conjunction with results of this study, it appears that *Pax6* is involved in conferring competence to cells to form lens placode, whether the cells being determined as "lens competent" are ectoderm or neurectoderm derived. However, tissue culture studies have identified only that regions of surface ectoderm that express *Pax6* are capable of being recruited into the lens morphogenetic pathway. Whether these regions are also capable of forming nasal epithelium has not been determined.

2.5.3. Thresholds for lens and nasal epithelial development in *Sey^{Neu}/Sey*↔+/+ chimaeras

The striking unilateral effects were observed in a *Sey^{Neu}/Sey*↔+/+ chimaera JC48, which exhibited presence of a lens in the left eye whilst no lens formation had occurred in the right eye (see Figure 2.9.), indicates a local sensitivity to the contribution of

mutant cells within the lens placode forming regions of surface ectoderm between the left and right sides of the head. Presumably, the threshold number of cells required for lens formation was achieved in the left eye of fetus JC48 but not in the right. Indeed, if the contribution of *Sey*^{Neu}*/Sey* cells is too great within the specified placode regions, lens morphogenesis is unable to proceed (e.g. chimaeras JC50 and JC17). Similar unilateral effects and complete tissue loss are observed in the nasal epithelium in these chimaeras. Therefore, a threshold of wild type cells is required for both lens and nasal tissue formation which is local, finite and tissue specific.

The need for a critical number of competent cells for initiation of tissue formation is an experimental concept known as the 'community effect' (Gurdon, 1988; Gurdon *et al.*, 1993). This defines an experimental phenomenon where the developmental fate of cells of an interacting population is different to that of the same cells grown individually. Using transplantation techniques, it has been shown that cells transplanted ectopically in groups are able to follow a pre-defined developmental pathway whilst cells transplanted individually either change cell fate or die (Gurdon *et al.*, 1993). Gurdon showed that there is a defined critical mass of cells needed for a pre-determined developmental pathway to be maintained in an ectopic environment and that the size of this cell mass is specific to the cell or tissue type. Indirectly, this experimental phenomenon indicates that uncommitted cells emit specific signals to identify themselves to like neighbours destined to undergo the same developmental processes so that developmental co-ordination can be achieved.

Figure 2.16. (Following page) Schematic representation of possible role of the 'community effect' in lens development in *Sey*^{Neu}*/Sey* ↔+/+ chimaeras. A critical number of +/+ cells in the lens forming region are needed for lens formation to be initiated and maintained. The number of cells competent to form placode directly confers size to the resultant tissue formed.

Figure 2.16.

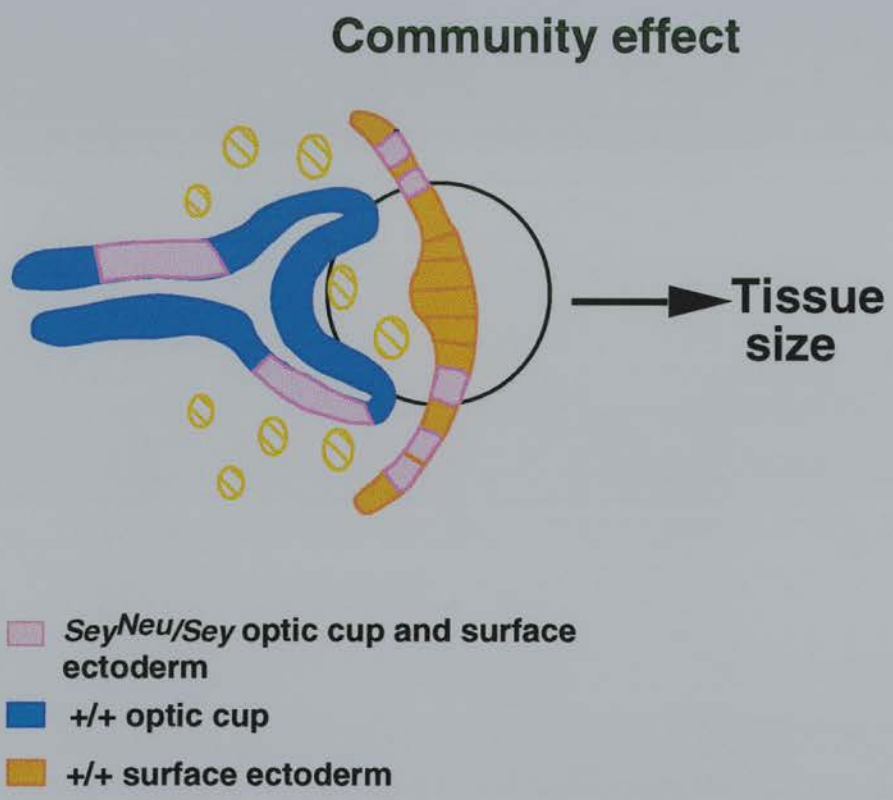
Community effect
Tissue size
Sey^Neu/Sey optic cup and surface ectoderm
+/+ optic cup
+/+ surface ectoderm

The development of lens and nasal epithelial tissues in $Sey^{Neu}/Sey \leftrightarrow +/+$ chimaeras appears be an example of this "community effect" occurring *in vivo* . The results of this study show that a critical mass of wild type cells is required before differentiation can occur and/or be maintained. Once the specification of the placode-forming regions has occurred in the $Sey^{Neu}/Sey \leftrightarrow +/+$ chimaeras, wild type cells make a developmental step *en mass*, this critical mass of cells directly conferring size to the developing tissue (see Figure 2.16.).

2.6. Conclusions

Using $Sey^{Neu}/Sey \leftrightarrow +/+$ chimaeras, it has been possible to define a cell autonomous role for *Pax6* in development of the lens and nasal epithelium with indication that *Pax6* is required to confer competence to surface ectoderm of the lens and nasal placodes to undertake the primary morphological step of its defined tissue developmental pathway, the transition from surface ectoderm to placode. Critical thresholds of +/+ cells are required for formation of lens and nasal epithelial tissues in $Sey^{Neu}/Sey \leftrightarrow +/+$ chimaeras, the kinetics of which are local, finite and tissue specific. Finally, although *Pax6* is required for conferring competence to the lens and nasal placodes, it does not determine their final tissue identity.

Chapter 3

Analysis of E12.5 and E14.5 *Sey^{Neu}/Sey*↔+/+ chimaeras - Roles for *Pax6* in optic cup development

3.1. Introduction

The optic cup is a simple structure from which the specialised and highly distinct cell populations of the neural retina and the retinal pigment epithelium (RPE) are derived. The optic cup is formed as an outgrowth of the forebrain, visible by E8.5 in the mouse embryo. The brain is immature at this early stage and the presumptive optic stalks are seen to be continuous with the ventricles of the forebrain. *Pax6* is expressed in a spatio-temporal pattern throughout development of the optic vesicle, optic cup and mature retina in the mouse embryo (Walther and Gruss, 1991; Grindley *et al.*, 1995).

Development of the optic cup is highly abnormal in the *Sey/Sey* homozygous fetus. Outgrowth of the forebrain occurs but no true optic cup structure is formed, although neural ectoderm does make contact with the surface ectoderm overlying the presumptive eye region of the head (Grindley *et al.*, 1995). This initial contact is subsequently lost as growth of the neural ectoderm structures appears to arrest and mesenchymal condensation occurs between the surface ectoderm and optic tissue. At E15.5 the abnormal optic structures resemble no more than abnormal 'optic stalks' with an extended lumenal space but no evidence of optic nerve formation. Grindley *et al* (1995) have suggested that failure of optic cup development in the *Sey/Sey* homozygous fetus occurs prior to contact with the surface ectoderm as the abnormal optic structures fail to invaginate. If this is the case, then failure of optic cup

development in the *Sey/Sey* homozygous fetuses is a separate event from failure of lens placode differentiation.

Retinal abnormalities have not been reported in mouse small eye heterozygous embryos to date. Studies of heterozygous small eye mutant rats; *rSey/+*, (Matsuo *et al.*, 1993) revealed some retinal dysplasia. Rat *rSey/rSey* embryos have a similar phenotype and aetiology to that of the mouse small eye homozygous fetus, with absence of lens and nasal tissue putatively resulting from failure of placode formation (Fujiwara *et al.*, 1990).

Until recently, the only human *PAX* gene mutations shown to exhibit neurectodermal abnormalities of the eye were those of a single family reported with mutations within the *PAX2* gene resulting in optic nerve colobomas (Sanyanusin *et al.*, 1995). However, recently the first human *PAX6* mutation to result in a primary retinal phenotype, isolated foveal hypoplasia, has been reported. The *PAX6* defect in this family was been identified as a missense mutation in the C-terminus of the paired domain (Azuma *et al.*, 1995). This report separates the more common anterior segment anomalies and primary retinal phenotypes caused by mutations within *PAX6*. It appears possible that these anterior versus posterior phenotypes may be caused by mutations which result in mutated splice variants with abnormal physiological effects (Sperbeck *et al.*, 1995).

It has been suggested that the presence of a lens is important for differentiation of the bi-layered structure of the optic cup. Development of the optic cup does not occur in the small eye homozygote although one of the markers of the optic cup outer layer, *Trp-2*, is expressed in the abnormal distal neurectodermal structures (Grindley *et al.*, 1995).

Expression of *Pax6* has been examined in the *Sey/Sey* homozygous mouse fetus and observed to be similar in pattern to that observed in the wild-type fetus, despite *Sey/Sey* optic structures being highly abnormal. Where there appeared to be a differentiation of optic cup from optic stalk, only the area resembling optic cup was seen to express *Pax6* (Grindley *et al.*, 1995). As *Pax6* is widely expressed in the presumptive optic cup in the wild-type fetus, this pattern being approximately maintained in the homozygous small eye fetus, it is possible that *Pax6* may therefore have a role to play in development of the retina proper. However, the absence of retinal structures in the small eye homozygote makes it impossible to elucidate what this role might be.

Despite the highly abnormal optic structures observed in the *Sey/Sey* homozygous fetus, development of the neurepithelium of the optic stalk appears to progress normally although optic nerve formation does not occur. However, it is difficult to ascertain from the published data whether the optic structures seen in the small eye homozygous fetus are optic cup proper or just developmentally specified distal optic stalk. Therefore it is difficult from the small eye homozygous *(Sey/Sey)* phenotype alone to define what role *Pax6* might play in development of the optic cup.

Concurrent with examination of roles for *Pax6* in development of the lens and nasal epithelium, E12.5 $Sey^{Neu}/Sey \leftrightarrow +/+$ chimaeras were utilised to attempt to answer questions regarding roles for *Pax6* in development of the optic cup. Elucidating a role for *Pax6* in optic cup development had previously been impossible due to the severity of optic cup dysmorphology in the homozygous *Sey/Sey* fetus, particularly as this severity might also be inherently related to loss of lens formation. The $Sey^{Neu}/Sey \leftrightarrow +/+$ chimaera provided a means of separating these divergent effects on optic cup development.

Additionally to the E12.5 chimaeric fetuses previously reported in Chapter 2, a group of E14.5 *Sey^{Neu}/Sey* ↔+/+ chimaeras were produced in order to investigate the reasons for absence of pigment formation in the *Sey^{Neu}/Sey* regions of chimaeric optic cups. In the wild-type fetus, pigmentation is complete by E12.5, therefore, by examining E14.5 *Sey^{Neu}/Sey*↔+/+ chimaeras it was hoped to confirm whether the lack of pigment formation in the eyes of E12.5 chimaeras was due do a functional inability to initiate pigment formation in all cells of the chimaera or if only *Sey^{Neu}/Sey* cells were unable to undergo RPE morphogenesis. Optic cup phenotypes in the E12.5 and E14.5 *Sey^{Neu}/Sey* ↔+/+ chimaeras and subsequent implications on *Pax6* function in development of the optic cup will be discussed in this chapter.

3.2. Methods: Analysis of *Sey^{Neu}/Sey* ↔+/+ chimaeras

Chimaeras were produced and analysed at E12.5 and E14.5 days. Of 285 embryos transferred, 57 fetuses were recovered at E14.5 of which 28 were chimaeric by GPI1 electrophoresis. However, only two of these chimaeric fetuses, JC113 and JC131, proved to be of *Sey^{Neu}/Sey* ↔+/+ genotype and were of mean percentage fetal GPI1B 70.6 and 35.6% respectively. These two chimaeras will be considered descriptively in this chapter, (see Chapter 2 and associated appendices for description of chimaera production and processing).

3.2.1. Spatial analysis of eye pigment in the RPE and Tg+ve cells in the optic cup

The proportions of albino and pigmented cells within the retinal pigment epithelium (RPE) were estimated from measurements on histological sections of chimaeric eyes. The numbers and lengths of pigmented and albino patches in mid-eye sections were determined by light microscopy. Patch lenghts were measured using an Olympus BH2

light microscope fitted with a Sony CCD/RBG video camera and analysis performed on a MacIntosh computer using Colour Vision Software, Improvision. The mean patch lengths were corrected for the effects of proportion of pigmented and albino cells and this "corrected" mean patch length used as a summary statistic for comparing patch sizes (West, 1976; West, unpublished 1996) The spatial distribution of cells in chimaeric mouse fetuses was studied in collaboration with Mr B.A. Hodson in our laboratory.

This basic approach was modified for use with the β-globin in-situ hybridisation endpoint (B.A. Hodson, unpublished). A hexagonal grid was superimposed over the tissue area and a line of hexagons at the edge of the tissue area scored. Each hexagon was classified as either Tg+ve or Tg-ve. This methodology was adopted to account for the loss of definition of cell boundaries that occurs due to the in-situ hybridisation process. The minor axis of the hexagonal grid was approximately equivalent to one cell length. This methodology was used to estimate the proportion of cell types, the mean patch length and corrected mean patch length in the optic cups of the different chimaera groups. In adddition, the proportion of Tg+ve cells from the grid analysis was compared to both the uncorrected hybridisation index score defined by cell counting and and mean percentage fetal GPI1B determined from fetal forelimb and tail samples.

Theoretically, if cells are arranged randomly within a tissue, the corrected mean patch length will be equivalent to one cell length, regardless of the size of the initial patches measured. Larger mean corrected patch sizes may be produced if cell mixing fails to keep pace with cell division (clonal expansion) or if cells of like genotype actively aggregate. Therefore, the corrected mean patch size can give a indication of the degree of cell mixing or aggregation within a chimaeric tissue. The proportion of pigmented

cells or Tg+ve cells were compared to the genotype of the fetus and its mean percentage fetal GPI1B.

3.2.2. 3-D reconstruction of chimaeric eyes

A 3-D reconstruction of the left and right eyes of chimaera JC48 was carried out to viualise the nature of the extreme cell segregation observed between *Sey*^{Neu}*/Sey* and +/+ cells in the optic cup. 3-D reconstruction was performed in collaboration with Mrs M. Stark, Dr D. Davidson and Dr R. Baldock at the MRC Human Genetics Unit, Edinburgh. All available sections for each eye were used for this analysis. In brief, a simple digital photograph was taken of each section of each eye and the tissue areas of *Sey*^{Neu}*/Sey* and +/+ cells were marked. A digital image of each section was then captured using a Zeiss Axioplan microscope with a Xilix Technologies Microimager-1400 12bit CCD camera connected to a Sun Microsystems Sparc station. Images were captured at x10 magnification. A template of each image was then produced using a single masking colour and the next serial section was aligned exactly to the first using this template. When the two sections were correctly oriented, the template was removed and the second image captured and stored. This process was repeated until all sections had been aligned and captured. Images were then stacked as a 3-D voxel image.

Once this process was complete, each image was recalled and correlated to its appropriate digital photograph and the areas of *Sey*^{Neu}*/Sey* cells and +/+ cells were highlighted by hand using "Paint", a program developed at the MRC Human Genetics Unit for manual separation of structures within a 3-D image. The *Sey*^{Neu}*/Sey* cells were highlighted in blue and the +/+ cells in pink. A third series of images was produced where the cells of the lens were highlighted in yellow. A series of four image layers were produced by this process, greyscale background, *Sey*^{Neu}*/Sey* cells,

+/+ cells and lens tissue. These layers were condensed, stacked and processed through 3-D reconstruction and the final image visualised using AVS (Advanced Visual System, AVS/UNIRAS Ltd.) [see Figure 3.6.].

A number of different approaches were used to attempt best visualisation of the relationship between the segregate areas of *Sey*^{Neu}*/Sey* and +/+ cells. Orientation and plane of section can be manipulated to invoke novel views from the original sections once the images have been converted into three dimensions. Two such methods proved to be worthwhile. Firstly, where sectioned images were shown in relationship to the background 'greyscale' image, with a right-angle section removed from the 3-D block increasing in depth by 28μm on each image. Secondly, a similar approach but sectioning the whole image at 28μm sections in the absence of the 'greyscale' background. These types of reconstructions were designated 'excavation' images and are shown in Figures 3.7. and 3.8.

Table 3.1. (Following page) Relationship between composition and eye morphology in E12.5 *Sey*^{Neu}*/Sey* ↔+/+ aggregation chimaeras. Using Spearman's Rank Correlation test the mean percentage fetal GPI1B in each fetus correlated positively with hybridisation index for the total optic cup (r_s = 0.731; *P* = 0.028). Degree of morphological abnormality in the optic cup correlated negatively with lens size (r_s=-0.899; *P*=0.0001) and positively with the hybridisation index for each total optic cup (r_s=0.781; *P*=0.019) and, in turn, with the mean % fetal GPI1B (r_s=0.933; *P*=0.001).

[a] %GPI1B is the % mean GPI1B from a tail and forelimb sample from each fetus.

[b] *Tg/-* in the optic cup is the hybridisation signal from three widely spaced sections. Where distinction between inner and outer layer of the optic cup could not be made in the case of those eyes that were so severely dysmorphic as to make identification of inner layer and outer layers impossible, only a total value is given. ND: not determined; NA: not applicable.

[c] (+); normal morphology with normal outer RPE layer and inner layer of neural retina. (++); slightly abnormal, small areas of ectopic growth in the outer layer. (+++); more abnormal tissue but double-layer structure of optic cup maintained. (++++); abnormal distortion of double layer structure with lens still present. (+++++); grossly abnormal convoluted structure with loss of double layer integrity, lens absent.

[d] Although no Tg signal was observed in the three sections used for analysis, qualitative analysis of all available sections revealed a few Tg+ve cells.

* Eyes that do not contain a lens.

Chimaera	Eye	%GPI1B in fetus[a]	*Tg/+* in optic cup[b]			Optic cup[c] dysmorphology
			Inner layer	Outer layer	Total	
JC63	left	11.0	0.3	0	0.2	+
JC63	right	11.0	0.3	0	0.2	+
JC35	left	27.5	N.D.	N.D.	N.D.	+
JC35	right	27.5	N.D.	N.D.	N.D.	+
JC56	left	42.8	0.3	38.2	20.5	+++
JC56	right	42.8	0[d]	0[d]	0[d]	+
JC61	left	46.9	0[d]	0[d]	0[d]	++
JC61	right	46.9	0[d]	19.3	7.3	++++
JC48	left	59.2	12.0	33.3	23.4	+++++
JC48	right*	59.2	N.A.	N.A.	18.1	+++++
JC50	left*	76.8	N.A.	N.A.	N.D.	+++++
JC50	right*	76.8	N.A.	N.A.	N.D.	+++++
JC17	left*	80.3	N.A.	N.A.	45.6	+++++
JC17	right*	80.3	N.A.	N.A.	29.6	+++++

Table 3.1. Relationship between composition and eye morphology in E12.5 fetal $Sey^{Neu}/Sey \leftrightarrow +/+$ aggregation chimaeras.

3.3. Results

3.3.1. Optic cup dysmorphology and presence or absence of a lens in E12.5 *Sey^{Neu}/Sey*↔+/+ chimaeras

The level of dysmorphology observed in the optic cups of E12.5 *Sey^{Neu}/Sey* ↔+/+ chimaeras was highly varied whilst no abnormalities were observed in any optic cups of chimaeras of the other genotype groups. Macromorphology of the optic cup in the *Sey^{Neu}/Sey* ↔+/+ chimaera group was graded according to dysmorphology on a scale of (+) to (+++++), with (+++++) indicating the most severe level of abnormality (see Table 3.1.).

None of the seven E12.5 *Sey^{Neu}/Sey* ↔+/+ chimaeras examined showed optic cup morphology similar to that observed in the *Sey^{Neu}/Sey* compound heterozygous or *Sey/Sey* homozygous fetus. Even the most severely affected eye (the left eye of chimaera JC17) showed an increased amount of optic cup tissue formation compared to the compound heterozygous or small eye homozygous fetus. In all *Sey^{Neu}/Sey* ↔+/+ chimaeras examined, areas of optic cup tissue were seen to maintain contact with the surface ectoderm, even when the tissue present was highly dysmorphic.

The severity of optic cup dysmorphology was observed to be related primarily to the absence of a lens or percentage of mutant cells in the chimaera. In those eyes where the lens tissue was absent, (both eyes of JC17 and JC50 and the right eye of JC48), optic cup morphology was highly abnormal with convoluted neurepithelial tissue filling the eye cavity. In the right eye of JC17, (see Figure 3.1.), these abnormal convolutions maintained the general spherical structure of the eye proper, but in other cases, as in the right eye of JC48, extreme proliferation was observed with the abnormal tissue extending beyond the normal boundary of the head. In *Sey^{Neu}/Sey* ↔+/+ chimaeric eyes where lens tissue was absent the spherical shape of the eye was lost, along with spatial orientation of the optic cup tissue present.

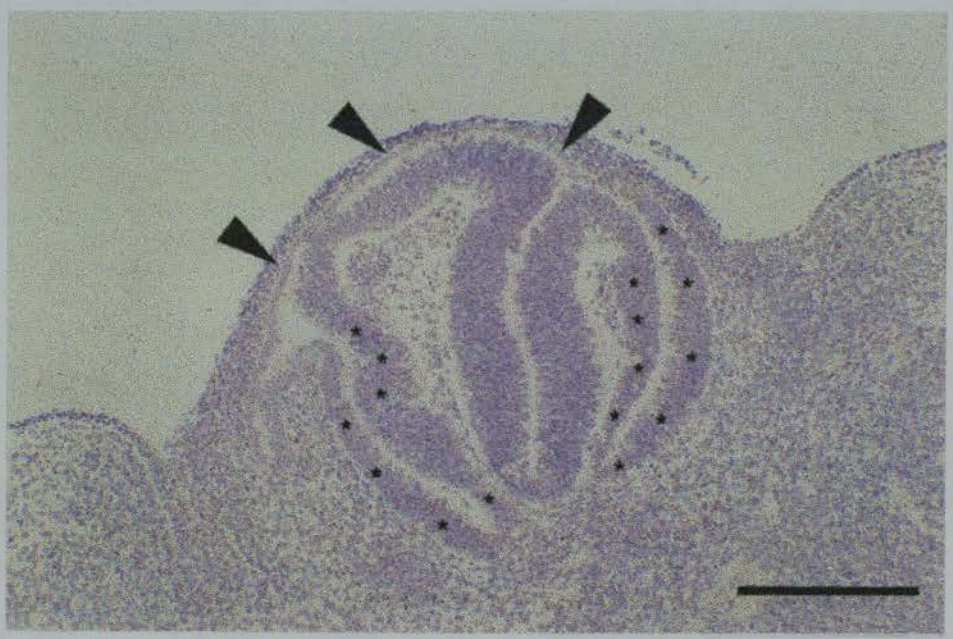

Figure 3.1. Histological section of the left eye of *Sey*^{Neu}*/Sey*↔+/+ chimaera JC17 showing hyperproliferation of optic cup tissue forming multi-layered structure. The optic cup is divided into areas of almost exclusively +/+ and *Sey*^{Neu}*/Sey* cells. Areas of *Sey*^{Neu}*/Sey* cells are marked *. Unmarked areas are composed of +/+ cells. Large arrowheads indicate area of morphologically normal retinal pigment epithelium (RPE) although these cells are ectopically oriented. Note that the abnormal eye structure maintains the spherical shape of the normal eye orbit. (Scale bar - 200μm).

3.3.2. Definition of optic cup tissue morphology in $Sey^{Neu}/Sey \leftrightarrow +/+$ chimaeras

On examination of $Sey^{Neu}/Sey \leftrightarrow +/+$ chimaeras it soon became apparent that the accepted definitions of the normal tissues of the eye present at E12.5 were not sufficent for accurate description of the highly abnormal optic cups observed. At E12.5 in the wild type fetus, the optic cup is defined as consisting of two layers, the inner layer of developing neural retina, and the outer layer constisting of retinal pigment epithelium. Normal retinal pigment epithelium is a highly distict simple cuboidal cell layer situated external to the inner layer of the optic cup. However, the highly abnormal optic cup structures of the $Sey^{Neu}/Sey \leftrightarrow +/+$ chimaeras did not exhibit normal inner layer/outer layer identity with areas of morphologically abnormal cells situated in inner layer positions as well as morphologically identifiable RPE positioned ectopically and in abnormal orientation.

Therefore, for purposes of identification, all morphologically normal RPE (that is, comprising a simple cuboidal cell layer) was designated as outer layer regardless of orientation or position. In addition, any abnormal tissue areas situated in the normal "outer layer" position were also classified as outer layer. Similarly, any tissue, morphologically normal or abnormal, situated in an inner layer position; that is, within the most apical boundary of the rim of the optic cup, was designated to be of inner layer type. Only areas of morphologically normal RPE could be accurately classified as to inner layer/outer layer identity in chimaeric eyes where lens tissue was absent as the integrity of the eye structure was completely lost in these cases.

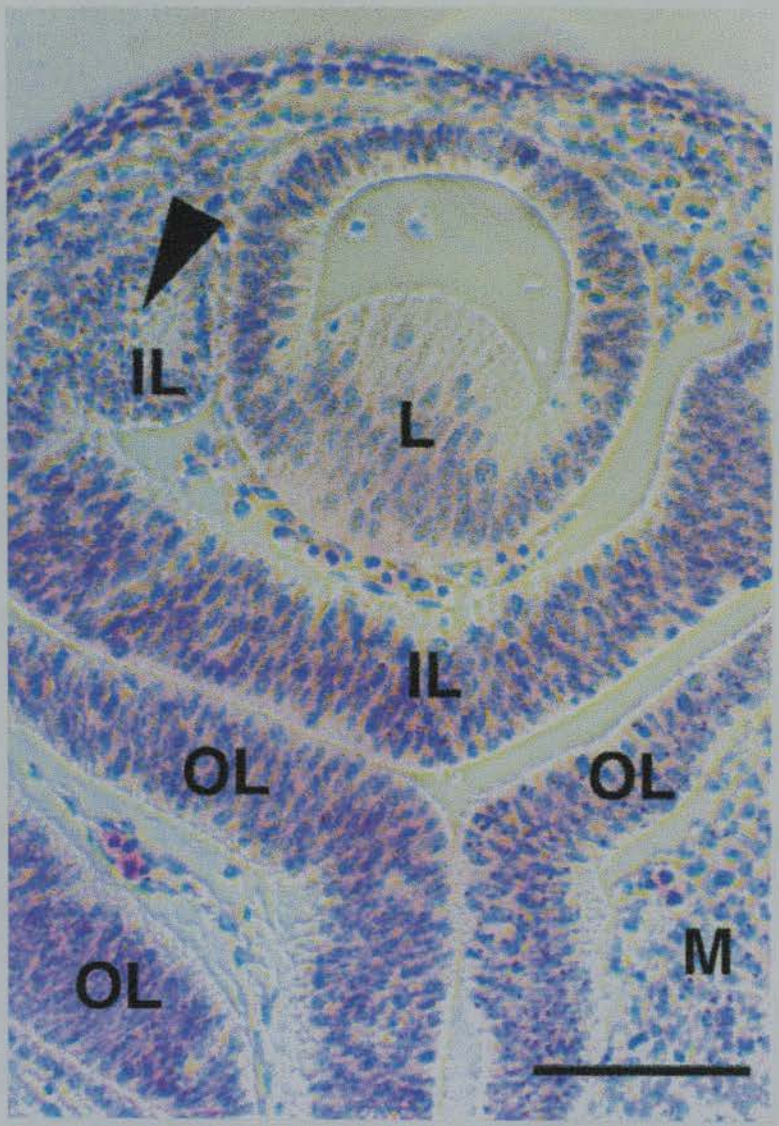

Figure 3.2. Histological section of the left eye of *Sey*^{Neu}*/Sey* ↔+/+ chimaera JC48 viewed under phase-contrast light microscopy. Note complete absence of nuclei with hybridisation signal (*Sey*^{Neu}*/Sey* cells) in the lens and areas of the optic cup. The optic cup is divided into large areas of +/+ without hybridisation signal and or *Sey*^{Neu}*/Sey* cells showing hybridisation signal. (L) lens, (M) mesenchyme, (IL) inner layer of optic cup, (OL) outer layer of optic cup. Arrowhead indicates an area of *Sey*^{Neu}*/Sey* cells situated in 'inner layer' position. (Scale bar - 80μm).

Areas of 'outer layer' RPE formation were observed ectopically, (see Figure 3.1.), for example, in the right eye of JC17 an area of histologically identifiable RPE was observed in the region underlying the surface ectoderm. Although areas of +/+ tissue could be identified as possessing cell morphology similar to normal inner layer of the optic cup, this was not always the case as some areas of +/+ tissue were found to be highly disorganised at a cellular level. No direct correlation was observed between the mean % fetal GPI1B and the hybridisation index in the total optic cup of these highly dysmorphic, lens-less eyes (see Table 3.1). Inner and outer layers could not be counted individually as it was impossible to define the the true identity of the abnormal tissue structures in spatial terms.

In those E12.5 $Sey^{Neu}/Sey \leftrightarrow +/+$ chimaeras that possessed lens tissue, the dysmorphology of the optic cup was seen to be less severe, with areas of ectopic growth being restricted to the outer layer, with outer and inner layers being generally identifiable. The only exception to this rule was the left eye of JC48 (see Figure 3.2.), where an area of abnormal growth was observed at the rim of the optic cup, this morphologically abnormal area found to be composed of Sey^{Neu}/Sey cells. These cells appeared disorganised and indicated no developmental characteristics of either inner or outer layer of optic cup, they were therefore classified to the inner layer purely by their position.

In three of the eyes with lenses (JC61 right eye, JC48 left eye and JC56 left eye), Sey^{Neu}/Sey cells contributed more significantly to the outer layer of the optic cup than the inner (see Table 3.1). Apart from the left eye of JC48 where the contribution of Sey^{Neu}/Sey cells to the inner layer was 12.0%, no significant contribution was made by Sey^{Neu}/Sey cells to the inner layer of any eye containing a lens (<1%). Moreover, the normal 'double cup' morphology of the eye was maintained in all eyes of $Sey^{Neu}/Sey \leftrightarrow +/+$ chimaeras that exhibited lens development.

3.3.3. The Retinal Pigment Epithelium

As was mentioned in Chapter 2, no pigmentation was noted at dissection in any eye of the E12.5 chimaeric fetuses genotyped as *Sey*^{Neu}*/Sey* ↔+/+. This observation was confirmed histologically at a cellular level as no melanin granule formation was observed in the RPE of any *Sey*^{Neu}*/Sey* ↔+/+ chimaeras. Where RPE was present, this was always found to be non-pigmented and negative for the β-globin transgene, indicating that these areas were derived solely of +/+ cells (see Figure 3.3.a and b). In addition, where areas of +/+ RPE were present, whether in normal or ectopic location, these were always seen to be juxtaposed to an area of +/+ cells resembling inner layer of the optic cup. This indicated that *Pax6* has a role to play in development of the RPE and that this role may be cell autonomous as only +/+ cells are able to contribute to this tissue.

Figure 3.3. (Following page) **a)** Histological sections of the right eye of *Sey*^{Neu}*/Sey*↔+/+ chimaera JC61. The lens and optic cup are relatively normal and show no hybridisation signal, (*Sey*^{Neu}*/Sey* cells). (Scale bar - 200μm). **b**) Higher magnification of area of eye shown in a). Hybridisation signal can be observed in cells of the mesenchyme but not in any cells in the inner or outer layers of the optic cup. Signal can be observed in a single cell in the hyaloid plexus. (M) mesenchyme, (IL) inner layer of optic cup, (OL) outer layer of optic cup, (hp) hyaloid plexus. (Scale bar - 50μm).

Figure 3.3.

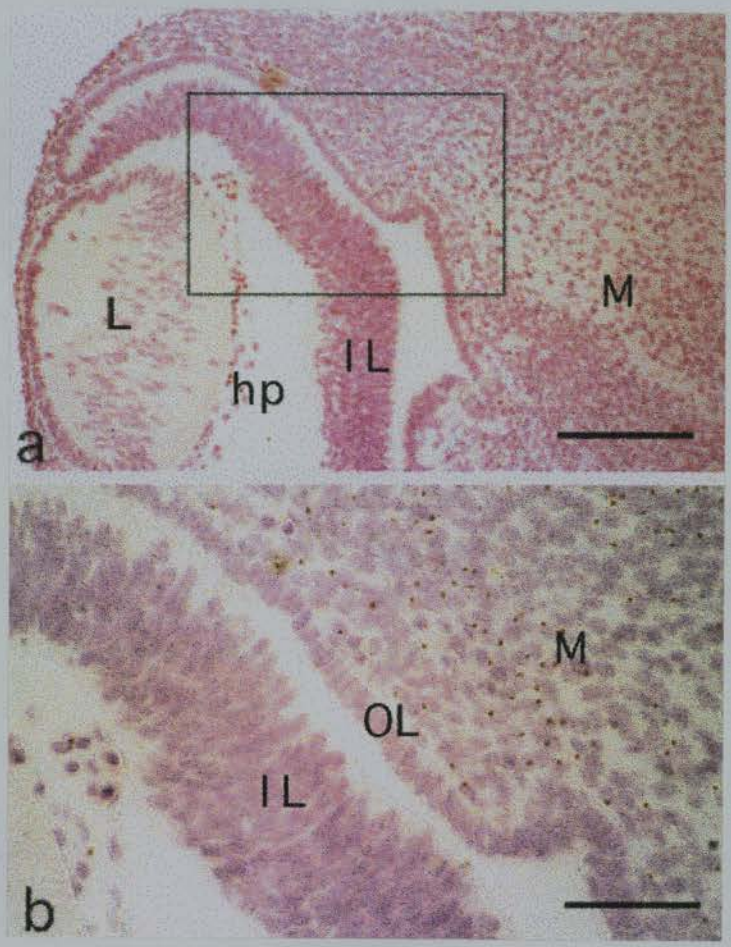

Although the two E14.5 *Sey*^{Neu}*/Sey* ↔+/+ chimaeras produced were not examined using the detailed scoring system devised for the E12.5 *Sey*^{Neu}*/Sey* ↔+/+ chimaeras, histological examination showed similar phenotypes to their E12.5 counterparts. *Sey*^{Neu}*/Sey* cells in these E14.5 *Sey*^{Neu}*/Sey*↔+/+ chimaeras did not contribute to the retinal pigment epithelium, and where RPE was present it was composed of entirely +/+ cells.

Sey^{Neu}*/Sey* cells were able to contribute to the "outer layer" of the optic cup in significant numbers (see Table 3.1., - JC56 left eye; 38.2%, JC61 right; 19.3% and JC48 left; 33.3%). However, these cells were never observed to be contributing to a normal RPE cellular monolayer. Where present, *Sey*^{Neu}*/Sey* cells formed thickened regions often ectopically situated. *Sey*^{Neu}*/Sey* cells were able to make significant contribution to the abnormal eyes possessing no lens tissue (JC48 right; 18.1%, JC17 left; 45.6% and JC17 right; 29.6%).

It appears significant that areas of RPE containing only +/+ cells are only found in conjunction with areas of +/+ 'inner layer'. This indicates that only optic cup cells able to express *Pax6* are able to initiate a normal developmental pathway for the outer layer of the optic cup. Particularly, where *Sey*^{Neu}*/Sey* cells were present in the outer layer of the optic cup in *Sey*^{Neu}*/Sey* ↔+/+ chimaeras, they could be flanked by histologically normal RPE on either side and situated external to an area of inner layer containing +/+ cells. Even when surrounded by a "normal" optic cup environment, *Sey*^{Neu}*/Sey* cells were unable to differentiate a normal RPE-like unicellular layer (see Figure 3.4.). It is therefore possible that development of RPE and interaction with +/+ inner layer may be inter-dependent in *Sey*^{Neu}*/Sey* ↔+/+ chimaeras.

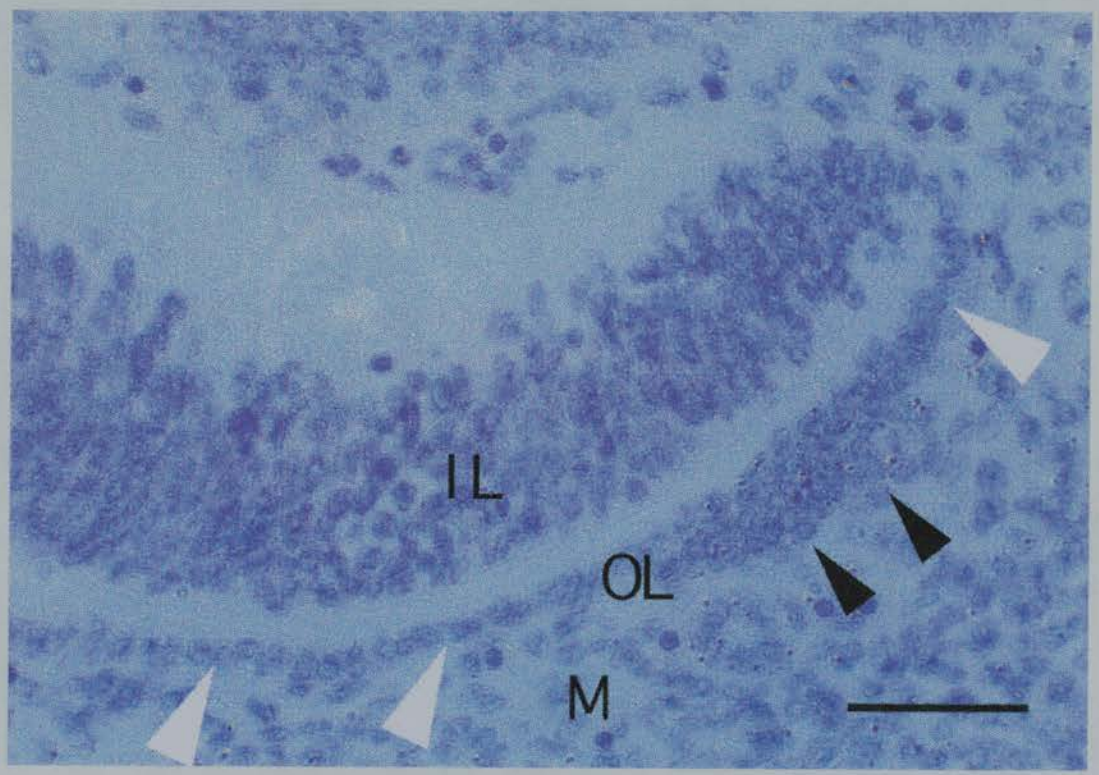

Figure 3.4. Histological section showing the right eye of $Sey^{Neu}/Sey \leftrightarrow +/+$ chimaera JC56. Hybridisation signal can be observed in the mesenchyme and a small area of disorganised, hyperproliferative cells in the outer layer of the optic cup (black arrowheads). Adjacent to this area of Sey^{Neu}/Sey cells are areas of +/+ morphologically normal retinal pigment epithelium (open arrowheads). (M) mesenchyme, (IL) inner layer of optic cup, (OL) outer layer of optic cup. (Scale bar - 80μm).

Table 3.2. (Following page) Results from 1-D analysis of % pigmented cells and corrected patch sizes for all genotype groups of chimaeras. Proportion of pigmented cells was analysed using measurements of pigmented patch lengths as a proportion of total length of RPE measured. The average RPE cell size was 9.008 μm, taken as the mean average of 20 cells measured from each chimaera. * No measurements of corrected patch size were available for the left eyes of chimaeras JC57 and JC22 as pigmentation was 100% in both of these cases making analysis impossible.

† For technical reasons, the estimated mean patch lengths and corrected mean cells per patch are equal for pigmented and albino patches when the patches are equal in number.This analysis does not, therefore, allow comparison between pigmented and albino patches but is suitable for comparison of like patches (e.g. all pigmented patches) between different genotypes of chimaeras. See West, (1976) for further details.

			% Pigmented cells	
Chimaera	**Genotype**	**Mean Fetal % GPI1B**	**Left eye**	**Right eye**
JC53	*Sey*/+ ↔+/+	20.1	7.9	8.9
JC54	*Sey*/+ ↔+/+	51.9	54.5	45.0
JC24	*Sey*/+ ↔+/+	54.0	38.4	30.7
JC21	*Sey*/+ ↔+/+	80.2	89.0	90.9
JC62	Sey^{Neu}/+/↔+/+	60.1	60.6	63.5
JC93	Sey^{Neu}/+/↔+/+	90.9	98.7	100
JC52	Sey^{Neu}/+ ↔+/+	96.5	97.8	99.1
JC45	+/+ ↔+/+	31.1	21.1	26.4
JC58	+/+ ↔+/+	61.0	56.1	58.4
JC49	+/+ ↔+/+	74.0	87.7	88.1
JC22	+/+ ↔+/+	79.6	86.7	89.5

Table 3.2. Analysis of correlation between left and right eye pigment in E12.5+/+ ↔+/+, Sey^{Neu}/+ ↔+/+ and *Sey*/+ ↔+/+ chimaeras as determined by 1-D measurements of single histological sections and mean fetal % GPI1B using Kendall Rank Correlation coefficient test. (Kendall's Rank Sum Correlation: Left eye pigment; τ= 0.8545, P=0.0003; right eye pigment; τ= 0.8182, P=0.0005).

Where areas of +/+ 'outer layer' cells were present, the associated +/+ 'inner layer' tissue often appeared to be morphologically normal. However, areas of morphologically abnormal +/+ 'inner layer' cells were also present without associated RPE-like tissue. Wherever areas of *Sey^{Neu}/Sey* were present, these appeared spatially and developmentally disorganised.

3.3.4. Cell mixing in the optic cup

The most striking phenomenon observed in the optic cups of the E12.5 *Sey^{Neu}/Sey* ↔+/+ chimaeras was that *Sey^{Neu}/Sey* and +/+ cells were segregated into distinct and highly separate areas (see Figure 3.2., Figure 3.5. a and b, also Figures 3.6., 3.7. and 3.8.). When these distinct areas of *Sey^{Neu}/Sey* and +/+ cells were analysed using the counting criteria devised for the optic cup discussed in Chapter 2, results showed that no +/+ cells could be detected within the areas of *Sey^{Neu}/Sey* cells and only a low level of transgenic signal (<0.03%) was observed in the areas containing predominantly+/+ cells, consistent with a low level of false positives. The boundaries between these areas of *Sey^{Neu}/Sey* and +/+ cells were highly distinct, containing little or no cell mixing (see Figure 3.5b).

Using the 1-D "grid" spatial analysis methodology described in section 3.2.1., it was possible to demonstrate this cell segregation more objectively (see Table 3.3.). Only a limited number of optic cups from the *Sey^{Neu}/Sey* ↔+/+ chimaera group could be analysed as some possessed no areas of Tg+ve cells. The results of the 1-D grid analysis showed that the number of Tg+ve cells per corrected patch length in the *Sey^{Neu}/Sey* ↔+/+ chimaeras (6.51) was significantly larger than for the other genotype groups (+/+ ↔+/+ ; 1.22; and *Sey*/+ ↔+/+ plus *Sey^{Neu}*/+ ↔+/+ ; 1.24).

Furthermore, the smallest value for the *Sey*^{Neu}*/Sey* ↔+/+ chimaera group was larger than any of the control corrected mean patch lengths.

The non-parametric Man-Whitney U showed that there was no significant difference in number of cells per patch between the +/+↔+/+ group and the combined*Sey*/+↔+/+ plus *Sey*^{Neu}/+↔+/+ groups. However, a significant difference was observed in number of cells per patch between the *Sey*^{Neu}*/Sey* ↔+/+ chimaera group and both +/+↔+/+. (P<0.01) and *Sey*/+↔+/+ plus *Sey*^{Neu}/+↔+/+ groups, (P<0.001), [see Appendix XII.II.II. for full data]

Figure 3.5. (Following page) **a)** Histological sections showing the left eye of *Sey*^{Neu}*/Sey*↔+/+ chimaera JC17. Hyperproliferation of the optic cup tissue creates a multi-layered structure in the absence of lens development. The optic cup is divided into large domains of almost entirely +/+ cells, those lacking a hybridisation signal, and *Sey*^{Neu}*/Sey* cells, those exhibiting hybridisation to the β-globin transgene probe. (Scale bar - 100μm). **b)** Enlargement of the area indicated in a) showing highly distinct boundary (black arrowhead) between area of +/+ cells and area of *Sey*^{Neu}*/Sey* cells. (Scale bar - 50μm).

Figure 3.5.

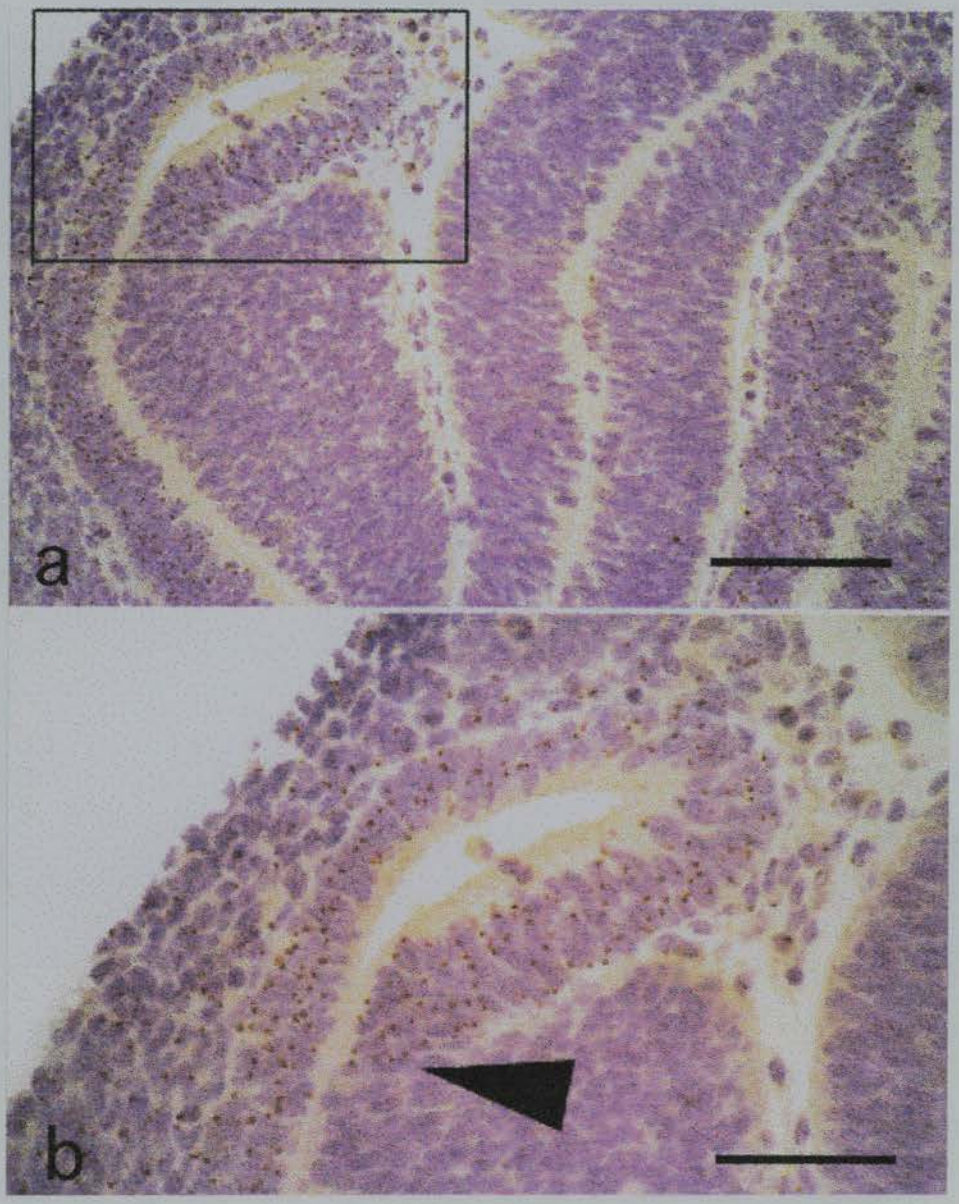

Table 3.3. (Following page) Results from 1-D analysis of % Tg+ve cells in the optic cups of all genotype groups of chimaeras. Tg+ve cells were analysed by superimposing a uniform hexagonal grid over the tissue section, the minor axis of which being approximately on cell size (9.25μm). A single continuous band of cells was scored around the edge of the optic cup and the parameters of corrected patch length and cells per corrected patch length were calculated. Note that the average number of cells per patch ranges from 1-2 cells. Using the non-parametric Mann-Whitney U test to compare the corrected patch sizes of *Sey*/+ x *Sey*^{Neu}/+ derived cells (Tg+ve) between genotype groups we find no significant difference in corrected patch size between the +/+↔+/+ and *Sey*/+ ↔+/+ and Sey^{Neu}/+↔+/+ chimaera groups, when the latter are compared together. However, a significant difference is observed between the *Sey*^{Neu}/*Sey* ↔+/+ chimaera group and both +/+↔+/+ (P=>0.001) and *Sey*/+ ↔+/+ and Sey^{Neu}/+↔+/+ groups (P=>0.01).

Chimaera	% mean fetal GPI1B	Genotype (χ ↔ +/+)	Eye Left/Right	Cells per mean corrected patch lenght (μm) Tg+ve cells
JC48	59.2	*Sey*^{Neu}/*Sey*↔ +/+	L	3.61
JC48	59.2	*Sey*^{Neu}/*Sey*↔ +/+	R	6.64
JC61	46.9	*Sey*^{Neu}/*Sey*↔ +/+	L	3.60
JC17	80.2	*Sey*^{Neu}/*Sey*↔ +/+	L	4.42
JC17	80.2	*Sey*^{Neu}/*Sey*↔ +/+	R	14.32
JC45	31.3	+/+↔+/+	L	1.05
JC24	54.1	+/+↔+/+	L	2.11
JC24	54.1	+/+↔+/+	R	1.48
JC22	79.6	+/+↔+/+	L	1.03
JC22	79.6	+/+↔+/+	R	1.34
JC58	61.0	+/+↔+/+	L	1.12
JC58	61.0	+/+↔+/+	R	1.0
JC49	74.5	+/+↔+/+	R	1.0
JC49	74.5	+/+↔+/+	L	0.85
JC53	20.1	*Sey*/+↔ +/+	R	1.28
JC54	51.9	*Sey*/+↔ +/+	L	1.48
JC54	51.9	*Sey*/+↔ +/+	R	1.98
JC21	80.2	*Sey*/+↔ +/+	L	0.82
JC25	75.8	*Sey*/+↔ +/+	L	1.28
JC25	75.8	*Sey*/+↔ +/+	R	0.95
JC57	83.05	*Sey*^{Neu}/+↔ +/+	R	0.78
JC62	60.1	*Sey*^{Neu}/+↔ +/+	L	1.58
JC62	60.1	*Sey*^{Neu}/+↔ +/+	R	1.06

Table 3.3. Results of 1-D analysis of % Tg+ve cells in the optic cups of all genotype groups of chimaeras.

3.3.5. 1-D analysis of RPE in all chimaera genotype groups

When considered together, *Sey*/+↔+/+ , *Sey*^{Neu}/+ ↔+/+ and +/+↔+/+ chimaera groups showed positive correlations bteween % pigment in histological sections of left and right eyes and the mean percentage fetal GPI1B (Left eye % pigment correlated to % GPI1B, P= 0.0003; right eye % pigment correlated to % GPI1B, P= 0.0005) [see Table 3.2].

When the corrected mean patch length of pigmented cells was compared between genotype groups using the Mann-Whitney U test, no significant difference was observed (See Appendix XII.II). The only significant variant was JC57 which showed very large corrected patch sizes of pigmented cells. This was probably the result of a sampling error because the high overall *Sey*^{Neu}/+ x *Sey*/+ derived cell contribution resulted in only a small number of patches in the histological section used for analysis.

Figure 3.6. (Following page) 3-D reconstruction of left eye of *Sey*^{Neu}/*Sey*↔+/+ chimaera JC48. Areas of +/+ cells (pink), and *Sey*^{Neu}/*Sey* cells (blue) have been highlighted. The lens is indicated in (yellow) allowing 3-dimensional visualisation of the structure. 3-D reconstruction allows visualisation of the large patches of +/+ cells and *Sey*^{Neu}/*Sey* cells, showing these areas to be highly distinct and larger than had been intimated from examination of histological sections. Note that the areas of *Sey*^{Neu}/*Sey* cells (blue) are integral to the structure as a whole and not isolated islands of tissue.

Figure 3.6.

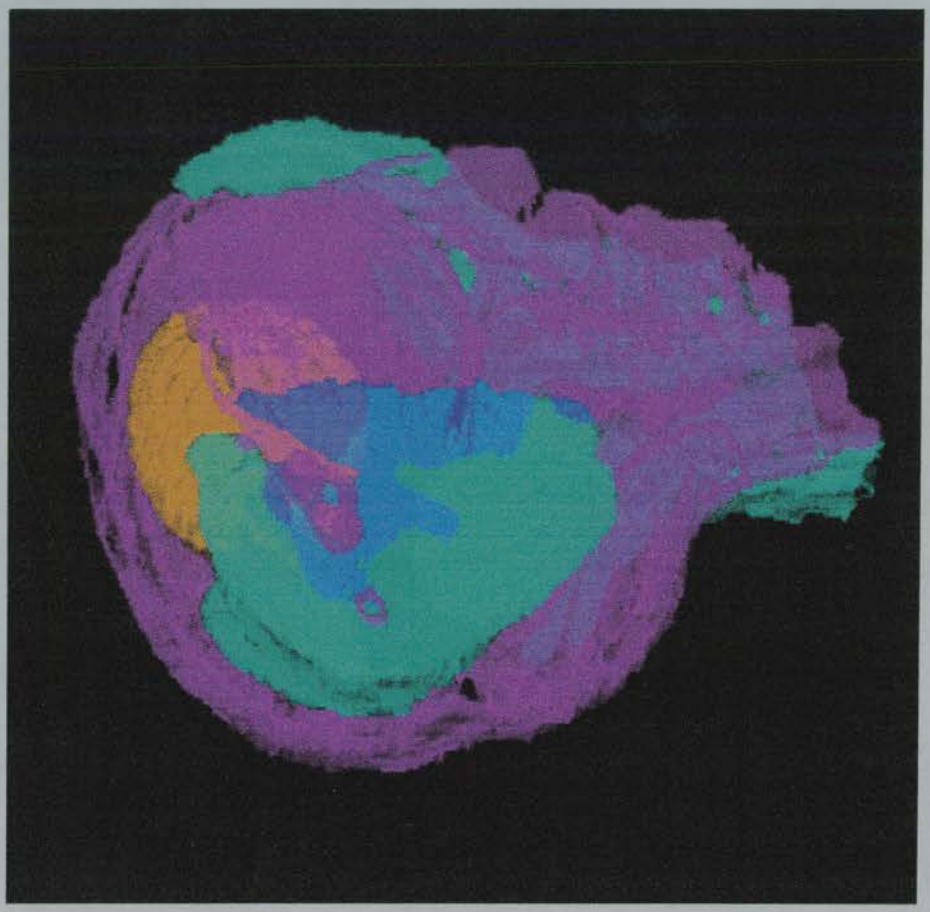

3.3.6. 3-D reconstruction of chimaeric eyes

In order to attempt to elucidate the nature of the segregation phenomenon, computerised 3-D reconstruction was performed on the left and right eyes of chimaera JC48. Due to the methodology employed for indication of cell type, i.e. blocking in a single colour areas of predominantly Sey^{Neu}/Sey and +/+ cells, reconstruction of the right eye of chimaera JC48 could only be visualised as an amorphous tissue mass. The blocking method proved too insensitive for recontruction of this highly convoluted structure as the technique could not highlight internal shape to give a three-dimensional effect. This procedure proved to be much more successful for the left eye of chimaera JC48 proved because a small lens was present which highlighted the three dimensional structure of the eye (see Figure 3.6.).

Visualisation using 3-D reconstruction proved the cell segregation to be much more distinct than had been apparent from histological sections alone. Cells of +/+ and Sey^{Neu}/Sey genotype were separated into large areas in a proximal to distal orientation. These segregated areas extended from the rim of the optic cup, through the outer layer region and along the optic stalk (see Figure 3.6.). Areas of Sey^{Neu}/Sey and +/+ cells, which had previously appeared to be ectopically positioned outside the abnormal optic cup structure, proved to be continuous with the structure as a whole and not isolated islands of tissue.

The lens was observed to be partially enclosed within the abnormal optic cup structure, with areas of +/+ cells extending over the normal margin of the optic cup rim (see Figures 3.7. and 3.8.). The 3-D reconstruction allowed visualisation of the complete structure of the abnormal eye, showing that the areas of Sey^{Neu}/Sey cells were integral to the eye structure as a whole and not merely randomly proliferating tissue areas as had been suggested from viewing histological sections alone.

Figure 3.7. (Following page) Excavation 3-D reconstruction showing left eye of *Sey*^{Neu}*/Sey*↔+/+ chimaera JC48. The image constructed in Figure 3.6. has been dissected with a 'box' into the middle of the image with 28μm sections stacking to complete the final construction. The 'greyscale' image allows visualisation of the position of the highlighted tissues within the surrounding mesenchyme and in orientation to the overlying ectoderm of the head.

Figure 3.8. (Following page but one) Excavation 3-D reconstruction showing left eye of *Sey*^{Neu}*/Sey*↔+/+ chimaera JC48. A similar method to that observed in Figure 3.7. The 'greyscale' image has been removed and the image manipulated in the opposite orientation. The image viewed in Figure 3.7. is shown stacking transverse 28μm sections. Removal of the 'greyscale' image allows clear orientation of the tissues relative to each other in space. This technique allows orientation of the lens relative to the surrounding abnormal tissue, note that +/+ tissue encloses the lens at the anterior surface.

Figure 3.7.

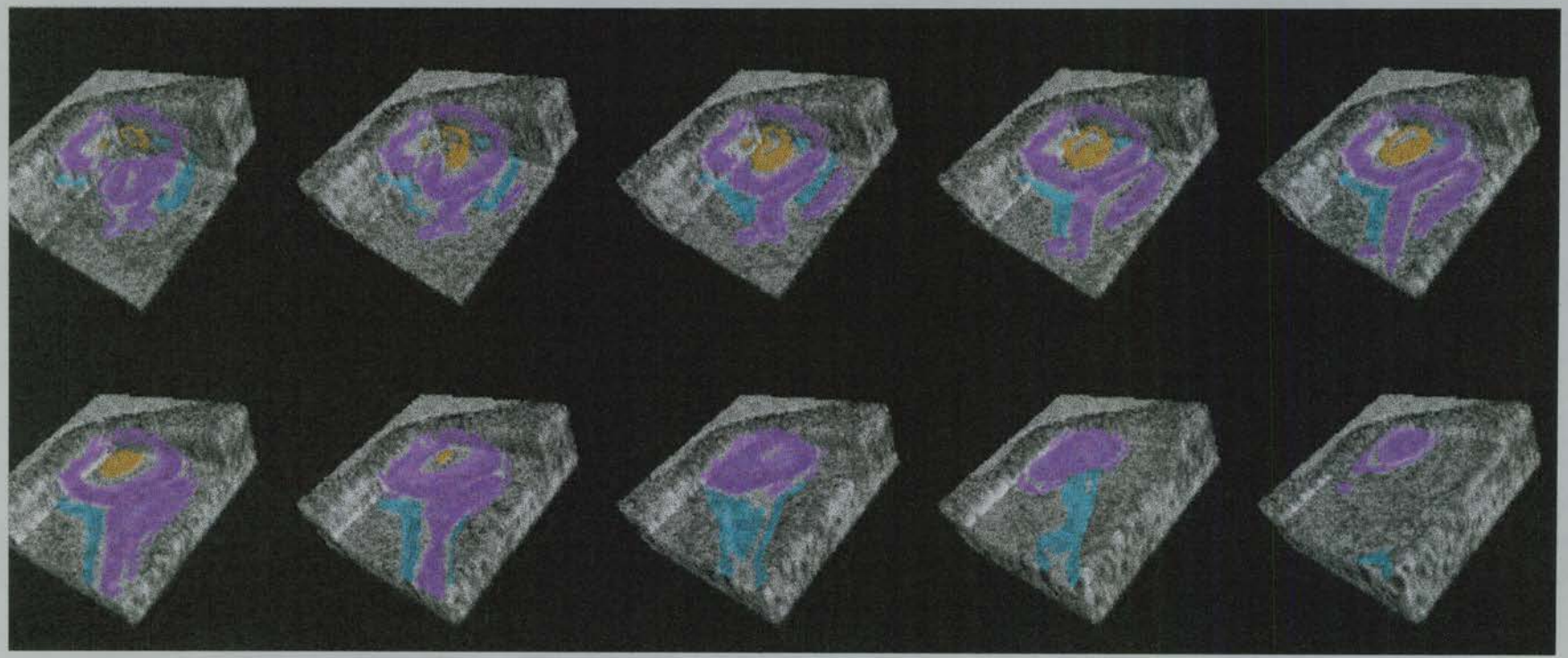

Figure 3.8.

Although the basis of chimaera experiments is to allow two genetically distinct cells types to interact *in vivo*, it is usual to see extensive cell mixing in most tissues of a chimaera. The level of cell segregation observed in these $Sey^{Neu}/Sey \leftrightarrow +/+$ chimaeras is highly unusual and indicates either an extremely low level of cell mixing or active segregation to achieve such an effect. Although it is not possible to define from this study alone the mechanism by which this extreme cell segregation might occur, the results indicate that *Pax6* must be playing a role in specification at the cell surface.

3.4. Discussion

Examination of the optic cups of $Sey^{Neu}/Sey \leftrightarrow +/+$ chimaeras indicates that *Pax6* may be playing a role in four major areas of optic cup development, formation of the inner layer of the optic cup, formation of the RPE, cell-to-cell interaction and proliferation of optic cup tissue.

3.4.1 Roles for *Pax6* in formation of the inner layer

As shown in Table 3.1, in those eyes of $Sey^{Neu}/Sey \leftrightarrow +/+$ chimaeras that possessed a lens, Sey^{Neu}/Sey cells were found to be almost completely excluded to the outer layer of the optic cup whereas in those eyes that do not contain lens tissue, the large patches of +/+ and Sey^{Neu}/Sey cells appeared randomly distributed. This indicates a possible cell autonomous role for *Pax6* in development of the inner layer of the optic cup prior to E12.5 days. Subsequent inner layer development may also be mediated through interaction of the developing optic cup with the forming lens after lens induction has occurrred.

Early tissue culture experiments focused on determining whether contact between optic vesicle and surface ectoderm was required for lens induction (Spemann, 1938). Contact was determined as functionally redundant for lens induction as lens cell differentiation was able to occur *in vitro* in the absence of neuroectodermal tissue (Spemann, 1912a; 1919; Rabl, 1898; Lehmann, 1933; Saha *et al.*, 1989; 1992; Grainger, 1992). Although it is now accepted that the optic vesicle is not required for lens induction, as eye development progresses, interaction between lens and optic cup is vital for both lens and retinal differentiation.

The lens/optic cup interaction plays a role in ensuring functional morphogenesis of the eye structure as a whole. The inverse relationship between percentage of Sey^{Neu}/Sey cells and lens size in the $Sey^{Neu}/Sey \leftrightarrow +/+$ chimaeras has been discussed in the previous chapter. Although lens size appears to be directly related to the number of cells within the presumptive lens placode region capable of undergoing transformation, there may also be a reciprocal effect on the developing optic cup. It is important to note that in those $Sey^{Neu}/Sey \leftrightarrow +/+$ chimaeric eyes where lenses were present but of small size, normal structural integrity of the eye was maintained in that optic cup structures were seen to be confluent with the smaller lens. These optic cups maintained contact with the lens at its lateral margins regardless of lens size. Although the mechanisms are highly complex, the overall picture is one of a constant reciprocal interaction between the lens and the developing retina in order that the final eye structure should be functional.

Interdependence between lens and retinal tissues is observed with regard to overall organ size in $Sey^{Neu}/+$ and $Sey/+$ heterozygous animals. The micropthalmic phenotype is produced by a reduction in retinal size coincident to the reduction in lens size. Lens ablation studies also show similar results to $Sey^{Neu}/Sey \leftrightarrow +/+$ chimaeras with regard to retinal morphology (Harrington *et al*, 1991; Breitman *et al*; 1987; 1989)

although in these cases lens induction had occurred prior to lens cell ablation. Interestingly, classical experiments by Coulombre and Coulombre (1963; 1964) also indicated a lens/retina interdependence, in that if the neural retina was ablated then lens development ceased. However, if a small area of neural retina was left then lens growth was observed to be proportional to the area of neural retina remaining (Coulombre and Coulombre, 1963; 1964).

Therefore, it appears that normal interaction between the lens and optic cup is required for eye development and that the restriction of *Sey*^{Neu}*/Sey* cells from the inner layer of the optic cup in *Sey*^{Neu}*/Sey*↔+/+ chimaeras where lens development had ocurred may be an indication of this normal interaction. Exclusion of *Sey*^{Neu}*/Sey* cells from the inner layer of the optic cup also definines a cell autonomous role for *Pax6* in development of this tissue.

3.4.2. Cells deficient for *Pax6* are unable to contribute to RPE

Analysis of *Sey*^{Neu}*/Sey*↔+/+ chimaeras shows that *Sey*^{Neu}*/Sey* cells are unable to contribute to morphologically normal retinal pigment epithelium (RPE). Although in all the eyes (both normal and abnormal) of *Sey*^{Neu}*/Sey* ↔+/+ chimaeras RPE can be identified, *Sey*^{Neu}*/Sey* cells were never observed contributing to an RPE-like cellular monolayer. When *Sey*^{Neu}*/Sey* cells were present in the outer layer of the optic cup, they formed large thickened areas with disorganised cell morphology, never exhibiting the normal simple cuboidal structural characteristics of differentiated RPE. Pigment formation was not observed in any of the seven *Sey*^{Neu}*/Sey* ↔+/+ chimaeras although pigment formation is usually complete by E12.5.

Two possible explanations could account for in inability of *Sey*^{Neu}*/Sey* cells to form RPE. It was possible that the *Sey*^{Neu}*/Sey* ↔+/+ chimaeras were immature relative to

their pigmented chimaeric siblings and that therefore pigment production had not yet been initiated in the cells destined to become RPE. However, this was not supported by comparison of hindlimb development (used as an index of developmental stage). The median developmental stage was the same for all groups of chimaeras.

The second possibility was that the RPE tissue itself might be dysmature in the *Sey*^{Neu}*/Sey* ↔+/+ chimaeras, that is, showing a relative immaturity to other tissues in the chimaeric eyes. However, examination of E14.5 *Sey*^{Neu}*/Sey* ↔+/+ chimaeras also showed a lack of pigmentation and inability of *Sey*^{Neu}*/Sey* cells to contribute to morphologically normal RPE, thus ruling out a relative cellular retardation and indicating a possible developmental arrest of *Sey*^{Neu}*/Sey* cells prior to pigment formation.

The results show that *Sey*^{Neu}*/Sey* cells are unable to form retinal pigment epithelium even in the presence of a +/+ cellular environment. Pigment formation was not observed in those *Sey*^{Neu}*/Sey* ↔+/+ chimaeras possessing only a small contribution of *Sey*^{Neu}*/Sey* cells. Overall, these results suggest a cell autonomous role for *Pax6* in formation of the RPE.

It had been previously shown that a neuroectodermal/mesenchymal interaction was necessary for differentiation of RPE in the wild-type eye (Stroeva, 1960). The right eye of JC17 (see Figure 3.1.) indicates that surface epithelium may also be able to provide the signals necessary for RPE development as ectopically located RPE in this eye is present at both neuroectodermal/mesenchyme and neuroectodermal/epithelial junctions. However, it is possible that small amounts of mesenchymal cells present under the surface ectoderm are capable of providing sufficient inducing signal for RPE formation to occur.

More recent tissue culture experiments have highlighted the requirement for normal inner layer/outer layer interaction for RPE development (Buse *et al.*, 1993). Buse (1993) suggested that the prospective neural retina was able to induce RPE development in culture. In $Sey^{Neu}/Sey \leftrightarrow +/+$ chimaeras analysed at both E12.5 and E14.5, morphologically normal RPE, containing only +/+ cells, was never observed internal to optic cup structures even in the most abnormal convoluted eyes. This supports the hypothesis that both an 'internal' and 'external' signal are required to give orientation to the inner and outer layer before RPE formation will occur, thus preventing RPE formation inappropriately within the eye structure.

The inability of Sey^{Neu}/Sey neurectoderm to form RPE in $Sey^{Neu}/Sey \leftrightarrow +/+$ chimaeras gives a clue to the timing of the primary defect in cells of the neuroectoderm unable to produce functional *Pax6* . Although a number of studies have reported that multiple extrinsic factors determine cell fate in the retina after differentiation of the inner and outer layers has occurred, (Watanabe *et al.*, 1990; Altshuler *et al.*, 1992; 1993; Kelley *et al.*, 1994; Cepko *et al.*, 1996), little work has been done to elucidate early factors involved in the primary steps towards optic cup development. It cannot be determined from the $Sey^{Neu}/Sey \leftrightarrow +/+$ chimaeras analysed in this chapter alone whether *Pax6* is required for early inner layer/outer layer determination of the optic vesicle or whether the Sey^{Neu}/Sey cells have developmentally arrested at a stage prior to inner layer/ outer layer formation. However, the results identify a requirement for *Pax6* in early development of both the inner layer and outer layers of the optic cup.

3.4.3. Proliferation in the optic cup

By E12.5, the *Sey/Sey* optic cup is highly abnormal and very retarded, having lost contact with the overlying surface ectoderm of the head. No recognisable inner layer/outer layer structure is apparent and the tissues that are present resemble a

truncated optic stalk. The hyperproliferation of optic cup tissue in the *Sey^{Neu}/Sey* ↔+/+ chimaeras was therefore unexpected as the primary defect in optic cup development in the *Sey/Sey* homozygous fetus had been previously suggested to be due to lens absence (Hogan *et al.*, 1986; 1988; Fujiwara *et al.*, 1994; Grindley *et al.*, 1995).

Optic cup structures in *Sey^{Neu}/Sey* ↔+/+ chimaeras were seen to be highly variable in the level of dysmorphology observed (see Table 3.1). The most severe morphology was observed in those eyes which did not possess any lens tissue (JC17 and 50 both eyes and the right eye of JC48). In these lens-less eyes, an extreme over proliferation of both *Sey^{Neu}/Sey and* +/+ cells was observed with the resulting convoluted optic cup structures often exceeding the normal limits of the eye capsule to extend beyond the margin of the head. Although some areas of optic cup could be observed to have both an inner and outer layer, identifiable by histological definition rather than orientation, much of the abnormal optic cup tissue present was highly disorganised showing few or no normal developmental characteristics.

Hyperproliferation phenotypes, similar to those observed in the *Sey^{Neu}/Sey* ↔+/+ chimaeras, have been reported in lens ablation studies although by the nature of these experiments lens induction has been allowed to occur prior to loss of lens tissue. Generation of transgenic mice in which the α-crystallin synthesising cells of the lens had been ablated resulted in a complete absence of lens structures (Kaur *et al.*, 1989). Kaur *et al.* reported proliferation of the retina beyond the normal margins of the ciliary body whilst the a normal laminar structure was maintained in this hyperproliferative retinal tissue. Similar normal laminar structure was observed in the hyperproliferative retina reported in a similar ablation experiment by Breitman *et al* (1989). Laminar differentiation was also shown in an early lens morphogenesis mutant, the *aphakia* mutant mouse, which exhibits convoluted retinal structures (Zwaan and Webster,

1984; 1985). Therefore, published data and results of this study indicate that hyperproliferation of neural retinal tissue occurs in response to loss of lens tissue.

Presence of a lens in eyes of *Sey*^{Neu}*/Sey* ↔+/+ chimaeras appears to induce reciprocal normal +/+ tissue formation in the inner and outer layers of the optic cup as discussed previously. However, the two cell genotypes present in the optic cup were seen to respond differently to the presence of a lens. The higher the contribution of *Sey*^{Neu}*/Sey* cells to the fetus, the greater the level of dysmorphology in the optic cup, even though the actual contribution of *Sey*^{Neu}*/Sey* cells to the overall optic structure was variable (see Table 3.1 for total optic cup hybridisation index data). Optic cups in *Sey*^{Neu}*/Sey* ↔+/+ chimaeras both with and without lenses showed areas of +/+ cells which were able to approximate the normal inner layer/outer layer 'double cup' identity, but not all areas of +/+ cells were seen to assume this normal morphology. The more dysmorphic the structure as a whole the greater the amount of disorganised +/+ tissue present.

One possible mechanism for the hyperproliferation observed in optic tissue of *Sey*^{Neu}*/Sey* ↔+/+ chimaeras could be a loss of apoptotic function in all *Sey*^{Neu}*/Sey* cells and those +/+ cells unable to assume normal inner layer/outer layer morphology. A large amount of cell death is known to occur during differentiation of the wild-type retina (Young, 1984). Although the roles *Pax* genes might play as mediators of apoptosis are as yet undetermined, some 50% of ganglion and amacrine cells undergo apoptosis during retinal development. *Pax6* has been shown to be expressed in neuronal progenitor cells as well as ganglion and amacrine cells post-differentiation (Hitchcock *et al.*, 1996; Beleckly-Adams *et al.*, 1996). If this control mechanism were lost in cells unable to express functional *Pax6,* or indeed, if these cells were unable to reach the stage of development at which these apoptotic processes begin, this could result in the hyperproliferation phenotypes observed in these *Sey*^{Neu}*/Sey* ↔+/+

chimaeras. The latter would fit the data most conveniently as ganglion cells are the first to be born in the developing retina, a loss of this cell type would add weight to an early retinal defect, such as suggested by the results of this study.

Therefore, the mechanisms by which *Pax6* is mediating the hyperproliferation of both +/+ and *Sey*^{Neu}*/Sey* cells remains uncertain. The hyperproliferation phenomenon and loss of developmental competence to assume the normal inner layer/outer layer optic cup morphology may be closely related. If both *Sey*^{Neu}*/Sey* and +/+ cells were locked into a hyperproliferative phase of development this could give rise to the hyperproliferative phenotypes observed in the chimaeras. As hyperproliferation in *Sey*^{Neu}*/Sey* cells must be indirectly due to a loss of functional *Pax6* product it is possible that these cells may be directly or indirectly influencing their +/+ neighbours and inducing a loss of appropriate (possibly *Pax6* mediated) developmental control. Although role of *Pax6* in this hyperproliferative process cannot be defined from these studies alone, both the presence of lens tissue and the relationship between the inner and outer layers of the optic cup affects proliferation and development of +/+ cells in the optic cups of *Sey*^{Neu}*/Sey* ↔+/+ chimaeras.

3.4.4. Cell-to-cell interaction in the optic cup

Perhaps the most striking effect observed in the optic cup tissue of the *Sey*^{Neu}*/Sey* ↔+/+ chimaeras was the extreme segregation of +/+ and *Sey*^{Neu}*/Sey* cells into highly distinct areas. As has already been discussed, *Sey*^{Neu}*/Sey* cells appear to be preferentially excluded from the inner layer of the developing cup and therefore the majority of *Sey*^{Neu}*/Sey* cell patches are located in the outer layer of the *Sey*^{Neu}*/Sey* ↔+/+ chimaeric optic cups. Also, *Sey*^{Neu}*/Sey* cells appear to be unable to make the transition from primitive neurectoderm to RPE in both E12.5 or E14.5

Sey^{Neu}*/Sey*↔+/+ chimaeras. Overall, this data indicates that the *Sey*^{Neu}*/Sey* cells are either severely retarded in their development or arrested at a stage prior to E12.5, although they maintain the ability to survive and proliferate.

Reasons for loss of ability of *Sey*^{Neu}*/Sey* cells to mix with +/+ cells may be due to inappropriate cell surface properties. The likely candidates to be affected at the cell surface by loss of *Pax6* function are the neural cell adhesion molecules (N-CAM's) and adhesive extracellular matrix molecules. Although the N-CAM expression pattern has been reported to be abnormal (Moase and Trasler, 1991) in the *Pax3* gene mutant, the *splotch* mouse (Epstein *et al.*, 1991), no similar expression studies have been performed in the small eye mutant.

Defects in cell adhesion between *Sey*^{Neu}*/Sey* and +/+ cells may be the most plausible explanation for the extreme cell segregation observed in the optic cups of *Sey*^{Neu}*/Sey* ↔+/+ chimaeras. *Pax6* has not only been shown to transactivate its own promoter and therefore regulate its own transcription (Plaza *et al.*, 1993; Czerny and Busslinger, 1995) but is also known to control, both directly and indirectly, transcription of other genes and transcription factors (Grindley *et al.*, 1995; Cvekl *et al.*, 1995; Wistow *et al.*, 1995; Kantorow *et al.*, 1995; Cvekl and Piatigorsky, 1996). *Pax6* has been shown to bind to the promoter region of the neural cell adhesion molecule L1 (Chalepakis *et al.*, 1994) and it has been recently reported that *Pax6, Pax1* and *Pax8* are able to bind to two paired domain binding site sequences within the N-CAM promoter (Chalepakis *et al.*, 1993; Holst *et al.*, 1994). These experiments support a hypothesis that *Pax6* might play a role in mediating cell-to-cell interactions at the cell surface.

Evidence supporting a possible loss of N-CAM function in small eye homozygous mutant cells comes from studies showing dynamic, transient N-CAM expression in

developing lens, otic and pharyngeal placode regions and particularly their underlying mesenchyme prior to tissue differentiation (Richardson *et al.*, 1987; Miragall *et al.*, 1989). Perhaps more pertinent support for this hypothesis comes from work using anti-N-CAM antibodies in retinal explant cultures (Hoffman *et al.*, 1986; Rutishauser, 1984). These experiments showed that in the presence of anti-N-CAM antibodies, explanted retinal cultures were unable to form the laminar layers of the retina whilst antibody-free cultures were able to differentiate all retinal layers. Similar results have been reported using anti-Ng-CAM antibodies, this antigen appearing to cross react with the L1 antigen (Hoffman *et al.*, 1986; Grumet *et al.*, 1984; 1985) to which *Pax6* has been shown to bind (Chalepakis *et al.*, 1994). However, it is difficult to make predictions as to the mediating role that *Pax6* may be playing with regard to the neural cell adhesion molecule family as no expression studies have yet been undertaken in the small eye homozygous fetus.

Cell clonality and clonal size in the optic cup could also be influencing the size of patches observed in the optic cups of the $Sey^{Neu}/Sey \leftrightarrow +/+$ chimaeras. Experiments injecting retroviral marked retinal cell precursors into undifferentiated retina have shown not only that these precursors cells can produce all of the cell types of the differentiated neural retina, but also that a wide range of clone size is generated (Turner and Cepko, 1987; Holt *et al.*, 1988; Turner *et al.*, 1990; Fekete *et al.*, 1994; Reese *et al.*, 1995). Similarly, the clonal nature of the neural retina could also provide a source for the highly discrete boundaries observed between the Sey^{Neu}/Sey and +/+ cells as highly discrete clonal boundaries have also been observed in the neurepithelial derived retinal tissue in other chimaera experiments (Williams and Goldowitz, 1992). It is possible that if the effect of loss of *Pax6* control of cell surface properties was early and widespread in the neurectoderm, only minor changes in cell adhesion might be needed to alter cell growth properties sufficiently for 'normal' clonal growth to produce patches of the the size observed in the $Sey^{Neu}/Sey \leftrightarrow +/+$ chimaeras.

3.5. Conclusions

Overall, the results obtained from analysis of optic cups of both E12.5 and E14.5 *Sey*^{Neu}*/Sey* ↔+/+ chimaeras indicates that *Pax6* is playing a role in three major areas of optic cup morphogenesis. Firstly, an effect is observed on proliferation of optic cup tissue with an indirect role for the lens indicated in this phenomoenon. Secondly, a cell autonomous effect for *Pax6* is shown in both the inner and outer layers of the optic cup, and thirdly, a role for *Pax6* is identified in cell-to-cell interaction. Overall, these results indicate an early and fundamental requirement for *Pax6* in development of the optic cup.

Chapter 4

Gene expression in the optic cup of *Sey^{Neu}/Sey* ↔+/+ aggregation chimaeras

4.1. Introduction

Results from analysis of *Sey^{Neu}/Sey* ↔+/+ aggregation chimaeras in this study have determined several crucial roles for *Pax6* in development of the mouse eye. Exclusion of *Sey^{Neu}/Sey* cells from the lens and nasal epithelium, discussed in Chapter 2, defined a cell autonomous role for *Pax6* in differentiation of tissue forming placode regions from surface ectoderm. A number of effects were observed in development of the optic cup (see Chapter 3), including a requirement for *Pax6* in development of the inner layer of the optic cup, a cell autonomous effect during development of the retinal pigment epithelium (RPE) and a role in cell-to-cell interaction.

The exact mechanisms by which a single gene product could be involved in such a variety of interactions within a highly complex structure, such as the eye, are difficult to elucidate. However, such diversity of function indicates temporal and cell specific responses both for and to *Pax6* expression. Published data shows that *Pax6* is required throughout eye development; from an early and general action in patterning of the anterior region of the head (Chisholm and Horovitz, 1995; Zhang and Emmons, 1995; Macdonald *et al.*, 1995), to interactions with genes and gene products involved in cell specific developmental processes (Cvekl *et al.*, 1995; Beleckly-Adams *et al.*, 1996; Wistow *et al.*, 1996). *Pax6* has been shown to be involved in its own transcriptional regulation (Plaza *et al.*, 1993; Czerny and Bussliger, 1995) with differential splice products controlling expression within the lens and retina (Kantorow *et al.*, 1996) giving an additional layer of complexity to *Pax6* function.

4.1.1. *Pax6* expression during fetal development

Development of the eye involves complex gene interactions controlling both the cellular and inter-cellular events needed for normal eye morphogenesis. A number of genes have been identified which play crucial roles in development of the eye but *Pax6* is deemed to be the "master gene" of eye development (Cvekl *et al.*, 1996; Halder *et al.*, 1995). Expression of *Pax6* during fetal development has been well studied, the most comprehensive to date by Walther and Gruss (1991) and Grindley *et al.* (1995) [see also Chapter 1].

Expression and cell cultures studies, along with our chimaera studies, indicate fundamental roles for *Pax6* in development of the lens and retina which appear to traverse temporal boundaries. *Pax6* appears to be required for normal induction, differentiation and maintenance from general specification of the lens and optic vesicle forming regions, placode formation, early lens and optic cup development to differentiation of specific cell types in the mature retina.

4.1.2. *Pax6* expression in the small eye (*Sey/Sey*) homozygous fetus

Expression of *Pax6* has been examined in the small eye *Sey/Sey* homozygous fetus (Grindley *et al*; 1995). Although the small eye mutant fetus is unable to produce a functional *Pax6* product, expression of mRNA transcript is still maintained. Grindley *et al.* showed that spatially "normal" *Pax6* expression is observed in the highly abnormal *Sey/Sey* optic vesicle and later optic structures. Where abnormal neuroepithelial structures were observed to form a bi-layered "cup", both layers of this cup were seen to express *Pax6* with no temporal restriction. No expression was

observed in the surface ectoderm of the head in the *Sey/Sey* homozygous mutant embryo (Grindley *et al.*, 1995).

As discussed in Chapters 2 and 3, highly abnormal optic cup development was observed in the $Sey^{Neu}/Sey \leftrightarrow +/+$ chimaeras. Areas of both ectopic and dysmorphic optic cup formation were observed, with Sey^{Neu}/Sey and +/+ cells seen to segregate into large patches. Sey^{Neu}/Sey cells failed to contribute to morphologically normal RPE. These results prompted a number of questions. Namely, were Sey^{Neu}/Sey cells unable to be recruited to RPE development due to a relative dysmaturity or were they fundamentally unable to commit to or carry out this developmental step? Were Sey^{Neu}/Sey cells able to be specified as optic cup or were they developmentally arrested prior to the earliest stage of optic cup formation, that of specification of the inner and outer layers from a multipotent population?

As was indicated in Chapter 3, preliminary analysis of E14.5 $Sey^{Neu}/Sey \leftrightarrow +/+$ aggregation chimaeras showed that Sey^{Neu}/Sey cells were unable to contribute to normal RPE even given extra developmental time in which to do so, thus indicating a cell autonomous role for *Pax6* in development of this tissue. However, analysis by in-situ hybridisation to positionally observe Sey^{Neu}/Sey cells within the highly abnormal optic cup formations in $Sey^{Neu}/Sey \leftrightarrow +/+$ chimaeras did not answer questions as to why these cells are unable to develop into normal RPE.

Therefore, a study was devised to attempt to identify whether a temporal or a developmental deficit was responsible for this loss of developmental potential to become RPE in those Sey^{Neu}/Sey cells correctly positioned in the outer layer of the optic cups of $Sey^{Neu}/Sey \leftrightarrow +/+$ chimaeras. To achieve this aim, two in-situ hybridisation methodologies were utilised: hybridisation to the β-globin transgene for spatial visualisation of Sey^{Neu}/Sey cells and hybridisation to two mRNA markers

using DIG-labelled mRNA riboprobes to determine temporal status and developmental potential of the two cell populations within abnormal optic cup structures. It was therefore necessary to identify expression markers that might indicate inherent temporal or developmental differences between Sey^{Neu}/Sey and +/+ cells in the abnormal optic cups. The results of investigation of both E12.5 and E14.5 $Sey^{Neu}/Sey \leftrightarrow +/+$ aggregation chimaeras using mRNA in-situ hybridisation will be discussed in this chapter.

4.1.3. Molecular markers of development in the optic cup

The RPE is a histologically distinct simple cuboidal epithelial cell layer, positioned external to the neural retina but in close communication with it. Pigmentation in the RPE results from melanin production in the simple cuboidal epithelial layer. Unlike the skin, where melanin-producing cells (melanocytes) are derived from neural crest and migrate to their final destination before initiating melanin production, cells of the RPE form melanin at the appropriate developmental stage *in-situ*.

Trp1 and *Trp2* are the earliest known expression markers of RPE. Expression is initiated prior to morphological determination of RPE from the outer layer of the optic cup. *Trp2* shows earliest expression in the optic vesicle at E9.5 (Jackson *et al.*, 1992; Steel *et al*; 1992). At this early stage *Trp2* is expressed in both layers of the optic vesicle, but later restricts to the outer layer and the iris region. *Trp2* expression is clearly localised to the presumptive RPE prior to its morphological determination or the appearance of visible pigment formation. *Trp1* and *Trp2* show similar expression patterns although *Trp2* is expressed prior to initiation of *Trp1* expression (Steel *et al.*, 1992). As *Trp2* is the earliest known marker of the RPE, this gene was selected for investigation of expression in $Sey^{Neu}/Sey \leftrightarrow +/+$ chimaeras.

Expression of *Trp2* has been examined in the small eye homozygote fetus (Grindley *et al.*, 1995). Grindley *et al* (1995) showed that expression of *Trp2* was not lost from the highly abnormal optic vesicles but was only expressed at the most proximal regions. It is therefore difficult to determine from this data if *Trp2* in the small eye homozygote fetus is delineating the presumptive RPE or just identifying developmentally specified proximal optic stalk.

As the expression pattern of *Trp2* has been characterised in the *Sey/Sey* homozygous fetus, and expression was seen to be initiated after expression of *Pax6* , *Trp2* appeared to be a good marker for early presumptive RPE. Differential expression between Sey^{Neu}/Sey and +/+ cells of this early RPE marker might indicate temporal and spatial differences between the Sey^{Neu}/Sey and +/+ cells in $Sey^{Neu}/Sey \leftrightarrow$+/+ chimaeras.

As discussed in Chapter 3, Sey^{Neu}/Sey cells appeared to be disorganised compared to most areas of +/+ cells within the abnormal optic cup structures, indicating that Sey^{Neu}/Sey cells might be developmentally dysmature relative to their +/+ neighbours. To determine if this was the case, *Pax6* expression was used as a marker of temporal maturity within the abnormal chimaeric eye structures.

4.1.4. Analysis of E14.5 and E12.5 chimaeras

The first chimaeras produced for this experiment were of a gestational stage of E14.5. This stage was used to corroborate the preliminary data observed in the E14.5 $Sey^{Neu}/Sey \leftrightarrow$+/+ chimaeras discussed in Chapter 3, but also because RPE is fully pigmented and RPE development and pigment production are unequivocally complete in the wild type fetus by this gestational stage. However, some E12.5 $Sey^{Neu}/Sey \leftrightarrow$+/+ chimaeras were also produced to allow direct comparison with results observed in Chapters 2 and 3 and corroborate data observed in the E14.5 $Sey^{Neu}/Sey \leftrightarrow$+/+ chimaera group.

4.2. Results

To produce *Sey*^{Neu}*/Sey* ↔+/+ chimaeras at E14.5 days, a total of 210 aggregated embryos were transferred which resulted in 46 fetuses at dissection, of which 24 were chimaeric. Of these 24 fetuses, only two proved to be of the *Sey*^{Neu}*/Sey* ↔+/+ genotype. Concurrently, E12.5 chimaeras were also produced. Of 147 aggregated embryos transferred, 28 fetuses were recovered at this gestational age, of which only 10 were chimaeric. Only a single *Sey*^{Neu}*/Sey* ↔+/+ aggregation chimaera was recovered from the E12.5 group. Although the total number of E14.5 and E12.5 *Sey*^{Neu}*/Sey* ↔+/+ chimaeras produced was small and therefore not ideal, time restrictions precluded production of more chimaeras. mRNA in-situ hybridisation analysis of the two E14.5 (JC148 and JC162) and one E12.5 (JC185) *Sey*^{Neu}*/Sey* ↔+/+ aggregation chimaeras will be discussed in this chapter.

Chimaeras were produced and analysed as described in Chapter 2, (see also Appendices III, V, VI, VII, VIII, IX, X and XI). For GPI analysis for estimation of *Sey*/+ x *Sey*^{Neu}/+ cell contribution, both left and right forelimbs, as well as tail and extra-embryonic membranes were taken for analysis. The mean % fetal GPI1B for the three chimaeras examined in this chapter are shown in Table 4.1.

Table 4.1.

Chimaera	Embryonic age	Mean percentage fetal GPI1B (%)
JC185	E12.5	72.8
JC162	E14.5	86.4
JC148	E14.5	26.7

4.2.1. Analysis of spatial position and expression of marker genes in *Sey^{Neu}/Sey* ↔+/+ chimaeras

Two in-situ methodologies were utilised for this study. Identification of *Sey^{Neu}/Sey* cells and determination of their position within chimaeric tissues was achieved by DNA-DNA in-situ hybridisation using β-globin transgene probe. mRNA in-situ hybridisation using DIG-labelled riboprobes was performed on semi-serial sections to those used for β-globin in-situ. This strategy ensured that the maximum spatial and expression information was achieved from any given tissue area within the eye.

Figure 4.1. (Following page) mRNA in-situ hybridisation using DIG-labelled anti-sense riboprobes to 4% paraformaldehyde fixed sections from E12.5 control fetal eyes. **a)** Wild type *Pax6* expression showing strong hybridisation in the lens, inner layer of the optic cup and surface ectoderm overlying the eye. **b)** Wild type *Trp2* expression showing discrete hybridisation of anti-sense *Trp2* riboprobe to the retinal pigment epithelium. Migrating melanocytes also show positive hybridisation in the mesenchyme of the head. (Scale bar - 200μm).

Figure 4.1.

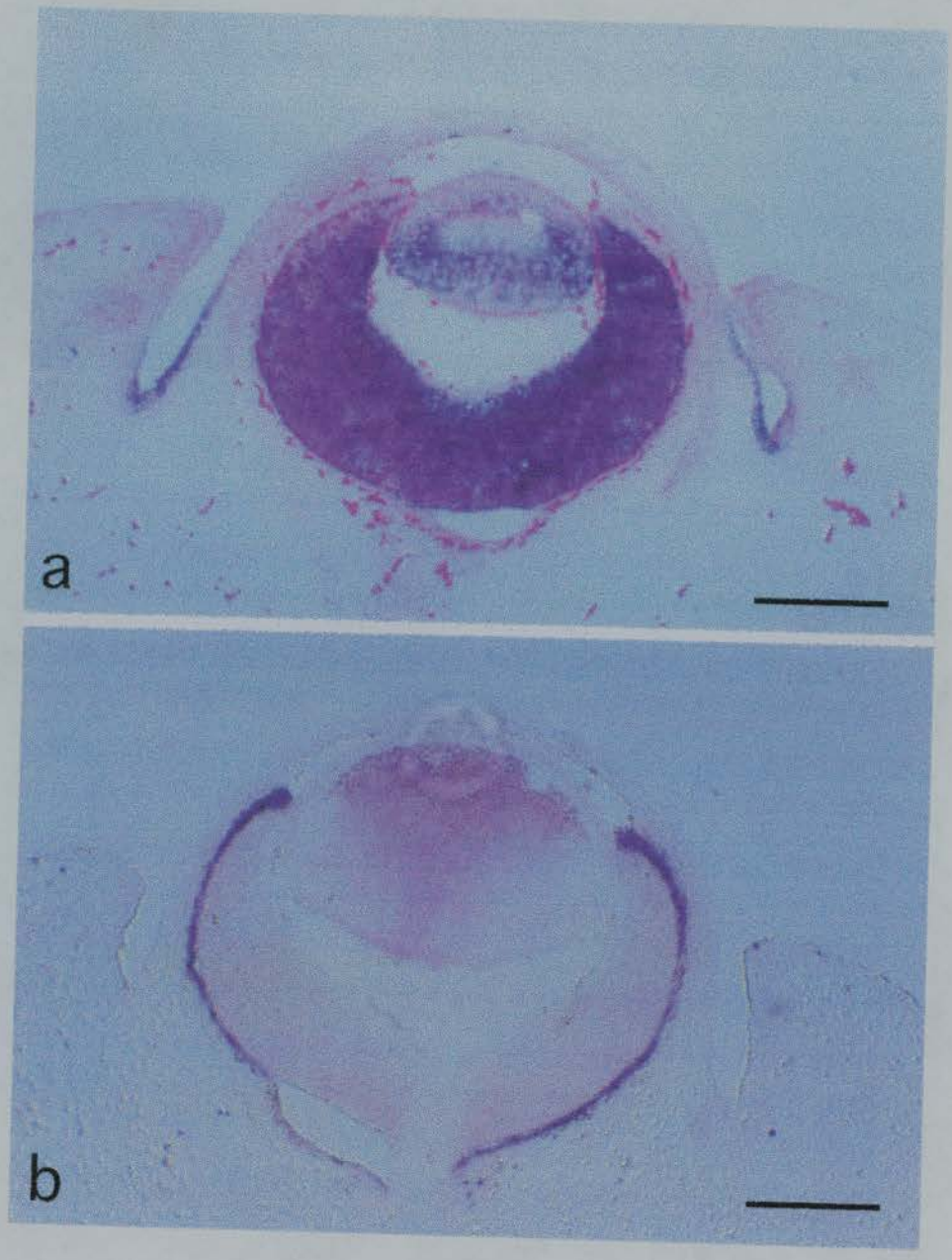

At dissection, the whole head was resected from each fetus and fixed. Sections were cut at 7μm and sections were arranged semi-serially in blocks of 16 across four slides. Therefore, slide a) contained sections 1,2,9 and 10, slide b); sections 3,4,11 and 12, slide c); sections 5,6,13 and 14 and slide d); sections 7,8, 15 and 16, etc. Sections from the whole eye region were semi-serially mounted in this way for the three chimaeras analysed.

Control sections were taken from the eyes of E12.5 and E14.5 embryos derived from timed matings between BALB/c parents. The BALB/c strain was used to make embryos for controls as the BALB/c strain is albino and therefore pigment granules would not be present in the RPE to obscure any *Trp2* or *Pax6* expression signal. Heads resected from these control fetuses were treated in an identical manner to those of the test chimaeras.

As discussed previously, mRNA probes for detection of *Trp2* and *Pax6* expression were used to determine inner layer/outer layer identity and temporal development in sections from eyes of $Sey^{Neu}/Sey \leftrightarrow +/+$ chimaeras, (for details of probes, see Appendices IV.III and IV.IV). A 4-day protocol for in-situ hybridisation to mRNA using DIG-labelled ribopobes was kindly provided by Dr. S. Wedden of the Department of Anatomy, University of Edinburgh; the protocol used for this study contained minor modifications from that original (see Appendix IV.VI.).

The mRNA in-situ protocol was refined for both *Pax6* and *Trp2* expression using control experiments incorporating sense and antisense DIG-labelled riboprobes on 4% paraformaldehyde fixed sections from eyes of control E14.5 and E12.5 fetuses. These control experiments proved strong and highly specific binding for both *Pax6* and *Trp2* anti-sense probes commensurate with published wild-type expression patterns (see

Figure 4.1.). No detection of any probe binding was observed for sense controls. Thereafter, for experimental in-situ runs, a positive control section from both an E12.5 and E14.5 mouse eye was included in each run for both *Pax6* and *Trp2* antisense probes to ensure run efficacy and as internal control for levels of stage related *Pax6* and *Trp2* expression.

As the mRNA in-situ hybridisation protocol required tissues to be fixed in 4% paraformaldehyde, a modified β-globin DNA-DNA in-situ hybridisation protocol was used to allow the two different in-situ methodologies to be carried out on semi-serial sections. A second β-globin DNA-DNA in-situ hybridisarion protocol from Keighren and West (1993) was used for this purpose, the probe used was identical to that used in Chapter 2 (see Appendices III.I, III.V and III.VI).

The major difference in the β-globin DNA-DNA in-situ hybridisation protocol used for 3:1 (ethanol:acetic acid) fixed tissues and that for tissue fixed in 4% paraformaldehyde was the requirement for a Proteinase K digestion step. Digestion with Proteinase K was necessary to allow full penetration of the probe into the cells by degradation of any proteins surrounding the target sequences. This digestion step proved to be highly variable between in-situ runs although time and concentration of reagents were kept constant. Tissue type and developmental age of the fetus also played a role in the efficacy of Proteinase K digestion. Unfortunately, the integrity of some tissue samples was lost by this digestion process, although the majority of eye tissues remained intact although in most cases some cellular definition was lost.

4.2.2. Morphological examination of E14.5 and E12.5 *Sey^{Neu}/Sey* ↔+/+ chimaeras

E14.5 chimaera JC148 was found to be of low mean *Sey^{Neu}/Sey* cell contribution (26.7%) determined by GPI1B analysis and exhibited no morphological abnormalities of eye or frontofacial development at dissection. No pigmentation was observed in either the left or right eye of this fetus with both eyes appearing morphologically normal (See Figure 4.1c).

E14.5 chimaera JC162 and E12.5 chimaera JC185 both contained a high *Sey^{Neu}/Sey* cell contribution, 86.4% and 72.8% respectively. E14.5 *Sey^{Neu}/Sey* ↔+/+ \chimaera JC162 exhibited a small eye opening on the left side, but no visible eye formation on the right (see Figure 4.2b). The snout of this fetus, when compared with a compound heterozygous (*Sey^{Neu}/Sey*) fetus, appeared well developed with the fronto-nasal area and upper jaw being larger that of the homozygous fetus (See Figure 4.2a and b). No observable pigmentation was recorded at dissection for any of the normal or abnormal eyes of the E14.5 or E12.5 *Sey^{Neu}/Sey* ↔+/+ chimaeric fetuses.

Figure 4.2. (Following page) Photographs of a E14.5 compound heterozygous *Sey^{Neu}/Sey* fetus and E14.5 *Sey^{Neu}/Sey* ↔+/+ chimaeric fetuses. **a)** *Sey^{Neu}/Sey* small eye fetus showing characteristic phenotype of anophthalmia and retrognathia with protruding tongue. **b)** *Sey^{Neu}/Sey* ↔+/+ chimaera JC162, mean fetal GPI1B 86.4%, showing slit-like eye formation on right side and more normal development of the upper mandible. **c)** *Sey^{Neu}/Sey* ↔+/+ chimaera JC148, mean fetal GPI1B 26.7%, showing wild type facial morphology and eye formation. Note absence of pigmentation in the normal right eye of this fetus.

Figure 4.2.

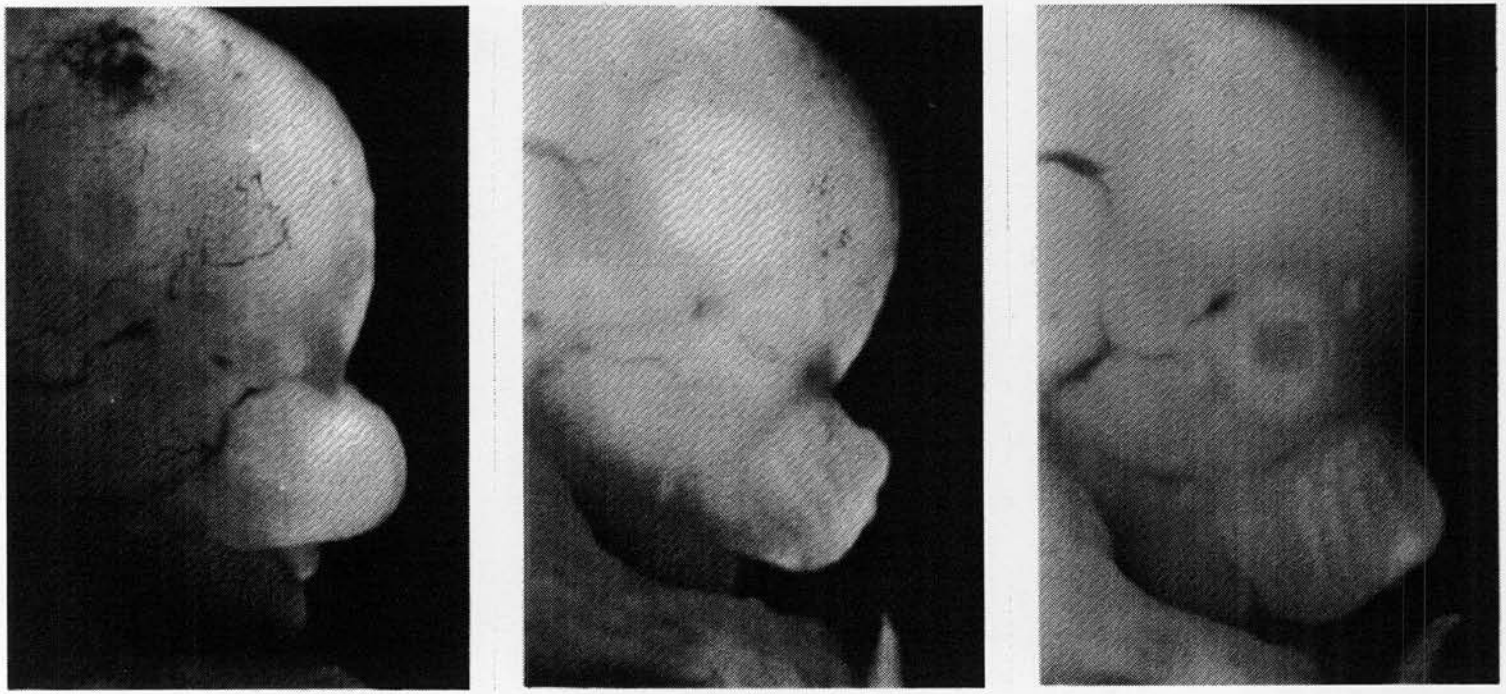

a) *Sey*^{Neu}/*Sey*

b) *Sey*^{Neu}/*Sey*↔+/+
86.4% GPI1B

c) *Sey*^{Neu}/*Sey*↔+/+
26.7% GPI1B

E12.5 *Sey*^{Neu}*/Sey* ↔+/+ chimaera JC185 showed a slight bulbous extension of the left eye beyond the margin of the head with an iris-like structure visible through the opaque cornea. The right eye of this chimaera appeared slit-like, similar in morphology to that of an E12.5 compound heterozygous (*Sey*^{Neu}*/Sey*) fetus.

4.2.3. Histological analysis of chimaeras JC148, JC162 and JC185.

Histological analysis of the three chimaeric fetuses used for this study showed similar morphology to those observed in *Sey*^{Neu}*/Sey* ↔+/+ fetuses of similar *Sey*^{Neu}*/Sey* cell contribution reported in Chapters 2 and 3.

Of the three *Sey*^{Neu}*/Sey* ↔+/+ chimaeras analysed, only E14.5 chimaera JC148 exhibited lens formation. Both the left and right eyes of this fetus contained lenses of normal size and morphology commensurate with E14.5 days of development (see Figure 4.3.). No *Sey*^{Neu}*/Sey* cells (Tg+ve) were observed in tissues of the lens and inner or outer layers of the optic cup in either the left or right eye of this chimaeric fetus.

Figure 4.3. (Following page) mRNA in-situ hybridisation using DIG-labelled anti-sense *Pax6* and *Trp2* riboprobes to E14.5 *Sey*^{Neu}*/Sey* ↔+/+ chimaera JC148.
a) *Pax6* is seen to follow a wild type expression pattern with strong hybridisation observed in the lens and lens epithelium, inner layer of the optic cup and the ciliary margins. Strong expression is also observed in the surface ectoderm of the head.
b) Wild type expression pattern of *Trp2* showing discrete restriction of hybridisation signal to the RPE. Migratory melanocytes are also observed to express *Trp2* in the mesenchyme of the head. (Scale bar - 200μm).

Figure 4.3.

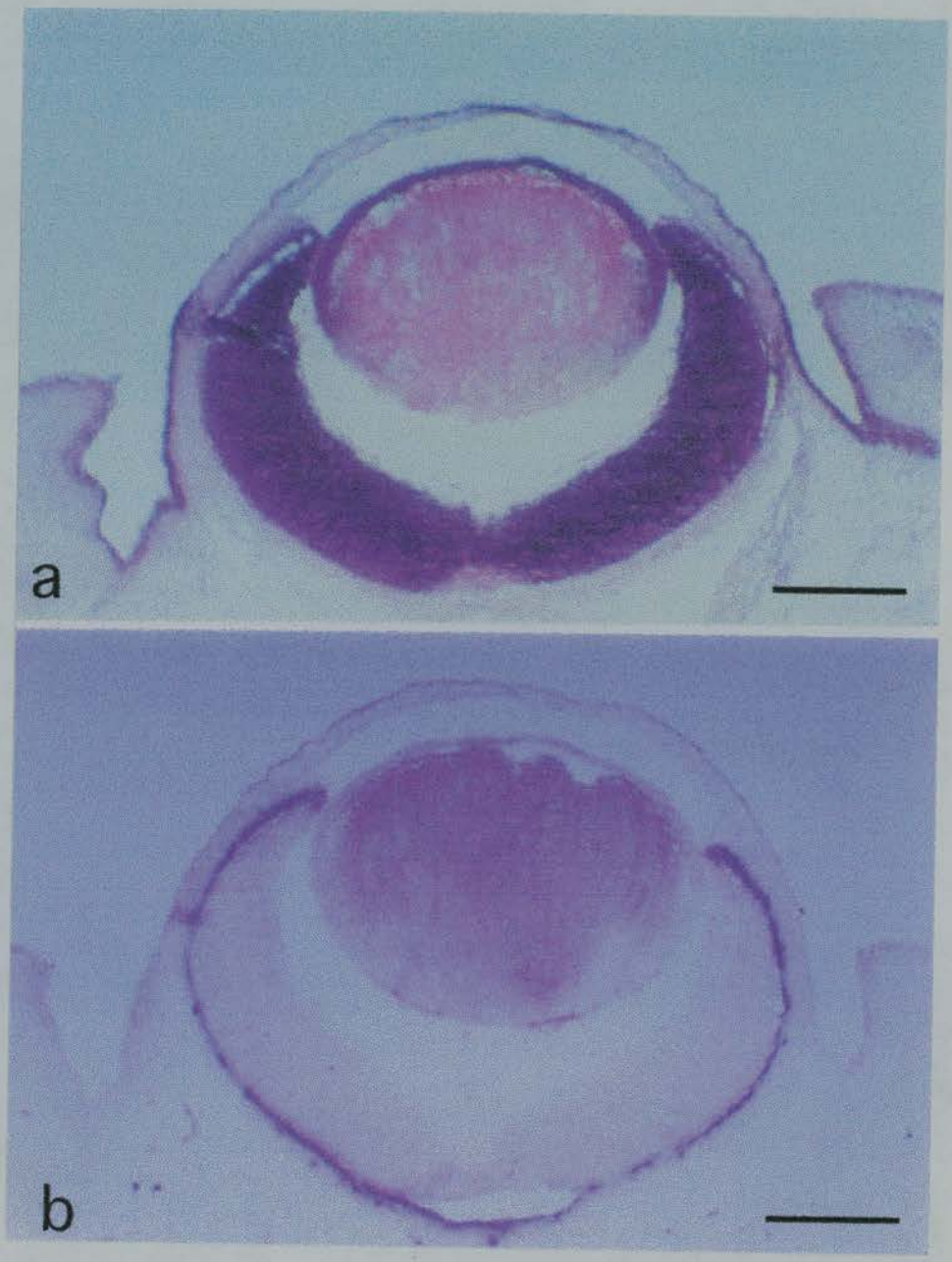

Figure 4.4.

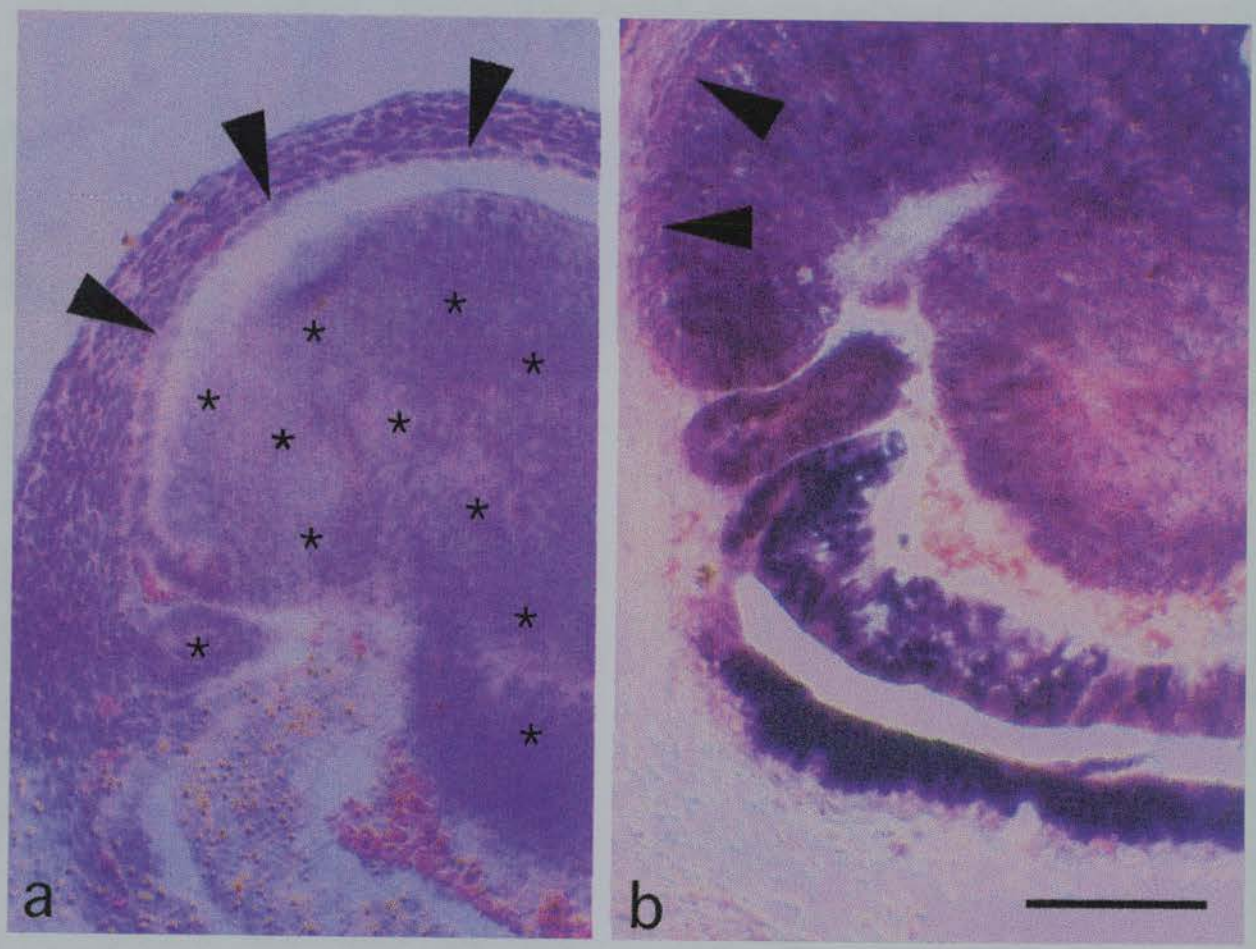

However, hybridisation to the β-globin transgene was observed in other tissues of the head. This result is similar to that reported in the low *Sey*^{Neu}*/Sey* cell contribution chimaeras at E12.5 days where *Sey*^{Neu}*/Sey* cells were excluded from all tissues of the eye, (JC63 both eyes, right eye of JC56 and the left eye of JC61; see Table 3.1 in Chapter 3).

E14.5 chimaera JC162 showed no evidence of lens formation in either the left or right eye. The right eye of this fetus was highly dysmorphic; optic tissue was seen to form a foreshortened optic cup structure which had lost contact with the surface ectoderm. As in the E12.5 *Sey*^{Neu}*/Sey* ↔+/+ chimaeric fetuses, *Sey*^{Neu}*/Sey* and +/+ cells were seen to segregate into discrete areas.

Figure 4.4. (Previous page) In-situ hybridisation using DIG-labelled probes to the left eye of E14.5 *Sey*^{Neu}*/Sey* ↔+/+ chimaera JC162. **a)** In-situ hybridisation using DIG-labelled probe to the β-globin transgene. Hybridisation signal is observed in *Sey*^{Neu}*/Sey* cells in the mesenchyme of the head and a region of ill-defined distal optic cup within a highly abnormal optic structure. A large area of unlabelled +/+ cells are seen proximal to this *Sey*^{Neu}*/Sey* "double cup" tissue . The +/+ cells constitute a large mass of 'inner layer' tissue with an associated ectopically-oriented area of morphologically normal, simple cuboidal +/+ RPE. **b)** Hybridisation with DIG-labelled anti-sense *Pax6* probe to a section serial to that shown in a). Note hybridisation to all +/+ and *Sey*^{Neu}*/Sey* cells, with a lower level of expression observed in the area of morpholocially normal RPE defined in a). Expression of *Pax6* is observed to be strongest in *Sey*^{Neu}*/Sey* cells, constituting both 'inner' and 'outer' layers of the distal "double cup" structure.
Arrowheads - areas of morphologically normal RPE, * area of "inner layer" composed of entirely +/+ cells. (Scale bar - 200μm).

Although the optic cup structure was highly abnormal in chimaera JC162, the areas of +/+ cells present were observed to be forming inner layer/outer layer structures, with areas of morphologically normal non-pigmented RPE composed of entirely +/+ cells juxtaposed with columnar inner layer-like +/+ areas. However, the overall morphology and spatial organisation of this optic cup was highly disorganised. *Sey*^{Neu}*/Sey* cells appeared as a single amorphous area distal in orientation to the areas of +/+ cells and showed no evidence of appropriate optic cup developmental by cell morphology (see Figure 4.4a and 4.5.a and c).

Figure 4.5. (Following page) In-situ hybridisation using DIG-labelled probes to the left eye of E14.5 *Sey*^{Neu}*/Sey* ↔+/+ chimaera JC162. In-situ hybridisation using DIG-labelled probe for the β-globin transgene in **a)** proximal and **c)** distal regions of the left eye of chimaeras JC162. In **a)**, note the morphologically normal +/+ RPE layer defining the proximal boundary of the abnormal eye structure. **c)** shows the abnormal "double cup" structure composed of entirely of *Sey*^{Neu}*/Sey* cells situated in the distal optic region. **b)** and **d)** show hybridisation with DIG-labelled *Trp2* anti-sense riboprobes to a section serial to those shown in a) and c). **b)** Note strong *Trp2* expression to the morphologically normal RPE indicated in a) [an area of +/+ cells situated in an 'outer layer' position] and in **d)** the 'outer layer' comprised of *Sey*^{Neu}*/Sey* cells in the distal "double cup" structure. Arrowheads - areas of morphologically normal RPE. (Scale bar - 200μm).

Figure 4.5.

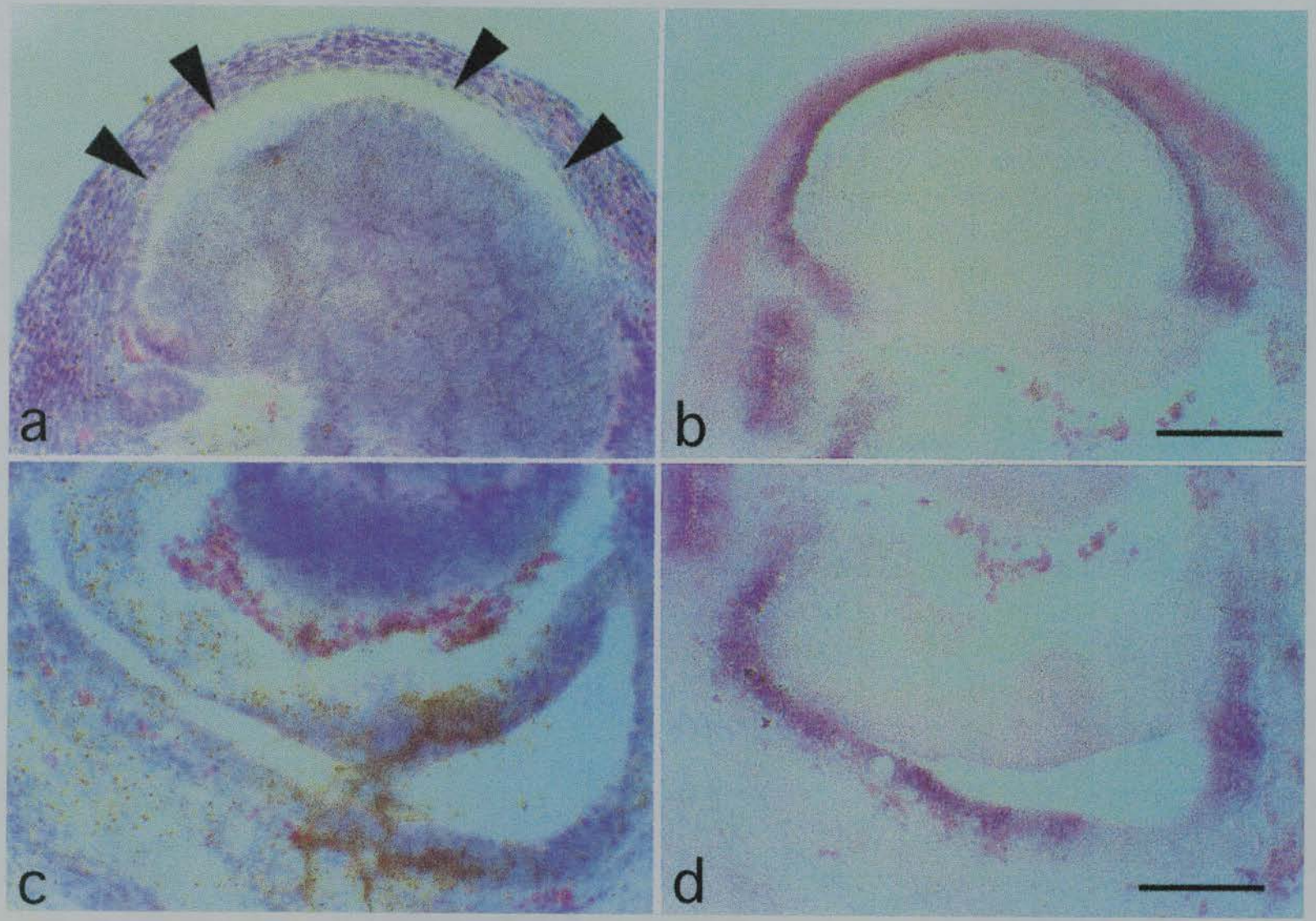

The left eye of this chimaera had extensive hyperproliferation of optic cup tissue which formed a spherical eye 'bulge', similar to that observed in the right eye of E12.5 chimaera JC17. Again, +/+ and *Sey*^{Neu}*/Sey* cells were highly segregated into large patches with the *Sey*^{Neu}*/Sey* cells appearing to constitute one large area distal to the areas of +/+ cells. Large, morphologically identifiable areas of unpigmented RPE containing only +/+ cells were present, juxtaposed with areas of +/+ "inner layer". However, the area of RPE containing only +/+ cells was seen to be ectopically situated at the most proximal border of the eye, underlying the surface ectoderm (see Figure 4.4a and 4.5a). Again, areas of +/+ cells appeared to have attained a maturity of development not achieved by *Sey*^{Neu}*/Sey* cell neighbours.

The left and right eyes of E12.5 *Sey*^{Neu}*/Sey* ↔+/+ chimaera JC185 showed a similar morphology to that observed in E14.5 chimaera JC162, as described above. Both eyes of this E12.5 chimaera JC185 were highly dysmorphic, showing no evidence of lens formation although an approximation to a "normal" optic cup structure was seen proximally in both the left and right eyes. As in the E14.5 *Sey*^{Neu}*/Sey*↔+/+ chimaeras, +/+ and *Sey*^{Neu}*/Sey* cells were segregated into large patches, with areas of *Sey*^{Neu}*/Sey* cells observed to be generally situated distal to areas of +/+ cells. In both the left and right eyes of this fetus, the cells forming the "normal" optic cup structure were those of a +/+ genotype (see Figures 4.6a and 4.7a).

4.2.4. *Pax6* expression in E14.5 and E12.5 *Sey*^{Neu}*/Sey*↔ +/+ chimaeras

Pax6 expression was observed to be higher in E12.5 controls than E14.5 controls, with expression restricted to the inner layer of the optic cup, lens and surface ectoderm (see Figure 4.2a).

Expression of *Pax6* in E14.5 *Sey*^{Neu}*/Sey* ↔+/+ chimaera JC148 was observed to be identical to that observed in a wild type fetus. Strong *Pax6* expression was seen in inner layer of the optic cup and the lens and lens epithelium. In this fetus, expression was observed in the most proximal tips of the outer layer of the optic cup, the presumptive iris region, although the fully differentiated RPE does not express *Pax6* (see Figure 4.3a).

Pax6 expression in both the left and right eyes of E14.5 chimaera JC162 was observed to be restricted to areas of *Sey*^{Neu}*/Sey* cells and areas of +/+ cell that had inner layer position and morphology (see Figure 4.4b). *Pax6* expression was not observed in those areas of morphologically normal RPE that contained only +/+ cells commensurate with its wild-type expression pattern. In both eyes of E14.5 *Sey*^{Neu}*/Sey* ↔+/+ chimaera JC162, expression of *Pax6* was observed to be at a considerably higher level in *Sey*^{Neu}*/Sey* cells than in their +/+ neighbours.

A similar *Pax6* expression pattern to that of JC162 was observed in E12.5 *Sey*^{Neu}*/Sey* ↔+/+ chimaera JC185. In this chimaera, *Pax6* was expressed in both the inner and outer layers of the abnormal "optic cup" structures, although a considerably lower level of expression was observed in areas of morphologically identifiable RPE, again, containing only +/+ cells (see Figures 4.6b and 4.7b). Indeed, in the both the left and right eyes of E12.5 chimaera JC185, where +/+ cells were forming identifiable 'double cup' structures, expression of *Pax6* within these structures was seen to be of wild-type pattern. Similarly to E14.5 *Sey*^{Neu}*/Sey* ↔+/+ chimaera JC162, areas of *Sey*^{Neu}*/Sey* cells were seen to be expressing *Pax6* at a considerably higher level than +/+ cells.

Figure 4.6. (Following page) Hybridisation using DIG-labelled probes to **a)** β-globin transgene, **b)** *Pax6* and **c)** *Trp2* in the right eye of E12.5 chimaera $Sey^{Neu}/Sey \leftrightarrow +/+$ JC185.

a) Hybridisation signal to the β-globin transgene can be observed in large areas of Sey^{Neu}/Sey cells situated distally within the highly abnormal optic cup structure. Large areas of +/+ cells are observed in the dorsal eye region and constitute a proximal optic cup structure. An area of normal inner layer/outer layer formation and a morphologically identifiable RPE can be observed (arrowheads). **b)** *Pax6* expression to a semi-serial section to that shown in a). Hybridisation to *Pax6* mRNA can be observed in both Sey^{Neu}/Sey and +/+ cells within the abnormal optic cup, although expression is seen to be down regulated in the area of morphologically normal +/+ RPE. *Pax6* expression is observed to be considerably stronger in Sey^{Neu}/Sey cells than in +/+ cells. **c)** *Trp2* expression in a semi-serial section to that shown in b). *Trp2* expression is observed in the morphologically normal area of RPE as well as an area of +/+ cells of abnormal appearance situated in an outer layer position. Interestingly, an area of +/+ cells forming a "middle layer" between two areas of +/+ cells are seen to be expressing *Trp2* at a low level, possibly indicating cells undergoing restriction of expression (open arrowhead). (Scale bar - 100μm).

Figure 4.6.

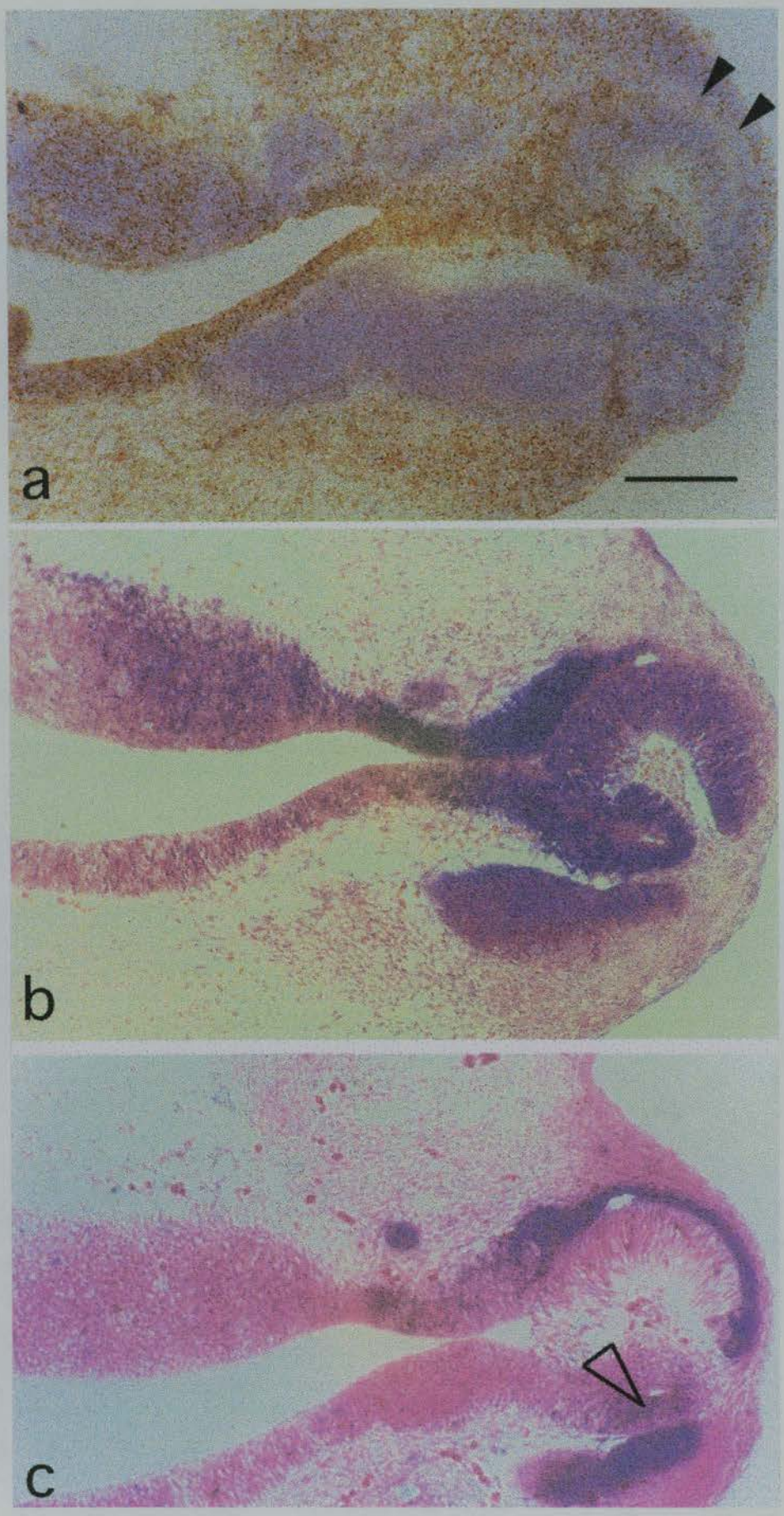

Figure 4.7. (Following page) Hybridisation using DIG-labelled probes for **a)** β-globin transgene, **b)** *Pax6* and **c)** *Trp2* in the left eye of E12.5 chimaera $Sey^{Neu}/Sey \leftrightarrow +/+$ JC185.

a) Hybridisation signal to the β-globin transgene can be observed in the entire distal region of this abnormal optic cup structure. A large area of +/+ cells is observed in the most proximal optic region with formation of an identifiable optic cup of normal apperance despite the absence of a lens (marked *). Areas of +/+ RPE are observed forming the outer layer of this structure (arrowheads). **b)** Hybridisation using DIG-labelled *Pax6* anti-sense riboprobes to a serial section to that shown in a). All optic cup cells are observed to strongly express *Pax6* with expression extending down the length of the optic stalk and into the presumptive pre-optic area. *Pax6* is seen to be down-regulated in +/+ cells forming morphogically normal areas of RPE (open arrowheads). Even though expression of *Pax6* is seen to be higher overall in this E12.5 chimaeric fetus to that observed in the E14.5 chimaeric fetuses, *Pax6* expression is still stronger in those cells of Sey^{Neu}/Sey genotype. **c)** Hybridisation using DIG-labelled *Trp2* anti-sense riboprobes to a semi-serial section to that shown in b). Expression of *Trp2* is seen to be restricted to those areas of morphologically normal RPE in the outer layer of the proximal optic cup structure. (Scale bar - 100μm).

Figure 4.7.

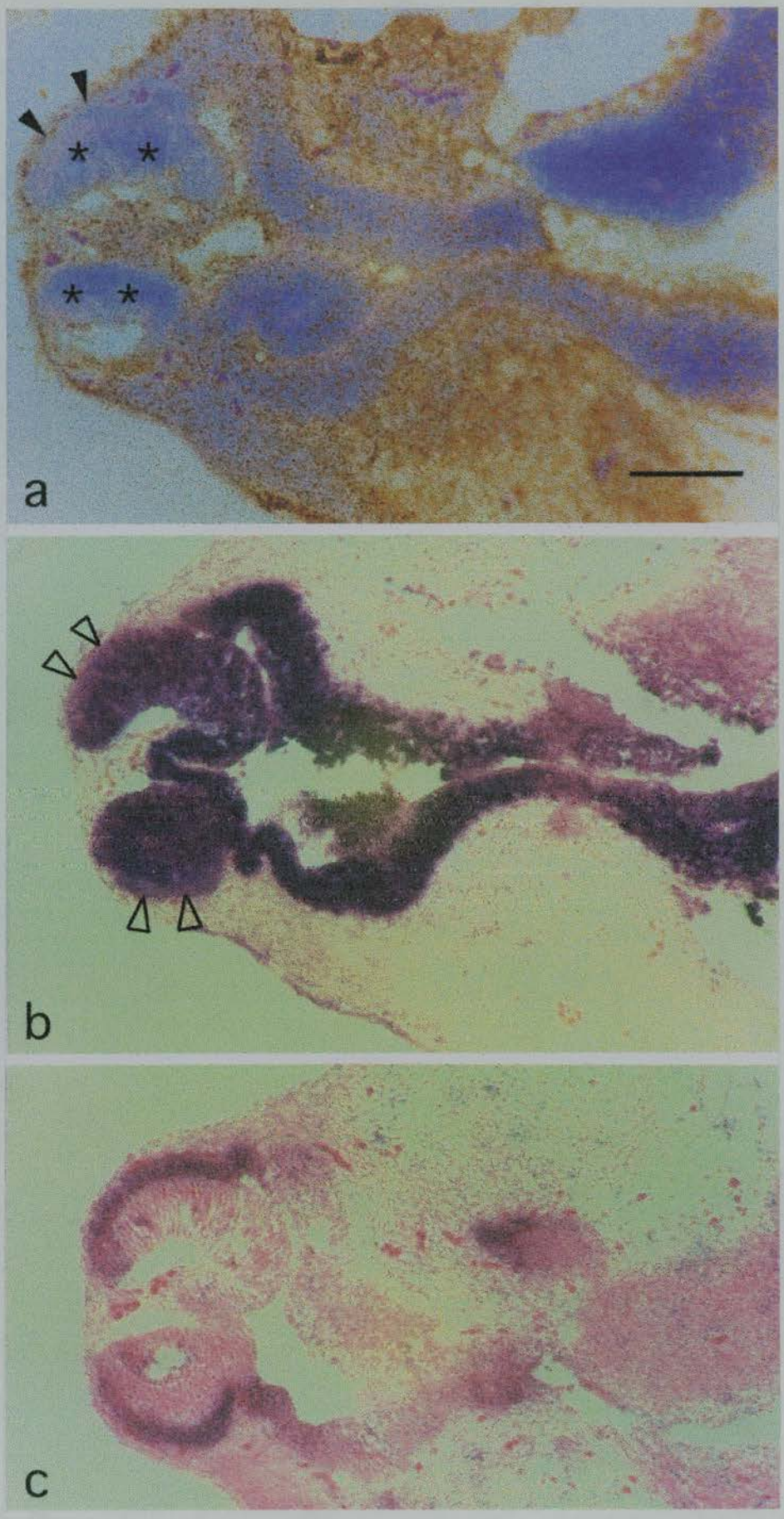

4.2.5.*Trp2* expression in E14.5 and E12.5 *Sey*^{Neu}*/Sey*↔+/+ chimaeras

Expression of *Trp2* maintained similar levels at both E12.5 and E14.5 in control sections. Expression of this marker was restricted exclusively to the RPE by E14.5. Migrating melanocytes were also observed by virtue of their *Trp2* expression at both E12.5 and E14.5 days (see Figure 4.2b).

Expression of *Trp2* in E14.5 *Sey*^{Neu}*/Sey* ↔+/+ chimaera JC148 was identical to the wild-type E14.5 pattern. *Trp2* expression was tightly restricted to the morphologically normal RPE (see Figure 4.3.b). *Trp2* expression was also observed in migratory melanocytes in both E12.5 and E14.5 *Sey*^{Neu}*/Sey* ↔+/+ chimaeras.

The most surprising results of this study were observed on analysis of *Trp2* expression in E14.5 *Sey*^{Neu}*/Sey* ↔+/+ chimaera JC162. Although the optic cup structures in this chimaera were highly dysmorphic, the pattern of *Trp2* expression was observed "normal"; that is, restricted to morphologically normal +/+ RPE where present, and cells of both genotypes situated in an "outer layer" position. Therefore, cells specified as outer layer purely by their position, including *Sey*^{Neu}*/Sey* cells and those +/+ cells not exhibiting RPE morphology but also positionally situated in the "outer layer", were all observed to express *Trp2* (see Figures 4.5.b and d). Most remarkably, where an area of exclusively *Sey*^{Neu}*/Sey* cells was seen to be forming an approximate "inner layer/outer layer" structure, as shown in Figures 5.5.c and d, only those *Sey*^{Neu}*/Sey* cells constituting the "outer layer" were observed to express *Trp2*.

Table 4.2a. Gene expression in the inner layer of *Sey*^{Neu}*/Sey* ↔+/+ chimaeric optic cups at E12.5 and E14.5 days. n/a, not applicable.

'Inner layer' genotype	***Pax6***	***Trp2***	**β-globin transgene**
Sey^{Neu}*/Sey*	+++	-	Tg+ve
+/+	+	-	Tg-ve
+/+ control -			
E12.5	++	-	n/a
E14.5	+	-	n/a

Table 4.2b. Gene expression in the outer layer of *Sey*^{Neu}*/Sey* ↔+/+ chimaeric optic cups at E12.5 and E14.5 days. n/a, not applicable.

'Outer layer' genotype	***Pax6***	***Trp2***	**β-globin transgene**
Sey^{Neu}*/Sey*	+++	+	Tg+ve
+/+	+/-	+	Tg-ve
+/+ control-			
E12.5	+/-	+	n/a
E14.5	-	+	n/a

Results of *Trp2* expression in E12.5 *Sey^{Neu}/Sey* ↔+/+ chimaera JC185 show that a wild type pattern of *Trp2* expression has been established by E12.5 days. A similar pattern of *Trp2* expression was observed in the E12.5 day chimaera JC185 to that of E14.5 day chimaera JC162, with only those cells either morphologically identifiable as RPE, (and therefore of +/+ genotype), or *Sey^{Neu}/Sey* cells positioned in the "outer layer" observed to express *Trp2* (see Figures 4.6c and 4.7.c).

Interestingly, chimaera JC185 gives an indication that this restriction of *Trp2* expression to the outer layer of the optic cup is both dynamic and temporally controlled. An area of *Sey^{Neu}/Sey* cells spatially positioned between two neurectodermal tissue areas, that is, in an ectopically formed "middle" layer position are observed to express a low level of *Trp2* , probably due to transcriptional regulation from its ectopic juxtaposed "outer layer" (see Figure 4.6c).

Expression data is summarised in Tables 4.2a and 4.2b. In *précis*, *Sey^{Neu}/Sey* cells were observed to express *Pax6* at a higher level than +/+ cells within the same optic cup structure at both E12.5 and E14.5 days indicating a possible cellular arrest at a stage prior to E12.5 where expression of this marker is high. *Pax6* was seen to be expressed by all *Sey^{Neu}/Sey* cells regardless of their position within the abnormal optic cups. *Pax6* expression in +/+ cells was normal with regard to cell type and level of expression, that is, between E12.5 and E14.5 *Pax6* was seen to be down regulated in +/+ cells forming morphologically normal RPE.

Expression of *Trp2* in both normal and abnormal optic cup structures of both E12.5 and E14.5 *Sey^{Neu}/Sey* ↔+/+ chimaeras was restricted to cells identified as morphologically normal RPE or cells in an "outer layer" position regardless of cell genotype. Indeed, *Sey^{Neu}/Sey* cells were able to be differentially specified as inner or

outer layer. There was no difference in level of *Trp2* expression between Sey^{Neu}/Sey and +/+ cells.

4.3. Discussion.

Investigation of expression of *Pax6* and *Trp2* expression in E12.5 and E14.5 $Sey^{Neu}/Sey \leftrightarrow$+/+ chimaeras allows us to determine both timing and effect of loss of *Pax6* function on Sey^{Neu}/Sey cells in the optic cups of $Sey^{Neu}/Sey \leftrightarrow$+/+ chimaeras. As the results show, expression of both *Pax6* and *Trp2* were observed to follow a wild type expression pattern in the morphologically normal left and right eyes of eyes of $Sey^{Neu}/Sey \leftrightarrow$+/+ chimaera JC148 with both the inner and outer layers of the optic cup exhibiting appropriate gene expression. Although no Sey^{Neu}/Sey cells were present in either eye of this chimaera, results indicate that the presence of Sey^{Neu}/Sey cells in the head mesenchyme does not have an inhibitory effect on expression of either gene in the developing eye.

Whilst interactions between mesenchyme and neurectoderm are important for formation of the RPE, results shown in Chapter 3 indicate that mesenchymal cells unable to express functional *Pax6* do not inhibit RPE formation in +/+ cells. In chimaeras with a high percentage of mutant cells, +/+ cells were seen to form areas of morphologically normal RPE, regardless of contribution of Sey^{Neu}/Sey cells to the head mesenchyme. This normal induction of RPE is reflected by induction of *Trp2* expression, with this outer layer marker seen to follow a wild type expression and restriction pattern in $Sey^{Neu}/Sey \leftrightarrow$+/+ chimaera of both low and high Sey^{Neu}/Sey cell contribution.

The results of *Trp2* expression in $Sey^{Neu}/Sey \leftrightarrow$+/+ chimaera gives an additional level of understanding regarding roles for *Pax6* in inner layer/outer layer specification to

that elucidated from *Trp2* expression in the homozygous small eye fetus alone. Although *Trp2* was seen to be expressed in the most proximal regions of the abnormal homozygous *Sey/Sey* optic cup structures, this gave no indication whether determination of inner layer/outer layer identity had been achieved. Examination of *Trp2* expression in the $Sey^{Neu}/Sey \leftrightarrow +/+$ chimaeras allows a definition of the potential of cells unable to express functional *Pax6* in that these cells are able to assume inner layer/outer layer identity but are unable to fulfil this potential.

The use of *Pax6* as a temporal marker in $Sey^{Neu}/Sey \leftrightarrow +/+$ chimaera allows determination of approximate developmental age of Sey^{Neu}/Sey cells within the abnormal optic cups. As a dramatically higher level of *Pax6* expression was observed in Sey^{Neu}/Sey cells at both E14.5 and E12.5 days, this indicates that the Sey^{Neu}/Sey cells are "stuck" at a developmental stage prior to that of E12.5 days.

4.4. Conclusions

If the results of expression studies of *Pax6* and *Trp2* are considered together, the increased level of *Pax6* expression in Sey^{Neu}/Sey cells, in relation to their ability to express *Trp2* and to assume an inner layer/outer layer identity, temporally specifies the developmental defect in these cells as lying between onset of *Trp2* expression and initiation of RPE development and/or pigment production. This narrows the window of requirement for *Pax6* expression in cells of the outer layer of the optic cup to lie between E9.5 and E11.5 days of embryonic development. The high levels of *Pax6* expression in Sey^{Neu}/Sey cells in the abnormal optic cups indicates a developmental arrest at a stage prior to E11.5 days.

As *Pax6* is expressed at a high level in the optic vesicle from the earliest morphological determination of this structure, the results of expression studies in $Sey^{Neu}/Sey \leftrightarrow +/+$

chimaeras supports a fundamental requirement for *Pax6* expression from the very earliest stages of eye morphogenesis in the mouse.

PART TWO

Chapter 5

Investigation of Luteinizing Hormone-Releasing Hormone (LHRH) neuron migration in the brains of *Sey^{Neu}/Sey^{Neu}*, *Sey^{Neu}*/+ and +/+ mice

5.1. Introduction

Although the eye and nasal phenotypes of the small eye homozygous fetus have been well characterised, associated brain abnormalities and their sequellae have been less well investigated. The morphology of the small eye homozygote brain is highly abnormal and both neural crest cell migration defects (Matsuo *et al.*, 1993) and hydrocephaly (Hogan *et al.*, 1988) have been cited in the literature in connection with mutations in the murine *Pax6* gene. However, the mechanism of these defects, or indeed, the most severe brain abnormality of holoprosencephaly and its relationship to the loss of fronto-facial structures remains undefined.

Pax6 has been shown to be expressed in a number of tissues of the developing brain (Walter and Gruss, 1991). Earliest expression is noted at E8.0 in the neurepithelium of the forebrain and hindbrain, this pattern being maintained throughout development to day E18.5. High levels of expression are seen in the lateral and dorsal aspects of the telencephalon with signal remaining restricted to the ventricular zone. High levels of *Pax6* expression are also noted in the olfactory lobes and cerebellum. A sharp boundary of expression is observed between the mesencephalon and diencephalon and also between the ventral and dorsal thalamus. Ventrally, signal extends into the anterior hypothalamus and the region of the preoptic area. Expression is also seen in the developing anterior pituitary. These observations indicate that *Pax6* is expressed in regionally defined pattern in the developing brain and also in the germinal zone of the

developing neocortex. Expression extends into the post-natal period with subsets of neurons in various areas of the brain, including the olfactory bulb and preoptic area, continuing to express *Pax6* (Stoykova and Gruss, 1994).

The only study to have been undertaken to examine the brain pathology of the homozygous small eye fetus has been carried out by Schmahl *et al* (1993). This study showed a variety of defects in both neuronal migration and differentiation in the cortex of the Sey^{Neu}/Sey^{Neu} homozygote. Neurons of the cortical plate cease to migrate at approximately E16.5 coinciding with reduced formation of axons and the degeneration of existing axons, glial cells and radial glial fibres.

Schmahl *et al* (1993) gave the most detailed description of the histology of the Sey^{Neu}/Sey^{Neu} homozygote brain, noting the complete absence of olfactory bulbs. This region was shown to contain only extensions of the arachnoid membranes. Schmahl *et al* note the enlargement of the ventricular zone in the forebrain of the Sey^{Neu}/Sey^{Neu} homozygote fetus and, although cortical plate formation is absent in the Sey^{Neu}/Sey^{Neu} homozygote, mitotic activity within the telencephalic ventricular zone was not reduced compared to wild type. Most significantly, Schmahl noted that cells were not able to migrate out of the intermediate zone after leaving the subventricular zone. Cells appeared to be blocked at this junction and unable to proceed with their migratory pathways resulting in disorganisation of orientation in the cortical plate. Schmahl *et al.* (1993) suggest that this pathology may be caused by arrest of post-mitotic cells in their resting phase in the subventricular zone. No abnormalities of the thalamic, hypothalamic areas or the pituitary were reported (Schmall *et al.*, 1993).

Interestingly, Schmahl (1993) were able to note some haploinsufficiency effects in the $Sey^{Neu}/+$ heterozygous fetus. Hypoplasia of the telencephalon with an increased

differentiation in the cortical plate. These heterozygous effects are interesting as no neural defects had been previously reported in small eye heterozygous embryos.

The reported defects in cell migration observed by Schmahl (1993) in association with our results observed regarding abnormal cell-to-cell interactions in the optic cup of $Sey^{Neu}/Sey\leftrightarrow+/+$ chimaeras (as described in Chapter 3) indicated that abnormal cell migration in the small eye homozygous fetus might result from abnormal cell-to-cell interaction. We have also suggested that this abnormal cell-to-cell interaction may be related to defects in cell surface molecules. Literature supports this hypothesis, with *Pax6* known to interact not only in its own regulatory pathway (Plaza *et al.*, 1993, Czerny and Busslinger, 1995) but also in those of the neural cell adhesion molecules (Chalepakis, 1994; Chalepakis *et al.*, 1993; Holst *et al.*, 1995) and neurotrophins (Kioussi and Gruss, 1994).

One of the most well defined neuronal migration pathways is that of the Luteinizing Hormone-Releasing Hormone (LHRH) neurons in the developing forebrain. Detailed studies of the route of neuronal migration of LHRH neurons have been achieved by Wray *et al* (1989a; 1989b) and Schwanzel-Fukuda and Pfaff (1989). LHRH neurons arise in the nasal tissues as a single neuronal population between E9.5 to E10.5, shortly after differentiation of the nasal placode but prior to expression of LHRH. These cells first begin to express LHRH mRNA at E12.5 and protein product can be detected at this time. Migration begins shortly after this stage and is complete by E16.5. LHRH neurons migrate across the nasal septum and enter the forebrain with the olfactory nerves, then arch into the preoptic area, migrating through to the hypothalamic region (Wray *et al.*, 1989a; 1989b; Schwanzel-Fukuda and Pfaff, 1989). LHRH neurons control the release of gonadotropic hormones from the anterior pituitary via their position in the hypothalamus.

Defects in LHRH neuron migration cause Kallman's syndrome, characterised by hypotrophic hypogonadism and anosmia (Schwanzel-Fukuda *et al.*, 1989b). The phenotype shows absence of olfactory bulbs and tracts. LHRH neuron migration in the Kallman's syndrome fetus is highly abnormal. LHRH neurons are born but fail to make contact with the brain (Schwanzel-Fukuda *et al.*, 1989b). This indicates a necessary interaction between innervation from nasal tissues and the development of the olfactory lobes, thus indicating a possible cause for loss of olfactory lobe development in the small eye homozygote fetus.

A genetic basis for Kallman's syndrome has been determined by isolation of a gene, identified on a critical region on human chromosome Xp22.3, that shares homology with molecules involved in cell adhesion and axonal pathfinding [N-CAM's and tyrosine phosphatases] (Franco *et al.*, 1991). More recent work has suggested that LHRH neurons may follow a "CAM-trail", involving multiple cell adhesion molecules [e.g. N-CAM, Ng-CAM and N-cadherins] along the medial surface of the forebrain (Norgreen and Brackenbury, 1993).

In view of this information, it appeared that if abnormal migration of LHRH neurons were observed in the small eye $Sey^{Neu}/+$ heterozygous fetus this might indicate interaction between neurons requiring cell adhesion molecules for migration and a role for *Pax6* in this process. This is particularly relevant as the areas through which LHRH neurons migrate (namely the nasal epithelium, nervus terminalis, olfactory lobe and preoptic area, hypothalamic area) and are born (the nasal placode) all express *Pax6* (Walther and Gruss, 1991).

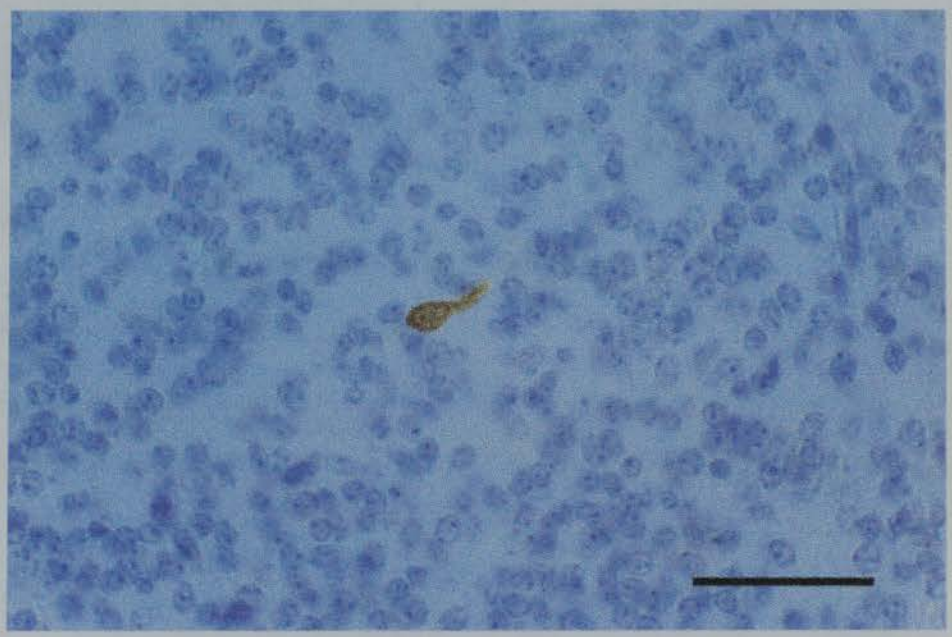

Figure 5.1. Anti-LHRH/DAB immunohistochemistry to single LHRH secreting neuron in the hypothalamic region of a +/+ E16.5 fetal mouse brain counterstained with haematoxylin. (Scale bar - 50μm).

A preliminary study was devised to determine if LHRH neuronal migration was affected in the $Sey^{Neu}/+$ heterozygous fetus using immunohistochemistry against LHRH secreting neurons. The experiments described in this chapter were carried out in collaboration with Dr N. Brook and Ms A. Aitkenhead of the MRC Reproductive Biology Unit, Edinburgh. Small eye fetuses were examined at E16.5, the stage by which most LHRH neuronal migration is complete in the wild type fetus. Development of the testis in the Sey^{Neu}/Sey^{Neu} homozygous fetus was also examined to determine if a complete loss of LHRH neuron development might have any effect on fetal testicular development. The Sey^{Neu} allele was chosen for this study as the brain phenotype of this small eye homozygote mutant allele had already been extensively described (Schmahl *et al.*, 1993).

5.2. Materials and Methods

5.2.1. Mice

As Sey^{Neu}/Sey^{Neu} homozygotes are early post-natal lethal, it was necessary to inter-cross $Sey^{Neu}/+$ heterozygous parents to produce homozygous fetuses. Homozygous fetuses were readily identifiable at dissection by the absense of eyes and characteristic domed head and micrognathia previously described in other small eye homozygous fetuses (Hogan *et al.*, 1986; 1988; Kaufman, 1995).An embryonic age E16.5 was used for his study as LHRH neuron migration is complete by this stage in the wild type embryo. Examination of testicular size and morphology was performed on the testes dissected from E17.5 Sey^{Neu}/Sey^{Neu} homozygous fetuses produced for investigation of tooth morphology (to be discussed in Chapter 6).

5.2.2. Tissues

Testes were dissected from E17.5 *Sey*^{Neu}/*Sey*^{Neu}, *Sey*^{Neu}/+ and +/+ fetuses using a Wild dissecting microscope, photographed and fixed in Bouin's solution at 4°C for 2 hours. Samples were then processed to wax blocks, sectioned at 7μm and stained with haematoxylin and eosin before examination using light microscopy. A total of 3 pairs of testis from each genotype group was examined.

Brains from E16.5 *Sey*^{Neu}/*Sey*^{Neu}, *Sey*^{Neu}/+ and +/+ fetuses were dissected from the skull and the left and right hemispheres separated before fixation in Bouin's solution at 4°C for 6 hours. Samples were transferred to 70% ethanol and automatically dehydrated to paraffin wax for embedding. Serial sagittal sections at 7μm were cut from the midline of one left hemisphere of each genotype group, *Sey*^{Neu}/*Sey*^{Neu}, *Sey*^{Neu}/+ and +/+ , with the first 2 serial sections from every run of 6 sections mounted on to TESPA (3-aminopropyltriethoxysilane, Sigma) coated slides. Slides were baked at 37°C overnight for immunohistochemistry.

Figure 5.2. (Following page) Photograph of ventral surfaces of E16.5 **a)** *Sey*^{Neu}/*Sey*^{Neu}, **b)** *Sey*^{Neu}/+ and **c)** +/+ fetal mouse brains. Note complete absence of olfactory lobes in a) *Sey*^{Neu}/*Sey*^{Neu} fetal brain and reduction in size of the pre-optic area and the midbrain area appears compacted. A slight reduction in size of the frontal lobes can also be observed in the *Sey*^{Neu}/*Sey*^{Neu} fetal brain although this difference in not marked.

Figure 5.2.

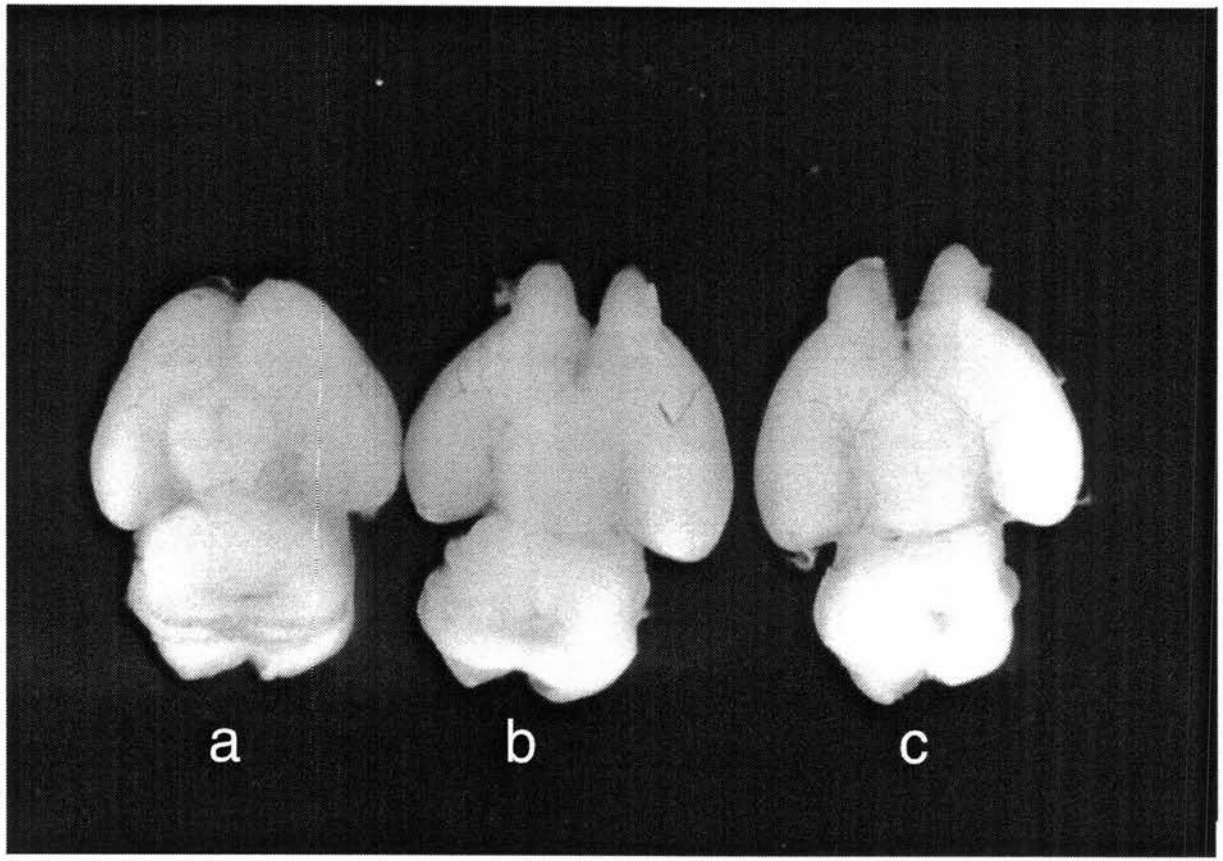

The left hemisphere of one fetus from each genotype group was selected for immunohistochemistry. A total of 31+/+ sections, 34 $Sey^{Neu}/+$ sections and 68 Sey^{Neu}/Sey^{Neu} sections were examined using immunohistochemistry to LHRH. The number of samples for this study was restricted due to the large number of sections required from each brain to traverse the entire left hemisphere to ensure that the number of neurons observed in each sample was representative.

5.2.3. Immunohistochemistry

Immunohistochemistry to LHRH secreting neurons was performed by Ms A. Aitkenhead in the MRC Reproductive Biology Unit Edinburgh from the protocol of Schwanzel-Fukuda and Pfaff (1989) with some modifications. Antiserum to LHRH, LR1 rabbit polyclonal antibody was provided by Dr R. Benoit (see Schwanzel-Fukuda and Pfaff, 1989; 1992).

In brief, slides were dewaxed in Xylene (BDH) before rehydrating through an alcohol series. Endogenous peroxidase activity was quenched by immersion in 10% H_2O_2/methanol before 80% alcohol. Slides were then washed in distilled water and placed in a 0.5% Triton-X100 in distilled water to permeate cell membranes. After further rinsing non-specific binding was prevented by incubation in blocking buffer containing normal swine serum and bovine serum albumin in Tris-buffered saline (TBS) to TBS at a 1:5 ratio. Blocking was carried out for 1 hour at room temperature. After blocking, slides were drained and primary anti-LHRH antibody applied at a 1:10000 dilution. Slides were incubated at 4°C for 24 hours.

After washing in TBS to remove any unbound primary antibody, the secondary antibody, a swine anti-rabbit biotinylated Fab fragment (Boehringer), was applied at a

1:500 dilution in blocking buffer. Slides were incubated for 1 hour at room temperature. Unbound secondary antibody was removed by further washes in TBS before addition of avidin-biotinylated horseradish-peroxidase complex (DAKO). A further incubation of 30 minutes was allowed before any unbound avidin complex was removed by washing with TBS. Visualisation was achieved by incubation in 0.05% H_2O_2/ 3'diaminobenzidine tetrahydrochloride (DAB) [DAKO] diluted in 0.05M Tris buffer, pH7.6 for 10 minutes. Slides were then rinsed in distilled water, counterstained with Harris' haematoxylin before dehydrating through the ethanol series. Slides were cleared in Xylene and mounted using Pertex mounting medium. Immunoreactive LHRH cells were observed as staining with dark brown granules in the cytoplasm and neurites (see Figure 5.1.).

5.2.4. Analysis of neuronal migration

Serial sections were ordered into sequence (31, 34 and 68 sections per individual hemisphere) and photographed using an Olympus BH2 microscope, a Sony CCD/RGB video camera attatced to a Mitsubishi colour printer. Positions of the LHRH positive nuclei were highlighted by hand. The position of each positive nuclei was marked on a tracing of each brain section in correct orientation to its neighbouring sections until the position of all neurons had been visualised. Each neuron was then marked on a diagrammatic representation of the mid-saggital section of the left hemisphere for visual comparison.

5.3. Results

5.3.1. Brain and testis development in Sey^{Neu}/Sey^{Neu}, $Sey^{Neu}/+$ and +/+ fetuses

Brains from $Sey^{Neu}/+$ and +/+ fetuses appeared similar in size and morphology with no macroscopic abnormalities of size or shape of brain areas (see Figure 5.2.). Olfactory lobes were of approximately equal size. Brains from Sey^{Neu}/Sey^{Neu} fetuses appeared similar to those from $Sey^{Neu}/+$ and +/+ fetuses with regard to external size and appearance of the frontal lobes and midbrain, although the latter appeared somewhat condensed. The main most obvious difference was the complete absence of olfactory lobe development in brains of Sey^{Neu}/Sey^{Neu} fetuses.

Testis size and development was found to be normal in the Sey^{Neu}/Sey^{Neu} homozygous fetuses with no visible abnormalities of cell type or development. All of the 6 individual testes examined from the three E17.5 Sey^{Neu}/Sey^{Neu} homozygote fetuses and the four testes examined each from two +/+ and 2 $Sey^{Neu}/+$ fetuses proved to be of equal size and shape at a macromorphological level and normal when examined histologically (see Figure 5.3. a and b).

Figure 5.3. (Following page) **a)** Photograph of section through E17.5 Sey^{Neu}/Sey^{Neu} mouse testis showing normal morphology. Photographs of left and right testis from **b)** +/+ and **c)** Sey^{Neu}/Sey^{Neu} E17.5 mouse fetuses. No difference in size or morphology is observed between testes from the wild type and small eye homozygous fetuses. (Scale bar - 80μm).

Figure 5.3.

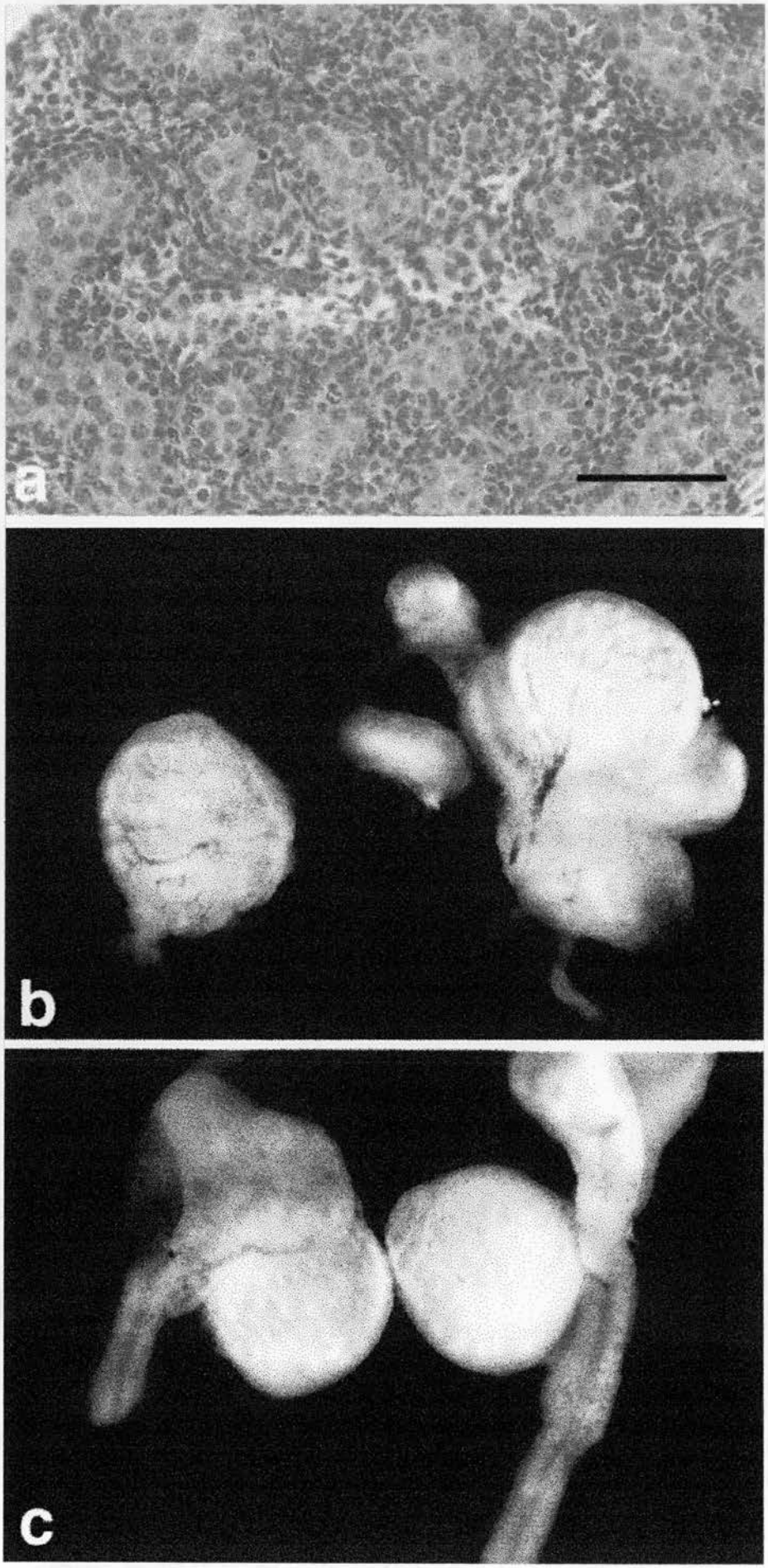

Figure 5.4.

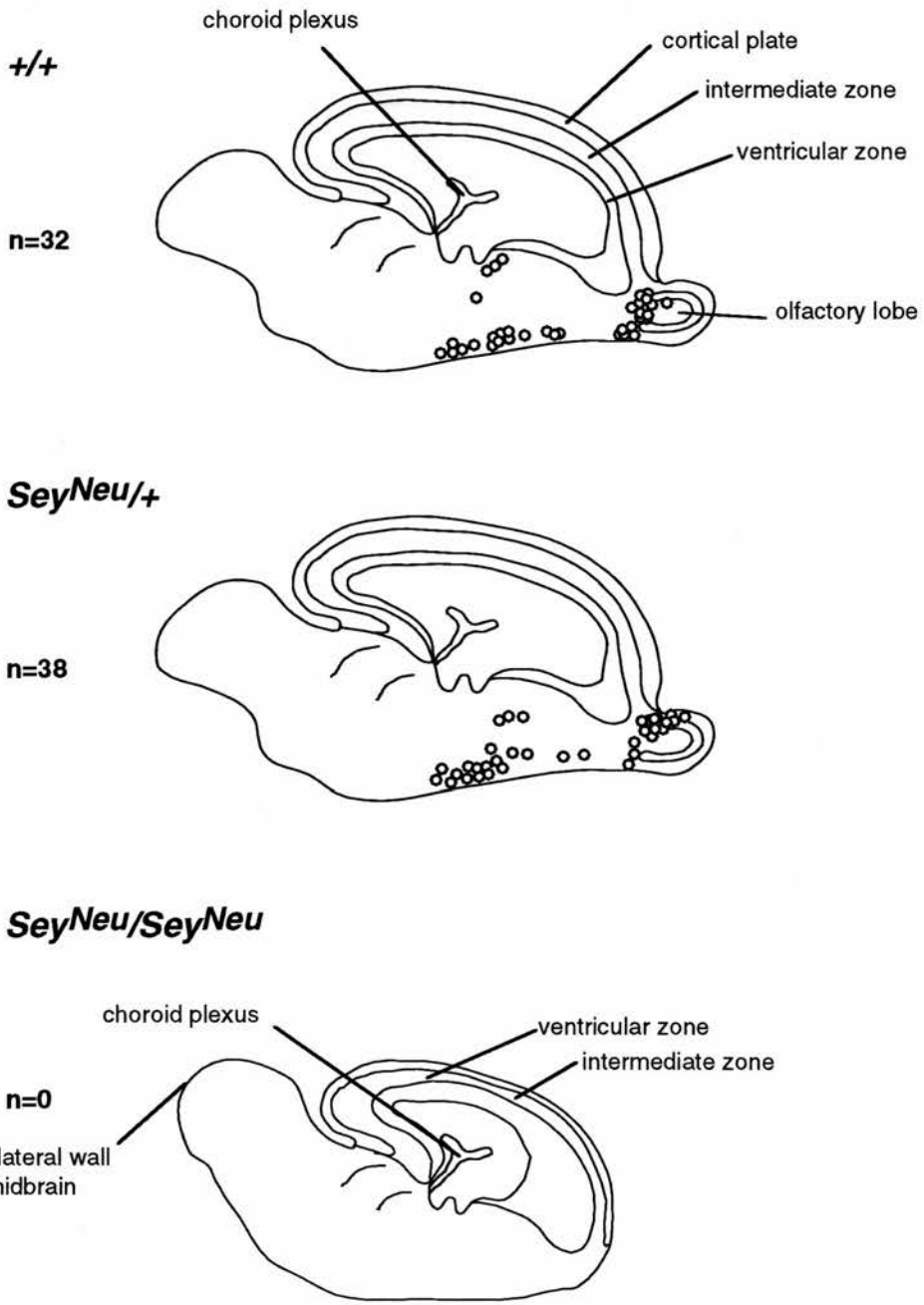
+/+
choroid plexus
cortical plate
intermediate zone
ventricular zone
n=32
olfactory lobe
SeyNeu/+
n=38
SeyNeu/SeyNeu
choroid plexus
ventricular zone
intermediate zone
n=0
left lateral wall
of midbrain

5.3.2. Analysis of LHRH neuron migration in E16.5 *Sey*^{Neu}/*Sey*^{Neu}, *Sey*^{Neu}/+ and +/+ fetuses

A total of 32 LHRH+ve neurons were identified in the frontal left hemisphere of the +/+ fetus and 38 in the *Sey*^{Neu}/+ fetus. The majority of these neurons were situated in the olfactory lobe and along the hypothalamic region as shown in Figure 5.4. A small number of neurons were identified in the preoptic area, three in the +/+ fetus and four in the *Sey*^{Neu}/+ fetus. There appeared to be no difference between the *Sey*^{Neu}/+ and +/+ fetal brains regarding efficacy of LHRH neuron migration although the number of samples was too small for statistical analysis. No LHRH secreting neurons were observed on any sections of brain from the*Sey*^{Neu}/*Sey*^{Neu} fetus (see Figure 5.5.).

Figure 5.4. (Previous page) Schematic representation of results of immunohistochemistry for LHRH secreting neurons in serial sagittal sections of the left hemisphere of E16.5 fetal brains from **a)** +/+, **b)***Sey*^{Neu}/+ and **c)***Sey*^{Neu}/*Sey*^{Neu} fetuses. Normal migration of LHRH secreting neurons from the olfactory bulb to the hypothalamic region can be observed in the +/+ and *Sey*^{Neu}/+ brains, whilst no LHRH neurons were observed in the *Sey*^{Neu}/*Sey*^{Neu} brain. **o** - single LHRH neuron. n= total number of LHRH positive neurons in all sections examined (+/+, 31 sections; *Sey*^{Neu}/+, 34 sections; *Sey*^{Neu}/*Sey*^{Neu}, 68 sections).

Figure 5.5. (Following page) Anti-LHRH/DAB immunohistochemistry to LHRH secreting neurons in the hypothalamic region of **a)** *Sey*^{Neu}/+ and **b)** *Sey*^{Neu}/*Sey*^{Neu} E16.5 fetal mouse brains. The area shown in a) and b) is shown in the schematic diagram above. Two migrating neurons are visualised in the *Sey*^{Neu}/+ brain (arrowheads) whilst no LHRH neurons were identified in the *Sey*^{Neu}/*Sey*^{Neu} brain examined. Arrowheads- LHRH positive neurons. (Scale bar - 200μm).

Figure 5.5.

Figure 5.5.

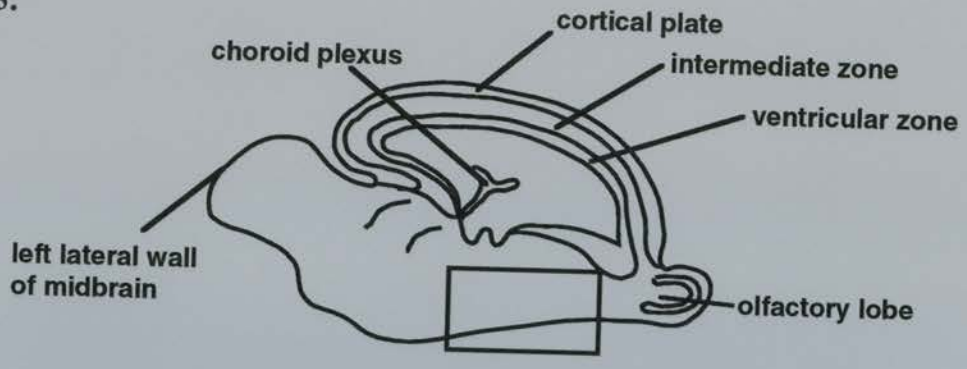

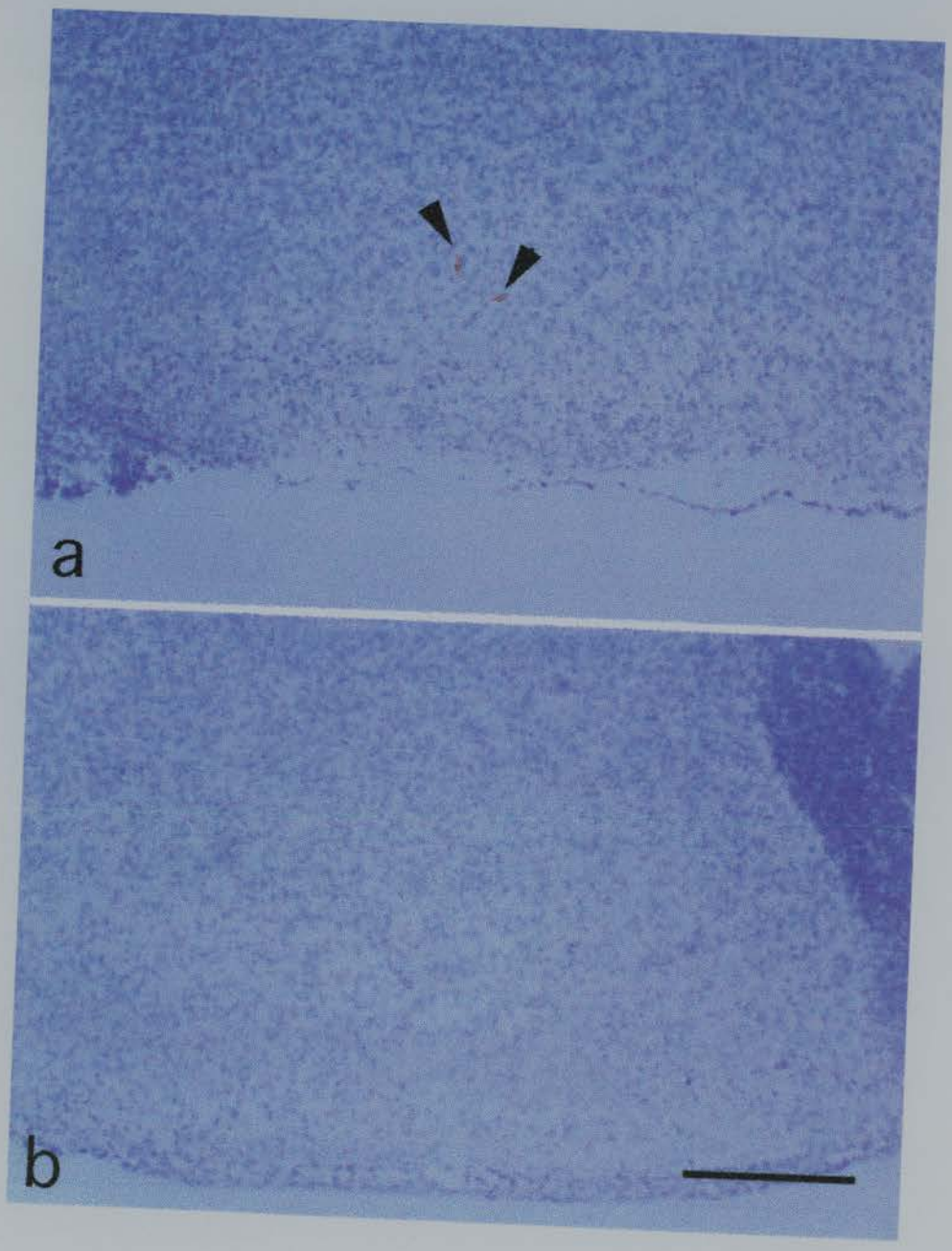

5.4. Discussion

The preliminary results from this study indicate that there is no major defect in LHRH secreting neuron migration in the brains of fetuses heterozygous for functional *Pax6*. Whatever cellular interactions occur in the developing brain with regard to migration of LHRH neurons, this interaction or induction is not perturbed by a loss of 50% of *PAX6* protein.

This result is perhaps not unexpected as, apart from cases of human patients with large deletions of the *Pax6* syntenic region on human chromosome 11q13, encompassing both the aniridia and Wilm's tumour regions (WAGR syndrome), no gonadal abnormalities have been reported in conjunction with anterior eye segment phenotypes. A complete loss of LHRH neuronal enervation during fetal life is unlikely to have a direct effect on fetal testicular size as fetal testis development is LHRH independant. It is during later pubertal development that abnormalities in testicular development would become apparent, as observed in Kallman's syndrome patients. As shown in Figure 5.3., Sey^{Neu}/Sey^{Neu} fetal testis development appeared normal at E17.5.

The complete absence of LHRH secreting neurons in the Sey^{Neu}/Sey^{Neu} homozygous fetuses examined supports the observations that LHRH neurons are born in the nasal placodes after placodal differentiation and are not, as perhaps might have been an alternative hypothesis, induced from some unspecified cell type in close relationship with the nasal placode. As in both the Kallman's syndrome fetus and the Sey^{Neu}/Sey^{Neu} homozygous fetus both the nasal apparatus and olfactory lobes are absent, this indicates that induction of the olfactory lobes is dependant upon enervation from the nasal and vomeronasal organs .

Although not conclusive, results from this preliminary study, supports other more direct evidence that LHRH neurons are derived from the nasal placodes (Wray *et al.*, 1989a; 1989b; Schwanzel-Fukuda and Pfaff, 1989). The results also show that LHRH neuron migration appears to progress normally in an environment heterozygous for *Pax6* and that therefore loss of a single copy of the *Pax6* gene is not sufficient to cause developmentally detrimental migrational defects in these specific neurons in the developing brain. This gives insight as to the rarity of overt neurological phenotypes in known human *PAX6* mutation syndromes.

Chapter 6

The effect of genetic background on tooth and craniofacial abnormalities in small eye mutant mice

6.1 Introduction

Although sigificant advances have been made in understanding the role of *Pax6* during eye and nasal development (Grindley *et al.*, 1995; see also Chapters 2 and 3), the effect of eye and nasal agenesis on frontofacial morphogenesis in the homozygous *Sey/Sey* fetus has been less well characterised. As the frontofacial region is normal in the *Sey/+* heterozygous animal, this model has provided little insight to the craniofacial phenotypes observed in the *Sey/Sey* homozygous fetus and their relevance to human craniofacial abnormalities.

Kaufman *et al.* (1995) reported 80% of small eye homozygous *Sey/Sey* fetuses examined possessed a complete or partial duplication of the upper incisor teeth. The homozygous *Sey/Sey* fetuses examined in Kaufman's study also exibited the presence of a midline cartilaginous rod-like structure protruding between the two maxillae in the abnormal nasal region, this rod-like structure appearing to be an extention of the chondrocranium.

In order to examine whether the incidence of supernumerary upper incisor teeth and the craniofacial abnormalities reported by Kaufman *et al.* (1995) were a direct result of mutations within the *Pax6* gene or were secondary effects of variable genetic background, a histological study was undertaken, in collaboration with Professor M.H. Kaufman of the Department of Anatomy, University of Edinburgh. We

compared the frontofacial/nasal phenotypes produced by two small eye alleles, *Sey* and *Sey*^{Neu} on different genetic backgrounds.

6.2. Mouse strains

The original small eye mutation (Roberts, 1967) arose in a stock called "CSR" (Roberts, 1966) and was subsequently outcrossed. The small eye strain used in the study by Kaufman *et al.* (1995) was maintained at the Institute of Cell, Animal and Population Biology, University of Edinburgh. This strain was of heterogeneous coat colour and were progeny of the original small eye strain described by Roberts (1967). The present genetic background of this strain is unclear, but probably contains elements of C57BL/Fa and JU/Fa. The stock is maintained by randomly intercrossing heterozygous mice. This small eye strain will be identified as MHK-*Sey* for the purposes of this study.

Four further small eye strains were used for test-mating. *Sey* and *Sey*^{Neu} alleles maintained on CBA/Ca backgrounds were obtained from the MRC Human Genetics Unit, Edinburgh. The CBA/Ca-*Sey*^{Neu} strain (Favor *et al.*, 1989) was originally provided by Dr J. Favor (Intitut fur Saugetiergenetik, Neuherberg, Germany). Stocks for use in this study were maintained by mating heterozygous CBA/Ca-*Sey*/+ or CBA/Ca-*Sey*^{Neu}/+ animals to CBA/Ca animals at the Centre for Reproductive Biology, Edinburgh. These *Sey* strains will be described as CBA/Ca-*Sey* and CBA/Ca-*Sey*^{Neu}.

Another small eye stock, SEYTG, was homozygous for the reiterated β-globin transgene (TgN(Hbb-b1)83Lo) [abbreviated to *Tg*] on chromosome 3, derived from strain "83" (Lo, 1987) [see also Chapter 2]. The SEYTG stock was derived from first generation matings between CBA/Ca-*Sey*/+ heterozygotes and TGB mice (Strain 83,

C57BL, CBA/Ca mixed background). Strain CBA/Ca is homozygous agouti (*A/A*) and strain C57BL is homozygous non-agouti (*a/a*) and CBA/Ca-*Sey*/+ mice are phenotypically agouti (*A/A* or *A/a*).

The small eye locus was observed to segregate with the agouti locus (*a/a, A/a or A/A*), which maps approximately 26cM proximal to the *Sey* locus on chromosome 2 (Davisson 1986, Hogan *et al.,* 1986; Hogan *et al.,* 1987). Mice from the TGB strain may be non-agouti (*a/a*) or agouti (*A/a* or *A/A*). As all first generation crosses between CBA/Ca-*Sey*/+ and TGB animals produced some non-agouti small eye offspring (*Sey a*/+ *a*), alleles for *Sey* and *a* must have been introduced from the CBA/Ca-*Sey*/+ stock; the *Sey* allele segregated preferentially with the non-agouti allele (*a*), confirming that *Sey* and *a* were in coupling. Progeny were backrossed to TGB for two further generations before resultant *Sey*/+, *Tg/Tg* animals were used to establish the SEYTG stock. The SEYTG stock was then maintained by crossing SEYTG animals (*Sey*/+, *Tg/Tg*, and *a/a, A/a or A/A*) to agouti TGB mice (+/+, *Tg/Tg* and *A/a* or *A/A*). The SEYTG stock continued to segregate at the agouti locus and separate agouti (*A/a or A/A*) and non agouti (*a/a*) sublines were established.

Table 6.1. Table showing number and percentage of fetuses in each strain and genotype group examined exhibiting supernumerary upper incisor teeth, cartilaginous "spurs" and a median nasal cartilaginous rod.

Strain	Genotype	Number of fetuses	No. fetuses with supernumerary upper incisors (%)	No. fetuses with cartilaginous 'spurs' (%)	No. fetuses with median cartilaginous nasal rod (%)
MHK	*Sey/Sey*	19*	16 (78)*	12 (63)†	19 (100)†
SEYTG(*A/?*)#	*Sey(A or a)/Sey(A or a)*	7	3 (43)	6 (86)	7 (100)
SEYTG(*a/a*)#	*Sey a/Sey a*	7	1 (14.2)	0 (0)	7 (100)
CBA/Ca-*Sey*	*Sey/Sey*	12	0 (0)	4 (33)	12 (100)
(CBA/Ca-Sey^{Neu} x SEYTG)F_1	Sey^{Neu}/Sey	9	2 (22)	2 (22)	9 (100)
CBA/Ca-Sey^{Neu}	Sey^{Neu}/Sey^{Neu}	11	0 (0)	3 (27)	11 (100)

#SEYTG (*a/a*) fetuses are from *a/a* x *a/a* matings. SEYTG (*A/?*) fetuses are from *A/?* x *A/?* matings where *A/?* is either *A/A* or *A/a*. Consequently SEYTG (*A/?*) fetuses may be *A/A*, *A/a* or *a/a* at the agouti locus. * Since Kaufman *et al.* (1995) was published, the histological sections from one of the fetuses reported has been misplaced, therefore, data pertaining to number of fetuses with supernumerary teeth is taken from the original publication whilst number of fetuses with cartilaginous 'spurs' considers only 19 of the original 20 fetuses. † Data from analysis of 19 extant fetuses.

6.2.1. Fetal dissection and analysis

Selected *Sey/+* or *Sey^{Neu}/+* small eye heterozygotes were mated to animals of appropriate strain and genotype and mating was confirmed by the presence of a vaginal plug the following morning. This was designated E0.5 days. Pregnant females were killed by cervical dislocation on days E14.5 to E18.5. Fetuses were dissected from the uterus into cold phosphate buffered saline (PBS) on ice and examined under a Wild M5 dissecting microscope.

Homozygous *Sey/Sey* or compound heterozygous *Sey^{Neu}/Sey* fetuses produced in the different matings were easily identified at dissection by the absence of eyes and characteristic cranio-facial phenotype of foreshortened upper jaw associated with a protruding tongue. Fetuses of desired phenotype were decapitated and their heads fixed in Bouin's fixative overnight. Samples were embedded in paraffin wax, serially sectioned at 7μm in the coronal plane and stained with haematoxylin and eosin (see Appendix II). Slides were examined using a Leitz Diaplan light microscope. Morphological abnormalities were verified by consultation with Professor M.H. Kaufman.

Table 6.2. Table showing number of supernumerary upper incisor teeth and cartilaginous 'spurs' possessed by each fetus examined for all genotype groups studied.

Genotype	***Sey/Sey***		***Sey (A* or *a)/Sey (A* or *a)***		***Sey a/Sey a***		***Sey/Sey***		***Sey^{Neu}/Sey^{Neu}***		***Sey ^{Neu}/Sey***	
Strain	**MHK**		**SEYTG(*A/?*)**		**SEYTG(*a/a*)**		**CBA/Ca-*Sey***		**CBA/Ca-*Sey^{Neu}***		**(CBA/Ca-*Sey^{Neu}* x SEYTG)F$_1$**	
Fetus No.	No. extra teeth	No. cart. 'spurs'	No. extra teeth	No. cart. 'spurs'	No. extra teeth	No. cart. 'spurs'	No. extra teeth	No. cart. 'spurs'	No. extra teeth	No. cart. 'spurs'	No. extra teeth	No. cart. 'spurs'
1	2	2	2	0	1	0	0	1	0	1	1	0
2	2	2	1	1	0	0	0	1	0	1	1	0
3	2	1	1	1	0	0	0	1	0	1	0	2
4	2	1	0	2	0	0	0	1	0	0	0	1
5	2	0	0	1	0	0	0	0	0	0	0	0
6	2	0	0	1	0	0	0	0	0	0	0	0
7	2	0	0	1	0	0	0	0	0	0	0	0
8	2	0	-	-	-	-	0	0	0	0	0	0
9	2	0	-	-	-	-	0	0	0	0	0	0
10	1	2	-	-	-	-	0	0	0	0	-	-
11	1	2	-	-	-	-	0	0	0	0	-	-
12	1	1	-	-	-	-	0	0	-	-	-	-
13	1	1	-	-	-	-	-	-	-	-	-	-
14	1	1	-	-	-	-	-	-	-	-	-	-
15	1	1	-	-	-	-	-	-	-	-	-	-
16	1	0	-	-	-	-	-	-	-	-	-	-
17	0	2	-	-	-	-	-	-	-	-	-	-
18	0	1	-	-	-	-	-	-	-	-	-	-
19	0	0	-	-	-	-	-	-	-	-	-	-

6.3. Results

A total of 46 homozygous (*Sey/Sey* or Sey^{Neu}/Sey^{Neu}) and compound heterozygous (Sey^{Neu}/Sey) fetuses were examined for the presence of supernumerary upper incisor teeth and a median cartilaginous nasal rod. The fetuses were separated into four groups by strain and genotype: 12 CBA/Ca-*Sey/Sey*, 11 CBA/Ca-Sey^{Neu}/Sey^{Neu}, 14 SEYTG-*Sey/Sey*, and 9 (CBA/Ca-Sey^{Neu} x SEYTG)F_1Sey^{Neu}/Sey fetuses.

Of the 14 SEYTG-*Sey/Sey* fetuses examined in this study, seven were from the non-agouti subline (SEYTG-*Sey a/Sey a* fetuses) and seven were from the agouti subline [SEYTG-*Sey*(*A* or *a*)/*Sey* (*A* or *a*) fetuses].

In addition, 19 MHK-*Sey/Sey* P1.0 animals from the original study by Kaufman *et al.* (1995) were reconsidered in this study. For ease of reference, these will be referred to as 'fetuses'. In all of the small eye homozygous (*Sey/Sey* or Sey^{Neu}/Sey^{Neu}) or compound heterozygous (Sey^{Neu}/Sey) fetuses examined, developing molar dentition was present appropriate to the developmental age of the fetus.

Figure 6.1. (Following page) (**a, b**) Representative coronal section through the fronto-nasal region of a *Sey/+* postnatal day 1 control mouse. Note the presence of the following: cartilaginous nasal capsule (cc), cartilaginous nasal septum (ns), nasal cavity (nc), upper incisor teeth (t). (**c,d**) Comparable coronal sections through the fronto-nasal region of (**c**) an E17.0 homozygous Sey^{Neu}/Sey^{Neu} fetus and (**d**) a day 1.0 postnatal homozygous *Sey/Sey* mouse. Note the presence in both (c) and (d) of a median cartilaginous rod-like structure (large arrows), two upper incisor teeth and, in fetus (d), two "spurs" (small arrows). Close-up views of the fronto-nasal region of the fetus illustrated in 1c are shown in Figures 2a-c, and those of the mouse illustrated in 1d are shown in figures 3d-f. (a.,b.,c. x 25; b. x 40) All sections illustrated in Figures 1-4 were stained with haematoxylin and eosin.

Figure 6.1.

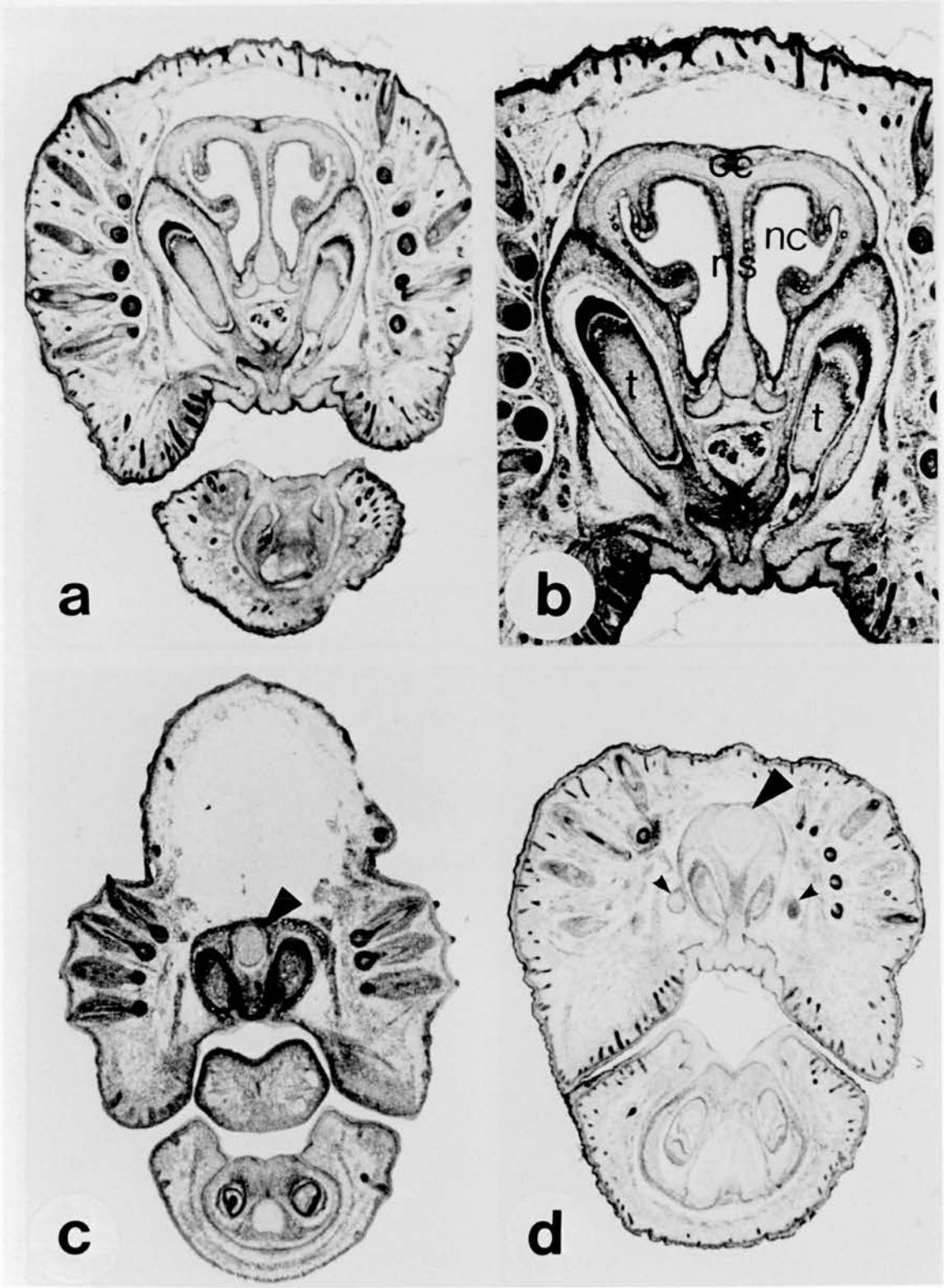

6.3.1. Incidence of supernumerary upper incisor teeth

The results of histological observations are shown in Table 6.1. and 6.2. No supernumerary upper incisor teeth were observed in any of the 12 CBA/Ca-*Sey/Sey* or 11 CBA/Ca-*Sey^{Neu}/Sey^{Neu}* fetuses examined (see Figures 6.1c and d). Of the seven SEYTG-*Sey*(*A* or *a*)/*Sey* (*A* or *a*) fetuses, three (43%) possessed supernumerary upper incisor teeth. Two fetuses possessed one extra upper incisor tooth positioned lateral to the normal left upper incisor. The third fetus posessed two supernumerary incisors, giving a total of four; one supernumerary tooth was slightly smaller than normal and located lateral to the normal left incisor, while the right supernumerary tooth was considerably smaller than normal resembling no more than a tooth bud. Of the seven SEYTG-*Sey a/Sey a* fetuses examined, only one possessed a single supernumerary upper incisor tooth (14.3%), this being located lateral to the normal left incisor.

Figure 6.2. (Following page) Representative intermittent serial sections through the fronto-nasal region of an E17.0 *Sey^{Neu}/Sey^{Neu}* fetus (**a-c**) and two postnatal day 1 *Sey/Sey* mice (**d-f**; **g-h**). The fetus illustrated in (a-c) possessed two upper incisor teeth; no cartilaginous "spurs" were present. The mouse whose fronto-nasal sections are illustrated in (d-f) possessed three upper incisor teeth, the "spur" (arrow) being present on the same side as the supernumerary upper incisor tooth. While the latter is not observed in this series of sections, it is shown in Figure 6.4b. The mouse illustrated in (g) and (h) possessed a left-sided supernumerary upper incisor tooth, but in this instance the single "spur" present (arrow) was located on the contralateral side. The "spurs" appear to originate in the cancellous bone in which the incisor teeth form. More distally they have a central cartilaginous "core" which appears to be surrounded by a fibrous capsule. (All illustrations, x 63).

Figure 6.2.

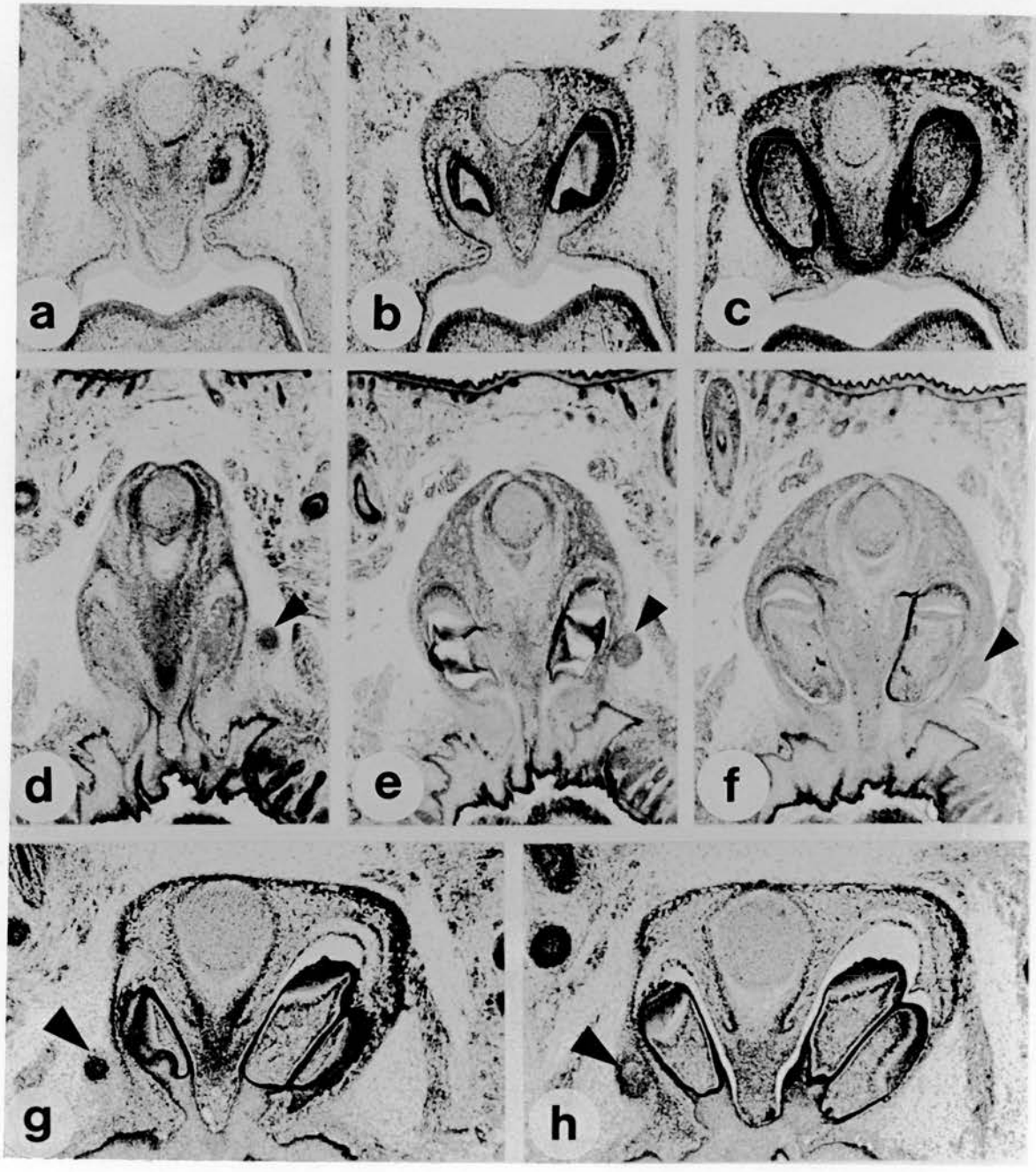

Table 6.3. Tables showing statistical comparisons between small eye homozygous fetuses on varying genetic backgrounds for presence or absence of abnormal phentoypic features.

a) Testing for differences between sublines of SEYTG strain of *Sey/Sey* genotype.

		Supernumerary upper incisor teeth						Cartilaginous 'spurs'					
		Ratios†				Test*	(*P*)	Ratios†				Test*	(*P*)
Sample 1	**Sample 2**	Sample 1 +ve	Sample 1 -ve	Sample 2 +ve	Sample 2 -ve			Sample 1 +ve	Sample 1 -ve	Sample 2 +ve	Sample 2 -ve		
SEYTG (*A/?*)	SEYTG (*a/a*)	3	4	1	6	FE	0.56	6	1	0	7	FE	**0.0047**

b) Testing for differences between differing *Sey* alleles on a similar (largely CBA/Ca) genetic background.

		Supernumerary upper incisor teeth						Cartilaginous 'spurs'					
		Ratios†				Test*	(*P*)	Ratios†				Test*	(*P*)
Sample 1	**Sample 2**	Sample 1 +ve	Sample 1 -ve	Sample 2 +ve	Sample 2 -ve			Sample 1 +ve	Sample 1 -ve	Sample 2 +ve	Sample 2 -ve		
CBA/Ca-*Sey*	CBA/Ca-Sey^{Neu}	0	12	0	11	FE	0.99	4	8	3	8	FE	0.99
CBA/Ca-*Sey*	(SEYTG x CBA/Ca-Sey^{Neu})	0	12	2	7	FE	0.17	4	8	2	7	FE	0.66
CBA/Ca-Sey^{Neu}	(SEYTG x CBA/Ca-Sey^{Neu})	0	11	2	7	FE	0.19	3	8	2	7	FE	0.99

Table 6.3. (continued)
c) Testing for differences between *Sey/Sey* genotypes on varying genetic backgrounds.

		Supernumerary upper incisor teeth						Cartilaginous 'spurs'					
		Ratios†				Test*	(*P*)	Ratios†				Test*	(*P*)
Sample 1	**Sample 2**	Sample 1 +ve	Sample 1 -ve	Sample 2 +ve	Sample 2 -ve			Sample 1 +ve	Sample 1 -ve	Sample 2 +ve	Sample 2 -ve		
MHK	CBA/Ca-*Sey*	16	3	0	12	χ^2	**0.0001**	12	7	4	8	χ^2	0.21
MHK	SEYTG (*A/?*)	16	3	3	4	FE	0.057	12	7	6	1	FE	0.37
MHK	SEYTG (*a/a*)	16	3	1	6	FE	**0.002**	12	7	0	7	FE	**0.006**
MHK	SEYTG (*a/a*) plus (*A/?*)	16	3	4	10	χ^2	**0.003**	12	7	6	8	χ^2	0.42
CBA/Ca-*Sey*	SEYTG (*A/?*)	0	12	3	4	FE	**0.036**	4	8	6	1	FE	0.057
CBA/Ca-*Sey*	SEYTG (*a/a*)	0	12	1	6	FE	0.37	4	8	0	7	FE	0.25
CBA/Ca-*Sey*	SEYTG (*a/a*) plus (*A/?*)	0	12	4	10	FE	0.10	4	8	6	8	FE	0.70

†Ratios indicate number of fetuses with phenotypic feature (+ve) verses number without (-ve).

* FE, Fisher's Exact test; χ^2, Chi Squared test. Statistically significant *p* values are shown in **bold.**

Of the nine Sey^{Neu}/Sey fetuses examined, two (22%) possessed a single supernumerary upper incisor tooth. In both cases this extra tooth was situated lateral to the normal left incisor. In one fetus the supernumerary incisor was of normal size and shape, but in the second fetus the extra tooth appeared smaller than its normal counterpart. The development of both supernumerary teeth was retarded and the connection between the developing tooth and the oral epithelium was still evident. This appearance confirmed that the normal incisor and the supernumerary incisor were both derived from invaginating oral epithelium rather than the supernumerary tooth having budded from the lateral aspect of the normal incisor tooth.

Of the 20 MHK-*Sey/Sey* fetuses reported in the original study (Kaufman *et al.*, 1995), five (25.0%) possessed a single supernumerary tooth lateral to the normal left upper incisor (see Figure 6.2. g,h), and two (10.0%) showed a single supernumerary tooth lateral to the normal right upper incisor tooth, only four fetuses possessing the normal complement of two upper incisor teeth (see Figure 6.4a). However, in nine fetuses (45.0%) a complete duplication of the upper incisor teeth was observed with a supernumerary incisor tooth located lateral to each normal upper incisor (see Figure 6.4c). Only one of the supernumerary teeth examined in this series appeared to be less well differentiated and smaller than its normal counterpart.

No teeth, whether supernumerary or normal, showed any evidence of pathology or abnormality of the enamel, dentine or pulp tissues where present. All fetuses examined possessed the normal number of upper and lower molars and lower incisor teeth.

Statistical analysis of frequency of supernumerary upper incisor teeth and the presence of cartilaginous 'spurs' between the different genotype and strain groups was performed on an Apple Macintosh computer using the statistical package "Statview 4.1" (Abacus Concepts, Berkeley, USA). Pairwise comparisons of the incidence of supernumerary upper incisor teeth (see Table 6.3.) indicate that there was no significant difference beween the *Sey/Sey* and Sey^{Neu}/Sey^{Neu} genotypes (when they are on a similar CBA/Ca genetic background). However, the genetic background appears to exert a significant effect on frequency in the different *Sey/Sey* stocks. More supernumerary teeth were found in fetuses from the agouti subline of SEYTG than in those from the non-agouti subline, although this difference (3/7 verses 1/7) was not statistically significant. Other differences were significant (see Table 6.3.) and this implies that genetic background affects the penetrance of this phenotype. The penetrance was highest in MHK-*Sey/Sey* fetuses (16/19; 84%) and lowest in CBA/Ca-*Sey/Sey* fetuses (0/12; 0%).

Figure 6.3. (Following page) (**a-f**) Representative intermittent serial sections through the fronto-nasal region of two day 1 postnatal *Sey/Sey* mice both of which possessed two spurs. The sections illustrated in (a-c) are from a mouse which possessed two upper incisor teeth, whilst those illustrated in (d-f) are from a mouse which possessed two supernumerary upper incisor teeth. The latter are illustrated in Figure 6.4c. (All illustrations, x 63).

Figure 6.3.

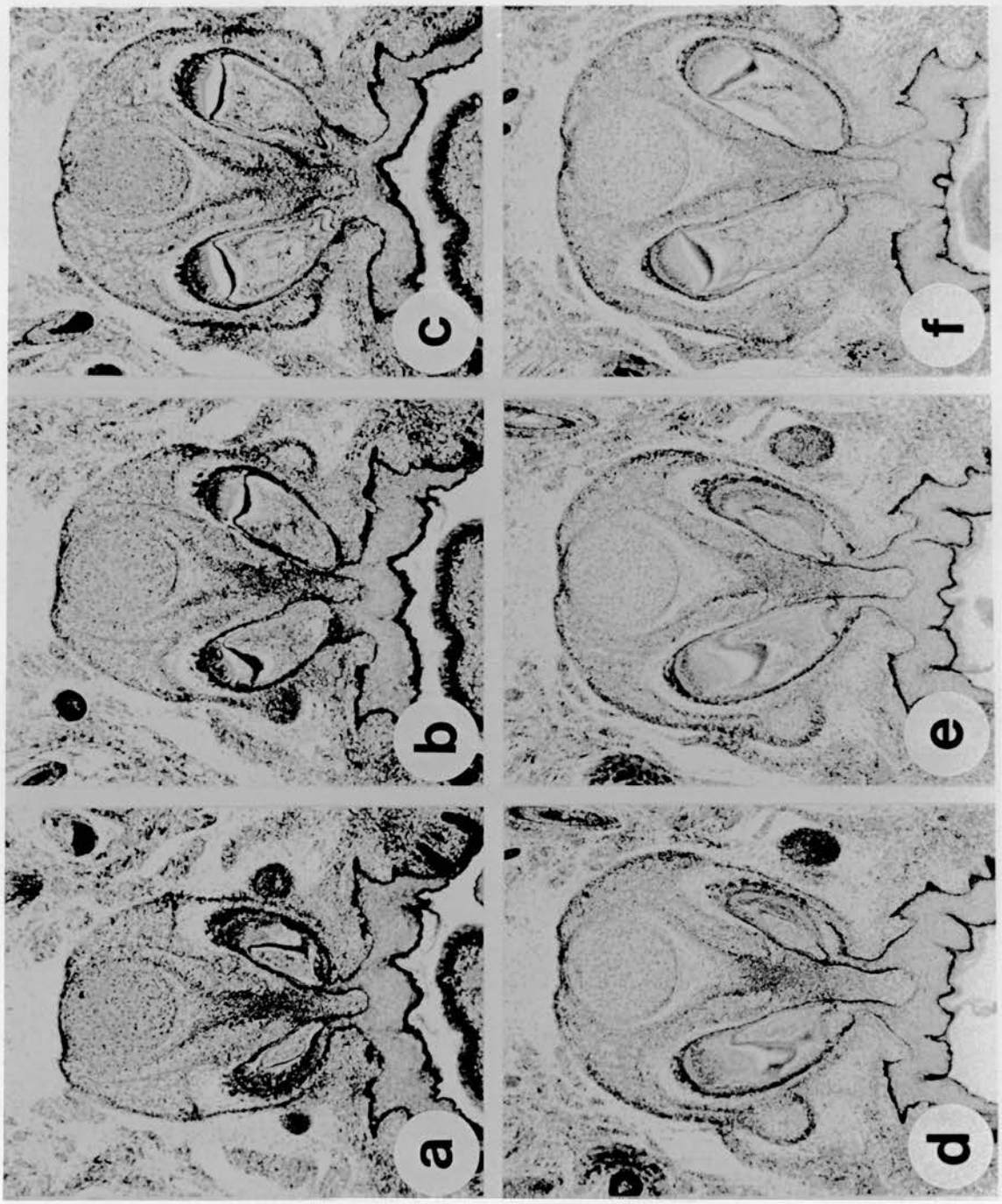

6.3.2. The median cartilaginous nasal rod

All 46 fetuses examined in this study, *Sey/Sey*, *Sey^{Neu}/Sey^{Neu}* and *Sey^{Neu}/Sey*, possessed a median nasal cartilaginous rod (see Tables 6.1 and 6.2., Figures 6.1c and d and Figures 6.2, 6.3, and 6.4). Thus, this phenotype was fully penetrant on all genetic backgrounds studied. No evidence of any nasal or eye tissues were observed in any of the small eye homozygous or compound heterozygous fetuses examined.

6.3.3. Presence of cartilaginous 'spurs'

A new phenotype was observed in the *Sey/Sey*, *Sey^{Neu}/Sey^{Neu}* and *Sey^{Neu}/Sey* fetuses on all strain backgrounds examined. Ectopic cartilaginous 'spurs', derived from the antero-lateral aspect of the nasal capsule, were present in some fetuses. At their origin, the 'spurs' appeared to have a central core of cancellous bone; more distally, a central cartilaginous core was present surrounded by a fibrous connective tissue capsule (see Figure 6.2. d-f, g-h; Figure 6.3. a-f.)

Figure 6.4. (Following page) Representative coronal sections through the fronto-nasal region of three postnatal day 1 *Sey/Sey* mice which possessed either (**a**) the normal complement of two upper incisor teeth, (**b**) a single supernumerary upper incisor, or (**c**) two supernumerary upper incisor teeth. (All illustrations, x 63).

Figure 6.4.

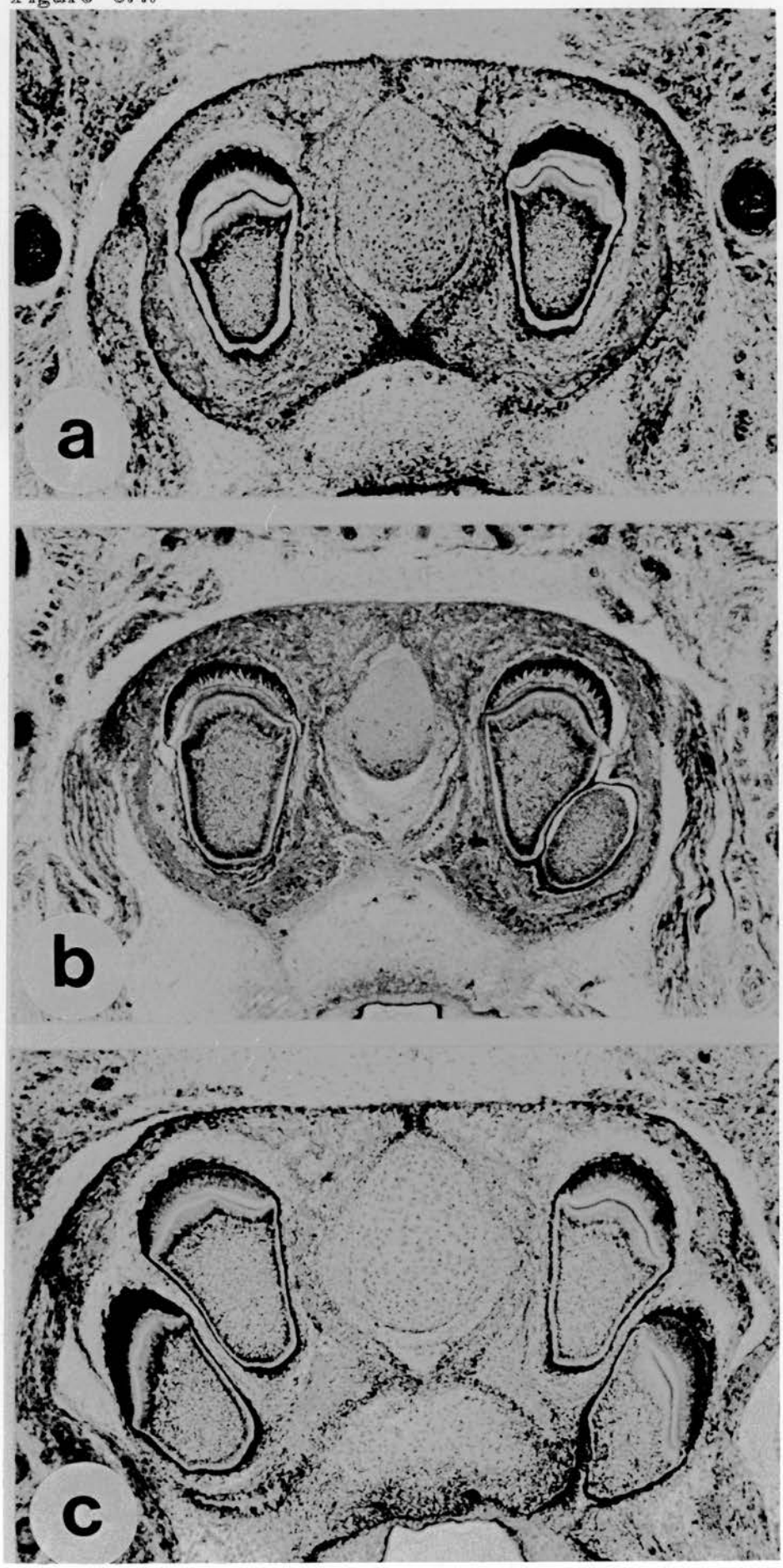

The 'spurs' extended forwards from the level of the normal incisor teeth towards the front of the snout, and measured up to 250μm in length. In the normal wild-type fetus, the nasal capsule surrounds the developing nasal tissues and septum, the area of the upper mandible in which the incisors are developing being outside this discrete nasal area (see Figure 1a and b). However, in the *Sey/Sey* homozygous fetus, the "nasal" capsule surrounds the entire area of the developing incisor teeth which are embedded in cancellous bone (see Figure 6.1.c and d). The 'spurs' are not dental derivatives as cartilage is never present in the developing tooth. 'Spurs' were present unilaterally or bilaterally in *Sey/Sey*, Sey^{Neu}/Sey^{Neu} and Sey^{Neu}/Sey fetuses and in all but one of the strains examined (see Table 6.1. and Table 6.2.) but were not observed in any wild type mice or in their small eye heterozygous littermates.

Pairwise comparisons of the incidence of cartilaginous 'spurs' between genotypes groups are shown in Table 6.3. No significant difference was found between *Sey/Sey* and Sey^{Neu}/Sey^{Neu} fetuses on a similar (mostly CBA/Ca) genetic background. However, as was observed for supernumerary teeth, genetic background appeared to influence the penetrance of the cartilaginous 'spurs' and there were some statistically significant difference between *Sey/Sey* fetuses from different strains.

The penetrance was highest in MHK-*Sey/Sey* fetuses (17/19; 63%) which was significantly higher (P= 0.0047) than for fetuses from the non-agouti subline of SEYTG (1/7; 14% penetrance). A significant difference between agouti and non-agouti SEYTG sublines also suggests that they differ for genes that affect the penetrance of cartilaginous 'spurs' (see Table 6.3.) but there is insufficient data to test whether the region of chromosome 2 close to the agouti locus is likely to be involved.

The stocks with the highest fequency of cartilaginous 'spurs' (MHK and the agouti subline of SEYTG) also had the highest frequency of supernumerary upper incisor teeth (see Tables 6.1. and 6.2.) which suggests that the penetrance of these phenotypes are affected by the same genes. The presence of cartilaginous 'spurs' was not, however, dependant on the presence of a supernumerary tooth as 'spurs' were present unilaterally or bilaterally in fetuses that possessed no supernumerary teeth (see Table 6.2., Figure 6.2.d-f, g-h and Figure 6.3.a-c). Moreover, division of the 19 MHK strain mice into three groups according to the number of supernumerary teeth, (0, 1 or 2) did not reveal a paralell trend in either the presence of cartilaginous 'spurs' (2/3; 6/7; 4/9) or the mean number of 'spurs' (1.0; 1.1; 0.67). When a single supernumerary tooth was present, the supernumerary tooth and 'spur' were not always on the same side (see Figure 6.2, g-h).

Variation in the number of supernumerary teeth or cartilaginous 'spurs' (see Table 6.2.) implies that these phenotypes show variable expressivity (1 or 2) as well as penetrance (presence or absence). Therefore, genetic backgound, but not allele type, appears to be playing the major role in the penetrance and expressivity of supernumerary upper incisor teeth and cartilaginous 'spur' formation in *Sey/Sey*, Sey^{Neu}/Sey^{Neu} and Sey^{Neu}/Sey fetuses. In contrast, in all small eye homozygotes studied, regardless of genetic background, the median cartilaginous rod was always present. However, as none of these phenotypes are reported in *Sey/+* heterozygote or wild-type littermates (see Figure 6.1.a and b), all these morphological abnormalities are causally related to a loss of functional *Pax6* product.

6.4. Discussion

6.4.1. Genetic influences on frontofacial morphogenesis

The presence of aberrant cartilaginous craniofacial structures in *Sey/Sey* homozygous fetuses appears to be consequential to the loss of *Pax6* function. Frontofacial/nasal development in the *Sey/Sey* homozygous fetus is grossly abnormal, with the absence of nasal structures clearly having a dramatic effect on the morphogenesis of the whole frontofacial/nasal region. A diminution of the primary palate is also observed (Kaufman *et al.*, 1995), with the upper incisors forming within a mass of cancellous bone. The severe degree of retrognathia observed in *Sey/Sey* fetuses reflects a deficiency of the frontal part of the maxillae and pre-maxilla. This suggests that the median nasal cartilaginous rod and cartilaginous 'spurs' may both be manifestations of an inherant need for structural support to overcome deformity of the middle part of the upper jaw resulting from loss of nasal derivatives.

A number of genes have been found to be involved in facial morphogenesis with loss of function mutations of relevance to the small eye homozygous phenotype. The homeobox-containing genes, *Msx1* and *Msx2*, are involved in epithelial-mesenchymal interactions during tooth morphogenesis (MacKenzie *et al.*, 1991a; 1991b; 1992; Jowett *et al.*, 1993) and are expressed in the cellular precursors of the developing skull bones (MacKenzie *et al.*, 1992). The *Msx1* knockout mouse exhibits cleft palate, oligodontia and limb abnormalities, indicating roles for *Msx1* in closure of the palatal shelves as well as tooth formation (Sakota & Maas, 1994). Other *Hox* gene knockout and gain of function mutants have been shown to exhibit bilateral cleft palate (Gendron-Maguire *et al.*, 1993) and other skeletal transformations (Lufkin *et al.*, 1992; Rijli *et al.*, 1993). The rat homolog of small eye, *rSey*, has been identified, with homozygous *rSey/rSey* fetuses exhibiting bilateral facial clefting (Matsuo *et al.*, 1993;

Fujiwara *et al.*, 1994). However, although a limited delay of palatal fusion has been reported in *Sey/Sey* fetuses (Kaufman *et al.*, 1995), cleft palate and facial clefting have not been observed in any mouse small eye strains to date.

Analysis of a recently reported mouse mutant, the *Otx2* knockout mouse, has indicated a general role for this homeobox-containing gene in rostral head formation (Matsuo *et al.*, 1995). In the heterozygous state, this mutant exhibits several phenotypes that bear relevance to the *Sey/Sey* phenotype, including microphthalmia or anophthalmia with associated agnathia, holoprosecephaly or anencephaly. Expression of *Otx2* is observed in both the eye and nasal epithelium (Simeone *et al.*, 1991; 1992). $Otx2^{+/-}$ heterozygous fetuses also exhibit areas of ectopic growth of cartilage and ossified bone, including abnormal formation of the basisphenoid bone of the skull. Most strikingly, a median nasal cartilaginous rod-like structure, similar to that observed in the small eye homozygote fetus, is also present in $Otx2^{-/-}$ fetuses that exhibit holoprosencephaly, agnathia and absence of nasal tissues. Although the highly variable degree of severity of the phenotype observed in the $Otx2^{-/-}$ mutant mouse indicates a broad function for this gene in patterning of the anterior head region, the presence of the median nasal cartilaginous rod in fetuses lacking nasal and forebrain tissues lends support to our hypothesis that the various cartilaginous structures reported in this study and in Kaufman *et al* (1995) might act as a novel support mechanism compensating for absent frontofacial structures.

The nature of interaction between *Pax6* and the genes involved in craniofacial morphogenesis are still unclear. *Pax6* is involved in both its own transcriptional regulation (Plaza *et al.*, 1993) and is also able to initiate the transcription of other genes (Chalepakis *et al.*, 1994; Cvekl *et al.*, 1995; Cvekl and Piatigorsky, 1996). Indirect evidence of *Pax6* interaction with *Msx1* in *Sey/Sey* mice has been reported, and there is some indication from abberrant expression of *Msx1* in the nasal region in

Sey/Sey embryos that *Msx1* may be involved in positional specification of both presumptive nasal and tooth regions (Grindley *et al.*, 1995).

In contrast to those reported mutants with cranial and bone dysgenesis phenotypes, few mouse mutants have been identified that exhibit abnormalities of tooth development. The homozygous tetraploid mouse embryo, in which incomplete separation of the telencephalic vesicles and a narrowing of the fronto-facial region are characteristic features (Kaufman & Webb, 1990), are deficient in upper incisor dentition (M.H.K. unpublished observation). In a recent study by Armstrong *et al* (1996), a high incidence of abnormalities of upper incisor dentition was observed in *p53*-deficient mice, the most extreme being fusion of the two mid-line upper incisors giving rise to a single mid-line tooth. Ocular abnormalities were also common in this mouse mutant. Absence of dentition may be a common feature of holoprosencephaly, as noted previously in the $Otx2^{-/-}$ mutant mouse, with reductions in number of upper incisor dentition reported in human holoprosencephalic and cyclopic fetuses (Ballantyne, 1904).

6.4.2. Genetic background effects on small eye phenotypes

Kaufman *et al.* (1995) reported that 80% of homozygous *Sey/Sey* fetuses examined possessed supernumerary upper incisor teeth, with 45% of fetuses showing a full duplication of the upper incisors. In most cases, supernumerary teeth were of similar size to their normal counterparts. The incidence of supernumerary upper incisor teeth we have observed in our crosses was considerably lower, from 12.5 to 43%, the highest incidence observed amongst fetuses with one or more parent from the SEYTG strain. No supernumerary teeth were observed in homozygous small eye offspring from the CBA/Ca-*Sey* or CBA/Ca-Sey^{Neu} strains. The very high incidence of complete upper incisor duplication reported by Kaufman (1995) was not emulated by

fetuses of any experimental genotypes or strain crosses. However, all fetuses examined showed a median rod-like cartilaginous structure.

Heterozygous effects of loss of *Pax6* function have been well documented in small eye strains of varying genetic backgound (Roberts, 1967; Pritchard, 1972; Hogan *et al.*, 1988). For example, Pritchard (1973) showed that the size of the eye and incidence of cataracts varied in *Sey/+* heterozygous mice when crossed onto the inbred strains C57BL/Fa, JU/Fa and JBT/Jd. Small eyes were most often observed on the JU/Fa background. Conversely, cataracts were less obvious on this background than on the C57BL/Fa background but this may partly reflect the difficulty in identification of small cataracts in eyes of albino JU/Fa strain mice. Overall, Pritchard (1973) reported that the *Sey* phenotype showed lowest penetrance on the JBT/Jd genetic background. The human disorders of aniridia and Peters' anomaly most closely resemble the mouse *Sey/+* ocular phenotypes when the small eye allele is expressed on outbred Swiss or inbred CBA genetic backgrounds (Jordan *et al.*, 1992).

Heterogeneity of ocular phenotype has been well documented in human anterior segment malformations (Hitner *et al.*, 1982; Holstrum *et al.*, 1991; Glaser *et al.*, 1994) and mutations in *PAX6* are involved in a variety of anterior segment disorders clinically distinct from aniridia and Peters' anomaly (Azuma *et al.*, 1995; Mirzayans *et al.*, 1995). Tooth abnormalities are associated with another anterior segment disorder; Rieger's syndrome, the diagnostic features of which include maxillary hypoplasia, microdontia, oligodontia and anodontia. Indirect evidence suggests that Peter's anomaly and Rieger's syndrome might be variable manifestations of the same underlying genetic disorder, although this has not been confirmed at a genomic level (Holstrum *et al.*, 1991). Familial differences in phenotype resulting from the same *PAX6* genomic defect have been reported, suggesting that variability in the human dominantly-inherited anterior segment malformation phenotypes may be the result of

underlying variability in background gene expression (Hanson *et al.*, 1994; Hanson and van Heyningen, 1995).

Although heterozygous human conditions resulting from defects in *PAX6* have been extensively reported, the homozygous condition is rare. A suspected aniridia homozygous human fetus was reported by Hodgson and Saunders (1980) which exhibited not only absence of the eyes and nose but also the adrenal glands. An absence of nasal bones and defects of the parietal bones was noted at necropsy but no deformities of the palate or dentition were recorded (Hodgson and Saunders, personal communication to M.H.K.). More recently, a human homozygote was reported which exhibited anophthalmia, absence of olfactory lobes, a high arched palate and micrognathia (Glaser *et al.*, 1994) showing a high degree of phenotypic similarity to the mouse small eye homozygous fetus.

6.5. Conclusions

Data from this study showed that the presence of supernumerary upper incisor teeth in small eye homozygous fetuses exhibited variable penetrance and expressivity. The variability was dependent on genetic background but no difference was found between *Sey* and Sey^{Neu} alleles. In contrast, the presence of the median cartilaginous rod-like structure was characteristic of all *Sey/Sey*, Sey^{Neu}/Sey^{Neu} and Sey^{Neu}/Sey fetuses tested. The novel findings reported here of cartilaginous 'spurs' originating from the lateral aspect of the abnormal nasal capsule adds further complexity to the *Sey/Sey* homozygous phenotype. This indicated that both direct and indirect effects of the loss of the functional *Pax6* product are affecting a variety of different tissue precursors.

The incidence of both supernumerary upper incisor teeth and ectopic cartilaginous 'spur' formation reported in this study show variable penetrance and expressivity

dependant on genetic background. Both the presence of the median cartilaginous rod-like structure and cartilagenous 'spurs' may be manifestations of an inherent need for structural support in the frontofacial region to overcome the loss of nasal tissues.

Evidence from mouse and man therefore suggests that *Pax6* is involved in a cascade of gene functions affecting numerous aspects of frontofacial/nasal and cranial morphogenesis, as well as eye and nasal development. Variability of phenotype in the human heterozygote, the *Sey/+* heterozygous mouse and the *Sey/Sey* homozygous fetus can be attributed to the "black box" of genetic background effects. However, it is unclear how the loss of *Pax6* function combines with the effects of other unknown genes to generate the different phenotypes described. The small eye homozygous mouse may be a useful model for analysis of the complex interactions that occur between gene families involved in patterning and development of the vertebrate head.

Chapter 7

Future Investigations

7.1. Introduction

The experiments described in this thesis have increased our understanding of the roles that *Pax6* is playing during development of the eye and nasal structures in the mouse embryo. *Sey*^{Neu}*/Sey*↔+/+ aggregation chimaeras have made it possible to define a cell autonomous role for *Pax6* during transition of surface ectoderm to lens and nasal placode regions. Chimaera studies have also defined roles for *Pax6* in the optic cup with cell autonomous effects observed in both the inner and outer layers. In addition, specification of inner layer/outer layer identity in the optic cup was found to be *Pax6* independent. *Pax6* was also observed to be involved in cell-to-cell interaction in the optic cup although the mechanisms by which *Pax6* influences cell interactions has not been defined.

A preliminary study investigating neuronal migration found LHRH neuron migration to be unaffected in the heterozygous small eye brain, although no LHRH neuron were present in the small eye homozygous fetal brain. This supports previous studies that have determined derivation of LHRH neurons in the nasal placodes.

Finally, study of homozygous small eye phenotypes showed genetic background effects on both penetrance and expressivity of abnormal manifestations of tooth and cartilage development during morphogenesis of the frontofacial region. Novel cartilaginous structures were observed indicating an inherent need for structural support in the absence of nasal tissues. Overall, these varied studies have highlighted

the widespread significance of the *Pax6* gene during fetal development. However, the studies reported herein have posed as may questions as they have answered.

7.2. Roles for *Pax6* in cell-to-cell interaction

Perhaps one of the most intriguing results reported in this study is that of the extreme cell segregation observed in the optic cups of $Sey^{Neu}/Sey\leftrightarrow+/+$ chimaeras. Possible candidates for analysis to determine the basis of this phenomenon are the neural cell adhesion molecules. Expression studies to determine N-CAM and N-cadherin expression patterns, or those of other cell adhesion molecules, in both small eye homozygous and $Sey^{Neu}/Sey\leftrightarrow+/+$ chimaeric fetuses might indicate if the abnormal cell-to-cell interactions observed in the chimaeric optic cups are the result of abnormal or absent cell adhesion molecule expression.

Similar studies would also be of relevance to the brain phenotypes reported in the small eye homozygous fetus. The preliminary investigation of LHRH neuron migration was an attempt to examine if loss of *PAX6* protein in the heterozygous small eye fetus was sufficient to cause abnormal migration of neurons known to follow N-CAM pathways. Although this preliminary study was not sufficient to identify subtle effects, a more detailed quantitative study might identify deficiencies of neuronal numbers or migrational ability.

7.3. Further investigations of nasal development

Little work has been done examining nasal phenotype of the small eye homozygous fetus. Using a chimaera approach, the interactions involved in development of the nasal tissues and olfactory lobes could be examined. It would also be interesting to examine neuronal migration and axonal outgrowth of the olfactory nerves in chimaeric

fetuses to identify if cells unable to express *Pax6* could contribute to olfactory system development. Similarly, investigation of odour receptor development in the small eye heterozygous animal may identify a role for *Pax6* in olfactory function. Preliminary examination of E14.5 $Sey^{Neu}/Sey \leftrightarrow +/+$ chimaeras indicates that olfactory lobe development occurs in these chimaeras with both Sey^{Neu}/Sey and+/+ cells able to contribute to this tissue. It would therefore be interesting to exmine the potential of cells unable to express *Pax6* during late development of the olfactory system to determine whether small eye homozygous cells were able to contribute to and function within the neural network of the olfactory system. Further examination of later developmental stages in aggregation chimaeras would be required to definitively answer these questions.

7.4. Roles for *Pax6* in development of the fetal brain

Perhaps the most intriguing questions remaining to be answered are regarding roles for *Pax6* during development of the fetal brain. The severely abnormal brain phenotype of the homozygous small eye fetus and observations of abnormal cell-to-cell interaction between Sey^{Neu}/Sey and +/+ cells in the optic cups of $Sey^{Neu}/Sey \leftrightarrow +/+$ chimaeras hints to roles for *Pax6* in cell migration and cell specification in the developing fetal brain. Examination of adhesion molecule expression in the brain of the small eye homozygous fetuses may help to identify interactions between *Pax6* and the cell adhesion molecules. Although expression of the neural cell adhesion molecule L1 is normal in the small eye fetus (Damira Caric, personal communication), this makes the study of other cell adhesion molecules even more relevant.

However, *Pax6* is undoubtedly playing a role in cell surface interactions in the developing brain. Preliminary observations (not shown) of E12.5 and E14.5 $Sey^{Neu}/Sey \leftrightarrow +/+$ chimaeric fetuses showed a degree of cell segregation in the brain,

similar but less dramatic than that observed in the optic cup. Bands of Sey^{Neu}/Sey or +/+ cells were observed radiating across the fetal neocortex, mid brain and hind brain regions.

Very recent examination of E14.5 $Sey^{Neu}/Sey \leftrightarrow +/+$ chimaeric fetuses (not shown) also indicates that *Pax6* does not act cell autonomously in cells of the developing cortex as Sey^{Neu}/Sey cells are able to migrate across to the developing outer cortical layers. However, there may be a diminution in the number of Sey^{Neu}/Sey cells able to migrate out of the ventricular and subventricular zones (Jane Quinn and Damira Caric, unpublished observations). However, the relationship between the apparent segregation and migration defects and the small eye homozygous brain phenotype have yet to be elucidated. Investigation of brain morphology and Sey^{Neu}/Sey cell potential in $Sey^{Neu}/Sey \leftrightarrow +/+$ chimaeric fetuses of late gestational stages would be a first step in defining roles for *Pax6* during brain development.

7.5. Roles for *Pax6* during formation of the inner layer of the optic cup

Pax6 and *Trp2* expression studies in $Sey^{Neu}/Sey \leftrightarrow +/+$ chimaeric fetuses at E12.5 and E14.5 were able to elucidate both timing and effect of loss of *Pax6* on development of the outer layer of the optic cup. However, these studies were not sufficient to determine roles for *Pax6* during development of the inner layer although examination of $Sey^{Neu}/Sey \leftrightarrow +/+$ chimaeric fetuses at E12.5 and E14.5 indicate that *Pax6* is playing a significant role both in interactions between lens and optic cup and development of the inner layer.

Expression studies in $Sey^{Neu}/Sey \leftrightarrow +/+$ chimaeras using expression markers for the inner layer might allow definition of *Pax6* function in the inner layer of the optic cup. Possible candidates as expression markers for specification of inner layer identity in

the highly abnormal chimaeric optic cups are markers such as *Msx2* or *Six3* , or indeed at later stages, genes expressed more widely during eye development such as *Pax2, Chox10, Dlx1*or *Otx2*. It would also be of interest to examine the expression of *sonic hedgehog* (*Shh*) in tissues of the the small eye homozygous or $Sey^{Neu}/Sey \leftrightarrow +/+$ chimaeric fetus. *Shh* has been reported to repress expression of *Pax6* in the zebrafish. Therefore, if overexpression of *Pax6* were observed in conjunction with expression of *Shh* this would indicated a loss of direct interaction between these two molecules.

In addition, studies could also be designed using tissue culture techniques to examine gene expression in small eye homozygote ↔ wild type chimaeric cell cultures *in vitro*. As *Pax6* may well be involved in both cell specific and temporally specific processes in the developing retina, a combination of chimaera and cell culture techniques might be needed to fully elucidate the multiple role *Pax6* might be playing in development and differentiation of the inner layer.

7.5. The role of *Pax6* in lens competence

Results from $Sey^{Neu}/Sey \leftrightarrow +/+$ chimaeric fetuses have identified that *Pax6* plays a cell autonomous role in the lens, possibly during transition of surface ectoderm to placode forming region. Examination of E9.5 $Sey^{Neu}/Sey \leftrightarrow +/+$ chimaeras, the stage at which lens placode formation is occurring, may give insight into the mechanisms by which Sey^{Neu}/Sey cells are excluded from lens development in these chimaeras.Whether expression of *Pax6* alone induces this transition, or whether *Pax6* purely determines the cells that are induced to form placode has yet to be unequivocally defined. Examination of $Sey^{Neu}/Sey \leftrightarrow +/+$ chimaeras at earlier stages of development may help to determine its role in early lens competence.

It might be possible to define the role of *Pax6* in lens competence by inducing expression of *Pax6* in undetermined epithelial cell cultures to elucidate whether expression of *Pax6* alone in epithelial cells is sufficient to induce lentoid body formation. It is possible that an endogenous inducer is still required for lens formation. It might also be possible to use cell culture techniques to determine if the lens developmental pathway is a morphogenetic "default" initiated by expression of *Pax6* in undetermined surface ectoderm such that nasal development cannot be induced *in vitro* without additional stimuli.

In conclusion, the results described in this thesis have only prompted more questions relating to roles for *Pax6* during fetal development than have been answered. However, using aggregation chimaeras at both earlier and later developmental stages may help to further define the actions and interactions of *Pax6* during organogenesis in the mouse fetus.

Bibliography

Austin, C.P., Feldman, D.E., Ida, J.A. and Cepko, C.L. (1995). Vertebrate ganglion cells are selected from competent progenitors by the action of *Notch*. *Development* **121**, 3637-3650.

Armstrong, J.F., Kaufman, M.H., Harrison, D.J. and Clarke, A.R. (1996). High frequency developmental abnormalities in p53-deficient mice. *Current Biology* **5**, 931-936.

Abitbol, M., Gerard, M., Delezoide, A.L., Sahly, I., Ribeaudeau, F., Mallet, J., Vekemans, M. and Dufier, J.L. (1995). PAX6 gene expression during human embryonic development at the cellular level. *Vis. Res.* **35**, 4235.

Adams, B., Dorfler, P., Aguzzi, A., Kozmik, Z., Urbanek, P., Maurer-Fogy, I., and Busslinger, M. (1992). *Pax-5* encodes the transcription factor BSAP and is expressed in B lymphocytes, the developing CNS and adult testis. *Genes and Dev.* **6**, 1589-1607.

Adler, R., Scheurer, D., Yang, J.M., Sundin, O. (1995). Expression of the Pax6 gene during retinal cell transdifferentiation in vitro. *Invest. Opthalmol. and Vis. Sci.* **35**, 689.

Allison, A.C. (1953). The morphology of the olfactory system in vertebrates. *Biol. Rev.* **28**, 195-244.

Altshuler, D. and Cepko, C. (1992). A temporally regulated, diffusable activity is required for rod photoreceptor development in vitro. *Development* **114**, 947-957.

Altshuler, D., LoTurco, J.J., Rush, J. and Cepko, C. (1993). Taurine promotes the differentiation of a vertebrate retinal cell type in vitro. *Development* **119**, 1317-1328.

Azuma, N., Nishina, S., Yanagisawa, H., Okuyama, T. and Yamada, M. (1995). Missense mutation in the PAX6 gene in a family with isolated foveal hypoplasia. *Invest. Opthalmol. Vis. Sci.* **37**, 707.

Azuma, N., Nishina, S., Yanagisawa, H., Okuyama, T. and Yamada, M. (1996). PAX6 missense mutation in isolated foveal hypoplasia. *Nature Genetics* **13**, 141-142.

Barabanov, V.M. and Fedstova, N.G. (1982). The distribution of lens differentiation capacity in the head ectoderm of chick embryos. *Differentiation* **21**, 183-190.

Barnstable, C.J. (1987). A molecular view of vertebrate retinal development. *Molecular Neurobiology* **1**, 9-46.

Ballantyne, J.W. (1904). *Manual of Antenatal Pathology and Hygeine: The Embryo.* p398. William Green and Sons, Edinburgh, U.K.

Balling, R., Deutsch, U. and Gruss, P. (1988) *Undulated*, a mutation affecting the development of the mouse skeleton, has a point mutation in the paired box of *Pax1*. *Cell* **55**, 531-535.

Barnes, R.D., Tuffrey, M., Drury, L. and Catty, D.L. (1974). Unequal rates of cell proliferation in tetraparental mouse chimaeras derived from fusion of early embryos. *Differentiation* **2**, 257-260.

Beleckly-Ada, T., Tomarev, S., Sundin, O., McInnes, R.R., Ploder, L. and Adler, R. (1996). Correlation of Prox1, Pax6 and Chx10 gene expression and phenotypic fate of chicken retinal precursor cells. *Invest. Ophthalmol. Vis Sci.* **suppl 37**, 4818.

Bell, E.T. (1906). Experimental studies on the development of the eye and nasal cavities in frog embryos. *Anat. Anz.* **29**, 185-194.

Bell, E.T. (1907). Some experiments on the development and regeneration of the eye and nasal organs in frog embryos. *Arch. Entw. Mech. d. Org.* **23**, 645-678.

Bok, D. (1985). Retinal photoreceptor-pigment epithelium interactions. *Invest. Ophthalmol. Vis. Sci.* **26**, 1659-1694.

Boland, N.I. and Gosden, R.G. (1994). Clonal analysis of chimaeric mouse ovaries using DNA in-situ hybridisation. *J. Reprod. and Fertil.* **100**, 203-210.

Bopp, D., Burri, M., Baumgartner, S., Frigerio, G. and Noll, M. (1986). Conservation of a large protein domain in the segmentation gene *paired* and in functionally related genes in *Drosophila. Cell* **47**, 1033-1040.

Bosch, E., Horwitz, J. and Bok, D. (1993). Phagocytosis of outer segments by retinal pigment epithelium. *J. Histochem. Cytochem.* **41**, 253-263.

Bradley, A., Evans, M., Kaufman, M.H. and Robertson, E. (1984). Formation of germline chimaeras from embryo derived teratocarcinoma cell lines. *Nature* **309**, 225-256.

Breitman, M.L., Clapoff, S., Rossant, J., Tsui, L.C., Glode, M., Maxwell, I.H., and Berstein, A. (1987). Genetic ablation: targeted expression of a toxin gene causes microphthalmia in transgenic mice. *Science* **238**, 1563-1565.

Breitman, M.L., Bryce, D.M., Giddens, E., Clapoff, S., Goring, D., Tsui, L.C., Klintworth, G.K. and Bernstein, A. (1989). Analysis of lens cell fate and eye morphogenesis in transgenic mice ablated for cells of the lens lineage. *Development* **106**, 457-463.

Buck, L. and Axel, R. (1991). A novel multigene family may encode odorant receptors: a molecular basis for odor recognition. *Cell* **65**, 175-187

Burgoyne, P.S., Buehr, M., Keepman, P., Rossant, J. and McLaren, A. (1988). Cell autonomous action of the testis determining gene: Sertoli cells are exclusively XY in XX↔XY chimaeric mouse testis. *Development* **102**, 443-450.

Burmeister, M., Novak, J., Liang, M.Y., Basu, S., Ploder, L., Hawes, N.L., Vidgen, D., Hoover, F., Goldman, D., Kalnins, V.I., Roderick, T.H., Taylor, B.A., Hankin, M.H. and McInnes, R.R. (1996). Occular retardation mouse caused by *Chx10* homeobox null allele: impaired retinal progenitor proliferation and bipolar cell differentiation. *Nature Genetics* **12**, 376-383.

Buse, E. and de Groot, H. (1991). Generation of developmental patterns in the neuroepithelium of the developing mammalian eye: the pigment epithelium of the eye. *Neurosci Lett.* **126**, 63-66.

Buse, E., Eichmann, T., de Groot, H. and Leker, A. (1993). Differentiation of the mammalian retinal pigment eptiehlium in vitro: influence of presemptive retinal neuroepithelium and head mesenchyme. *Anat. Embryol.* **187**, 259-268.

Carter, N.D. and Parr, C.W. (1967). Isoenzymes of phosphoglucose isomerase in mice. *Nature* **216**, 511.

Cepko, C.L., Austin, C.P., Yang, X., Alexiades, M. and Ezzeddine, D. (1996). Cell fate determination in the vertebrate retina. *Proc. Natl. Acad. Sci. USA* **93**, 589-595.

Cevkl, A., Kashanchi, F., Sax, C.M., Brady, J.N. and Piatgorsky, J. (1995). Transcriptional regulation of the mouse α-crystallin gene: activation dependant on a cyclic AMP responsive element (DE1/CRE) and a *Pax6* binding site. *Mol.Cell. Biol.* **15**, 653-660.

Chalepakis, G., Fritsch, R., Fickenscher, H., Deutsch, U., Goulding, M. and Gruss, P. (1991). The molecular basis of the *undulated/Pax1* mutation. *Cell* **66**, 873-884.

Chalepakis, G., Tremblay, P. and Gruss, P. (1992). Pax genes, mutants and molecular function. *J. Cell. Sci.* **suppl. 16**, 61-67.

Chalepakis, G., Stoykova, A., Wijnholds, J., Tremblay, J. and Gruss, P. (1993). Pax gene regulators in the developing nervous system. *J Neurobiol.* **24**, 1367-1384.

Chalepakis, G., Wijnholds, J., Giese, P., Schachner, M., and Gruss, P. (1994). Characterisation of Pax-6 and Hox-1a binding to the promoter region of the neural cell adhesion molecule L1. *DNA Cell. Biol.* **13**, 891-900.

Chalepakis, G., Goulding, M., Read, A., Strachan, T. and Gruss, P. (1994). Molecular basis of splotch and Waardenburg *Pax3* mutations. *Proc. Natl. Acad. Sci. USA* **91**, 3685-3689.

Chapman, V.M., Whitten, W.K. and Ruddle, F.H. (1971). Expression of paternal glucose phosphate isomerase-1 (*Gpi-1*) in preimplantation stages of mouse embryos. *Dev. Biol.* **26**, 153-158.

Chisholm, A.D. and Horvitz, H.R. (1995). Patterning of the *Caenorhabditis elegans* head region by the *Pax-6* family member *vab-3*. *Nature* **377**, 52-55.

Chung, W.W., Lagenaur, C.F., Yan, Y. and Lund, J.S. (1991). Developmental expression of neural cell adhesion molecules in the mouse neocortex and olfactory bulb. *J. Comp. Neurol.* **314**, 290-305.

Clayton, R.M. and Campbell, J.C. (1968). Small eye, a mutant in the house mouse apparently affecting the synthesis of extracellular membranes. *J. Physiol.* **198**, 74P-74P.

Condamine, H., Custer, R.P. and Mintz, B. (1971). Pure-strain and genetically mosaic liver tumours histochemically identified with the β-glucuronidase marker in allophenic mice. *Proc. Natl. Acad. Sci. USA* **68**, 2032-2036.

Conrad, U., Walter, G., Helbing, R., Mantueffel, R. and Schoneich, J. (1987). Immunochemical differentiation of glucose phosphate isomerase (GPI) allozymes of the mouse. *Biochem. Genets.* **25**, 739-754.

Coulombre, A.J. (1965). Experimental embryology of the vertebrate eye. *Invest Ophthalmol.* **4**, 411-419.

Coulombre, A.J. and Coulombre, J.L. (1963). Morphogenesis of the vertebrate eye. Proceedings VXI Internat. Congre. Zool., Wasington D.C., Aug 20-27, **2**, 231.

Coulombre, A.J. and Coulombre, J.L. (1964). Lens development I: Role of the lens in eye growth. *J. Exper. Zool.* **156**, 39.

Coulombre, A.J. and Coulombre, J.L. (1965). Regeneration of neural retina from the pigmented epithelium in the chick embryo. *Dev. Biol.* **12**, 79-92.

Coulombre, A.J. and Coulombre, J.L. (1970). Influence of mouse neural retina on regeneration of chick neural retina from chick embryonic pigmented epithelium. *Nature* **228**, 559-560.

Curtis, A.S.G. (1960). Area and volume measurements by random sampling methods. *Med. Biol. Illust.* **10**, 261-266.

Cuschieri, A. and Bannister, L.H. (1975). The development of the olfactory mucosa in the mouse: light microscopy. *J. Anat.* **119**, 277-286.

Cvekl, A., Sax, C.M., Li, X., Bresnick, E.H. and Piatigorsky, J. (1994). Complex array of positive and negative elements regulates the chicken αA-crystallin gene: involvement of Pax-6, CREB and AP-1 proteins. Mol. Cell. Biol. **14**, 7363-7367.

Cvekl, A., Sax, C.M., Li, X., McDermott, J.B. and Piatigorsky, J. (1995a). Pax-6 and lens-specific transcription of the chicken δ1-crystallin gene. *Proc. Natl. Acad. Sci. USA* **92**, 4681-4685.

Cvekl, A., Kashanchi, F., Sax, C.M., Brady, J.N. and Piatigorsky, J. (1995b). Transcriptional regulation of the mouse αA-crystallin gene: Activation dependant on a cyclic AMP-responsive element (DE1/CRE) and a Pax-6-binding site. *Mol .Cell Biol.* **15**, 653-660.

Cvekl, A., Kashanchi, F., Epstein, J., Rauchman, M., Maas, R. and Piatigorsky, J. (1996). Pax6, a "master gene" for eye development: target genes and mechanisms of action. *Invest. Ophthalmol. Vis. Sci.* **37**, 715.

Cvekl, A. and Piatigorsky, J. (1996) Lens development and crystallin gene expression: many roles for Pax-6. *Bioessays* **18**, 621-630.

Czerny, T., Schaffner, G. and Busslinger, M. (1993). DNA sequence recognition by Pax proteins: bipartite structure of the paired domain and its binding site. *Genes. Dev.* **7**, 2048-2061.

Czerny, T. and Busslinger, M. (1995). DNA-binding and transactivation properties of Pax-6: Three amino acids in the paired domain are responsible for the different sequence recognition of Pax-6 and BSAP (Pax-5). *Mol .Cell Biol.* **15**, 2858-2871.

Daniloff, J.K., Chuong, C.M., Levi, G. and Edelman, G. (1986) Differential distribution of cell adhesion molecules during histogenesis of the chick nervous system. *J. Neurosci.* **6**, 739-758.

Davisson, M.T. (1986). Position of Dey on Chr 2. *Mouse News Lett.* **75**, 30-31.

De Lorenzo, R.J. and Ruddle, F.H. (1969). Genetic control of two eletrophoretic variants of glucosephosphate isomerase in the mouse (*mus musculus*). *Biochem. Genets.* **3**, 151-162.

Deutsch, U., Dressler, G. and Gruss, P. (1988). Pax1, a member of the paired box homologous murine gene family, is expressed in segmented structures during development. *Cell* **53**, 617-625.

Dietrich, S., Schubert, F. and Gruss, P. (1993). Altered Pax gene expression in murine notochord mutants: the notochord is required to initiate and maintain ventral identity in the somite. *Mech. Dev.* **44**, 189-207.

Dolle, P., Price, M. and Duboule, D. (1992). Expression of the murine Dlx1 homeobox gene during facial, ocular and limb development. *Differentiation* **49**, 93-99.

Dozier, C., Carrierre, C., Grevin, D., Martin, P., Quatannens, B., Stehelin, D. and Saule, S. (1993). Structure and binding properties of PaxQNR, a paired box and homoebox containing gene. *Cell Growth Diff.* **4**, 281-289.

Dressler, G.R., Deutsch, U., Chowdhury, K., Nornes, H.O. and Gruss, P. (1990). Pax2, a new murine paired box containing gene and its expression in the developing excretory system. *Development* **109**, 787-795.

Eakin, R.M. (1947). Determination and regulation of polarity in the retina of *Hyla regilla. Uni California Publ Zool* **51**, 245-288.

Edwards, J.G., Lampert, R.P., Hanner, M.E. and Young, S.R. (1984). Ocular defects and dysmorphic features in three generations. *J. of Clin. Dysmorph.* **2**, 8-13.

Ekker, S.C., Ungar, A.N., Greestein, P., ven Kessler, D.P., Porter, J.A., Moon, R.T. and Beachy, P.A. (1995). Patterning activities of vertebrate hedgehog proteins in the developing eye and brain. *Curr. Biol.* **5**, 944-955.

Epstein, D.J., Vekemans, M. and Gruss, P. (1991). Splotch (Sp2H)., a mutation affecting development of the mouse neural tube, shows a deletion within the paired homeodomain of Pax-3. *Cell* **67**, 767-774.

Epstein, J.A. Glaser, T., Cai, J., Walton, D.S. and Maas, R.L. (1994a). Two independent and interactive DNA-binding subdomains of the Pax6 paired domain are regulated by alternative splicing. *Genes Dev.* **8**, 2022-2034.

Epstein, J., Jiexing, C., Glaser, T., Jepeal, L. and Maas, R. (1994b). Identification of a Pax paired domain recognition sequence and evidence for DNA-dependent conformational changes. *J. Biol. Chem.* **269**, 8355-8361.

Evans, M.J. and Kaufman, M.H. (1981). Establishment in culture of pluripotential cells from mouse embryos. *Nature* **292**, 154-156.

Everett, C.A., Keighren, M. and West, J.D. (1994). New transgenic Robersonian strain. *Mouse Genome* **92**, 668.

Everett, C.A. and West, J.D. (1996). The influence of ploidy on the distribution of cells in chimaeric mouse blastocysts. *Zygote* **4**, 59-66.

Falconer, D.S. and Avery, P.J. (1978). Variability of chimaeras and mosaics. *J. Embryol. Exp. Morph.* **43**, 195-219.

Fantes, J., Redeker, B., Breen, M., Boyle, S., Fletcher, J., Jones, S., Bickmore, W., Fukushima, Y., Mannens, M., Danes, S., van Heyningen, V. and Hanson, I. (1995). Aniridia-associated cytogenetic rearrangements suggest that a position effect may cause the mutant phenotype. *Hum. Mol. Genet.* **4**, 415-422.

Favor, J., Neuhauser-Klaus, A. and Erhling, U.H. (1988). The effect of dose fractination on the frequency of erithrolnitrousourea induced dominant cataract and resessive specific locus mutations in germ cells of the mouse. *Mutation Research* **198**, 269-275.

Fekete, D.M., Perez-Miguelsanz, J., Ryder, E. and Cepko, C.L. (1994). Clonal analysis of the chicken retina reveals tangential dispersion of clonally related cells. *Dev. Biol.* **166**, 666-682.

Fujii, J.T and Martin, G.R. (1980). Incorporation of teratocarcinoma cells into blastocysts by aggregation with cleavage stage embryos. *Dev. Biol.* **7**, 239-244.

Fujiwara, M., Uchida, T., Osumi-Yamashita, N. and Eto, K. (1994). Uchida rat (*rSey*): a new mutant with craniofacial abnormalities resembling that of the mouse *Sey* mutant. *Differentiation* **57**, 31-38.

Franco, B., Guioli, S., Pragliola, A., Incerti, B., Bardoni, B., Tonlorenzi, R., Carrozza, R., Maestrini ,E., Pieretti, M., Taillon-Miller, P., Brown, C.J., Willard, H.F., Lawrence, C., Persico, M.G., Camerino, G. and Ballabio, A. (1991). A gene deleted in Kallman's syndrome shares homology with neural cell adhesion and axonal pathfinding molecules. *Nature* **353**, 529-537.

Fundele, R., Norris, M.L., Barton, S.C., Wolf, R. and Surani, M.A. (1989). Systematic elimination of parthenogenetic cells in mouse chimaeras. *Development* **106**, 29-35.

Gardner, R.L. (1968). Mouse chimaeras obtained by injection of cells into the blastocyst. *Nature* **22**, 596-597.

Gardner, R.L. (1984). An in situ marker for clonal analysis on devlopment of the extraembryonic endoderm in the mouse. *J. Embryol. Exp. Morphol.* **80**, 251-258.

Gardner, R.L. and Papaioannou, V.E. (1975). Differentiation in the trophectoderm and inner cell mass. In *The Early Development of Mammals. The Second Symposium of the British Society for Developmental Biology.* (M. Balls and A.E. Wilds, eds), pp 107-132. cambridge University Press, Cambridge.

Garner, W. and MCLaren, A. (1972). Cell distribution in chimaeric embryos before implantation. *J. Embryol. Exp. Morphol.* **32**, 495-503.

Gearhart ,J., Oster-Granite, M.L., and Musser, J.M. (1981). Immunoreactivity of the two common alleles of murine glucose phosphate isomerase. *Biochem. Genet.* **19**, 445-455.

Gendron-Maguire, M., Zhang, M., Mallo, M., and Gridley, T. (1993). *Hoxa2* mutant mice exhibit homeotic transformations of skeletal elements derived from cranial neural crest. *Cell* **75**, 1317-1331.

Glaser, T., Walton, D.S. and Maas, R.L. (1992). Genomic structure, evolutionary conservation and aniridia mutations in the human PAX6 gene. *Nature Genetics* **2**, 232-239.

Glaser, T., Jepal, L., Edwards, J.G., Young, S.R., Favor, J. and Maas, R.L. (1994). PAX6 gene dosage effects in a family with congenital cataracts, aniridia, anophthalmia and central nervous system defects. *Nature Genetics* **7**, 463-471.

Gong, Q. and Shipley, M.T. (1995). Evidence that pioneer olfactory axons regulate telencephalon cell cycle kinetics to induce formation of the olfactory bulb. *Neuron* **14**, 91-101.

Goomer, R.S., Holst, B.D., Wood, I.C., Edelman, G.M., and Jones, F.S. (1994). Regulation in-vitro of an L-cam enhancer by homeobox genes Hoxd9 and HNF-1. *Proc. Natl. Acad. Sci. USA* **91**, 7985-7989.

Goulding, N.D., Chalepakis, G., Deutsch, U., Erelius, J.R. and Gruss, P. (1991). Pax3, a novel murine DNA binding protien expressed during early neurogenesis. *EMBO J.* **10**, 1135-1147.

Grainger, R.M. (1992). Embryonic lens induction: Shedding new light on tissue determination. *Trends Genet.* **8**, 349-355.

Green, M.C. (1989). *Genetic Strains and Variants of the Laboratory Mouse.* (eds Lyon M.F. and Searle P.G). pp12-403. Oxford University Press.

Grindley, J., Davidson, D.R. and Hill, R.E. (1995). The role of *Pax6* in lens and nasal placode development. *Development* **121**, 1433-1442.

Grumet, M., Hoffman, C., Choung, M. and Edelman, G.M. (1984). Polypeptide components and binding functions of neuron-glia cell adhesion molecules. *Proc. Natl. Acad. Sci. USA* **81**, 7989-7996.

Grumet, M., Hoffman, C., Crossin, K.L. and Edelman, G.M. (1985). Cytotactin, an extracellular matrix protein of neural and non-neural tissue that mediates glia-neuron interaction. *Proc. Natl. Aacad. Sci. USA* **82**, 8075-8079.

Grunberg, H. (1953). The relations of microphthalmia and white in the mouse. *J. Genet. 51*, 359-362.

Grunberg, H. (1954). Genetical studies on the skeleton of the mouse. XII. The development of *undulated. J. Genetics* **52**, 441-455.

Gurdon, J.B., Lemaire, P. and Kato, K. (1993). Community effects and related phenomena in development. *Cell* **75**, 831-834.

Gurdon, J.B. (1988). A community effect in animal development. *Nature* **336**, 772-774.

Halder, G., Callaerts, P. and Gehring, W. Induction of ectopic eyes by targeted expression of the *eyeless* gene in *Drosophila. Science* **267**, 1778-1792.

Hanson, I.M., Seawright, A., Hardman, K., Hodgson, S., Zaletayev, D., Fekete, G. and van Heyningen, V. (1993). PAX6 mutations in aniridia. *Hum. Mol. Genet.* **2**, 915-920.

Hanson, I.M., Seawright, A., Hardman, K., Hodgson, S., Zaletayev, D., Fekete, G. and van Heyningen, V. (1992). PAX6 mutations in aniridia. *Hum. Molec. Genet.* **2**, 915-920.

Hanson, I.M., Fletcher, J.M., Jordan, T., Brown, A., Taylor, D., Adams, R.J., Punnett, H.H. and van Heyningen, V. (1994). Mutations at the PAX6 locus are found in heterogeneous anterior segment malformations including Peters' anomaly. *Nature Genetics* **6**, 348-356.

Hanson, I. and van Heyningen, v. (1995). Pax6: more than meets the eye. *Trends in Genetics* **11**, 268-272.

Harrington, L., Klintworth, G.K., Secor, T.E. and Breitman, M.L. (1991). Developmental analysis of ocular morphogenesis in αA-crystallin/diptheria toxin transgenic mice undergoing ablation of the lens. *Dev. Biol.* **148**, 508-516.

Harris, W.A. and Hartsein, V. (1991). Neuronal cell determination without cell division in Xenopus embryos. *Neuron* **6**, 499-515.

Harrison, D. and Astle, C.M. (1976). Population of lymphiod tissue is cured in *W*-anaemic mice by donor cells. *Transplantation* **22**, 42-46.

Henry, J.J. and Grainger, R.M. (1990). Early tissue interactions leading to embryonic lens formation in *Xenopus laevis*. *Dev. Biol.* **141**, 149-163.

Hill, R.E., Favor, J., Hogan, B.L.M., Ton, C.C.T., Saunders, G.F., Hanson, I.M., Prosser, J., Jordan, T., Hastie, N.D. and van Heyningen, V. (1991). Mouse *Small eye* results from mutations in a paired-like homeobox containing gene. *Nature* **354**, 522-525.

Hitchcock, P.F., Macdonald, R.E., van De Ryt, J. and Wilson, S.W. (1996). Antibodies against Pax6 immunostain amacrine and ganglion cells and neuronal progenitors, but not rod precursors, in the normal and regenerating retina of the goldfish. *J. Neurobiol.* **3**, 399-413.

Hittner, H.M., Kretzer, F.L., Antoszyk, J.H., Ferrell, R.E. and Mehta, R.S. (1982). Variable expressivity of autosomal dominant anterior segment mesenchymal dysgenesis in six generations. *Am. J. Ophthalmol.* **93**, 57-70.

Hodgson, S.V. and Saunders, K.E. (1980). A probable case of the homozygous condition of the aniridia gene. *J. Med. Genet.* **6**, 478-480.

Hodgkinson, C.A., Moore, K.J., Nakayama, A., Steingrimsson, E., Copeland, N.G., Jenkins, N.A. and Arnheiter, H. (1993). Mutations at the mouse microphthalmia locus are associated with defects in a gene encoding a novel basic-helix-loop-helix-zipper protein. *Cell* **74**, 395-404.

Hoffman, S. and Edelman, G.M. (1983). Kinetics of homophilic binding by E and A forms of the neural cell adhesion molecule. *Proc. Natl. Acad. Sci. USA* **80**, 5762-5766.

Hoffman, S., Friedlander, D.R., Choung, C.M., Grumet, M. and Edelman, G.M. (1986). Differential contributions of Ng-CAM and N-CAM cell adhesion in different neural regions. *J. Cell Biol.* **103**, 145-158.

Hogan, B.L., Horsburgh, G., Cohen, J., Hetherington, C.M., Fisher, G. and Lyon, M.F. (1986). Small eyes (Sey): a homozygous lethal mutation on chromosome 2 which affects the differentiation of both lens and nasal placodes in the mouse. *J. Exp. Morph.* **97**, 95-110.

Hogan, B.L., Hetherington and Lyon, M.F. (1987). Alleleism of small eyes (Sey) with Dickie's small eye (Dey) on Chr 2. *Mouse News Lett.* **77**, 135-138.

Hogan, B.L., Hirst, E.M., Horsburgh, G. and Hetherington, C.M. (1988). Small eye (Sey): A mouse model for the genetic analysis of craniofacial abnormalities. *Development* **103 Suppl.**, 115-119.

Hollander, W.F. (1968). Complementary alleles at the *mi*-locus in the mouse. *Genetics* **60**, 189.

Holst, B.D., Goomer, R.S., Wood, I.C., Edelman, G.M. and Jones, F.S. (1994). Binding and activation of the promoter for the neural cell adhesion molecule by Pax-8. *J. biol. Chem.* **269**, 22245-22252.

Holstrom, G.E., Reardon, W.P., Baraitser, M. and Elson, J.S. and Taylor, D.S. (1991). Heterogeneity in dominant anterior segment malformations. *Br. J. Opthalmol.* **75**, 591-597.

Holt, C.E., Bertsch, T.W., Ellis, H.M. and Harris, W.A. (1988). Cellular determination in the Xenopus retina is independant of cell lineage and birth date. *Neuron* **1**, 15-26.

Jackson, I.J. (1988). A cDNA encoding a tyrosinase-related protien maps to the mouse brown locus. *Proc. Natl. Acad. Sci. USA.* **85**, 4392-4396.

Jackson, I.J. and Bennett, D.C. (1990). Molecular characterisation of the mouse albino mutation of tyrosinase and an in-vitro revertant. *Proc. Natl. Acad. Sci. USA.* **87**, 7010-7014.

Jackson, I.J., Chambers, D.M., Tsukamoto, K., Copeland, N.G., Gilbert, D.J., Jenkins, N.A. and Hearing, V. (1992). A second tyrosinase-related protein, TRP-2, maps to and is mutated at the mouse *slaty* locus. *EMBO J.* **11**, 527-535

Jacobson, A.G. (1958). The roles of neural and non-neural tissues in lens induction. *J. Exp. Zool.* **134**, 525-557

Jacobson, A.G. (1966). Inductive processes in embryonic development. *Science* **152**, 25-34

Jacobson, A.G and Slater, A.K. (1988). Features of embryonic induction. *Development* **104**, 341-359.

James, R.M., Flockhart, J.H., Keighren, M. and West, J.D. (1993). Quantitative analysis of mid-gestation mouse aggregation chimaeras: non-random composition of the placenta. *Roux's Arch. Dev. Biol.* **202**, 296-305.

James, R.M., Klerkx, A.H.E., Keighren, M., Flockhart, J.H. and West, J.D. (1995). Restricted distribution of tetraploid cells in mouse tetraploid↔diploid chimaeras. *Dev. Biol.* **167**, 213-226.

Jones, F.S., Holst, B.D., Minowa, O., DeRobertis, E.M., and Edelman, G.M. (1993). Binding and transcriptional activation of the promoter for the neural cell adhesion molecule by Hoxc6. *Proc. Natl. Acad. Sci. USA* **90**, 6557-6561.

Jordan, T., Hanson, I., Zaletayev, D., Hodgson, S., Prosser, J., Seawright, A., Hastie, N. and van Heyningen, V. (1992). The human PAX6 gene is mutated in two patients with aniridia. *Nature Genetics* **1**, 328-332.

Jostes, B., Walther, C. and Gruss, P. (1990). The murine paired box gene, *Pax7*, is expressed specifically during development of the nervous and muscular systems. *Mech. Dev.* **33**, 27-38.

Jowett, A.K., Vainio, S., Ferguson, M.W.J., Sharpe, P.T. and Thesleff, I. (1993). Epithelial-mesenchymal interactions are required for *msx-1* and *msx-2* gene expression in the developing murine molar tooth. *Development* **117**, 461-470.

Kahle, W. (1986). *Colour Atlas and Textbook of Human Anatomy. Vol. 3: Nervous System and Sensory Organs.* Trans. H.L. Dayan and A.D. Dayan. Geog Theime Verlag, Stuttgart, New York.

Kantorow, A., Cvekl, A. and Piatigorsky, J. (1995). Regulation of Pax-6 gene expression in the lens. *Invest. Opthalmol. Vis. Sci.* **37**, 4528.

Kaufman, M.H. and Webb, S. (1990). Postimplantation development of tetraploid mouse embryos produced by electrofusion. *Development* **110**, 1211-1132.

Kaufman, M.H., Chang, H.H. and Shaw, J.P. (1995). Craniofacial abnormalities in homozygous small eye (Sey/Sey) embryos and newborn mice. *J. Anat.* **186**, 607-617.

Kaur, S., Key, B., Stock, J., McNeish, J.D., Akeson, R. and Potter, S.S. (1989). Targeted ablation of alpha-crystallin-synthesising cells produces lens deficient eyes in transgenic mice. *Development* **105**, 613-619.

Keighren, M. and West, J.D. (1993). Analysis of cell ploidy in histological sections of mouse tissues by DNA-DNA in-situ hybridisation with digoxygenin labelled probes.
J. Histochem. **25**, 30-44.

Keighren, M. and West, J.D. (1994). Two partially congenic transgenic strains. *Mouse Genome* **92**, 666.

Kelley, A. (1995). The developmental of embryos and cells that are deficient in glycolysis. Ph.D. thesis, Edinburgh.

Kelley, M.W., Turner, J.K. and Reh, T.A. (1994). Retinoic acid promotes differentiation of photoreceptors in vitro. *Development* **120**, 2091-2102.

Kioussi ,C. and Gruss, P. (1994). Differential induction of Pax genes by NGF and BDNF in cereballar primary cultures. *J. Cell Biol.* **125**, 417-425.

Kobayashi, T., Urabe, K., Winder, A., Jiminez-Cervantes, C., Imokawa, G., Brewington, T., Solano, F., Garciaborron, J.C. and Hearing, V.J. (1994). Tyrosinase-related protein-1 (Trp-1) functions as a DHICA oxidase in melanin biosynthesis. *EMBO J.* **13**, 5818-5825.

Konyukhov, B.V., Kindyakov, B.N. and Malinina, N.A. (1994). Effects of the white allele of the Mi-locus on coat colour pigmentation in chimaeric mice. *Genet.Res. Camb.* **63**, 175-181.

Kozmik, Z., Kurzbauer, R, Dorfler, P. and Busslinger, M. (1993). Alternative splicing of *Pax-8* gene transcripts is developmentally regulated and generates isoforms with different transactivation properties. *Mol .Cell Biol.* **13**, 6024-6035.

Krauss, S., Johansen, T., Korzh, V., Moens, U., Ericson, J.U. and Fjose, A. (1991). Zebrafish Pax ZF-A: a paired box gene expressed in the neural tube. *EMBO J.* **10**, 3609-3619.

Kusakabe, M., Yokoyama, M., Sakakura, T., Nomura, T., Hosick, H.L. and Nisizuka, Y. (1988). A novel methodology for analysis of cell distribution in chimaeric mouse organs using a strain specific antibody. *J.Cell Biol.* **107**, 257-265.

Lamoreux, M.L., Boissy, R.E., Woimack, J.E. and Nordlund, J.J. (1968). The *vit* gene maps to the *mi* (microphthalmia) locus of the laboratory mouse. *J. Hered.* **83**, 435-439.

Langman, J. (1959a). The first appearance of specific antigens during the induction of the lens. *J. Embryol. Exp. Morphol.* **7**, 193-202.

Langman, J. (1959b). Appearance of antigens during development of the lens. *J. Embryol. Exp. Morphol.* **7**, 264-274.

LaVail, M.M. and Sidman, R.L. (1971). Patchy retinal degeneration in tetraparental mice. *Nature* **230**, 333-334.

LaVail, M.M. and Mullen, R.M. (1976a). Role of pigment epithelium in inherited retinal degeneration analysed with experimental mouse chimaeras. *Expl. Eye Res.* **23**, 227-245.

LaVail, M.M. and Mullen, R.M. (1976b). Inherited retinal dystrophy: Primary defects in pigment epithelium determined with experimental rat chimaeras. *Science* **192**, 799-801.

Layer, P.G. and Willbold, E. (1989). Embryonic chicken retinal cells can generate all cell layers in-vitro, but ciliary pigmented cells induce their correct polarity. *Cell Tissue Res.* **258**, 233-242.

Lehmann, F.E. (1933). Die Augen-und Linsenbildung von Amphibienembryonen unter dem Einfluss chemischer Mittel. *Rev. Suisse de Zool.* **40**, 251-264.

Lerner, A.B. (1986). Designation of a provisional gene symbol for a new mouse mutant. *Mouse News Lett.* **74**, 125.

Lewis, W.H. (1904). Experimental studies on the development of the eye in amphibia. I. On the origin of the lens. *Rana palustris. American Journal of Anatomy* **3**, 505-536.

Li, H.-S., Yang, J.-M., Jacobson, R.D., Pasko, D. and Sundin, O. (1994). Pax-6 is first expressed in a region of ectoderm anterior to the early neural plate: implications for stepwise determination in the lens. *Dev. Biol.* **81**, 143-162.

Lo, C. (1986). Localisation of low abundance DNA sequences in tissue sections by in-situ hybridisation. *J. Cell Sci.* **81**, 143-162.

Lo, C. W., Coulling, M. and Kirby, C. (1987). Tracking of mouse cell lineage using microinjected DNA sequences: analysis using genomic southern blotting and tissue section in-situ hybridisation. *Differentiation* **35**, 37-44.

Lo, C.W., Diaz, R. and Kirkby, C. (1992). Iontophoretic DNA injections and the production of transgenic mice. *Mouse Genome* **90**, 684-686.

Lufkin, T., Mark, M., Hart, C.P., Dolle, P., Le Meur, M. and Chambon, P. (1992). Homeotic transformation of the occipital bones of the skull by ectopic expression of a homeobox gene. *Nature* **359**, 835-841.

Lui, I.S.C., Chen, J., Ploder, L., Vidgen, D., van der Kooy, D., Kalnins, V.I. and McInnes, R.R. (1994). Developmental expression of a novel murine homeobox gene (Chx10): evidence for roles in determination of the neuroretina and inner nuclear layer. *Neuron* **13**, 377-393.

Macdonald, R., Barth, K.A., Xu, Q., Mikkola, I. and Wilson, S. (1995). Midline signalling is required for Pax gene regulation and patterning of the eyes. *Development* **121**, 3267-3278.

Mackenzie, A., Leeming, G.L., Jowett, A.K., Ferguson, M.W.J. and Sharpe, P.T. (1991a). The homeobox gene Hox7.1 has specific regional and temporal expression patterns during early murine craniofacial embryogenesis, especially tooth development *in vivo* and *in vitro*. *Development* **111**, 269-285.

Mackenzie, A., Ferguson, M.W.J. and Sharpe, P.T. (1991b). Hox7 expression during murine craniofacial development. *Development* **113**, 610-611.

Mackenzie, A., Ferguson, M.W.J. and Sharpe, P.T. (1992). Expression patterns of the homeoboxgene Hox-8 in the mouse embryo suggests a role in specifying tooth initiation and shape. *Development* **115**, 403-420.

Maisel, H. and Langman, J. (1961). An immunological study of the chick lens. *J. Embryol. Exp. Morphol.* **7**, 191-201.

Mansouri, A., Stoykova, A. and Gruss, P. (1994). *Pax* genes in development. *J. Cell Sci.* **18**, 35-42.

Mansouri, A., Stoykova, A., Torres, M. and Gruss, P. (1996). Dysgenesis of cephalic neural crest derivatives in *Pax7-/-* mutant mice. *Development* **122**, 831-838.

Margo, C.E. (1983). Congenital aniridia: A histopathological study of the anterior segment in children. *J.Ped. Opthalmol. Strabismus* **20**, 192-198.

Martha, A.D., Ferrell, R.E. and Saunders, G.F. (1994). Nonsense mutation in the homeobox region of the aniridia gene. *Human Mutation* **3**, 297-300.

Martin, G.R. (1981). Isolation of a pluripotent cell line from early mouse embryos cultured in medium conditioned by teratocarcinoma cells. *Proc. Natl. Acad. Sci. USA* **78**, 7634-638.

Martin, P., Carriere, C., Dozier, D., Quatannens, B., Mirabel, M.A., Vandenbunder, B., Stehelin, D. and Saule, S. (1992). Characterisation of a paired box and homeobox containing quail gene (PAX-QNR) expressed in the neuroretina. *Oncogenes* **7**, 1721-1728.

Matsunaga, M., Hatta, K. and Takeichi, M. (1988). Roles of N-cadherin cell adhesion molecules in the histogenesis of the neural retina. *Neuron* **1**, 289-295.

Matsuo, T., Osumi-Yamashita, N., Noji, S., Ohuchi, H., Koyama, E., Myokai, F., Matsuo, N., Taniguchi, S., Doi, H., Ninomiya, Y., Fujiwara, M., Wanatabe, T. and Eto, K. (1993). A mutation in the *Pax-6* gene in rat small eye is associated with impaired migration of midbrain neural crest cells. *Nature Genetics* **3**, 299-304.

Matsuo, I., Kuratani ,S., Kimura, C., Takeda, N. and Aizawa, S. (1995). Mouse Otx2 functions in the formation and patterning of the rostral head. *Genes Dev.* **9**, 2642-2658.

McCaffery, P., Tempst, P., Cara, G. and Drager, U.C. (1991). Aldehyde dehydrogenase ia a positional marker in the retina. *Development* **112**, 693-702.

McGinnis, W., Levine, M., Hafen, E., Kuriowa, A. and Gehring, W.J. (1984). A conserved DNA sequence in homeotic genes of the Drosophila *antennapedia* and *bithorax* complexes. *Nature* **308**, 428-433.

McLaren, A. (1976). *Mammalian Chimaeras.* Cambridge University Press, Cambridge.

McLaren, A. and Michie, D. (1956). Transfer of fertilised mouse eggs to uterine foster mothers: Factors affecting the implantation and survival of native and transferred eggs. *J. Exp. Biol.* **33**, 394-416.

McLaren, A. and Buehr, M. (1990). Development of mouse germ cells in cultures of fetal gonads. *Cell. Diff. Dev.* **31**, 185-195.

Meer de Jong, R.V.D., Dickinson, M.E., Woychik, R.P., Stubbs, L., Hetherington, C. and Hogan, B.L. (1990). Location of the gene involving the small eye mutation on mouse chromosome 2 suggests homolgy with human aniridia 2 (AN2). *Genomics* **7**, 270-275.

Mintz, B. (1967). Gene control of mammalian pigmentary differentiation. I. Clonal origin of melanocytes. *Proc. Natl. Acad. Sci. USA* **58**, 344-351.

Mintz, B. (1971). The clonal basis of mammalian differentiation. In *Control Mechanisms of Growth and Differentiation, Symposia of the Society for Experimental Biology.* (D.D. Davis and M. Balls, eds.), pp. 345-370. Cambridge University Press, London.

Mintz, B. and Illmensee, K. (1975). Normal genetically mosaic mice produced from malignant teratocarcinoma cells. *Proc. Natl. Acad. Sci. USA* 72, 3585-3589.

Mintz, B. and Palm, J. (1969). Gene control of haematapoesis. I. Erythrocyte mosaicism and permanent immunological tolerance in allophenic mice. *J. Exp. Med.* **129**, 1013-1027.

Miragall, M., Kadmon, G. and Schachner, M. (1989). Expression of L1 and N-CAM cell adhesion molecules during development of the mouse olfactory system. *Development* **135**, 272-286.

Mirzayans, F., Pearce, W.G., MacDonald, I.M. and Walter, M.A. (1995). Mutations of the PAX6 gene in patients with autosomal dominant keratinitis. *Am. J. Hum. Genet.* **3**, 539-548.

Moase, C.E. and Trasler, D.G. (1991). N-CAM alterations in splotch neural tube mouse embryos. *Development* **113**, 1049-1058.

Monaghan, P., Davidson, D.R., Sime, C., Graham, E., Baldock, R., Battacharya, S.S. and Hill, R.E. (1991). The Msh-like homeobox genes define domains in the developing vertebrate eye. *Development* **112**, 1053-1061.

Moore, W.J. and Mintz, B. (1972). Clonal model of vertebral column and skull development derived from genetically mosaic skeletons in allophenic mice. *Dev. Biol.* **27**, 55-70.

Muggleton-Harris, A.L., Hardy, K. and Higbeen, N. (1987). Rescue of developmental lens abnormalities in chimaeras of non-cataractous and congenital cataractous mice. *Devlopment* **99**, 473-480.

Mullen, R.J. and Whitten, W.K. (1971). Relationship of genotype and degree of chimaerism in coat colour to sex ratios and gametogenesis in chimaeric mice. *J. Exp. Zool.* **178**, 165-176.

Nagy, A., Paldi, A., Dezso, L., Varga, L. and Magyar, A. (1987a). Prenatal fate of parthenogenetic cells in mouse aggregation chimaeras. *Development* **101**, 67-71.

Nagy, A., Gosca, E., Diaz, E.M., Prideaux, V.R., Markulla, M. and Rossant, J. (1987b). Systematic non-uniform distribution of parthenogenetic cells in adult mouse chimaeras. *Development* **106**, 321-324.

Nagy, A., Miklos, S. and Markulla, M. (1989). Systematic non-uniform distribution of parthenogenetic cells in adult mouse chimaeras. *Devlopment* **106**, 321-324.

Norgreen ,R.B and Brackenbury, R. (1993). Cell adhesion molecules and the migration of LHRH neurons during development. *Dev. Biol.* **160**, 377-387.

Nornes, H.O., Dressler, G.R., Knapik, E.W., Deutsch, U. and Gruss, P. (1990). Spatially and temporally restricted expression of Pax-2 during murine neurogenesis. *Development* **109**, 797-809.

Okada, T.S. (1980). Cellular metaplasia of transdifferentiation as a model for retinal cell differentiation. *Curr. Top. Dev. Biol.* **16**, 349-380.

Padua, R.A., Bullfield, G. and Peters, J. (1978). Biochemical genetics of a new glucose phosphate isomerase allele (*Gpi-1*^{c}) from wild mice. *Biochem. Genets.* **16**, 127-143.

Palmer, S.J. and Burgoyne, P.S. (1991a). The *Mus musculus domesticus Tdy* allele acts later than *Mus musculus musculus Tdy* allele: a basis for XY sex reversal in C57BL/6-Y^{POS} mice. *Development* **113**, 709-714.

Palmer, J.S. and Burgoyne, P.S. (1991b). In situ analysis of fetal, prepubertal and adult XX↔XY testes: Sertoli cells are predominantly, but not exclusively, XY. *Development* **112**, 265-268.

Pappaioannou, V.E., and Gardner, R.L. (1976). Investigation of the lethal yellow A^y/A^y embryo using mouse chimaeras. *J. Embryol. Exp. Morphol.* **52**, 153-163.

Pappaioannou, V.E., Gardner, R.L., McBurney, M.W., Babinet, C. and Evans, M.J. (1978). Participation of cultures teratocarcinoma cells in mouse embryogenesis. *J. Embryol. Exp. Morphol.* **44**, 93-104.

Peyman, G.A. and Bok, D. (1972). Peroxidase diffusion in the normal and laser-coagulated primate retina. *Invest. Ophtalmol.* **11**, 35-45.

Pittack, C., Jones, M., Reh, T.A. (1991). Basic Fibroblast Growth Factor induces retinal pigment epithelium to generate neural retina *in vitro. Development;* **113**, 577-588.

Pituello, F., Yamada, G. and Gruss P. (1995). Activin A inhibits Pax-6 expression and purturbs cell differentiation in the developing spinal cord in vitro. *Proc. Natl. Acad. Sci. USA* **92**, 6952-6956.

Plachov, D., Chowdhury, K., Walther, C., Simon, D., Guene, J.L. and Gruss, P. (1990). Pax8, a murine paired box gene expressed in the developing excretory system and thyroid gland. *Development* **110**, 643-651.

Plaza, S., Dozier, C. and Saule, S. (1993). Quail Pax-6 (PAXQNR) encodes a transcription factor able to bind and trans-activate its own promotor. *Cell Growth and Diff.* **4**, 1041-1050.

Plaza, S., Dozier, C., Langlois, M-C. and Saule, S. (1995). Identification and characterisation of a neuroretina-specific enhancer element in the quail (*Pax-QNR*) gene. *Mol. Cell Biol.* **15**, 892-903.

Puschel, A.W., Gruss, P. and Westerfield, M. (1992). Sequence and expression pattern of Pax-6 are highly conserved between zebrafish and mice. *Development* **114**, 643-651.

Pritchard, J.D. (1973). A biochemical investigation of a dominant mutation associated with cellular invasiveness. PhD thesis, Edinburgh.

Pritchard, J.D., Clayton, R.M. and Cunningham, W.L. (1974). Abnormal lens capsule carbohydrate associated with the dominant gene "small-eyes" in the mouse. *Exp. Eye Res.* **19**, 335-340.

Quinn, J.C., West ,J.D. and Hill, R.E. (1996). Multiple functions for *Pax6* in mouse eye and nasal development. *Genes Dev.* **10**, 435-446.

Quinn, P., Barros, C. and Whittingham, D.G. (1982). Preservation of hamster oocytes to assay the fertilising capacity of human spermatozoa. *J. Repr. Fert.* **66**, 161-168.

Quiring, R., Walldorf, U., Kloter, U. and Gehring, W. (1994). Homology of the *eyeless* gene of *Drosophila* to the *Small eye* gene in mice and *Aniridia* in humans. *Science* **265**, 785-789.

Rabbachi, S.A., Neve, R.I. and Drager, U.C. (1990). A positional marker for the dorsal embryonic retina is homologous to the high affinity laminin receptor. *Development* **109,** 521-531.

Rabl, C. (1938). Uber den Bau und die Entwicklung der Linse. I. Slanchier und Amphibien. *Ztschr. f. wiss. Z. Zool.* **63**, 496-572.

Rashbass, P., Cooke, L.A., Herrman, B.G. and Beddington, R.S.P. (1991). A cell autonomous function of *Brachyury* in *T/T* embryonic stem cell chimaeras. *Nature* **353**, 348-351.

Raymond, S.M. and Jackson, I.J. (1995). The retinal pigment epithelium is required for development and maintenance of the mouse neural retina. *Current Biology* **5**, 1286-1295.

Reese, D.E., Harvey, A.R. and Tan, S.S. (1995). Clonal restriction in the mouse retina is cell class specific. *Invest. Ophthalmol. Vis. Sci.* **suppl. 35**, 3797.

Richardson, G.P., Crossin, K.L., Choung, C.-M. and Edelman, G.M. (1987). Expression of cell adhesion molecules during embryonic induction. III. Development of the otic placode. *Dev. Biol.* **119**, 217-230.

Richardson, J., Cvekl, A. and Wistow, G. (1995) Pax-6 is essential for lens specific expression of ζ-crystallin. *Proc. Natl. Acad. Sci. USA* **92**, 4676-4680.

Rijli, F.M., Mark, M., Dierich, P., Dolle, P. and Chambon, P. (1993). Homeotic transformation is generated in the rostral branchial region of the head by disruption of *Hoxa2* which acts as a selector gene. *Cell* **75**, 1333-1349.

Roberts, R.C. (1966). The limits to artificial selection for body weight in the mouse. *Genet. Res. Cambs.* **8**, 361-375.

Roberts, R.C. (1967). Small eyes - a new dominant eye mutation in the mouse. *Genet. Res. Cambs.* **9**, 121-122.

Rossant, J., Vijh, M., Siracusa, L.D. and Chapman, V.M. (1983). Identification of embryonic lineage in histological sections of *Mus musculus* ↔*Mus caroli* chimaeras. *J. Embryol. Exp. Morphol.* **73**, 179-191

Rutishauser, U. (1984). Developmental biology of a neural cell adhesion molecule. *Nature* **310**,549-554.

Sanyanusin, P., Schimmenti, L.A., McNoe, L.A., Ward, T.A., Pierpont, M.E.M., Sullivan, M.J., Dobyns, W.B. and Eccles, M.R. (1995). Mutation of the PAX2 gene in a family with optic nerve colobomas, renal anomalies and vesicouretal reflux. *Nature Genetics* **9**, 358-363.

Saha, M.S., Servetnick, M. and Grainger, R.M. (1992). Vertebrate eye development. *Curr. Op. Genet. Dev.* **2**, 582-588.

Saha, M.S., Spann, C.L. and Grainger, R.M. (1989). Embryonic lens induction: more than meets the optic vesicle. *Cell. Diff. Dev.* **28**, 153-172.

Sakota, I. and Maas, R. (1994). *Msx1* deficient knockout mice exhibit cleft palate and abnormalities of craniofacial and tooth development. *Nature Genetics* **6**, 348-356.

Sanyal, S. and Zeilmaker, G.H. (1977). Cell lineage in retinal development of mice studied in experimental chimaeras. *Nature* **265**, 731-733.

Schedl, A., Ross, A., Lee, M., Engelkamp, D., Rashbass, P., van Heyningen, V. and Hastie, N.D. (1996). Influence of *Pax6* gene dosage on development - overexpression causes severe ete abnormalities. *Cell* **86**, 71-82.

Schmahl, W., Knoedlseder, M., Favor, J and Davidson, D. (1993). Defects in neuronal migration and pathogenesis of cortical malformations are associated with small eye (Sey) in the mouse, a point mutation of the Pax-6 locus. *Acta Neuropathol.* **86**, 126-135.

Schwanzel-Fukuda, M. and Pfaff, D. (1985). Ontogenesis of neurons producing luteinizing hormone-releasing hormone (LHRH) in the nervus terminalis of the rat. *J. Comp. Neurol.* **338**, 161-163.

Schwanzel-Fukuda, M. and Pfaff, D. (1989a). Origin of leuteinising hormone-releasing hormone neurons. *Nature* **238**, 348-364.

Schwanzel-Fukuda, M., Bick, D. and Pfaff, D. (1989b). Luteinizing hormone-releasing hormone (LHRH) expressing cells do not migrate normally in an inherited hypogonadal (Kallman's) syndrome. *Mol. Brain Res.* **6**, 311-326.

Scott, M.P., Tamkun, J.W. and Hartzell, G.W. The strucure and function of the homeodomains. *Biochem. Biophys. Acta Rev. Cancer* **989**, 25-48.

Silvers, W.K. (1979). *The Coat Colours of Mice: A Model for Mammalian Gene Action and Interaction.* Springer Verlag, New York.

Simeone, A., Acampora, D., Stornaiuolo, A. and Boncinelli, E. (1991). Nested expression domains of four homoebox genes in developing rostral brain. *Nature* **358**, 687-690.

Simeone, A., Acampora, D., Mallamac, A., Stornaiuolo, A., Rosarina D'Apice, M., Nigro, V. and Boncinelli, E. (1992). A vertebrate gene related to *orthodenticle* contains a homeodomain of the *bicoid* class and demarcates anterior neuroectoderm in the gastrulating mouse embryo. *EMBO J.* **12**, 2735-2747.

Smesler, G.K. (1965). Embryology and morphology of the lens. *Invest. Opthalmol.* **4**, 398-410.

Southard, J.L. (1974). *Mouse News Lett.* **51**, 23.

Sparrow, J.R. and Barnstable, C.J. (1986). Expression of cell and synapse specific antigens in rat retinal explant cultures. *Soc. Neurosci. Abstr.* **12**, 643.

Spemann, H. (1912a). Uber Enticklung des Wirbeltierauges. *Zool. Jahrb. Abt.f.* **suppl. 3**, 1-48.

Spemann, H. (1912b). Die Erzeugung tierischer Chimaeren durch heteroplastische embryonale Transplatation zwischen Triton crtistarus u. taeniatus. *Arch. f. Entw. Mech.* **48**, 533-570.

Spemann, H. (1919). Experimentelle Firschungen zum Determinations und Individualitatsproblem. *Naturwissenschaften* **7.**

Spemann, H. (1938). *Embryonic Development and Induction.* Oxford University Press, Oxford.

Sperbeck, S., Jaworski, C., Richardson, J. and Wistow, G. (1996). Alternative splicing of Pax6. *Invest. Ophthalmol. Vis. Sci.* **37**, 706.

Spindle, A. (1982). Cell allocation in preimplantation mouse chimaeras. *J. Exp. Zool.* **219**, 361-367.

Stapleton, P., Weith, A., Urbanek, P., Kozmik, Z. and Busslinger, M. (1993). Chromosomal localisation of seven PAX genes and cloning of a novel family member, PAX9. *Nature Genetics* **3**, 292-298.

Steel, K.P., Davidson, D.R. and Jackson, I.J. (1992). TRP-2/DT, a new early melanoblast marker, shows that steel growth factors (c-kit ligand) is a survival factor. *Development* **115**, 1111-1119.

Stelzner, K.F. (1964). *Mouse News Lett.* **31**, 40.

Stelzner, K.F. (1966). *Mouse News Lett.* **34**, 41.

Stephenson, R.A., Glenister, P.H. and Hornby, J.E. (1985). Site of *beige* (*bg*) and *leaden* (*ln*) pigment gene expression determined by recombinant embryonic skin grafts and aggregation mouse chimaeras employing sash (*Wsh*) homozygotes. *Genet. Res.* **46**, 193-205.

Stroeva, O.G. (1960). Experimental analysis of eye morphogenesis in mammals. *J. Embryol. Exp. Morphol.* **8**, 349-368.

Stuart, E.T., Kioussi, C. and Gruss, P. (1994). Mammalian Pax genes. *Ann. Rev. Genet.* **28**, 219-236.

Struhl, G., Struhl ,K. and MacDonald, P.M. (1989). The gradient morphogen *bicoid* is a concentration dependent transcriptional activation factor.*Cell* **57**, 1259-1273.

Stoykova, A. and Gruss, P. (1994). Roles of Pax genes in developing and adult brain as suggested by expression patterns. *J. Neurosci.* **14**, 1395-1412.

Surani, M.A.H., Barton, S.C. and Kaufman, M.H. (1977). Development to term of chimaeras between diploid parthenogenetic and fertilized embryos. *Nature* **270**, 601-603.

Surani, A., Barton, S.C., Howlett,S.K. and Norris, M.L. (1988). Influence of chromosomal determinants on development of androgenetic and parthenogenetic cells. *Development* **103**, 171-178.

Tanaka, M. and Herr, W. (1990). Differential transcription by Oct-1 and Oct-2: Interdependent activation domains induce Oct-2 phosphorylation. *Cell* **60**, 375-386.

Tarkowski, A.K. (1964). Patterns of pigmentation in experimentally produced mouse chimaeras. *J. Embryol. Exp. Morph.* **12**, 575-585.

Tassabehji, M., Read, A.P., Newton, V.E., Harris, R., Balling, R., Gruss, P. and Strachan, T. (1992). Waardenburg's syndrome patients have mutations in the human homologue of the *Pax-3* paired box gene. *Nature* 355, 635-636.

Theiler K., Varnum, D.S. and Stevens, L.C. (1980). Development of Dickie's small eye, an eary lethal mutation in the house mouse. *Anatomy and Embryology* **161**, 115-120.

Theiler, K., Varnum, D.S. and Stevens, L.C. (1978). Development of Dickie's small eye, a mutation in the house mouse. *Anatomy and Embryology* **155**, 81-86.

Thomson, J.A. and Solter, D. (1988a). The developmental fate of androgenetic, parthenogenetic and gynogenetic cells in chimaeric gastrulating mouse embryos. *Genes and Dev.* **2**, 1344-1351.

Thomson, J.A. and Solter, D. (1988b). Transgenic markers for mammalian chimaeras. *Dev. Biol.* **197**, 63-65.

Thomson, J.A. and Solter, D. (1989). Chimaeras between parthenogenetic and androgemetic blastomeres and normal embryos: allocation to the inner cell mass and trophectoderm. *Dev. Biol.* **131**, 580-583.

Tomarev, S., Callaerts, P., Kos, L., Zinovieva, R., Halder, G. and Gehring, W. (1996). Pax6 and eye development in invertebrates. *Invest. Ophthalmol. Vis. Sci.* **suppl. 37**, 927.

Ton, C.C.T., Hirvonen, H., Miwa, H., Weil, M.M., Monaghan, P., Jordan, T., van Heyningen, V., Hastie, N.D., Meijer-Heijboer, H., Dreschler, M., Royer-Pokora, B., Collins, F., Swaroop, A., Strong, L.C. and Saunders, G.F. (1991). Positional cloning and characterisation of a paired box and homeobox containing gene from the aniridia region.*Cell* **67**, 1059-1074.

Ton, C.C., Miwa, H. and Saunders, G.F. (1992). Small eye (*Sey*): Cloning and characterisation of the murine homologue of the human aniridia gene. *Genomics* **13**, 251-256.

Treisman, J., Harris, E. and Desplan, C. (1991). The paired box encodes a second DNA-binding domain in the paired homeodomain protein. *Genes Dev.* **5**, 594-604.

Turner, D.L and Cepko, C.L. (1987). A common progenitor for neurons and glia persists in the rat retina late in development. *Nature* **328**, 131-136.

Turner, D.L., Snyder, E.Y. and Cepko, C.L. (1990). Lineage independant determination of cell type in the embryonic mouse retina. *Neuron* **2**, 833-845.

Vollmer, G., Layer, P.G. and Cierer, A. (1984). Reaggregation of embryonic chicken retina cells: pigment epithelial cells induce a high order of stratification. *Neurosci. Lett.* **48**, 191-196.

Waddington, C.H. and Cohen, A. (1936) Experiments on the development of the head of the chick embryo. *J. Exp. Biol.* **13**, 219-236.

Wallin, J., Witting, J., Haruhiko, K., Fritsch ,R., Christ, B. and Balling, R. (1994). The role of Pax-1 in axial skeletal development. *Development* **120**, 1109-1121.

Walther, C. and Gruss, P. (1991). Pax-6, a murine paired box gene, is expressed in the developing CNS. *Development* **113**, 1435-1449.

Walther C., Guenet, J.L., Deutsch, U., Goulding, M.D., Plachov, D., Balling, R. and Gruss, P. (1991). Pax: a murine multigene family of paired box-containing genes. *Genomics* **11**, 424-434.

Watanabe, T. and Raff, M.C. (1990). Rod photoreceptor development in vitro: properties of proliferating neuroepithelial cells change as development proceeds in the rat retina. *Neuron* **2**, 461-467.

West, J.D. (1976). Clonal analysis of the retinal epithelium in mouse chimaeras and X-inactivation mosaics. *J.Embryol. Exp. Morphol.* **35**, 445-461.

West, J.D. (1977). Red blood cell selection in chimaeric mice. *Exp. Haematol.* **5**, 1-7.

West, J.D. (1978). Analysis of clonal growth using chimaeras and mosaics. *Development in Mammals* Vol. 3, 413-460. Ed. M.H. Johnson,. Elseiver, Amsterdam.

West, J.D. (1984). Cell markers. In *Chimaeras in developmental Biology*. (N.L. Dourin and A. McLaren, eds.), pp. 39-63.

West, J.D. and Flockhart, J.H. (1994). Genotypically unbalanced diploid↔diploid foetal mouse chimaeras: Possible relevance to human confined placental mosaicism. *Genet. Res.* **63**, 87-99.

West, J.D., Everret, C.A. and Keighren, M. (1995). Corrections to transgenic nomenclature. *Mouse Genome* **93**, 145.

West, J.D., Keighren, M.A., Flockhart, J.H. (1996). A quantatative test for developmental neutrality of a transgenic lineage marker in mouse chimaeras. *Genet. Res. Camb.* **67**, 135-146.

West, J.D., Hodson, B.A. and Keighren, M.A. (1996). Quantitative and spatial information on the composition of chimaeric fetal mouse eyes from single histological sections. *In press.*

West, J.D. and McLaren, A. (1978). The distribution of melanocytes in the dorsal coats of a series of chimaeric mice. *J.Embryol. Exp. Morphol.* **35**, 87-93

Whittingham, D.G. (1971). Culture of mouse ova. *J. Reprod. Fertil.* **suppl. 14**, 7-21.

Williams, R.W. and Goldowitz, D. (1992). Structure of clonal and polyclonal cell arrays in chimaeric mouse retina. *Proc. Nat. Acad. Sci.* **89**, 1184-1188.

Williams, B.A. and Ordahl, C.P. (1994). Pax-3 expression in segmental mesoderm marks early stages in myogenic cell specification. *Development* **120**, 785-796.

Winder, A., Kobayashi ,T., Tsukamoto, K., Urabe, K., Aroca, P., Kameyama, K. and Hearing, V.J. (1994). The Tyrosinase gene family - interactions of melanogenic proteins to regulate melanogenesis. *Cell Mol. Biol. Res.* **40**, 613-626.

Wistow, G., Richardson, J., Lee, D., Friling, R., Sperbeck, S. and Graham, C. (1995). ζ-crystallin: Pax-6 dependance and expression in epithelial cells. *Invest. Opthalmol. Vis. Sci.* **37**, 4175.

Wolf, R. and Ready, D.F. (1993). *The Development of Drosohila melanogaster.* Eds; M. Bate and A. Martinez-Arias. Cold Spring Habour Laboratory Press, Cold Spring Harbour, NY.

Wolfe, H.G. and Coleman, D.L. (1964). Mi-spotted: a mutation in the mouse. *Genet. Res.* **46**, 309-324.

Wood, S.A., Allen, N.D., Rossant, J., Auerbach, A. and Nagy, A. (1993). Non-injection methods for the production of embryonic stem cell-embryo chimaeras. *Nature* **365**, 87-89.

Wray, S., Nieburgs, A. and Elkabes, S. (1989a). Spatiotemporal cell expression of leuteinisng hormone-releasing hormone in the prenatal mouse: evidence for an embryonic origin in the olfactory placode. *Dev. Brain Res.* **46**, 309-318.

Wray, S., Grant ,P. and Gainer, H. (1989b). Evidence that cells expressing luteinizing hormone-releasing hormone mRNA in the mouse are derived from progenitor cells in the olfactory placode. *Proc. Nat. Acad. Sci. USA* **86**, 8132-8136.

Yoshiki, A., Hanazono, M., Sen-ichi, O., Kakasugi, N., Sakakura, T. and Kusakabe, M. (1991). Developmental analysis of the eye lens obsolescence (*Elo*) gene in the mouse: cell proliferation and *Elo* gene expression in the aggregation chimaera. *Development* **113**, 1293-1304.

Young R.W. (1984). Cell death during differentiation of the retina in the mouse. *J. Comp Neurol.* **229**, 362-373.

Zhang, Y.H. and Emmons, S.W. (1995). Specification of sense organ identity by a *Caenorhabditis elegans* Pax-6 homologue. *Nature* **377**, 55-59.

Zannini, M., Francis-Land, H., Plachov, D. and Di Lauro, R. (1992). Pax-8, a paired domain-containing protein, binds to a sequence overlapping the recognition site of a homeodomain and activates transcription from two thyroid specific promotors. *Mol. Cell Biol.* **12**, 4230-4241.

Zwaan, J. and Webster, E.H. (1984). Histochemical analysis of extracellular matrix material during embryonic mouse lens morphogenesis in an aphakic strain of mice. *Dev. Biol.* **104**, 380-389.

Zwaan, J. and Webster, E.H. (1985). Localisation of keratin in the cells of the cornea in *aphakia* and normal mouse eyes. *Exp. Eye Res.* **40**, 127-133.

Zwilling, E. (1934). Induction of the olfactory placode by the forebrain in *Rana pipiens*. *Proc. Soc. Exp. Biol.* **31**, 933-935.

Appendices

Appendix I
Mouse strains

Abbreviated Stock name	Details	Genotype *Gpi1*	Genotype β-globin transgene
Sey	*CBA/Ca-Sey*	*b/b*	-/-
Sey^{Neu}	*CBA/Ca-Sey^{Neu}*	*b/b*	-/-
SEYTG	*CBA/Ca-Sey* x TGB inbred stock	*b/b*	+/+
MHK-*Sey*	C57BL x JU-*Sey* stock, mixed background	?/?	-/-
BALB/c	BALB/c/Eumm	*a/a*	-/-
C57BL	C57BL/6	*b/b*	-/-
CBA	CBA/Ca	*b/b*	-/-
CF_1	(CC female x CALB male)F_1 hybrid	*c/c*	-/-
TGB	derived from strain 83 (Lo *et al.*, 1986,1987), which carries the reiterated TgN(Hbb-b1)83Clo β-globin transgene (abbreviated to Tg)	*b/b*	+/+

Appendix II

Basic Histology

Reagents used:

Bouin's Fixative	500mls 40% formaldehyde (Sigma) 100mls Acetic acid (BDH) 2000mls Picric acid (BDH) Fix for 5-6 hours for E12.5 fetuses, overnight for >E14.5 fetuses
Acid/Alcohol Fixative	3:1 vol./vol. 100% ethanol/ acetic acid (Sigma)
Harris' Haematoxylin	(Pioneer research Chemicals Ltd.)
Eosin	1% aqueous eosin (BDH): 1% alcohol/eosin solution, 3:1. Add 0.05% acetic acid before use.
Acid/alcohol	70% alcohol: Concentrated Hydrochloric acid, 99:1
Scotts Tap water	2g Potassium bicarbonate 20g Magnesium sulphate make up to 1litre with H_20.

Routine histology:

Samples were processed to paraffin wax using an automatic processor. Samples were then embedded and allowed to cool. Once cold, blocks could be stored at room temperature until required. Sections for routine histology were cut at 7μm. All slides were dried overnight at 37°C before use.

For routine staining slides were dewaxed in Histoclear (National Diagnostics) for 2 x 10 minutes before rehydration in 100% and 70% ethanol for 2 x 5 minutes each and finally washed in 1 x PBS for 2 x 5 minutes. Slides were then stained for 1-1.5 minutes in Harris' haematoxylin, cleared in acid/alcohol for 2-5 seconds before 'blueing' in Scott's Tap Water (20-30 seconds). Slides were then counter-stained in eosin for 10-30 seconds depending on the strength of the eosin stain. Between each of the staining steps, slides were thoroughly rinsed in tap water. After staining, slides were dehydrated by immersion for 20 seconds in an ethanol series of 70%, 80% and 95%, before full dehydration in 100% ethanol for 2 minutes. Slides were finally cleared for mounting in Histoclear for 3 minutes before immersion briefly into Xylene (BDH) befor mounting. Slides were mounted using Pertex mounting medium (CellPath) under glass coverslips and allowed to air dry before viewing.

Appendix III

DNA-DNA in-situ hybridisation to the β-globin transgene

III.I.Digoxygenin Labelling of Probes:

Reagents used:

Hexanucleotide mix	(Boehringer 1277 081)
Dig DNA Labelling mix	Contains 1mM/l dATP, 1mM/l dCTP, 1mM/l dGTP,. 0.65mM/l dTTP & 0.35mM/l Dig-dUTP (Boehringer, 1277 065)
Klenow enzyme	2U/μl Labelling grade (Boehringer 1008 404)
Stop buffer	0.2M EDTA pH8.0
Absolute Ethanol	
TE buffer	10mM Tris pH7.5 - 8.0, 1mM EDTA

The transgene which was inserted into embryos to produce the Strain 83 mice consisted of approximately 1000 tandem repeats plasmid pMβδ2, comprising plasmid pBR322 and a 7kb insert of *Hbb*^{b1} , located on chromosome 3 (Lo et al; 1992 and Everett et al; 1994). The probe used for in-situ hybridisation was derived from the pMβδ2 plasmid used for to create the transgenic strain. The probe contains 1 copy of the mouse β-globin gene. The plasmid pMβδ2 was linearised by incubation at 37°C with *Eco*RI (10 units/μl) for 90min. Phenol/chloroform extraction was performed and the DNA was ethanol precipitated overnight at -20°C The precipitate was dissolved in TE buffer and stored as a stock of 100ng/μl.

III.II.Random Prime Labelling Method

Probe was denatured by boiling 1μg of DNA for 5 min then removing to ice.The labelling reaction was carried out using reagents from the Boehringer Mannheim DIG DNA Labelling and Detection Kit.

Add to the probe	10x hexanucleotide mix	2μl
	10x dNTPlabelling mix	2μl
	sterile distilled H_2O	5μl
	Klenow enzyme 2U/μl	1μl
	Total volume	20μl

1. Incubate for 6hr after addition of Klenow enzyme.

2. Add 2μl of 'stop buffer'.

3. Add 2μl of 3M sodium acetate and 60μl of cold EtOH. Place in -20°C freezer overnight.

4. Spin down precipitate. Decant supernatant and dry.

5. Redissolve in 50μl of TE buffer to give a final stock concentration of 20 ng/μl of labelled DNA. Store in freezer.

III.III. Nick Translation Labelling Method

Additional reagents used:

DNase I, RNase free Stock is 1mg/ml in 0.15M NaCl; 50% glycerol. (Boeringer, 776 785) Store at -20°C. Make a fresh 1:500 dilution in dH_2O for labelling.

DNA Pol 1 Stock is 10U/µl. Store at -20°C.(Gibco BRL,510 80105A)

dNTPs dATP (Pharmacia, 27-2050-01)
dCTP (Pharmacia, 27-2060-01)
dGTP (Pharmacia, 27-2070-01)
Stocks for nick translation reaction are at 0.5mM, prepared by a 1:200 dilution in dH_2O of 100mM stocks. Store at -20°C.

Dig-11-dUTP 1mM stock Store at -20°C (Boehringer, 1093 088.)

Dig DNA Labelling Contains 1mmol/l dATP, dCTP, dGTP, 0.65mmol/l (as before) dTTP & 0.35mmol/l Dig-dUTP (Boehringer, 1277 065) Store at -20°C

Nick translation salts 0.5M Tris pH 7.5; 0.1M $MgSO_4$; 1mM dithiothreitol; 500µg/ml BSA fraction V (Sigma). Store at -20°C in small aliquots

NICK Spin Columns Prepacked spin columns containing Sephadex G-50 fine, DNA grade.(Pharmacia, 17-0862-01)

1.0 µg of probe was in each reaction mix. The DNA must be clean as nick translation is sensitive to contaminants. All components of the reaction must be kept on ice. It is particularly important to dilute the DNase in cold distilled H_2O. The nucleotides may be added separately, alternatively a DIG DNA labelling mix can be used.

1. The following reagents were mixed in a 1.5ml Eppendorf tube:

	EITHER		OR
2µl	10X Nick translation salts.	2µl	10X Nick translation salts.
2.5µl	0.5mM dATP	2µl	DIG DNA labelling mix
2.5µl	0.5mM dCTP		
2.5µl	0.5mM dGTP		
2.5µl	1.0mM dig-11-dUTP		
1µl	1:500 fresh dilution of DNase (1mg/ml)	1µl	1:500 fresh dilution of DNase (1mg/ml)
xµl	probe (1µg)	xµl	probe (1µg)
yµl	dH2O	yµl	dH2O

The final volume in each tube was 19µl

2. All reagents were mixed together and collected in the bottom of the tube by spinning briefly in a microfuge.

3. 1µl of DNA Polymerase 1 enzyme (Pol 1) was then added.

4. The mixture was then incubated for 4 hours on ice or overnight at 4°C.

5. The reaction was stopped the reaction by adding 2µl 0.2M EDTA and 1µl 5% SDS. Samples were pooled together and made up to 100µl with TE buffer.

After the labelling reaction the probe is separated from unincorporated nucleotides using a Sephadex spin column (Pharmacia).

1. The column was inverted several times to resuspend the gel, then placed upright to allow the gel to settle.

2. The top cap was removed and then the bottom cap and the column allowed to drain Tap the column gently to remove any air bubbles.

3. The column was placed in a centrifuge tube and 2ml of TE buffer added. The column was allowed to drain.

4. The tube was centrifuged for 4 min at 500g in a swinging bucket rotor. The column was then removed and the eluate discarded.

5. The sample was then slowly applied (75-150µl) to the centre of the flat gel surface.

6. An Eppendorf™ tube was placed in the bottom of the column and the loaded column placed in a centrifuge tube. The sample was eluted by centrifugation for 4 minutes at 500g.

It was assumed that 80% (800ng) was of total labelled probe was recovered and the volume made up to a concentration of 20ng/ml in TE buffer.

III.IV. Quantification of probe labeling using 'Test Strips'

Products used:

Boehringer DIG Quantification Test strips (Boehringer 1660958)

Boehringer DIG Control Test strips (Boehringer 1669 966)

Boehringer Blocking Reagent (Boehringer 1096 176)

Reagents used:

Blocking buffer	From 10X stock, dilute to 1x in buffer 1
Antibody buffer	1.5ml anti-DIG Fab-AP antibody in 3 mls buffer 1
Wash buffer	Buffer 1
Equilibration buffer	Buffer 3
Colour substrate	3 mls buffer 3, 27µl NBT, 21µl x-phos
Buffer 1	0.1M Maleic acid 0.15M Nacl make up to 1 litre, pH 7.5
Buffer 3	0.1M TRIS 0.1M NaCl make up to 1 litre, pH 9.5 0.05M $MgCl_2$
X- Phos	5-Bromo 4chloro 2-indolyl phosphate (Boehringer-Mannheim)
NBT	Nitros blue tetrazolium (Boehringer-Mannheim)
Antibody	Anti-digoxygenin anti-sheep alkaline phosphatase Fab fragment conjugate (Boehringer -Mannheim)

10ml Sterilin™ conical tubes were used for this procedure. Test strips were placed back-to-back to allow two strips per tube. 3mls of each solution was used per tube and strips transferred using forceps. One control test strip was used per batch of experimetal strips for probe quantification. Control test strips had concentrations of 1, 3, 10, 30 and 100pg per spot.

Dilutions: Assume labelled probe test stock has start concentration of 10ug/100µl

Dilute original stock 1:100 to 'give' 1ng/µl

Further dilute this:

	Dilution	**Assumed Conc.**
a)	1:10	100pg/µl
b)	1:33	30pg/µl
c)	a dil 1:10	10pg/µl
d)	b dil 1:10	3pg/µl
e)	c dil 1:10	1pg/µl

1µl each test dilution was dotted onto the test strip and allowed to air dry for 10 mins. N.B. The lowest concentrationwas dotted in the space furthest from labelling area, this allowed easy comparison to the control test strip.

Washes were as follows **:**

Blocking buffer	2 mins	
Antibody buffer	1 min	
Blocking buffer	3 mins	
Washing buffer	1 min	
Eqilibrate	1 min	
Colour substrate	15 mins	In the dark

All strips were viewed after 15 minutes, blotted with tissue and allowed to airdry. Once dry, test strips were compared to the control test strip to identify amount in original probe stock. Stock sample was then diluted if necessary and routinely stored at 20ng/µl.

III.V.In-situ hybridisation using β-globin DIG-labeled probes on 3:1 fixed sections

Reagents used:

3:1 fix	3:1 ethanol:acetic acid (Sigma)
10 X PBS	Made up from tablets (Oxoid Code BR14a)
1 X PBS	1:10 dilution of 10 X PBS in distilled H_2O
Deionised formamide	(Sigma)
50 x Denhardt's	0.5g BSA (Sigma) , 0.5g PVP (Polyvinylpyrrolidine, Sigma), 0.5g Ficoll (Pharmacia) in 50mls H_20. Store in freezer.
20 X SSC	3M NaCl, 0.3M Na_3 Citrate [pH7-7.4]
2 X SSC	1:10 dilution 20 x SSC in distilled H_2O
TE buffer	10mM Tris[pH7.5], 1mM EDTA (BDH)
Salmon sperm DNA (sonicated)	Stock is 10mg/ml in TE buffer
Triton-X-100	(Sigma)
Buffer 1	0.1 M Tris, 0.15M NaCl [pH7.5]
Antibody:	Anti-digoxigenin polyclonal sheep Fab ragments conjugated to HRP-antibody horseradish peroxidase, 150U/ml.(Boehringer-Mannheim)
DAB buffer	0.05mM Tris [pH7.3]
Development Reagent	0.5mg/ml diaminobenzidine tetrahydrochloride in DAB buffer. Add 3µl H_2O_2 0.003% v/v) per 10ml (of reagent) just before use.

Samples for in situ hybridisation were fixed for 8 hours in 3:1 ethanol/acetic acid fixative and 70% ethanol before processing to wax blocks. Sections were cut at 7µm and mounted on TESPA coated slides.

Preparation washes were as follows:

Histoclear	2 x 10 mins	
100% Ethanol	2 x 5 mins	
3% H_2O_2/MeOH	30 mins	HRP endpoint
70% Ethanol	2 x 5 mins	
1 x PBS	2 x 5 mins	
1mM NaOH	3 mins	70°C
1 x PBS	5 mins	ice-cold (4°C)

Prehybridsation:

Amounts noted are for 10 slides:

Solution	**Volume**	**Final concentration**
50 x Denharts	40µl	5x
Deionised formamide	180µl	45%
20 x SSC	120µl	6 x
Salmon Sperm DNA (10mg/ml)	20µl	500µg/ml
dH_2O	40µl	

35µl of prehybridisation mix was transferred onto a clean glass coverslip before being picked up onto the slide. Slides were prehybridised at 60°C for 15 mins.

Hybridistion:

Amounts are for 10 slides:

Solution	**Volume**	**Final concentration**
20 x SSC	100µl	5x
20% Dextran sulphate	200µl	10%
Salmon Sperm DNA (10mg/ml)	20µl	500µg/ml
dH_2O	60µl	
probe*	20µl	approx. 20ng/slide

40µl of hybridisation mixture was used per slide and and slides incubated at 60°C overnight. Hybridisation mix was placed onto hydrophobic coverslips (Gelbond) and pick up onto slides before sealing with nail varnish. (Probe was routinely stored at 20ng/µl). The volume used depended upon strength of signal required). Slides were then placed into sealed sandwich boxes humidified with 2 x SSC to prevent slides dryng out.

Post hybridisation washes were performed as follows:		**Temperature**
2 x SSC, 0.1% Triton-X	2 x 5 mins	RT
0.1xSSC,0.1% Triton-X	1 x 5 mins	RT
0.1xSSC,0.1% Triton-X	1 x 5 mins	50°C
0.1xSSC,0.1% Triton-X, 5% BSA	1 x 5 mins	RT

Visulaisation:

1. Slides were washed in buffer 1 for 5 mins.
2. Slides were placed in a humidified chamber and flooded with antibody, (1:100 dilution of the anti-digoxigenin HRP-antibody in buffer 1) for 30 mins.
3. Slides were washed again in buffer 1 for 2 x 10 mins before a single wash in DAB buffer (HRP) for 5 mins.
4. Slides were placed again into a humidified chamber and flooded with development reagent for 30-40 mins. It was critical that slides were kept in the dark for colour development.
6. After colour had developed, slides were washed in water, dehydrated through an alcohol series, 70%, 80%, 95% to 100% ethanol, cleared in Histoclear (National Diagnostics) and Xylene (BDH) before mounting under glass coverslips using Pertex (CellPath) mounting medium.

If required, slides were counterstained before mounting.

III.VI. In-situ hybridisation using β-globin DIG-labeled probes on 4% paraformaldehyde fixed sections

Additional reagents used:

4% PFA	4% paraformaldehyde (Sigma) in 1x sterile PBS, pH7.2
0.02M HCl	425µl conc. HCl in 250mls dH_2O
Proteinase K Buffer	50mM TRIS, 5mM EDTA
Proteinase K	10mg/ml stock (Boehringer-Mannheim)

		Amount in 20 mls
Hybridisation buffer	50% Formamide	10 mls
	2xSSC	2 mls 20xSSC
	0.05g/ml Dextran sulphate	1g
	2mg/ml Marvel	0.04g
	dH_2O	8 mls

Samples were fixed for up to eight hours in 4% paraformaldehyde and washed in 1 x PBS before processing to wax blocks. Sections were cut at 7µm, mounted on TESPA coated slides and slides dried overnight at 55°C before use.

Prehybridisation washes were as follows:

Histoclear	2 x 10 minutes	
100% ethanol	2 x 5 minutes	
3% H_2O_2/MeOH	10 minutes	HRP endpoint only
70% ethanol	2 x 5 minutes	
1 x PBS	2 x 5 minutes	
0.02M HCl	10 minutes	
1 x PBS	2 x 5 minutes	
Proteinase K (50µg/ml)	7.5 minutes @ RT	200µl 10mg/ml Proteinase K in 40mls Proteinase K buffer.
1 x PBS	2 x 10 minutes	
4% PFA	5 minutes	
PBS	2 x 5 minutes	
70%, 80%, 95%, 100% ethanol	2 minutes each	

Slides were allowed to air dry.

Hybridisation:

For 10 slides: xµl probe (20ng/slide)
400µl hybridisation buffer

40µl of hybridisation mixture per slide was placed onto on a cleaned hydrophobic coverslip (40mm x 25mm) [Gelbond-MC Bioproducts]. Coverslips were picked up onto the slide and sealed with nail varnish.

Slides were then placed into an oven at 90°C for 10 minutes to denature before hybridisation overnight at 42°C. After hybridisation, coverslips were removed using a scalpel blade and slides immersed in 2 x SSC.

Post-hybridisation washes were as follows:

2 X SSC	RT	10 minutes
2 X SSC	60°C	20 minutes
0.2 X SSC	RT	10 minutes
0.2 X SSC	42°C	20 minutes

Visualisation was carried out as for the protocol of 3:1 fixed sections, as reported in section III.III.

Slides were then counterstained, dehydtrated through an alcohol series and cleared in Histoclear for 3 minutes before mounting with Pertex mounting medium as before.

III.VII. Protocol to detect β-globin transgene in blood cell smears.

Additional reagents used:

		Amount in 1 litre
Buffer 3	0.1M Tris	12.1g
	0.1M NaCl	5.8g
	0.05M MgCl	10.15g
	make up to 1l , pH to 9.5	

Marvel™ powdered milk

Antibody Anti-digoxygenin anti-sheep alkaline phsphatase Fab fragment conjugate (Boehringer -Mannheim)

Stain 3 mls buffer 3, 27µl NBT, 21µl x-phos

A fresh blood sample was taken and smeared onto a cleaned slide, (10µl of blood was sufficient). Slides were allowed to air dry for a minimum of 30 minutes.

Prehybridisation washes were as follows:

Wash:	**Time:**	
Ethanol / acetic acid 3:1	60 mins	Air dry after fix.
Acetone	10 mins	Air dry.
70% ethanol	2 mins	
80% ethanol	2 mins	
95% ethanol	2 mins	
100% ethanol	2 mins	

Slides could be stored before hybridisation if allowed to air dry after the 100% ethanol step.

Probe was boiled for 10 minutes to denature and then cooled rapidly on ice before adding to the hybridisation mix. 40µl of hybridisation mixture per slide was placed onto a hydrophobic coverslip (22x50mm, Gelbond - FMC Bioproducts), picked up onto the slide and sealed with nail polish. Slides were then placed at 75°C for 10 mins to denature sample DNA. On removal from the 75°C oven, slides were placed in a preheated sandwhich box, humidified with 2 x SSC, and hybridisation carried out at 37°C overnight.

HYBRIDISATION:

The following amounts are for 10 slides:

Hybridisation mix:

Solution	Volume	Final Concentration
Deionised formamide	200µl	50%
20 x SSC	40µl	2 x SSC
Salmon Sperm DNA(10mg/ml)	40µl	500µg/ml
50% Dextran	80µl	10%
dH_2O	30µl	
Probe	10µl	20ng/slide

Post-hybridisation:

Post-hybridisation washes were as follows:

Wash:	Time:	Temperature:
50% formamide, 2 x SSC	3 x 5 mins	45°C
2 x SSC	3 x 5 mins	45°C
4 x SSC,0.05% Triton-X	Holding Step	RT
5% Marvel, 4 xSSC, 0.05% Triton-X	5 mins	RT

Visulaisation:

Visualisation was achieved as follows:

Wash:	Time:	
Anti-digoxigenin AP-antibody in buffer 1 (1:2500)	30 mins	Humidified chamber
Buffer 1	2 x 10 mins	
Buffer 3	5 mins	
Stain	30-60 mins	In the dark.

Colour was allowed to develop in a dark chamber. Once colour had developed, slides were viewed without coverslips to check signal number.

Appendix IV
In-situ hybridisation to mRNA using Digoxygenin-labelled probes

IV.I. Production of probes for mRNA-DIG in-situ hybridisation

Isolation of mRNA probes from plasmid stocks

Reagents used:

L-Broth: (Luria-Bertani Medium)
To 950mls of deionised H2O add:
10g bacto-tryptone
5g bacto-yeast extract
10g NaCl

Dissolve solutes. Adjust pH to 7.0 with 5N NaOH (approximately 0.2mls). Adjust the volume of the solution to 1 litre with deionised H_2O. Autoclave.

LB-Plates: Make up media as above, but before autoclaving add:
15g/litre agarose
Allow media to cool to approx 50°C before adding antibiotics.

E. coli/plasmid stocks are stored at -70°C in 20% glycerol.

1. 1µl/ml of a 50mg/ml ampicillin stock (final con. 50mg/µl) was smeared onto the surface of L-broth plates with 500µl of sterile dH_2O and then air dried in sterile fume hood. Each L-broth plate was approximately 25mls in volume. A single loop of gylcerol stock was the streaked onto the ampicillin innoculated (50µg/ml ampicillin) plate.

2. Plate were left to incubate overnight at 37°C and a single colony selected to grow on. Isolates could be stored at 4°C if further colonies were required.

3. 5mls of L-broth (50µg/ml ampicillin) was innoculatedwith a single selected colony and allow to grow at 37°C to the exponential phase (approx 8 hours).

4. This mini-culture was then added to 500mls L-broth (50μg/ml ampicillin) and allow to grow for 14-16 hours (to saturation) at 37°C.
For use in a Quiagen Maxi-Prep (Qiagen), aliquot final culture colume into into 200ml samples.

IV.II. Isolation of plasmid from maxi-prep using Quiagen Maxi-Prep kit

Reagents used:

Buffer P1: 50mM Tris-HCl, pH8.0 Store at 4°C
10mM EDTA
100mg/ml RNAase A

Buffer P2: 200mM NaOH
1% SDS

Buffer P3: 3.0M potassium acetate pH5.5

Buffer QBT: 750mM NaCl
50mM MOPS pH7.0
15% ethanol
0.15% Triton-X100

Buffer QC: 1.0M NaCl
50mM MOPS pH7.0
15% ethanol

Buffer QF: 1.25M NaCl
10mM Tris-HCl pH8.5
15% ethanol

1. 200mls of maxi-prep was placed into a Sorval centrifuge spin container and cetrifuged at 13,000rpm for 30 minutes to pellet bacterial cells. Supernatant was then discarded.

2. The cellular pellet was resuspend in 10mls of buffer P1, by forcefull pipetting using a disposable plastic pipette.

3. 10mls of buffer P2 was added, mixed gently and left at room temperature for 5 minutes. Cells began to lyse immediately and the solution was seen to "clear". P2 buffer contains SDS which was suspensed before addition to the cell suspension by mixing until the buffer was clear.

4. 10mls of chilled buffer P3 was then added, and gently mixed by inverting the container 5-6 times before incubation on ice for 15 minutes.
[A whiteish substance formed in the solution. At this stage, precipitation of SDS captures denatured proteins, chromosomal DNA and cell debris, allowing the plasmid to renature and remain in solution. Incubation with prechilled buffer P3 on ice facilitates precipitation.]

5. The suspension was then centrifuge for 30 minutes at 4°C at 13,000rpm in a Sorval rotor. After centrifugation the supernatant was seen to be clear. Supernatant was then removed promptly before filtration through a pre-wetted muslin filter.

6. A Quiagen-tip 500 was equilabrated by applying 10mls of buffer QBT and allowing the colunm to empty by gravity flow.

8. Filtered supernatant was applied to the Quiagen-tip and allowed to empty by gravity flow. Plasmid DNA should be trapped in the resin of the tip. The 250-125 mls of supernatant can be kept to check retreival by running on an agarose gel if needed.

9. The Quiagen-tip with washed with 2 x 30mls of buffer QC. Washes removed any bacterial contaminants, small traces of buffer QC will not affect later elution.

10. DNA was eluted with 15mls of buffer QF and the elute collected in a sterilin of plastic centrifuge tube.

11. Plasmid DNA was precipitated with 10.5mls (0.7 volumes) of propan-2-ol (isopropanol), centrifuged for 30 minutes at 4°C at 13,000rpm in a Sorval rotor and the supernatant removed.
[No "pellet" is visible at this stage although the DNA should be observed as a clear gel-like substance at the bottom of the tube. Position of the presumptive pellet was marked on the centrifuge tube before centriugation so that the location of the pellet could be easily identified.]

12. The pellet was washed in 5 mls of 70% ethanol/TE pH8.0) and then vacuum dried before redissolving in 500ml TE buffer (pH8.0). [If full retreival has been acheived, this stock should be at a concentration of approximately 1mg/ml.]

13. 1μg of final stock was run on a 1% agarose/TBE gel containing ethidium bromide and visualised under UV to ascertain efficacy of retreival. (N.B. A 18ml mini-gel will contain 0.7μl of 10μg/ml ethidium bromide.)

IV.III. Linearisation of mRNA probes

Trp2 probe was kindly donated by Ian Jackson at the MRC Human Genetics Unit, Edinburgh. This probe was derived from a HindIII (Boehringer-Mannheim) digest of plasmid pA57, pA57 being a pBS plasmid containing an 1200bp insert of cDNA *Trp2* sequence. Sense control was derived from plasmid pA53 by HindIII digestion, pA53 contained the same cDNA *Trp2* sequence to that of pA57 but cloned in the opposite orientation (See Steel et al., 1992). Sense and anti-sense probes were labelled by transcription with T7 RNA polymerase using DIG-labelled dUTP (Boehringer-Mannheim DIG-RNA labelling kit, see Appendix IV.IV).

Pax6 probe was created by linearisation of the plasmid pM1 which contained a 1.7kb insert of *Pax6* cDNA sequence cloned into Bluescript II SK+ vector. Anti-sense probe was linearised from pM1 plasmid using restriction enzyme XbaI (Boehringer-Mannheim). Linearised plasmid was labelled by transcription with T7 polymerase using DIG-dUTP (Boehringer-Mannheim DIG-RNA labelling kit) to create labelled anti-sense probe. Sense probe was linearised with SalI (Boehringer-Mannheim) before transcription and labelling with T3 RNA polymerase and DIG-labelled dUTP (See Appendix IV.IV).

Probes were digested with the appropriate restriction enzyme as follows:

10µl (approximately 10µg) uncut probe
10µl restriction enzyme (Boehringer-Mannheim)
10µl 10X restriction enzyme buffer (Boehringer-Mannheim)
70µl sterile distilled H_2O

The reaction mixture was incubated overnight at 37°C. Linearised probe samples were then purified of exogenous protein and enzymes using Gene Clean II Kit (Bio 101 Inc.).

IV.III.I. Cleaning of digested probe samples using the "Gene Clean" Kit

Reagents in Gene Clean II Kit (Bio 101 Inc.):

6M NaI solution

NaCl/Tris/EDTA- ethanol water mix (NEW Wash)

'Glassmilk' - silica matrix

The following protocol is for a digestion samples of approximately 100µl:

1. 300µl of NaI solution was added to the reaction mixture and mixed.

2. 15µl of fully suspended "glassmilk" was then added and vortex mixed and place on ice. This reaction mixture was then briefly vortexed again once every minute for five minutes.

3. Glassmilk was pelleted to the botton of the tube by allowing the tube to reach full speed in a microfuge for 5 seconds. After each centrifugation the NaI supernatant was removed from tube.

4. The pellet was washed three times with New Wash, adding 1ml each time and fully resuspending the pellet by forceful pipetting. The tubes were spun at full speed in a microfuge to repellet after each wash.

5. After the final wash, tubes were spun for a further 5 seconds to ensure all New Wash had been removed before resuspending the cleaned pellet in 20µl of TE buffer.

6. This mixture was then incubated at 45-55°C for 2-3 minutes.

7. Tubes were centrifuged again for a full 30 seconds to make a firm pellet before removing the resultant supernatant to a separate tube. This supernatant now contained the 'cleaned' probe.

8. Steps 6 and 7 were repeated to ensure full recovery.

Assuming full recovery, a 0.5µg sample of cleaned probe was submitted to electrophoresis in a 1% agarose/TBE gel for 30 minutes at 100 volts. 0.5µg of uncleaned probe stock was also run as a conrol to give an approximate recovery rate. Probes were only used for DIG labelling if a single, clean band was visualised after linearisation and cleaning.

IV.IV. Labeling of mRNA probes using digoxigenin-UTP by in vitro transcription with T7 RNA polymerase

Reagents Used:

		Final Conc.
NTP labeling mixture	10mM ATP	1mM
	10mM CTP	1mM
	10mM GTP	1mM
	6.5mM UTP	0.65mM
	3.5mM DIG-UTP	0.35mM
	pH7.5	
10 X Transcription buffer		
DIG RNA labelling Kit	(Boehringer-Mannheim) cat. no. 1175 025	

The following protocol was for labelling of mRNA probes after linearisation and cleaning as previously described:

1. The following reagents were measured into a sterile 500µm Eppendorf™ tube:

   1µl probe (4µl volume) or control DNA
   2µl 10 X transcription buffer
   2µl NTP labelling mix
   10µl sterile DEPC dH_2O
   2µl T7 RNA polymerase (20 units / µl)

2. Tubes were incubated for 2 hours at 37°C.

3. 2µl DNase1, RNase free (10 units / µl) was added and tubes incubated at 37°C for 15 minutes.

4. 2µl 0.2M EDTA(pH8.0) was then added to stop this reaction.

5. Labelled probe was precipitated with 2.5µl 4M LiCl and 75µl chilled ethanol by incubation at -20°C overnight.

6. Precipitation mixture was then cetrifuged for 15 minutes at 15,000rpm and supernatant removed. The pellet was washed in 70% ethanol and centrifuged again to remove all supernatant.

7. Tubes were covered with peirced "Parafilm" and left in a sterile fume hood to dry for 1 hour.

8. Once dry, the pellet was was resuspend in 100µl of sterile DEPC dH_2O. Placing tubes in a 37°C oven for 1 hour facilitated this process.
Probe-DIG incorporation was quantified using Test strips.

IV.V. Quantification of DIG-labelled mRNA probes using test strips

Quantification of DIG labellled riboprobes was performed using the protocol as described in Appendix III.IV.

IV.VI. In-situ hybridisation to mRNA using DIG-labelled probes

Reagents used:

50 x Denhardt's: 0.5g BSA (Sigma) , 0.5g PVP (Polyvinylpyrrolidine, Sigma), 0.5g Ficoll (Pharmacia) in 50mls H_20.
Store in freezer.

1 x TEA: 10X (1.0M) Buffer: 92.85g Triethanolamine (TEA) in 500mls pH to 7.5. Store as 10 x stock.
Dilute to 1X (0.1M) and autoclave before use.

Proteinase K Buffer: 50mM TRIS, 5mM EDTA

20 x SSC:		500mls
	NaCl	87.66g
	Trisodium Citrate	44.12g
	pH 7.5	

Buffer 3:		Amount in 100mls
	0.1M Tris	12.1g
	0.1M NaCl	5.8g pH to 9.5 before adding $MgCl_2$
	0.05M $MgCl_2$	10.15g

0.2M HCl:		Amount in 500mls
	Conc. HCl	8.61mls

4% PFA:		Amount in 250mls sterile 1 x PBS
	PFA	10g
	pH to 7.2	

Acetic anhydride - Sigma

Stain - 100mls Buffer 3
90µl NBT
35µl X-Phos

X- Phos 5-Bromo 4-chloro 2-indolyl phosphate (Boehringer)

NBT Nitros Blue tetrazolium (Boehringer-Mannheim)

Slides were floated from sterile distilled water onto TESPA coated slides, sealed in fiol and baked overnight at 55°C before storing until use in sealed boxes containing silica gel to prevent unnecessary hydration. All glassware was baked to 250°C and all solutions and plasticware autoclaved before use.

DAY 1

Pre-hybridisation washes were as follows:

Wash:	Time:	
Histoclear	2 x 10 mins	
100% ethanol	2 x 5 mins	
70% ethanol	2 x 5 mins	
2xSSC	5 mins	
Proteinase K buffer (50µg/ml)	7.5 mins @ RT	200µlProt K (10mg/ml stock per 40ml coplin jar
2XSSC	30 mins	
4% PFA	15 mins	
0.2M HCL	15 mins	
1xTEA pH 8.0	30 secs	
1xTEA + acetic anhydride	10 mins	625µl in 200 mls fume cupboard on stirrer

Prehybridisation:

Make up 1ml of mix, remove amount needed for pre-hybridisarion or hybridisation, (75µl per slide) adding one extra slide volume for every 5 slides.

	Amount	Final Concentration
Formamide	500µl	50%
20xSSC	100µl	2X
50xDenharts	100µl	5X
50% dextran	200µl	10%
yeast tRNA (10mg/ml stock)	20µl	200µg/ml
20% SDS	25µl	0.5%
depc H2O	30µl	

75µl prehybridisation mixture per slide was placed under a hydrophobic 40mm x 25mm coverslip (Gelbond -FMC Bioproducts). Prehybridisation was carried out in a 5 x SSC, 50% formamide humidified box at 50°C for 30 minutes.

Hybridisation:

Amounts needed were aliquoted as before.

Solution	Amount	Final Concentration
Formamide	500µl	50%
20xSSC	100µl	2X
50xDenharts	100µl	5X
50% dextran	200µl	10%
yeast tRNA (10mg/ml stock)	20µl	200µg/ml
20% SDS	25µl	0.5%
depc H2O	30µl	
Probe	**4-8µl per slide**	**Approx. 120ng per slid**

Probe was added to hybridisation mix at a concentration of approximately 120ng per slide. Hybridisation mix containing probe was heated to 80° for 2 mins and then cooled rapidly on ice. 75µl of hybridisation mixture was placed onto hydrphobic 40mm x 25mm coverslips (Gelbond - FMC Bioproducts) and picked up onto each slide.

Slides were placed in 5 x SSC humidified box, seal with tape and hybridisation allowed to proceed at 50°C overnight.

DAY 2

Post-hybridisation:

Post hybridisation washes were as follows:

Wash:	Time:	Temperature:
2 x SSC	10 mins +++	50°C
2 x SSC 50% formamide	45 mins	**60°C**
4 x SSC	5 mins	50°C
4 x SSC plus RNAase A (100µlof 10mg/ml stock in 50mls 4 x SSC in coplin jar)	30 mins	37°C (20µg/ml RNAase A - final concentration)
2 x SSC 50% formamide	45 mins	**60°C**
2 x SSC	allow to cool 30' plus	50°C

Antibody washes were as follows:

Wash:	Time:	
PBS 0.1% Triton-X	10 mins	
PBS 0.1% Triton -X plus 1% BSA	30 mins	
Anti-DIG AP Fab antibody 1:5000 dilution in PBS (10µl in 50ml coplin jar)	**overnight**	**4°**

DAY 3

Colour detection:

Wash:	Time:	
1 X PBS, 0.1% Triton-X	3 x 20 mins	
Buffer 3	5 mins	
Stain - 100mls	overnight	wrap and place in dark

DAY 4

Visulaisation:

Slides in were rinsed in distilled H_2O and examined using light microscopy for intensity of blue staining before staining lightly with eosin for 5 seconds. Slides were then dehydrated through and ethanol series, dipping quickly into each dilution. Slides must not be left in alcohol for any lenght of time as this causes the stain to precipitate. Slides were then cleared in Histoclear (National Diagnostic) for 2 minutes before immersion in Xylene (BDH) for mounting. Coverslips were mounted with Pertex (CellPath) mounting medium under glass coverslips.

Appendix V

Embryo culture medias

V.I.Stock solution:

Stock A (10x)	1M NaCl
	0.05M KCl
	1.2M KH_2PO_4
	0.01M $MgSO_4.7H_2O$
	0.23M Na lactate (60% solution)
	5.5mM Glucose
	10^5 units penicillin (Stock -)
	750 units/mg streptomycin (Stock -)
Stock B (10x)	0.25M $NaHCO_3$
	0.01g phenol red
Stock C (100x)	0.33M Sodium pyruvate
Stock D (100x)	0.17M $CaCl_2.2H_20$
Stock E (10x)	0.25M HEPES (Ultrapure Calbiochem)
	0.01g phenol red

Adjusted to pH to 7.4 with 5M NaOH before making up to 100ml.

100mls of stocks A, B and E and 10ml of C and D were made using sterile cell culture grade H_2O (BDH). All stocks were filter sterilised using a millipore filter (0.22µm)and stored at 4°C. Stocks A, D and E were kept for 3 months and B and C renewed every two weeks.

Appendix VI

Embryo collection

M2 Handling Medium

(HEPES buffered modified Kreb's-Ringer solution; Quinn *et al.*, 1982)

Stock	A	1.00ml
	B	0.16ml
	C	0.10ml
	D	0.10ml
	E	0.84ml
Double distilled H_2O (BDH)		7.8ml
BSA		4mg/ml

Filter sterilise before use.

Acid Tyrode's solution

0.14M NaCl

2.6mM KCl

1.4mM $CaCl_2$

0.5mM $MgCl_2.6H_2O$

0.2mM$NaH_2PO_4.H_2O$

5.5mM Glucose

0.12M $NaHCO_3$

0.4%polyvinyl pyrrolidone

Adjusted to pH 2.5 with 5M HCl. Filter sterilise and stored at 4°C.

M16 Culture Medium

(modified Kreb's-Ringer bicarbonate solution, [Whittingham, 1971])

Stock	A	1.0ml
	B	1.0ml
	C	0.1ml
	D	0.1ml
Double distilled H_2O		7.8ml
	BSA	4mg/ml

Filter sterilise before use.

Method:

Preimplantation embryos were removed from the uterus and oviducts by inserting a syringe needle into one end of the uterus and oviduct and flushing with M2 medium. Embryos were collected and placed in a fresh drop of M2. To remove the zona pellucidae, groups of approximately 6 embryos were placed in a watchglass containing acid Tyrode's solution, previously warmed to 37°C, and watched closely until the zonas began to disappear. This process only took a matter of seconds. The embryos were then rinsed in a fresh drop of M2 to remove any traces of the acid Tyrode's solution (pH 2.5). Chimaeras were produced by aggregating pairs of 8-cell embryos together. To aid fusion, the two selected embryos were placed together in a drop a of M2 + PHA (1 part phytohaemagglutinin [M form, GIBCO 670-0576] plus 19 parts M2 medium) and pushed gently together.

Embryo pairs were left for 2-3mins to ensure that they had aggregated sufficiently and were then removed to a fresh drop of M2 medium. Embryos were then transferref to drops of M16 culture medium under oil which had been allowed to equilibrate at 37°C in 5% CO_2 and allowed to develop overnight. By the next day the aggregated embryos had reached late morullae to blastocyst stage. Those embryos that had not aggregated properly were discarded. The aggregated embryos were then surgically transferred to pseudopregnant females (see Appendix VII).

Appendix VII

Superovulation

Reagents used:

Pregnant Mares serum gonadotrophin (PMSG) Stock solution of 50Units/ml.

Dosage : 5U per mouse

Human chorionic gonadotrophin (hCG) Stock solution of 50Units/ml.

Dosage : 5U per mouse

Females to be superovulated were injected intraperitoneally with 0.1ml pregnant mares serum gonadotrophin (PMSG) at 12 noon, followed 48hrs later by injection of 0.1ml human chorionic gonadotrophin (hCG). After the second injection, females were mated to males of the required strain. Mating was confirmed by the presenc of a vaginal plug the following morning. The day of plug detection was designated 0.5 day *post coitum* (*p.c.*) or embryonic day 0.5 (E0.5). Pregnant females were killed by cervical dislocation on day E2.5 and the oviducts and uterus removed. On the day of detection of vaginal plug, a group of CF_1 females were examined and those in oestrus were mated to vasectomised CF1 males to provide pseudopregnant females for subsequent embryo transfer (see Appendix VIII).

Appendix VIII

Transfer of embryos

Anaesthetics:

Hypnorm (0.315 mg/ml fentanyl citrate and 10mg/ml fluanisone;
Janssen Pharmacuticals)

Hypnovel (2mg/ml midazlam hydrochloride; Roche)

Females to be used as transfer recipients were selected in oestrus by vaginal inspection and mated to vasectomized males. Vaginal plugs were checked the following morning, the day of detection was designated as day E0.5. Transfer took place on day E2.5. Pseudopregnant females were anaesthetised with 0.25 ml per 30 g body weight of a 1:1 v/v mixture of Hypnorm and Hypnovel. Both the Hypnorm and Hypnovel were diluted 1:1 v/v with sterile distilled water before being mixed together. Pregnancies were timed according to the pseudopregnant female.

The embryos were collected in a small amount of M2 handling medium in a fine glass pipette before surgical transfer to the uterus. Embryos were inserted in to the uterus as close to the oviduct as possible via a small incision made with a fine needle (McLaren and Michie, 1956).

Appendix IX

Gel Electophoresis for GPI-1 Activity

Reagents used:

Fructose 6 phosphate (F6P)	Sigma (F3627)
Glucose 6 phosphate dehydrogenase (1000 units/ml) (G6PD)	Sigma (G8878)
Glycine	Sigma (G7126)
$MgCl_2.6H_2O$	BDH (10149)
NADP	Sigma (N0505)
Nitro blue tetrazolium (NBT)	Sigma (N6876)
Phenozine methosulphate (PMS)	Sigma (P9625)
Tris	Sigma(T1503)
Glycerol	BDH (28454)
Sodium citrate	BDH (10242)
Electrophoresis Buffer	0.02M Tris 0.2M Glycine

Adjust to pH 8.1 and store for one month at 4°C.

Stock Solutions for Stain:

F6P	20mg/ml
$MgCl_2$	0.2%
NADP	2.7mg/ml
NBT	2.7mg/ml
PMS	2.5mg/ml
Tris citrate buffer pH 8.0	0.3M Tris 0.08M Citric acid

Stain amounts for 1 plate:

Glycerol/$MgCl_2$ (50:50)	1.5ml
Tris citrate buffer	170µl
F6P	170µl
NBT	170µl
NADP	170µl
G6PD	6-10units
PMS	20µl

Method

Electrophoresis was carried out using electrophoresis tanks and Super Z-8 applicators obtained from Helena Laboratories used in conjunction with a Consort Bioblock Scientific power pack. Titan III cellulose acetate plates (Helena Laboratories) were soaked in electrophoresis buffer for 30min before use. The tank reservoirs were filled with electrophoresis buffer and Whatman filter paper was used to form wicks. Tissue samples were frozen and thawed three times before dilution to ensure full cell lysis. Samples were diluted 1:5 in water, applied to blotted plates and run from anode to cathode at 200V for 60min. Plates were then stained for glucose phosphate isomerase (GPI1) activity for up to 20min in the dark on a 37°C hotplate.The staining reaction is shown in Chapter 2, Figure 2.3. After rinsing in water, the plates were fixed in 5% acetic acid for 5min then washed in distilled water for 15min. Plates were allowed to air dry before densitometry.

Densitometry \was carried out using a Helena Process-24 gel scanner to determine the relative proportions of GPI-1A and GPI-1B and GPI-1C in the samples (West *et al.*, 1986).

Appendix X

PCR and restriction digest analysis of genomic DNA from chimaeric fetuses

Reagents used:

5 x Proteinase K Buffer (Stock):

50mM Tris
250mM KCl
25mM $MgCl_2$ (ph7.8)
2.25% N-P40 (Nonidet-P40) (Sigma)
2.25% TWEEN (Polyoxyethelene-sorbitan-monolaurate) (Sigma)
0.5mg/ml gelatine (Sigma)

Diluted to 1X in sterile distilled H2O plus 300µg of (10mg/ml) Proteinase K (Sigma) per 0.5mls final volume.

10 X PCR buffer (stock)

500mM KCl
100mM Tris-HCl (pH8.3)
15mM $MgCl_2$
1% Triton-X100 (Sigma)

Preparation of 2 x PCR buffer:

200µl 10 x PCR buffer
2µl dATP
2µl dTTP
2µl dGTP
2µl dGTP
2µl Triton-X100 (Sigma)
790µl DEPC distilled H_20

10 X PCR buffer was diluted 2:5 with sterile distilled H2O and 0.2mM of dATP, dTTP, dCTP and dGTP added. [dNTPs are kept as 100mM stocks (Boehringer-Mannheim)]. Final working concentration of 1 X PCR buffer containing 1mM of each dNTP was used in the final PCR by dilution of 2 X stock with distilled H_2O containing template DNA.

HindII restriction digest buffer

10mM / litre Tris-HCl
50mM / litre NaCl
10mM / litre $MgCl_2$
DTT1mM / litre
(pH 7.5)(Boehringer-Mannheim)

DdeI restriction digest buffer

50mM / litreTris-HCl
100mM / litre NaCl
10mM / litre $MgCl_2$
DTT1mM / litre
(pH7.5) (Boehringer-Mannheim)

TBE (Tris-borate) buffer (pH 8.0):

1 X	**5 X**
9mM Tris-borate (Sigma)	45mM Tris-borate (Sigma)
2mM EDTA (Sigma)	10mM EDTA
(pH to 8.0)	(pH to 8.0)

TE (Tris-EDTA) buffer:

1 x	
10mM Tris-Cl	(pH8.0)
1mM EDTA	(pH8.0)

DEPC distilled H_20

1:1000 dilution in distilled H_20, autoclaved

TEMED

(N,N,N',N'-Tetramethylethylenediamine, Sigma)

10% Ammonium persulphate

(Sigma) in distilled H_2O

15% Polyacrylamide gel:

15 mls 40% acrylamide: bis:acrylamide 19:1
(Northumbria Biologicals Ltd)
300µl 10% Ammonium persulphate (Sigma)
8 mls 5 x TBE
30µl TEMED (Sigma)
16 mls distilled H_2O

X.I.Purification of oligonucelotides from ammonia stocks:

Oligonucelotides for Polymerase Chain Reaction (PCR) were produced by an automated oligonucleotide synthesis processor at the Medical Research Council Human Geneitcs Unit, Western General Hospital, Edinburgh. Oligonucleotides were produced in an ammonia stock for long term preservation.

To purify oligonucelotides from ammonia stock add:

1. 300µl oligo/ammonia suspension
   50µl 3M NaAc (Sigma)
   900µl ethanol

2. Tubes were vortex mixed before placing at -70°C for 1 hour.

3. Tubese were then spun at 1500rpm in microcentrifuge for 15 minutes. Supernatant was then removed and discarded.

4. The pellet was washed in 4:1 ethanol:TE buffer (pH8.0).

5. Tubes were spun and washed again.

6. Tube were then placed into vacuum chamber, the open tops of the tubes being covered with Parafilm and the pellets to dried.

7. Pellets were resuspended in 200µl of TE buffer pH8.0). This process was facilitated by placing tubes at 37°C for upto 4 hours.

To quantify retrieval of oligonucelotides from ammonia stock, samples were 1:100 in dH_20 and absorbance read at A260 nm. An optical density of 0.330 at A260 gave a concentration of 1µg/µl for a 21mer oligonucleotide. Concentrations of longer or shorter oligonucelotides were be calculated similarly. Oligonucleotides were used for PCR at a working concentration of 50pg/µl.

X.II.Isolation of genomic DNA

The trunk of each fetus was dissected into cold, sterile PBS and then placed into an sterile Eppendorf™ tube containing 0.5mls of Proteinase K buffer and 300µg (30µl) of 10mg/ml Proteinase K. Tubes were incubated at 55°C for 8 hours, the tubes being subjected to vortex mixing every 2-3 hours during the incubation period. After digestion, the tubes were heated to 97°C for 3 minutes and then cooled on ice. Tubes were spun at 1,500 rpm for 10 minutes to pellet the cellular debris. 1µl of the supernatant was used directly for PCR from E12.5 fetuses, 1µl of a 1:100 dilution of the supernatant used for E14.5 fetuses.

X.III. Analysis of genomic DNA

DNA samples prepared from the fetal trunk of all four classes of chimaeras ($Sey^{Neu}/Sey \leftrightarrow +/+$, $Sey^{Neu}/+ \leftrightarrow +/+$, $Sey/+ \leftrightarrow +/+$ and $+/+ \leftrightarrow +/+$) were distinguished by PCR analysis of genomic DNA.

PCR Mix:

1µl template DNA suspension (undiluted or 1:100 dilution)
22µl DEPC DH_2O
25µl 2x PCR Buffer
2µl primer mix (1µl each of relevant 5' and 3' primers)
1µl (1.5 units)Taq DNA Polymerase (Boehringer-Mannheim)

Tubes were denatured for 2 minutes at 97°C and then subjected to 30 cycles at:

95°C 0.5 mins
55°C 0.75 mins
72°C 1.0 mins

Extension was assured to completion by a final step of 72°C for 5.0 mins.

In addition to tubes containing test template DNA, a single tube contining the full PCR mix, but ommitting any template, was added to each run. A negative result from this tube, when visualised on an agarose gel, assured that test samples had not been contaminated with exogenous DNA during preparation.

Primers Hax5 GGAGGAAGTGTAGTCCCAGGAGGTA and G15 GCACACCTCCTAGTCCACTTCC or MC130/3

CTTTCTCCAGGGCCTCAATCTG and G459 CGTTGTCCTTCCTCCCCCTCT were used to amplify 220bp or 148bp fragments from within the *Pax-6* gene for identification of the Sey^{Neu} and *Sey* mutations respectively. PCR fragments were visualised by electrophoresis at 100 volts for 20 minutes in a 1.2% (TBE) agarose gel containing 0.75µl 10mg/ml ethidium bromide (Sigma) per 15ml gel volume. 1mg of the size marker $\phi\chi$ was added to each gel for fragment size comparison. After electrophoresis, gels were viewed under UV light and photographed.

In order to veryify the genotype of chimaeras identified as being $Sey^{Neu}/Sey\leftrightarrow+/+$ genotype where mutant sequences were present in low proportion; a second 'nested' PCR reaction was carried out to reduce possible mis-genotyping due to the prescence of low level background sequence amplification. The PCR mix and enzyme concentrations were as before. First round primers for *Sey* and Sey^{Neu} fragments were B509/3 TGCCAGCAACAGGAAGGAGG and F769 GGGCAAAGACATCTGGATAATG, Hax5 GGAGGAAGTGTAGTCCCAGGAGGTA and F772 CATTATCCAGATGTGTTTGCCCC respectively. Samples were subjected to 15 cycles at 95°C, 0.5 mins, 56°C 0.75 mins and 72°C 1.0 mins. 1µl of the resultant "first round" PCR mix was transferred to a new Eppendorf™ tube containing either second round *Sey* primers MC130 CTTTCTCCAGGGCCTCAATCTG and G459 CGTTGTCCTTCCTCCCCCTCT or Sey^{Neu} primers Hax5 GGAGGAAGTGTAGTCCCAGGAGGTA and G15 GCACACCTCCTAGTCCACTTCC. This 'nested' mixture was then subjected to a further 30 cycles at 95°C, 0.5 mins, 55°C 0.75 mins and 72°C 1.0 mins. Nested PCR products were of identical size to original PCR fragments; *Sey* being 148bp and Sey^{Neu} 220bp. Nested fragment sizes were again visulaised on 1.2% agarose/TBE gel before being digested and subjected to polyacrylamide gel electrophoresis and silver staining.

When the proportion of genomic DNA sequence containing either mutation site was very low, (e.g. chimaera JC63 where percentage of genomic DNA containing the *Sey* or Sey^{Neu} sequence was approximately 5%), genotype results were duplicated using the nested PCR procedure. Thus, specificity and sensitivity of the original genotyping procedure was confirmed.

X.IV. Restriction digests of PCR fragments

Identification of the *Sey*^{Neu} mutation:

20µl of PCR product
3µl 10 x HindII buffer (Boehringer-Mannhein)
1µl (3 units/10ml) HindII (Boehringer-Mannheim)
6µl sterile dH_2O

Restriction fragment sizes:
(undigested - 220bp)

wild-type	no digestion
Sey^{Neu}	140bp 80bp

Identification of the *Sey* mutation:

30µl of PCR product
4µl 10 x DdeI buffer (Boehringer-Mannhein)
2µl (10 units/10ml) DdeI (Boehringer-Mannheim)
4µl sterile dH_2O

Restriction fragment sizes:
(undigested - 148bp)

wild-type	83bp 65bp
Sey	46bp 19bp

Samples were loaded into a 15% polyacrylamide gel (19:1 acrylamide: bisacrylamide) (Northumbria Biologicals Ltd.) and subjected to electrophoresis at 280 volts for 2 hours. Fragment sizes were visualised by silver staining. 1µg of $\phi\chi$ 174/HaeIII marker (Boehringer-Mannheim) and pBR322-DNA HaeIII digest (New England Biolabs) marker were also run on each gel for fragment size comparison (see Appendix XI for marker fragment sizes).

Appendix XI

Silver staining of polyacrylamide gels

Reagents used:

Fix	10% ethanol, 0.5% Acetic acid (BDH)
Silver Nitrate	$AgNO_3$ solution, (Sigma)
Sodium hydroxide	NaOH (Sigma)
Sodium borohydrate	$NaBH_4$ (Sigma)
Formaldeyde	40% w/v (BDH)

Samples were loaded into a 0.6mm polyacrylamide gel and subjected to eletrophoresis at 280 volts for 2 hours in 1 x TBE buffer. After electrophoresis, polyacrylamide gels were stained to visualise restriction digest fragments. The staining protocol was as follows:

Step:	**Solution:**	**Time:**	**Preparation:**
Fix:	10% ethanol, 0.5% Acetic acid	2 x 2 mins	100 mls Ethanol 5 mls Acetic acid 795 mls dH_2O
Incubation:	6mM $AgNO_3$	10 mins	0.4g $AgNO_3$ 400 mls dH_2O
Wash:	dH_2O	2 x 1 min	
Stain:	375mM NaOH 3mM $NaBH_4$ 16% formaldehyde	20 mins	7.5g NaOH 0.05g $NaBH_4$ 2mls 40% formalde

After staining, gels were transferred to distilled H_2O and photographed immediately.

Fragment size markers:

pBR322-DNA MspI digest	**$\phi\chi$174 / HaeIII digest**
(New England Biolabs, USA.)	(Boehringer Mannheim)
622	1,353
527	1,078
404	872
307	603
242	310
238	281
217	271
201	234
190	194
180	118
160	72
160	
147	
147	
123	
110	
90	
76	
67	
34	
34	
26	
26	
15	
9	
9	

Appendix XII
Statistics

XII.I.Statistics for Chapter 2.

XII.I.I. Results for Spearman's Rank correlation coefficient test for correlation between % mean fetal GPI1B and hybridisation index score for tissues of the eye and head in all chimaera groups. Significant correlations are noted in **bold** type. N/A - not applicable.

	Mean fetal % GPI1B			
	Sey^{Neu}/+ ↔+/+, +/*Sey* ↔+/+ and +/+↔+/+		*Sey*^{Neu}/*Sey*↔+/+	
Tissue hybridisation index score	**r_s**	**Probability**	**r_s**	**Probability**
Left nasal epithelium	0.918	**0.004**	0.000	1.000
Right nasal epithelium	0.964	**0.004**	0.000	1.000
Left lens	0.891	**0.005**	0.000	1.000
Right lens	0.842	**0.012**	0.000	1.000
Left optic cup inner layer	0.945	**0.003**	N/A	N/A
Right optic cup inner layer	0.927	**0.005**	N/A	N/A
Left optic cup outer layer	0.964	**0.002**	0.615	0.296
Right optic cup outer layer	0.976	**0.003**	0.947	**0.004**
Left total optic cup	0.982	**0.002**	0.700	0.181
Right total optic cup	0.952	**0.004**	0.900	**0.037**
Left optic stalk	0.788	**0.013**	0.900	**0.037**
Right optic stalk	0.600	0.090	0.700	0.188
Surface ectoderm overlying left eye	0.900	**0.004**	0.700	0.188
Surface ectoderm overlying right eye	0.855	**0.010**	0.900	**0.037**
General head ectoderm	0.782	**0.013**	1.000	**<0.01**
Hindbrain	0.964	**0.002**	1.000	**<0.01**
General head mesoderm	0.961	**0.002**	1.000	**<0.01**

XII.I.II. Corrected hybridisation index data for all chimarea genotype groups for all tissues examined using designated scoring systems, as referred to in Chapter 2 and 3 and used for statistical calculations in XIII.I.II. N/A-not applicable, N/K-not known.

XII.I.II.I.

+/+ ↔+/+ chimaeras Tissue hybridisation index	JC45	JC58	JC49	JC22
Left nasal epithelium	18.29	42.94	65.59	53.3
Right nasal epithelium	29.6	45.2	51.5	91.8
Left lens	6.6	54.0	62.6	39.3
Right lens	11.0	68.5	68.7	29.0
Left optic cup inner layer	14.9	64.6	63.7	78.8
Right optic cup inner layer	13.9	79.0	88.7	91.0
Left optic cup outer layer	21.6	56.1	87.7	86.7
Right optic cup outer layer	26.4	58.4	88.1	89.5
Left total optic cup	13.4	46.6	53.5	62.6
Right total optic cup	13.7	54.3	66.9	69.1
Left optic stalk	32.5	64.5	43.6	53.7
Right optic stalk	32.9	58.6	48.1	54.7
Surface ectoderm overlying left eye	7.6	58.6	48.8	95.3
Surface ectoderm overlying right eye	11.1	32.7	88.8	49.7
General head ectoderm	11.0	58.9	74.3	88.7
Hindbrain	29.4	53.5	88.3	84.2
General head mesoderm	30.0	55.3	79.2	80.5
Mean % fetal GPI1B	31.1	61.0	74.5	79.6

XII.I.II.II.

Sey/+ ↔+/+ chimaeras Tissue hybrdisation index	JC53	JC54	JC24	JC21
Left nasal epithelium	19.1	50.1	34.1	74.6
Right nasal epithelium	21.7	42.6	35.6	66.0
Left lens	0.7	29.4	9.5	48.5
Right lens	0.9	27.6	8.6	50.3
Left optic cup inner layer	12.3	54.3	28.5	105.9
Right optic cup inner layer	5.2	54.3	38.6	84.6
Left optic cup outer layer	7.9	54.5	38.4	89.0
Right optic cup outer layer	8.9	45.0	30.7	90.0
Left total optic cup	8.1	41.0	23.4	75.5
Right total optic cup	5.2	38.5	27.0	65.5
Left optic stalk	24.8	64.5	36.6	100.8
Right optic stalk	N/K	68.7	30.5	96.3
Surface ectoderm overlying left eye	1.05	22.3	30.1	69.5
Surface ectoderm overlying right eye	5.7	44.2	14.4	83.0
General head ectoderm	16.0	70.0	46.5	66.0
Hindbrain	14.9	51.6	40.4	91.8
General head mesoderm	16.5	48.0	48.0	93.3
Mean % fetal GPI1B	20.1	51.9	54.0	80.2

XII.I.II.III.

Sey^{Neu}/+ ↔+/+ chimaeras Tissue hybridisation index	JC62	JC93	JC52
Left nasal epithelium	39.4	101.4	90.4
Right nasal epithelium	50.4	N/K	97.6
Left lens	12.6	82.8	78.4
Right lens	24.0	N/K	75.1
Left optic cup inner layer	62.1	105.4	102.1
Right optic cup inner layer	71.4	N/K	90.1
Left optic cup outer layer	60.6	98.7	97.8
Right optic cup outer layer	63.5	N/K	99.1
Left total optic cup	46.7	78.3	78.4
Right total optic cup	52.0	N/K	75.8
Left optic stalk	68.5	95.7	98.5
Right optic stalk	77.4	N/K	101.7
Surface ectoderm overlying left eye	13.5	83.6	85.0
Surface ectoderm overlying right eye	47.6	N/K	77.5
General head ectoderm	71.5	85.9	88.4
Hindbrain	68.6	105.4	101.5
General head mesoderm	65.9	89.5	93.1
Mean % fetal GPI1B	60.1	90.9	96.5

XII.I.II.IV.

Sey^{Neu}/*Sey*↔+/+ chimaeras Tissue hybridisation index	JC63	JC56	JC61	JC48	JC17
Left nasal epithelium	0	0	0	0	0
Right nasal epithelium	0	0.2	0	0	0
Left lens	0	0	0	0	0
Right lens	0	0	0	0	0
Left optic cup inner layer	0.3	0.3	0.0	12.0	N/A
Right optic cup inner layer	0.0	0.0	0.0	N/A	N/A
Left optic cup outer layer	0.0	38.2	0.0	33.3	N/A
Right optic cup outer layer	0.0	0.0	19.3	N/A	N/A
Left total optic cup	0.2	20.4	0.0	23.4	45.5
Right total optic cup	0.2	0.0	7.3	18.1	29.6
Left optic stalk	4.7	55.1	46.7	57.7	70.3
Right optic stalk	2.0	69.8	56.3	57.4	90.7
Surface ectoderm overlying left eye	5.7	28.8	63.7	25.0	76.4
Surface ectoderm overlying right eye	3.4	4.5	33.5	5.7	58.6
General head ectoderm	3.5	32.6	51.6	57.9	73.2
Hindbrain	6.1	34.8	44.8	74.8	94.4
General head mesoderm	32.2	35.7	55.4	69.6	90.6
Mean % fetal GPI1B	11.0	42.8	46.9	59.2	80.2

XII.II. Statistics for Chapter 3

IIX.II.I. Results from 1-D analysis of % pigmented cells and corrected patch sizes for all genotype groups of chimaeras.

Chimaera	% mean fetal GPI1B	Genotype ($\chi \leftrightarrow$ +/+)	Eye	Corrected mean patch lenght in μm (Corrected mean cells per patch)	
				% pigment	Pigmented cells
JC21	80.2	*Sey*/+	L	80.29	13.89 (1.51)
		Sey/+	R	89.14	9.79 (1.06)
JC25	75.8	*Sey*/+	L	89.34	15.49 (1.64)
		Sey/+	R	83.24	12.08 (1.27)
JC53	20.1	*Sey*/+	L	6.17	9.65 (1.03)
		Sey/+	R	11.61	10.11 (1.08)
JC54	51.9	*Sey*/+	L	64.61	13.34 (1.38)
		Sey/+	R	57.77	14.76 (1.55)
JC62	60.1	Sey^{Neu}/+	L	64.8	14.87 (1.54)
		Sey^{Neu}/+	R	65.01	11.96 (1.28)
JC57*	83.1	Sey^{Neu}/+	R	85.09	111.96 (11.66)

Continued overleaf....

XII.I.I.continued: Results from 1-D analysis of single histological section for % pigmented cells and corrected patch sizes for all genotype groups of chimaeras.

Chimaera	% mean fetal GPI1B	Genotype ($\chi \leftrightarrow$ +/+)	Eye	Corrected mean patch lenght in μm (Corrected mean cells per patch)	
				% pigment	Pigmented cells
JC22*	79.6	+/+	R	87.79	8.35 (0.90)
JC24	54.1	+/+	L	35.04	14.48 (1.51)
		+/+	R	18.98	13.02 (1.37)
JC45	31.3	+/+	L	18.02	11.27 (1.22)
		+/+	R	20.92	9.78 (1.05)
JC49	74.5	+/+	L	83.45	17.01 (1.79)
		+/+	R	89.03	14.86 (1.59)
JC58	61.0	+/+	L	66.95	10.31 (1.08)
		+/+	R	54.98	16.78 (1.79)

XII.II.I. Statistical comparison of mean corrected patch size of pigmented cells in the RPE or Tg+ve cells in the optic cups of heterozygous small eye (*Sey/+* and *Sey^{Neu}/+*), compound heterozygous *(Sey/Sey^{Neu})* and wild type (+/+) to wild type chimaeras using the non-parametric, unpaired Man-Whitney U test. x = mean of corrected patch sizes, n = number of chimaeras. Significant *P* values are shown in **bold**.

1) Comparison between corrected patch size of pigmented cells in the RPE:

Genotype sample 1	Genotype sample 2	Probability(*P*)
a) *Sey/+* ↔*+/+* and *Sey^{Neu}/+* ↔*+/+* (x=1.26; n=10)	+/+↔+/+ (x=1.42; n=9)	>0.05

2) Comparison between corrected patch sizes of Tg+ve cells in the optic cup

Genotype sample 1	Genotype sample 2	Probability(*P*)
a) *Sey/+* ↔*+/+* and *Sey^{Neu}/+* ↔*+/+* (x=1.24; n=9)	+/+↔+/+ (x=1.22; n=9)	>0.05
b) *Sey/+* ↔*+/+* and *Sey^{Neu}/+* ↔*+/+* (x=1.24; n=9)	*Sey/Sey^{Neu}* ↔*+/+* (x=6.58; n=5)	**<0.001**
c) +/+↔+/+ (x=1.22; n=9)	*Sey/Sey^{Neu}* ↔*+/+* (x=6.58; n=5)	**<0.01**

Multiple functions for *Pax6* in mouse eye and nasal development

Jane C. Quinn,[1] John D. West,[1] and Robert E. Hill[2,3]

[1]Department of Obstetrics and Gynecology, University of Edinburgh, Centre for Reproductive Biology, Edinburgh, EH3 9EW, UK; [2]MRC Human Genetics Unit, Western General Hospital, Edinburgh EH4 2XU, UK

Mouse embryos, homozygous for the small eye (*Sey*) mutation die soon after birth with severe facial abnormalities that result from the failure of the eyes and nasal cavities to develop. Mutations in the *Pax6* gene are responsible for the *Sey* phenotype. As a general disruption of eye and nasal development occurs in the homozygous *Sey* embryos, it is unclear, from the mutant phenotype alone, which tissues require functional *Pax6*. To examine the roles for *Pax6* in eye and nasal development we produced chimeric mouse embryos composed of wild-type and *Sey* mutant cells. In these embryos we found that mutant cells were excluded from both the lens and nasal epithelium. Both of these tissues were smaller, and in some cases absent, in chimeras with high proportions of mutant cells. The morphology of the optic cup was also severely affected in these chimeras; mutant cells were excluded from the retinal pigmented epithelium and did not intermix with wild-type cells in other regions. The evidence shows that *Pax6* has distinct roles in the nasal epithelium and the principal tissue components of the embryonic eye, acting directly and cell autonomously in the optic cup and lens. We suggest that *Pax6* may promote cell surface changes in the optic cup and control the fate of the ectoderm from which the lens and nasal epithelia are derived.

[*Key Words*: *Pax6*; *Sey*; small eye; mouse; chimera; eye; lens; nose; nasal epithelium]

Received November 1, 1995; accepted in revised version January 18, 1996.

Mutations in the *Pax6* gene result in a range of abnormalities. In man these include the autosomal dominant conditions of aniridia (Ton et al. 1991; Jordan et al. 1992; Hanson et al. 1993) and Peter's anomaly (Hanson et al. 1994), which both affect the anterior chambers of the eye. In both mouse (Hill et al. 1991) and rat (Matsuo et al. 1993), *Pax6* lesions are responsible for the semidominant phenotype small eye (*Sey*). The heterozygous phenotype of *Sey* in mouse shows related manifestations seen in human conditions (Jordan et al. 1992; Hanson et al. 1994) with additional associated micropthalmia. More severe phenotypes are seen in homozygous condition in rats (Matsuo et al. 1993) and mice (Hogan et al. 1986, 1988) and in a compound heterozygous human (Glaser et al. 1994). In mice, homozygous *Sey/Sey* is lethal at birth, leads to disruption of eye development and lack of nasal cavities in the embryo (Hogan et al. 1986, 1988), and lack of olfactory bulbs and abnormal cortical plate formation in the brain (Schmahl et al. 1993).

Pax6 and other members of the *Pax* gene family have the characteristics of being important regulatory elements whose roles are central to normal development (for a recent review, see Stuart et al. 1994). We have exploited the small eye phenotype to define more clearly the developmental roles of *Pax6*, focusing primarily on the overt eye and nasal abnormalities. Eye development proceeds from two principal tissue components: the neural ectoderm, which buds from the forebrain to form the optic vesicle, and the surface ectoderm, which forms the lens. The optic vesicle invaginates, producing the optic cup with an inner layer, which forms the neural retina, and an outer layer, which forms the retinal pigmented epithelium (RPE). The lens placode is a morphological intermediate of lens formation, characterized as an area of thickened columnar epithelium, which comes into contact with the optic vesicle. Continued eye development is dependent on the mutual interaction and invagination of these two tissues (Coulombre 1965; Smelser 1965; Saha et al. 1989; Grainger 1992). In the *Sey/Sey* homozygous mouse and rat the initial contact between the optic vesicle and head ectoderm occurs; however, there is no evidence for the formation of the lens primordium. The optic vesicle subsequently loses contact with the surface and degenerates (Hogan et al. 1986; Fujiwara et al. 1994; Grindley et al. 1995).

Like the lens, the nasal cavities form from the invagination of ectodermal placodes. Hogan et al. (1986) have considered this similarity and suggested that the eye and nasal phenotype of *Sey/Sey* mice may result from defective placode formation. In support of this suggestion, *Pax6* is initially expressed broadly in the head ectoderm and subsequently becomes localized in the placodes of these two tissues (Li et al. 1994; Grindley et al. 1995). However, in the eye, *Pax6* is also expressed in the optic vesicle and later in both the inner and outer layers of the

[3]Corresponding author.

optic cup, and in the distal optic stalk (Walther and Gruss 1991; Grindley et al. 1995). Defects in any of these expressing components of the eye could interfere with essential tissue-tissue interactions and lead to a phenotype resembling that of *Sey/Sey*.

To investigate the relevance of the expression pattern of *Pax6* to the *Sey/Sey* phenotype we have produced fetal mouse aggregation chimeras composed of a mixture of wild-type and small eye mutant cells. Chimeras of four genotype combinations were produced and distinguished retrospectively by PCR analysis. The distribution of mutant *Sey* cells was determined by the inclusion of three genetic markers. These studies have enabled us to investigate the developmental potential of the cells that express *Pax6* before 12.5 days gestation (E12.5) in different tissues of the developing eye and nose. We have also investigated the suggestion that the *Sey* mutation may have similar effects in the lens and nasal epithelium.

Results

Production of chimeras

Production of $Sey/Sey \leftrightarrow +/+$ chimeras is hampered by lethality of the *Sey/Sey* mice. This means that *Sey/Sey* embryos must be produced by $(Sey/+ \times Sey/+)$ matings and distinguished from other genotypes retrospectively. To facilitate identification of different genotypic classes of chimeras, we produced chimeras with compound heterozygous (Sey^{Neu}/Sey) embryos, rather than homozygous (Sey/Sey) embryos (Fig. 1). Both the *Sey* and Sey^{Neu} small eye alleles contain point mutations that result in loss of functional PAX6 protein (Hill et al. 1991) and are distinguishable by a PCR assay (Fig. 2). The same phenotypic abnormalities are seen in homozygous *Sey/Sey*, Sey^{Neu}/Sey^{Neu} (Hill et al. 1991; Schmahl et al. 1993) and Sey^{Neu}/Sey compound heterozygous embryos (J.C. Quinn, unpubl.). To distinguish between different classes of chimeras, we used embryos from crosses between heterozygous $Sey^{Neu}/+$ females and heterozygous $Sey/+$ males, both of which are pigmented (C/C) and homozygous for the glucose phosphate isomerase $Gpi1^b$ allele. The $Sey/+$ males were also homozygous (Tg/Tg) for the reiterated TgN(Hbb-b1)83Clo, β-globin transgene (Lo 1986; Lo et al. 1987; West et al. 1995). Consequently all of the embryos produced by the $Sey^{Neu}/+ \times Sey/+$ cross were $Tg/-$ heterozygotes. These embryos were aggregated to albino BALB/c strain embryos ($Gpi1^a,c/Gpi1^a c$) to produce chimeric fetuses, which were analyzed at E12.5 days (Fig. 1). Four groups of chimeras were distinguished by PCR analysis of *Pax6* DNA: $Sey^{Neu}/Sey \leftrightarrow +/+$, $Sey^{Neu}/+ \leftrightarrow +/+$, $Sey/+ \leftrightarrow +/+$, and $+/+ \leftrightarrow +/+$. The contribution of the $(Sey^{Neu}/+ \times Sey/+)$ embryo was estimated in different tissues to test the developmental potential of Sey^{Neu}/Sey compound heterozygous cells in the $Sey^{Neu}/Sey \leftrightarrow +/+$ fetal chimeras. This estimate was based on a combination of GPI electrophoresis, eye pigmentation, and DNA in situ hybridization to the β-globin transgene.

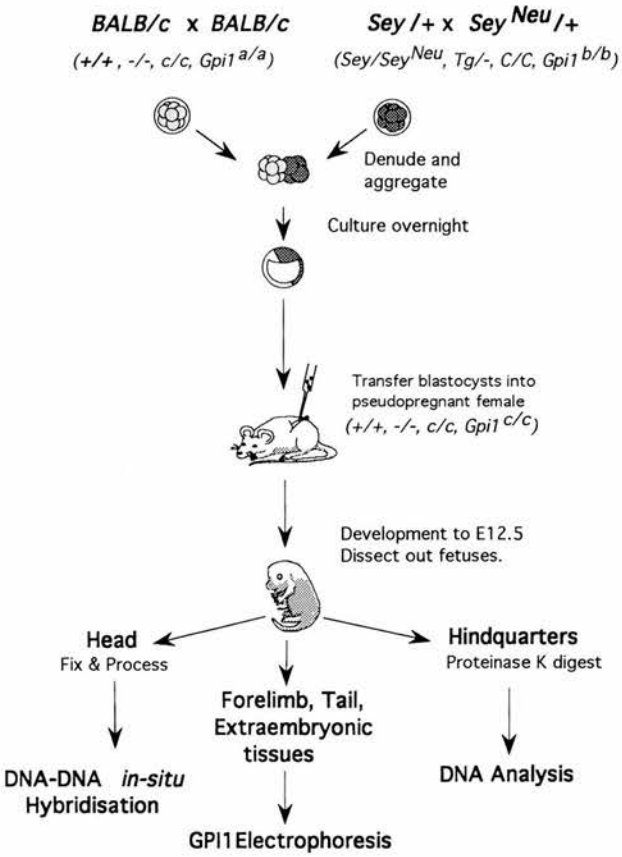

Figure 1. Schematic representation of the experimental design for investigation of the role of *Pax6* in eye and nasal development. Two small eye mutant strains were intercrossed to produce eight-cell stage embryos that were all genetically pigmented (C/C), homozygous $Gpi1^b/Gpi1^b$, hemizygous for the β-globin transgene ($Tg/-$) but differed at the small eye locus (Sey^{Neu}/Sey, $Sey^{Neu}/+$, $Sey/+$ or $+/+$). These were aggregated to inbred BALB/c embryos (albino, c/c, homozygous $Gpi1^a/Gpi1^a$, nontransgenic, $-/-$, and wild-type for small eye, $+/+$) to produce aggregation chimeras. At E12.5, $Sey^{Neu}/Sey \leftrightarrow +/+$ and the three control groups ($Sey^{Neu}/+ \leftrightarrow +/+$, $Sey/+ \leftrightarrow +/+$ and $+/+ \leftrightarrow +/+$) of chimeras were distinguished by DNA analysis. The contribution from the $(Sey/+ \times Sey^{Neu}/+)$ embryo was quantified by DNA in situ hybridization to various tissues in the head and GPI1 electrophoresis of the tail, forelimb, amnion, whole yolk sac, and placenta.

Thirty-seven fetal chimeras were produced (7 $Sey^{Neu}/Sey \leftrightarrow +/+$, 7 $Sey^{Neu}/+ \leftrightarrow +/+$, 7 $Sey/+ \leftrightarrow +/+$, and 16 $+/+ \leftrightarrow +/+$). Although the presence of GPI1A and GPI1B confirmed that these were all chimeric, eye pigment was not observed in any of the $Sey^{Neu}/Sey \leftrightarrow +/+$ chimeras (discussed below). Absence of eye pigment was not attributable to retarded development, as statistical analysis revealed no significant differences, among the four groups, in median developmental stage (Kruskal Wallis test of hindlimb morphology), mean conceptus weight, fetus weight, placental weight or crown–rump length (analysis of variance). The chimeras in the other groups had variegated eyes, as expected.

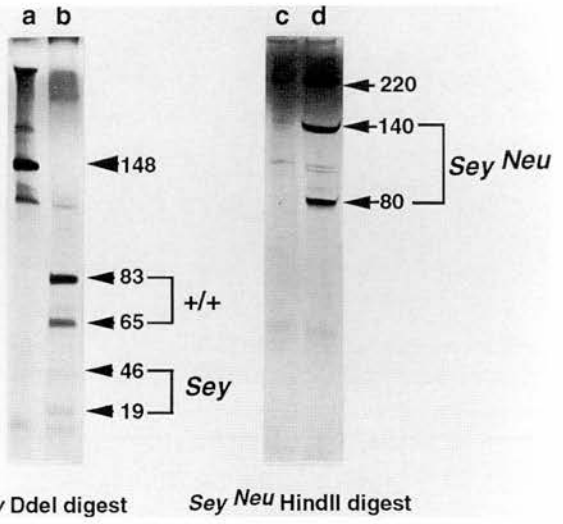

Figure 2. Analysis of genomic DNA from chimeric fetuses allows identification of *Sey* genotypes. Both the *Sey* and Sey^{Neu} alleles have single-base-pair changes within the *Pax6* gene that give rise to novel *Dde*I and *Hin*dII restriction enzyme sites, respectively. Digestion of a 148-bp PCR product with *Dde*I gives fragment sizes of 83 and 65 bp in the wild type with additional 46- and 19-bp fragments in the *Sey* mutant (lane *a* is undigested; lane *b* is digested). After digestion, the Sey^{Neu} mutation gives rise to 140- and 80-bp fragments from a 220-bp PCR product (lane *c* is undigested; lane *d* is digested).

Histological sections revealed several striking morphological abnormalities in $Sey^{Neu}/Sey{\leftrightarrow}+/+$ chimeras but none in the other groups of chimeras. Three (JC17, JC48, and JC50) of the seven $Sey^{Neu}/Sey{\leftrightarrow}+/+$ chimeras had abnormal bulging eyes with overgrown abnormal optic cup tissue but no lenses (Fig. 3). The lenses were absent from both eyes of chimeras JC17 (Fig. 3D) and JC50 and from the right eye of chimaera JC48 (Fig. 3A). In two other chimeras (JC56 and the left eye of JC61) the lenses were present but markedly smaller than normal. This was also the case in the left eye of JC48 (Fig. 3A,C).

Thresholds for proper lens and nasal epithelium development

Initial analysis of the chimeras was based on an estimate of the overall contribution of ($Sey^{Neu}/+ \times Sey/+$) cells to the fetus [mean percent GPI1B (mean %GPI1B) in the tail and forelimb] and histology of the eye and nasal epithelium. GPI analysis showed that the contribution of the Sey^{Neu}/Sey cells to the $Sey^{Neu}/Sey{\leftrightarrow}+/+$ chimeras that lacked lenses was high (80% for JC17, 76% for JC50, and 56% for JC48, missing one lens). The mean %GPI1B for each of the other four $Sey^{Neu}/Sey{\leftrightarrow}+/+$ chimeras was lower (range 11%–46%; Table 1). A similar relationship was seen for the nasal epithelium.

The sizes of lenses and nasal epithelia were estimated in the $Sey^{Neu}/Sey{\leftrightarrow}+/+$ chimeras and found to be inversely correlated with the %GPI1B (Sey^{Neu}/Sey) contribution to the fetus (Fig. 4). This suggests that the sizes of the lenses and nasal epithelia are quantitatively dependent on the proportion of wild-type cells in the $Sey^{Neu}/Sey{\leftrightarrow}+/+$ chimeras. In the 10 chimeras from the other three groups that were analyzed, the sizes of the lenses or nasal epithelia were not affected by the presence of $Sey^{Neu}/+$ or $Sey/+$ cells and showed no relationship with the percent fetal GPI1B. There was no reduction in lens size in $Sey/+{\leftrightarrow}+/+$ or $Sey^{Neu}/+{\leftrightarrow}+/+$ chimeras even though both $Sey/+$ and $Sey^{Neu}/+$ heterozygous adults have small eyes.

In $Sey^{Neu}/Sey{\leftrightarrow}+/+$ chimeras, lens development appeared to be more sensitive than nasal epithelium development, showing a critical threshold at ~50%–70% contribution of Sey^{Neu}/Sey cells (Fig. 4a). Chimeras approaching this threshold formed small lenses, and beyond this threshold lenses were not formed. The threshold is likely to exert its effect in the surface ectoderm or the lens placodes and if the proportion of Sey^{Neu}/Sey cells differs between left and right lens primordia this may result in unilateral effects. Several examples of chimeras with different sized lenses are shown in Table 1. The right lens of JC61 was much larger than the left lens, and JC48 had only a lens in the left eye, as shown in Figure 3A. Presumably the proportion of Sey^{Neu}/Sey cells was just below the critical threshold in the head ectoderm that produced the lens placode in the left eye of JC48 (with a small lens) but was above this level in the right eye (no lens).

The lens and nasal epithelia sizes are both related to the chimeric composition in the $Sey^{Neu}/Sey{\leftrightarrow}+/+$ chimeras, and either tissue may be absent unilaterally (Table 1). The shapes of the curves in Figure 4, a and b, appear to differ, and this suggests that the kinetics of the relationships between composition and tissue size may differ. In Figure 4b there is a nearly linear relationship between the extent of nasal epithelia and the %GPI1B (Sey^{Neu}/Sey) contribution to the fetus, whereas Figure 4a appears more sigmoidal and the size of the lens appears constant until the proportion of mutant cells reaches ~40%. It is clear that a critical percentage of wild-type cells is required to coordinate formation of both these tissues, below which they cannot form. Although there are too few animals to draw firm conclusions, it appears that different thresholds of normal cells are required for the production of the lens and nasal epithelium.

Cellular composition of lens and nasal epithelium

The tissue composition of 16 chimeras (3–5 in each group) was analyzed in more detail by estimations of the percent eye pigment and the percentage of $Tg/-$ cells, by DNA in situ hybridization to the β-globin transgene (Fig. 3). The quantitative results of the analysis of three widely spaced sections of each tissue are shown in Figure 5 and Table 1. For most of the tissues analyzed from the 11 $Sey^{Neu}/+{\leftrightarrow}+/+$, $Sey/+{\leftrightarrow}+/+$ and $+/+{\leftrightarrow}+/+$ chimeras, the hybridization index correlated significantly with the mean percent fetal GPI1B (see Fig. 5 legend for statistical analysis). In $Sey^{Neu}/Sey{\leftrightarrow}+/+$ chimeras, contributions from both parental genotypes in each

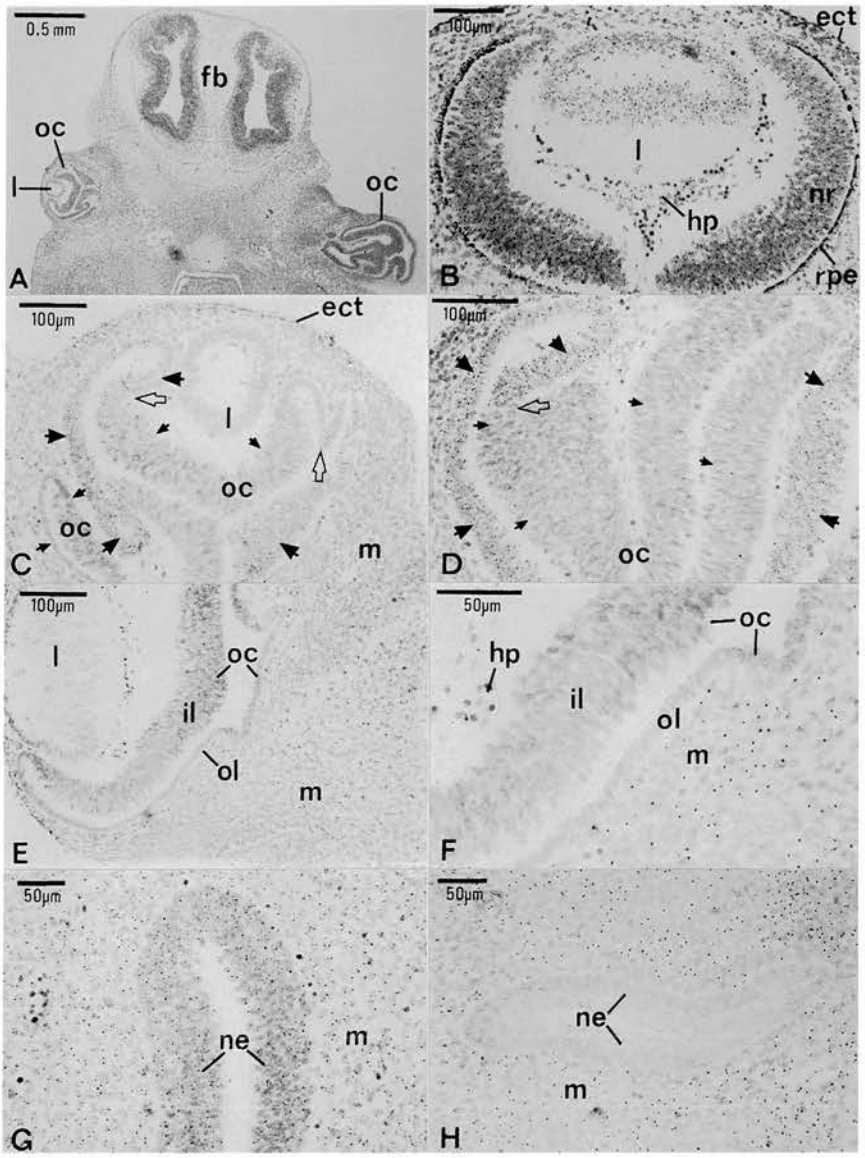

Figure 3. (*A*) Low-power photograph of a transverse histological section of the head of $Sey^{Neu}/Sey{\leftrightarrow}+/+$ chimera JC48, showing both eyes. The right eye has no lens, and the optic cup is overgrown. The left eye has a small lens and is shown in higher magnification in *C*. (*B*) Histological section of the left eye of $+/+{\leftrightarrow}+/+$ chimera JC49, showing a high contribution of $Tg/-$ cells (positive signal seen as dark spots in the nuclei after in situ hybridization) in all tissues and pigmented cells in the retinal pigmented epithelium (outer layer). (*C*) Histological section of the left eye of $Sey^{Neu}/Sey{\leftrightarrow}+/+$ chimera JC48 shown in *A*, showing complete absence of nuclei with in situ hybridization signal (absence of Sey^{Neu}/Sey cells) in the lens and division of the optic cup into large domains of almost entirely wild-type cells (no hybridization signal; small arrows) and almost entirely Sey^{Neu}/Sey cells (with hybridization signal; large arrows), respectively. Two boundaries between the domains of mutant and wild-type cells are indicated with open arrows. (*D*) Histological section of the left eye of $Sey^{Neu}/Sey{\leftrightarrow}+/+$ chimera JC17 with a multilayered optic cup and no lens. The optic cup is divided into large domains of almost entirely wild-type cells (central region with no hybridization signal; small arrows) and almost entirely Sey^{Neu}/Sey cells (with hybridization signal; large arrows), respectively. One boundary between the domains of mutant and wild-type cells is indicated with an open arrow. (*E*) Histological section of the right eye of $Sey^{Neu}/Sey{\leftrightarrow}+/+$ chimera JC61. The lens and optic cup are more normal but both lack mutant cells (no nuclei with hybridization signal). (*F*) Higher magnification of part of the eye shown in *E*. Hybridization signal can been seen in some mesoderm cells and one cell in the hyaloid plexus but not in the inner or outer layers of the optic cup. (*G*) Histological section of the head of $+/+{\leftrightarrow}+/+$ chimera JC49 showing in situ hybridization to some cells in both the left nasal epithelium and surrounding mesoderm. (*H*) Histological section of the head of $Sey^{Neu}/Sey{\leftrightarrow}+/+$ chimera JC61 showing in situ hybridization to some of the mesoderm cells but not to the nasal epithelium cells (absence of Sey^{Neu}/Sey cells). (ect) Ectoderm; (fb) forebrain; (hp) hyaloid plexus; (il) inner layer of optic cup; (l) lens; (m) mesoderm; (ne) nasal epithelium; (nr) neural retina; (oc) optic cup; (ol) outer layer of optic cup; (rpe) retinal pigmented epithelium.

chimera were found in regions unaffected by the *Sey* genotype, including tail, forelimb, head mesoderm, head ectoderm, proximal optic stalk, and hindbrain (Fig. 5) plus amnion, yolk sac, and placenta (not shown). In striking contrast, however, no hybridization signals to $Tg/-$ (Sey^{Neu}/Sey) cells were found in the lenses and nasal epithelia (where present) of the five $Sey^{Neu}/Sey{\leftrightarrow}+/+$ embryos analyzed (Fig. 3C,E,H). Hybridization signals were found, however, in all three control groups, and $+/+{\leftrightarrow}+/+$ tissues are illustrated in Figure 3, B and G. Further analysis of every available section of $Sey^{Neu}/Sey{\leftrightarrow}+/+$ eyes (13–25 sections containing lens tissue) confirmed that mutant cells were completely absent from all of the lenses. Similarly, in the nasal epithelia, only 2–14 scattered cells were found in all available sections of the five $Sey^{Neu}/Sey{\leftrightarrow}+/+$ chimeras (10–32 sections per chimera). This is consistent with the low false-positive frequencies seen in this (data not shown) and other (Everett and West 1996) studies. We conclude that Sey^{Neu}/Sey cells are effectively excluded from the nasal epithelium as well as the lens. This exclusion shows that they cannot be rescued by neighboring wild-type cells and implies that *Pax6* acts cell autonomously within prospective lens and nasal epithelium.

Table 1. *Relationships between chimera composition, eye morphology, and sizes of lens and nasal epithelia in E12.5 fetal* $Sey^{Neu}/Sey\leftrightarrow+/+$ *chimeras*

Chimera	Side	%GPI1B in fetus[a]	*Tg*/− in optic cup[b]			Optic cup dysmorphology[c]	Area in section ($\mu m^2 \times 10^4$)[d]	
			inner layer	outer layer	total		lens	nasal epithelium
JC63	left	11.0	0.3	0	0.2	+	4.5	14.7
JC63	right	11.0	0.3	0	0.2	+	5.7	15.9
JC35	left	27.5	N.D.	N.D.	N.D.	+	5.5	9.8
JC35	right	27.5	N.D.	N.D.	N.D.	+	4.7	13.5
JC56	left	42.8	0.3	38.2	20.5	+ + +	3.9	7.4
JC56	right	42.8	0[e]	0[e]	0[e]	+	5.7	11.0
JC61	left	46.9	0[e]	0[e]	0[e]	+ + +	2.1	1.2
JC61	right	46.9	0[e]	19.3	7.3	+ +	6.1	2.5
JC48	left	59.2	12.0	33.3	23.4	+ + + +	2.6	4.9
JC48	right	59.2	N.A.	N.A.	18.1	+ + + + +	0	2.5
JC50	left	76.8	N.A.	N.A.	N.D.	+ + + + +	0	0
JC50	right	76.8	N.A.	N.A.	N.D.	+ + + + +	0	0
JC17	left	80.3	N.A.	N.A.	45.6	+ + + + +	0	2.5
JC17	right	80.3	N.A.	N.A.	29.6	+ + + + +	0	0

Treating each eye as a separate sample, the mean percent fetal GPI1B correlated positively with the percent *Tg*/− cells in the total optic cup (Spearman's rank correlation coefficient, $r_s = 0.731$; $P = 0.028$), and the size of the lens correlated positively with the size of the nasal epithelium ($r_s = 0.736$; $P = 0.008$). The degree of morphological abnormality of the optic cup correlated negatively with lens size ($r_s = -0.899$; $P = 0.001$) and positively with percent *Tg*/− cells in the whole optic cup ($r_s = 0.781$; $P = 0.019$) and percent fetal GPI1B ($r_s = 0.933$; $P = 0.001$). Lens size also correlated inversely with percent fetal GPI1B ($r_s = -0.789$; $P = 0.004$) but not with the percent *Tg*/− cells in the whole optic cup ($r_s = -0.588$; $P = 0.078$).

[a]%GPI1B is the mean %GPI1B in the tail and one forelimb.

[b]*Tg*/− in optic cup is the hybridization index in three widely spaced sections. Separate values are shown for the inner and outer layers of the optic cup where these layers can be clearly distinguished; otherwise the total value is shown (as plotted in Fig. 5). None of the *Tg*/− cells in the outer layer were pigmented and so they were not normal RPE cells. (N.D.) Not determined; (N.A.) not applicable.

[c]Optic cup dysmorphology is shown on a subjective 5-point scale: (+) Normal morphology with double-cup comprising an outer layer of RPE and inner neural retina; (+ +) slightly abnormal; (+ + +) abnormal tissue present but double-cup shaped morphology largely retained; (+ + + +) abnormal with distortion of the double-cup shape; (+ + + + +) grossly dysmorphic and multilayered.

[d]Area was estimated with a Chalkley grid as described in Materials and methods.

[e]Although no hybridization signal was seen in the three histological sections examined for the quantitative analysis, qualitative analysis of all of the available sections revealed a few *Tg*/− *cells.*

Cellular composition of the optic cup

Development of the optic cup was also abnormal in the $Sey^{Neu}/Sey\leftrightarrow+/+$ chimeras but not in any of the other groups of chimeras. At the stage of development examined (E12.5) the optic cup is normally composed of an outer unicellular layer of RPE and a closely opposed thicker inner layer of prospective neural retina (Fig. 3B). The state of the optic cup in the $Sey^{Neu}/Sey\leftrightarrow+/+$ chimeras was highly variable. Some of the gross abnormalities made it difficult to assign cells to normal tissues; therefore, in Figure 5 the optic cup is considered as a whole. The extent of the morphological abnormalities was apparently influenced by the size of the lens and the proportion of the Sey^{Neu}/Sey cells in the chimera, two parameters that are interdependent and negatively correlated (Fig. 4; Table 1). Two distinctive classes of embryonic eyes arose in the $Sey^{Neu}/Sey\leftrightarrow+/+$ chimeras. One class includes the optic cups that are associated with lenses, all having the characteristic double layer cup shape. Morphologically, these range from optic cups that appear normal (JC63, JC35, and JC56 right eye; Table 1) to dysmorphic cups that are distorted with ectopic tissue overgrowth (JC56 left eye, JC61 and JC48 left eye; Table 1; Fig. 3C,E). The second class of optic cup structures have no associated lenses and are highly disorganized and overgrown (JC48 right eye, JC50 and JC17; Table 1; Fig. 3A,D).

Figure 5 shows that in $Sey^{Neu}/Sey\leftrightarrow+/+$ chimeras, the proportion of mutant cells was lower in the optic cup than in other unaffected tissues. Although the contribution was lower in the whole optic cups (mean hybridization index = 14.5) than the fetal limb and tail (mean %GPI1B = 48.0), the significance of this is uncertain because there was also a difference in the other groups of chimeras (47.4% vs. 62.3%). The inner and outer layers of the optic cup were considered separately for seven $Sey^{Neu}/Sey\leftrightarrow+/+$ eyes in Table 1. The inner layer had a lower proportion of mutant cells, which made up <1% except for the JC48 left eye (12%). Here, the mutant cells were specifically at the tip of the optic cup in a morphologically abnormal region (Fig. 3C). In the outer layer, the Sey^{Neu}/Sey cells contributed more significantly to three of the seven eyes (19%–38% in JC61 right, JC48 left, and JC56 left; Table 1) but were not incorporated into the thin monolayer of the RPE (Fig. 3E,F). The mutant cells were usually associated with regions of the outer layer that are either abnormally thickened or situated ectopi-

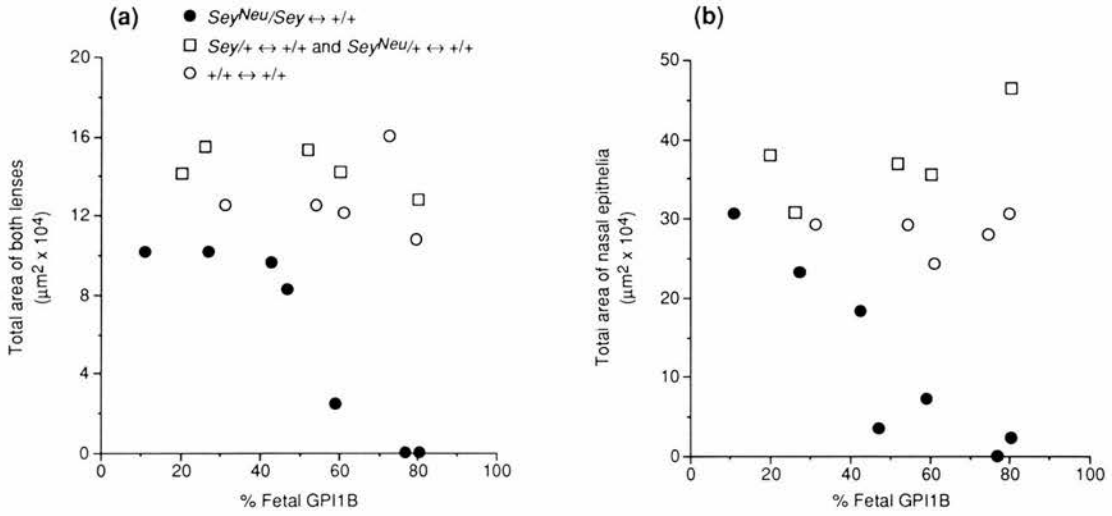

Figure 4. Relationship between the percent fetal GPI1B and the estimated sizes of both lenses (*a*) and both nasal epithelia (*b*) for different groups of chimeras. (*a*) The total size of both lenses showed a statistically significant negative correlation with the %GPI1B in $Sey^{Neu}/Sey \leftrightarrow +/+$ chimeras ($r_s = -0.982$; $P = 0.016$) but not in the other groups of chimeras analyzed ($r_s = -0.564$; $P = 0.259$ for $Sey^{Neu}/+ \leftrightarrow +/+$ plus $Sey/+ \leftrightarrow +/+$ and $r_s = -0.359$; $P = 0.473$ for $+/+ \leftrightarrow +/+$). Similarly, the total size of the nasal epithelia was also negatively correlated with the %GPI1B in $Sey^{Neu}/Sey \leftrightarrow +/+$ chimeras ($r_s = -0.929$; $P = 0.023$) but not in the other groups ($r_s = 0.300$; $P = 0.549$ for $Sey^{Neu}/+ \leftrightarrow +/+$ plus $Sey/+ \leftrightarrow +/+$ and $r_s = 0.154$; $P = 0.758$ for $+/+ \leftrightarrow +/+$). The estimated sizes of the lenses and nasal epithelia were positively correlated, both when left and right sides were pooled ($r_s = 0.946$; $P = 0.021$) or when they were considered separately (Table 1).

cally. These regions were not composed exclusively of mutant cells but contained significant proportions of wild-type cells, which occurred as segregated patches and were not intermingled with the mutant cells. The optic cups that appeared normal showed little or no Sey^{Neu}/Sey contribution to either layer (Table 1; Fig. 3D). Furthermore, the inability of the Sey^{Neu}/Sey cells (the pigmented component of the chimeras) to successfully contribute to the RPE is supported by the observation that none of the eyes of the $Sey^{Neu}/Sey \leftrightarrow +/+$ chimeras showed any detectable pigmentation.

Mutant Sey^{Neu}/Sey cells made a significant contribution to the morphologically abnormal optic cups of the second class of eyes (with no lenses) as well as the morphologically abnormal regions of optic cups in the eyes with lenses. In both cases, the mutant cells were nonrandomly distributed and not finely mixed with wild-type cells. There was a striking partitioning of the two cell types (Fig. 3D), which was not seen in the control chimeras. In the wild-type domains there were few mutant ($Tg/-$) cells and no detectable wild-type cells in the mutant domains. (Because not all mutant $Tg/-$ cells show a hybridization signal, it is not known whether wild-type cells were completely absent from mutant domains or present at a low level). Segregation of cell types is unusual in mouse chimeras and implies that the interactions between Sey^{Neu}/Sey and $+/+$ cells are abnormal so that they either fail to mix and intermingle or actively sort themselves out into homogeneous patches. This suggests that *Pax6* expression defines early cellular properties (possibly affecting the cell surface) within the optic vesicle. The evidence that Sey^{Neu}/Sey cells are excluded from the RPE and at a selective disadvantage in other regions of the optic cup, as well as being distributed nonrandomly, implies that *Pax6* has a direct, cell-autonomous effect not only in the lens and nasal epithelium (see above) but also in the optic cup.

Discussion

The eye is a complex organ that develops from the interaction of two embryologically distinct ectodermal layers: the head surface ectoderm and the neural ectoderm. Analysis of *Sey/Sey* homozygous and phenotypically equivalent, Sey/Sey^{Neu} compound heterozygous mutant mice shows that the development of the embryonic eye is disrupted but provides only a few clues as to the mechanism. Thus, a clear understanding of the role of the gene responsible, *Pax6*, is difficult to surmise. To investigate the developmental potential of the Sey/Sey^{Neu} compound heterozygous mutant cells, we produced mouse chimeras by aggregating mutant (Sey/Sey^{Neu}) and wild-type eight-cell stage embryos. The resulting $Sey/Sey^{Neu} \leftrightarrow +/+$ chimeric embryos provided an environment in which wild-type and Sey/Sey^{Neu} mutant cells could mix and interact. Each mutant cell carried a reiterated transgene to distinguish between mutant and wild-type cells. This provided a means of testing whether Sey/Sey^{Neu} cells were rescued by surrounding wild-type cells in the affected tissues and, if so, whether the two types of cells mixed normally. Specifically, the failure of wild-type cells to rescue mutant cells in a tissue implies that *Pax6* gene expression is required in that tissue and acts cell autonomously. Although a system-

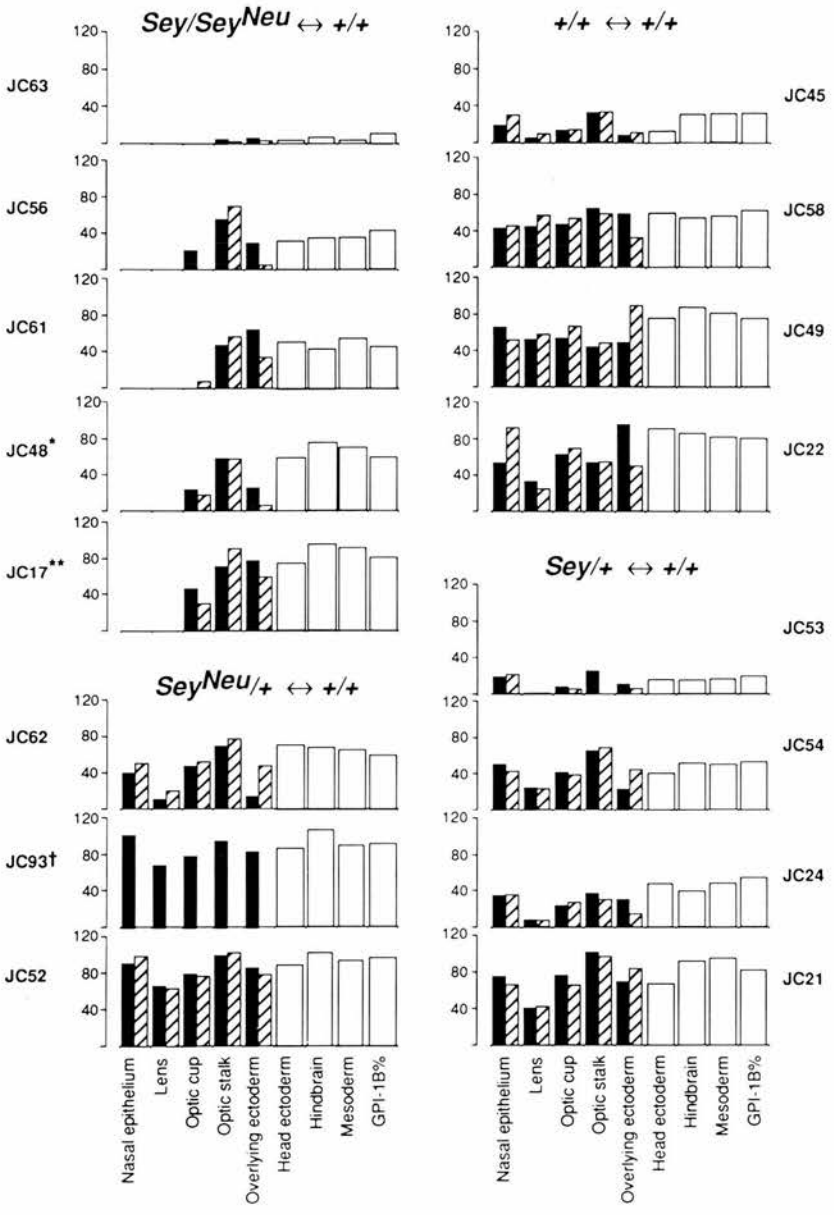

Figure 5. Histograms showing the contribution of ($Sey^{Neu}/+ \times Sey/+$) cells to different tissues of 16 chimeric fetuses of four different genotypes. The contribution to the fetal trunk is given as the mean %GPI1B (calculated from separate estimates of %GPI1B in the tail and one forelimb). The contributions to normal RPE (where present) was estimated as the percent pigmented RPE cells. The contributions to other tissues were estimated by the corrected hybridization index (see Materials and methods) from three widely separated histological sections. (Solid bar) left; (hatched bar) right; (open bar) unpaired tissues. For eye tissues, these were the midsection of the eye and the two sections that were halfway between the midsection and the first or last section, respectively. Results for the neural retinal and RPE are presented together as the optic cup because these tissues were morphologically abnormal in some $Sey^{Neu}/Sey \leftrightarrow +/+$ chimeras. For the 11 control, $Sey^{Neu}/+ \leftrightarrow +/+$, $Sey/+ \leftrightarrow +/+$ and $+/+ \leftrightarrow +/+$ chimeras, the mean %GPI1B correlated well (Spearman's rank correlation coefficient, r_s) with the hybridization index for all of the tissues analysed apart from the right optic stalk: left nasal epithelium ($r_s = 0.918$; $P = 0.004$); right nasal epithelium ($r_s = 0.964$; $P = 0.004$); left lens ($r_s = 0.891$; $P = 0.005$); right lens ($r_s = 0.842$; $P = 0.012$); left neural retina ($r_s = 0.945$; $P = 0.003$); right neural retina ($r_s = 0.927$; $P = 0.005$); left RPE ($r_s = 0.964$; $P = 0.002$); right RPE ($r_s = 0.976$; $P = 0.003$); left total optic cup ($r_s = 0.982$; $P = 0.002$); right total optic cup ($r_s = 0.952$; $P = 0.004$); left optic stalk ($r_s = 0.788$; $P = 0.013$); right optic stalk ($r_s = 0.600$; $P = 0.090$); ectoderm overlying left eye ($r_s = 0.900$; $P = 0.004$); ectoderm overlying right eye ($r_s = 0.855$; $P = 0.010$); head ectoderm ($r_s = 0.782$; $P = 0.013$); hindbrain ($r_s = 0.964$; $P = 0.002$); and mesoderm ($r_s = 0.961$; $P = 0.002$). (*) Chimera JC48 had no lens in its left eye; (**) chimera JC17 had no lens in either eye; †tissues from the left side of the head were not analyzed from chimera JC93.

atic analysis of cell mixing was not undertaken, the distribution of the transgenic and nontransgenic cells, in various embryonic tissues unaffected by the *Sey* mutation, was apparently similar in the $Sey/Sey^{Neu} \leftrightarrow +/+$ and control chimeras. In contrast, the developing eyes and nasal epithelium showed abnormal participation of the Sey/Sey^{Neu} cells and highlighted similarities in the developmental requirements of the lens and nasal epithelium.

Role of Pax6 *in lens and nasal epithelium formation*

In the $Sey/Sey^{Neu} \leftrightarrow +/+$ chimeras, Sey/Sey^{Neu} cells were not detected in the lens or nasal epithelium at E12.5. The inability to participate in the development of these epithelial tissues, populated by $+/+$ cells, shows that the Sey/Sey^{Neu} cells are incapable of rescue and that *Pax6* activity is direct and cell autonomous. Thus, *Pax6* has a cell-autonomous role at a stage of lens and nasal epithelia formation preceding E12.5. The lens and nasal epithelium are derived from the head ectoderm. Figure 5 shows that the proportion of Sey/Sey^{Neu} cells in other regions of the head ectoderm was similar to that in the fetal trunk (%GPI1B) and other tissues, in which *Pax6* has no apparent influence. This proportion is probably representative of the chimera as a whole. Thus, initially, the regions of head ectoderm that form the lens and nasal placodes are likely to have been composed of a similar mixture of mutant and wild-type cells. Mutant cells would subsequently be lost from the lens and nasal lineages at the stage of earliest *Pax6* function. Previous

analysis of *Sey/Sey* homozygous mice showed not only that lens and nasal cavities fail to form but that at E9.5 there is no evidence for thickening of the surface ectoderm indicative of lens and nasal placode formation (Hogan et al. 1986; Grindley et al. 1995). Placode formation is the earliest morphological indicator of lens and nasal differentiation. It was suggested (Grindley et al. 1995) that in *Sey/Sey* homozygous mice the normal transition from head ectoderm to placode formation is interrupted. The observations in the $Sey/Sey^{Neu} \leftrightarrow +/+$ chimeras argue that *Pax6* has a direct role in this early developmental decision such that head ectodermal cells, deficient in *Pax6*, are unable to proceed to the initial stages of epithelial morphogenesis. Thus, *Pax6* is a necessary component of the system that specifies the pattern of the head. However, because the fates of lens and nasal epithelial cells are ultimately different, additional, perhaps exogenous, signals (Jacobson and Slater 1988) are necessary to specify the identity of these cells as either lens or nasal epithelium.

In the $Sey/Sey^{Neu} \leftrightarrow +/+$ chimeras, there were inverse relationships between the %GPI1B (overall percentage of the Sey/Sey^{Neu} mutant cells) and the amount of both lens and nasal epithelia. In addition, the production of both of these structures is dependent on a threshold of normal cells, below which no epithelium is detectable at the embryonic stage examined (E12.5). These observations lead to two predictions. First, we predict that the size of the lens and nasal tissues is solely dependent on the number of cells that are competent to form these tissues; that is, the wild-type cells. We cannot rule out the possibilities that Sey/Sey^{Neu} cells are active inhibitors of lens development or that the level of a concentration-dependent exogenous signal (from outside the lens) is reduced in $Sey/Sey^{Neu} \leftrightarrow +/+$ chimeras. However, our results, combined with failure of nasal and lens placode formation in nonchimeric, homozygous *Sey/Sey* mutants suggest that the size of these epithelia-derived structures is determined by the number of wild-type cells that constitute the placodal domains. Thus, in the chimeras, the primordia forming these specialized epithelia are smaller than normal and there is no subsequent compensatory growth mechanism.

Second, we predict that the there is a critical proportion of wild-type cells in the lens and nasal primordia needed to initiate the development of these structures. This is reminiscent of an experimental phenomenon referred to as the community effect (Gurdon et al. 1993). Briefly, this suggests that in development, cells communicate with like neighbors and that a critical number of interacting cells is required to proceed to the next stage in development. Thus, in the $Sey/Sey^{Neu} \leftrightarrow +/+$ chimeras, the presence of a high percentage of Sey/Sey^{Neu} cells interrupts the sparse population of wild-type cells and the critical number of interacting wild-type cells is not reached. However, the possibility also exists that lens or nasal epithelium development begins in these tissues as a mixture of mutant and wild-type cells but subsequently degenerates because of the burden of the abnormal Sey/Sey^{Neu} cells.

Role of Pax6 *in optic cup development*

Optic vesicle-derived tissue developed in all $Sey/Sey^{Neu} \leftrightarrow +/+$ chimeras examined, and no simple correlation was observed between size and %GPI1B. In contrast, the %GPI1B correlated with the degree of tissue abnormality in the optic cup. This we attribute, at least in part, to abnormally small or absent lenses. Lens tissue is important as a regulator of retinal growth and in the maintenance of retinal development (Saha et al. 1992). In either the absence of the lens resulting from lens ablation (Breitman et al. 1987; Kaur et al. 1989; Harrington et al. 1991) or the presence of an abnormally small lens as in the mutant aphakia (Zwaan and Webster 1985; R.E. Hill, unpubl.) convoluted overgrowth of retinal tissue occurs. However, neither of these situations show the degree of abnormality demonstrated in the $Sey/Sey^{Neu} \leftrightarrow +/+$ chimeric eyes that lack a lens. It is not clear whether the Sey/Sey^{Neu} cells in the optic cup increase the degree of abnormality in this tissue.

In the $Sey/Sey^{Neu} \leftrightarrow +/+$ chimeras the wild-type and Sey/Sey^{Neu} cells did not mix freely, resulting in large partitions consisting predominantly, if not exclusively, of either wild-type or mutant cells. Sharp boundaries with no detectable intermingling occurred between the cell types. In the lensless eyes the ocular tissue was highly convoluted and normal inner and outer layers were not identifiable. In these eyes the partitioning of the two cell types suggests a mechanism, operating at an earlier developmental stage, which sorts the cells into large patches of like cells. This failure of cell types to mix illustrates that differences exist between the wild-type and Sey/Sey^{Neu} cells consistent with differences in cellular properties that define identity. It is likely that these differences lie at the cell surface.

It has been suggested that homeo domain-containing proteins control the expression of genes encoding extracellular matrix proteins and cell adhesion molecules (Edelman and Jones 1992; Jones et al. 1993; Goomer et al. 1994; Holst et al. 1994). Furthermore, *Pax6* and other members of the *Pax* gene family are known to interact with the promoters of cell surface molecules and, in particular, those that belong to the immunoglobulin superfamily. For example, the evidence is strong that *Pax5* regulates the B-lymphocyte receptor CD19 (Kozmik et al. 1992), and *Pax6* interacts with the neural cell adhesion molecule L1 promoter region in in vitro DNA-binding assays (Chalepakis et al. 1994). Thus, *Pax6* deficiency may influence the expression of adhesion molecules or other cell surface molecules to effect the cell sorting.

In the eyes of $Sey/Sey^{Neu} \leftrightarrow +/+$ chimeras, the optic cup appears more normal in the presence of a lens than in those where the lens is absent. In addition, there appears to be a relationship between the size of the lens (and therefore the overall contribution of Sey/Sey^{Neu} cells; %GPI1B) and the degree of tissue abnormalities. In the eyes with lenses the mutant cells were excluded more rigorously from the inner layer of the optic cup than from the outer layer. In all but one case (Fig. 3C), no appreciable patches of Sey/Sey^{Neu} cells were detected in

the inner layer. Most *Sey/Sey*^{Neu} cells in these optic cups were in the outer layers, either in abnormally thickened or ectopic tissue. In no cases examined were these cells found in the single cell layer of RPE. In the embryos with low %GPI1B and larger lenses, the degree of tissue abnormalities was reduced, coincident with more extreme reduction of mutant cells in the optic cup. We suggest that the presence of a lens provides an environment in which the developmental conditions for the optic cup are more stringent. Therefore, the optic cup develops more normally and the mutant cells make only a very low overall contribution. The evidence that *Sey/Sey*^{Neu} cells were excluded from the RPE and apparently at a selective disadvantage in other regions of the optic cup, as well as being distributed nonrandomly, implies that *Pax6* has a direct, cell-autonomous effect on the optic cup as well as the lens and nasal epithelium.

These chimeras provide evidence that *Pax6* has a role in all the primary tissues of the eye, including the inner and outer layers of the optic cup. *Pax6* exerts an effect prior to E12.5 at a time when overt differentiation is still undetectable in the inner layer. Because the fates of cells in the inner and outer layers differ and the optic cup is of different embryological origin than the lens and nasal epithelium, we suggest that *Pax6* has multiple roles in eye and nasal development.

Evolution of the role of Pax6

Pax6 is highly conserved in evolution, and homologs have been found in *Drosophila* and *Caenorhabditis elegans*. Quite surprisingly, *Drosophila Pax6* is also involved in eye development being responsible for the *eyeless* phenotype (Quiring et al. 1994; Halder et al. 1995). The similarity of the phenotype led to the suggestion that *Pax6* may have a homologous role in the development of these highly divergent eye structures separated by extreme evolutionary distances. In *C. elegans Pax6* has a role in patterning the head region (Chisholm and Horvitz 1995; Zhang and Emmons 1995). Thus, in vertebrates the roles of *Pax6* in head ectoderm and in the eye may have descended from very ancient conserved functions.

A problem with generalization of conserved function based on phenotype alone is the possible fortuity of the observations (Hill and Davidson 1994). *Pax6* is expressed in multiple domains of the head and brain in both mouse and *Drosophila*. Thus, a role for *Pax6* may incidentally overlap in the eye. In addition, eye structure and development differ dramatically between the two species. Thus, similar phenotypic characteristics observed in *Pax6* mutants in the two species may well be attributable to unrelated developmental defects. However, analysis of the *Sey/Sey*$^{Neu}\leftrightarrow+/+$ chimeric mice provides evidence that *Pax6* has an early role in neural retina development, prior to the appearance of differentiating retinal cells. In comparison, the *Drosophila eyeless* mutant shows that *Pax6* also functions in retinal development and development is defective in the mutant at a stage prior to differentiation (Quiring et al. 1994). This provides further evidence that the *Pax6* homologs have equivalent functions in development, strengthening the argument for conserved developmental roles.

Materials and methods

Mice

Inbred BALB/c/Eumm mice were purchased from the Department of Medical Microbiology, University of Edinburgh. The founder stock of *Sey*^{Neu}/+ mice was kindly supplied by Dr. Jack Favor, Institüt für Genetik, Neuherberg, Germany. *Sey*^{Neu} arose on a (C3H×102)F_1 genetic background and was crossed to a CBA/Ca genetic background. The *Sey* allele (Roberts 1967) was maintained on a partially congenic CBA/Ca-Sey/+ stock. Other stocks were produced and maintained in the Centre for Reproductive Biology (Edinburgh). Transgenic strain 83 (Lo 1986) carries the reiterated β-globin, TgN(Hbb-b1)83Clo transgene (abbreviated to *Tg*) and was used to derive the randombred, homozygous *Tg/Tg* stock TGB on a largely (C57BL/Ola×CBA/Ca) genetic background (Keighren and West 1994; West et al. 1995). A *Sey*/+ stock (SEYTG), which was homozygous for the transgene (*Tg/Tg*), was produced by intercrossing CBA/Ca-*Sey*/+ and TGB and backcrossing *Sey*/+ individuals to TGB; *Sey*/+, *Tg/Tg* mice were used in the experiment after two to four backcross generations. The albino, *Gpi1*^{c}/*Gpi1*^{c}, CF_1 hybrid stock was produced from crosses between C57BL–*Gpi1*^{c}, *c*/Ws females and BALB/c–*Gpi1*^{c}/Ws males (West and Flockhart 1994).

Production and dissection of chimeras

Eight-cell embryos were obtained from two crosses. CBA/Ca-*Sey*^{Neu}/+ females were mated to SEYTG (*Sey*/+, *Tg/Tg*) males to produce a mixture of *Sey*^{Neu}/*Sey*, *Sey*^{Neu}/+, +/*Sey*, and +/+ embryos, all of which were *Gpi1*^{b},*C*/*Gpi1*^{b}, *C* −/*Tg*. Inbred BALB/c mice were intercrossed to produce wild-type, albino embryos (*Gpi1*^{a},*c*/*Gpi1*^{a},*c*) without the transgene. Chimeras were made by aggregating embryos from the two crosses and the four groups of chimeras (*Sey*^{Neu}/*Sey*↔+/+, *Sey*^{Neu}/+↔+/+, *Sey*/+↔+/+, and +/+↔+/+) were distinguished retrospectively by PCR analysis as described below.

BALB/c and CBA/Ca–*Sey*^{Neu}/+ females were induced to ovulate by intraperitoneal (i.p) injection of 5 IU of pregnant mares' serum gonadotrophin (PMSG) at ~12 noon, followed 48 hr later by i.p. injection of 5 IU of human chorionic gonadotrophin (hCG). Females were caged overnight with males of the appropriate stock, and mating was confirmed the following morning by the presence of a vaginal copulation plug; the day of the vaginal plug was designated 0.5 day postcoitum (d.p.c.). On the same day as vaginal plugs were identified, CF_1 females in estrus were paired overnight with vasectomized CF_1 males and mating was verified the following morning by the presence of a vaginal plug. These provided homozygous, *Gpi1*^{c}/*Gpi1*^{c} pseudopregnant females for embryo recipients.

Embryos were flushed from the CBA/Ca–*Sey*^{Neu}/+ and BALB/c females at 2.5 d.p.c. with HEPES-buffered M2 handling medium (Quinn et al. 1982). Aggregations were carried out according to methods used by West and Flockhart (1994). After overnight culture, the aggregated embryos were surgically transferred to the uteri of pseudopregnant CF_1 females. Pregnancies were timed according to the pseudopregnant female, with the plug day being 0.5 d.p.c; the recipient female was sacrificed at 12.5 d.p.c (E12.5). This age was chosen because normal RPE pigmentation is well established and provides a marker for the chimera analysis (see below).

Fetuses were dissected into cold PBS. The weight of the total conceptus, fetus, and placenta were recorded along with the crown–rump length and morphological index based on hindlimb development (McLaren and Buehr 1990; Palmer and Burgoyne 1991). Different samples of the conceptus were analyzed by GPI electrophoresis, PCR, and in situ hybridization to the reiterated transgene (Fig. 1). Tissue samples dissected for GPI1 electrophoresis into H_2O/glycerol 50:50 from the tail, forelimb, amnion, whole yolk sac, and placenta. Methods used for GPI1 electrophoresis as described in West and Flockhart (1994). The trunk was digested for 24 hr at 55°C in 0.5 ml of proteinase K buffer (5 mM Tris, 25 mM KCl, 25 mM $MgCl_2$ at pH 7.8, 0.45% NP-40, 0.45% Tween, 0.1 mg/ml of gelatin) plus 300 μg of proteinase K. The head of each fetus was fixed in ethanol/acetic acid [3:1 (vol/vol)] and then processed to wax for analysis by DNA–DNA in situ hybridization.

Analysis of genomic DNA

The four groups of chimeras ($Sey^{Neu}/Sey \leftrightarrow +/+$, $Sey^{Neu}/+ \leftrightarrow +/+$, $Sey/+ \leftrightarrow +/+$, and $+/+ \leftrightarrow +/+$) were distinguished by PCR analysis of *Pax6* genes in samples of fetal trunk DNA. After digestion in proteinase K buffer (see above), the resulting suspension was denatured at 95°C for 5 min. One microliter was then added to a PCR mixture containing 50 mM KCl, 10 mM Tris-HCl (pH 8.3), 1.5 mM $MgCl_2$, 0.1% Triton X-100, 0.1 mM of each dNTP, and 1.5 units of *Taq* DNA polymerase (Boehringer Mannheim) per 50-μl volume. Primers *Hax-5* (ATGGAACCTGATGTGAAGGAGG) and *G15* (GCAACACTCCTAGTCACATTCC) or *MC130* (CTTTCTCCAGGGCCTCAATCTG) and *G459* (GCAACAGGAAGGAGGGGGAGA) were used to amplify 220- and 148-bp fragments, respectively, from within the *Pax6* gene for identification of the Sey^{Neu} and *Sey* mutations. For the analysis of the Sey^{Neu} mutation, 20 μl of PCR product was digested with 9 units of *Hin*dII, and for the *Sey* mutation 30 μl of PCR product was digested with 30 units of *Dde*I (as per manufacturer's instructions; Boehringer Mannheim). Samples were loaded onto a 15% polyacrylamide gel (19:1, acrylamide/bis-acrylamide) and subjected to electrophoresis in TBE buffer at 280 V for 2 hr. Restriction fragments were fixed in the gel by washing twice in 10% ethanol, 0.5% acetic acid, before incubation for 10 min in 6 mM $AgNO_3$. Gels were washed twice in distilled water and then stained for 20 min in 375 mM NaOH, 3 mM $NaBH_4$ and 0.16% formaldehyde to visualize fragments (C.M. Abbott, unpub.). After transfer to distilled water, the gels were photographed.

To verify the genotype of chimeras where mutant sequences were present in low proportion, a second "nested" PCR reaction was carried out to reduce possible low-level nonspecific sequence amplification. The PCR mixture and enzyme concentrations were as before. First round primers for *Sey* fragments were *B509/3* (TGCCAGCAACAGGAAGGAGG) and *F769* (GGGCAAAGACATCTGGATAATG), and for Sey^{Neu} were *Hax-5* (see above) and *F772* (CATTATCCAGATGTGTTTGCCC). These were subjected to 15 cycles at 95°C for 0.5 min, 56°C for 0.75 min, and 72°C for 1.0 min. One microliter of the resultant PCR mixure was transferred to a new tube containing either second-round *Sey* primers *MC130* and *G459* or Sey^{Neu} primers *Hax-5* and *G15*. This mixture was then subjected to a further 30 cycles at 95°C, for 0.5 min, 55°C for 0.75 min, and 72°C for 1.0 min. Nested PCR products were of identical size to original PCR assay, with *Sey* being 148 bp and Sey^{Neu} being 220 bp. Fragments were digested and subjected to polyacrylamide gel electrophoresis and silver staining as described above. Original genotype results for chimeras where the proportion of mutant sequence was very low (e.g., chimera JC63 where ~5% of genomic DNA contained the *Sey* or Sey^{Neu} sequence) were duplicated using the nested PCR procedure and thus specificity and sensitivity of the original genotyping procedure confirmed.

DNA–DNA In Situ Hybridization

Sections were cut at 7 μm and mounted on slides coated with 3-aminopropyltriethoxysilane (Sigma) and analyzed by in situ hybridization to the transgene as described by Keighren and West (1993). Hybridized digoxygenin-labeled DNA probe was detected by diaminobenzidine (DAB) staining for peroxidase-labeled antibody (nonradioactive DNA labeling and detection kit; Boehringer Mannheim). Slides were counter stained with hematoxylin and eosin and examined by bright-field and phase-contrast light microscopy.

Analysis of E12.5 chimeras

The %GPI1B contribution was estimated by scanning densitometry of GPI electrophoresis plates (West and Flockhart 1994). The average %GPI1B in the fetal tail and forelimb was used as an estimate of the overall contribution of ($Sey^{Neu}/+ \times Sey/+$) cells to the fetus.

After DNA in situ hybridization, the percentage of transgene-positive cells in each of the selected test tissues was estimated (James et al. 1995) in each of the fetuses examined by phase-contrast light microscopy. The contribution of transgenic ($Tg/-$) cells was estimated for each tissue in three widely spaced sections. For tissues in the eye, the midsection and the two sections that were halfway from the mid- to the first or last section were selected for examination. An eyepiece grid and a standardized sampling protocol was used for each separate tissue, and ~150–1000 cells were classified, depending on the tissue. For some tissues, for example, where cells were densely packed, individual cells were not classified but the total number of cells and the total number of hybridization signals were counted in the same field of view. For morphologically normal RPE, ($Sey^{Neu}/+ \times Sey/+$) cells were identified as pigmented and/or positive for the hybridization signal.

The primary estimates of percent hybridization-positive cells were corrected to allow for the failure to detect a hybridization signal in a proportion of the $Tg/-$ ($Sey^{Neu}/+ \times Sey/+$) cells. The tissue-specific correction factors were derived from the following estimates of percent hybridization for tissues from two hemizygous transgenic ($Tg/-$) E12.5 fetuses: nasal epithelium, 105.5%; lens, 83.3%; optic cup, 84.5%; overlying ectoderm (overlying the eye), 64.5%; head ectoderm, 56.8%; hindbrain, 89.1%; head mesoderm, 88.5%. Most of these estimates are below 100%, because in histological sections, a proportion of nuclei fail to include a hybridization signal. In densely packed tissues, the number of hybridization signals may be greater than the number of identifiable nuclei in the field of view, because of overlapping nuclei (e.g., nasal epithelium estimate of 105.5%). The final corrected hybridization index may also exceed 100% if the contribution of $Tg/-$ cells in the chimaera is close to 100% and the correction factor overcompensates.

Estimation of lens and nasal epithelium size

The area of the lens or nasal epithelium in one histological section (where the area was maximum) was used as a measure of tissue size. Areas were estimated (Curtis 1960) using a modified Chalkley grid (Graticules Ltd., Tonbridge Kent, UK).

Statistical analysis

Statistical tests were performed on an Apple Macintosh computer using the statistical package StatView 4.1 (Abacus Concepts Inc., Berkeley, CA).

Acknowledgments

We thank Margaret Keighren, Jean Flockhart, Denis Doogan, Maureen Ross, and Jim Macdonald (Centre for Reproductive Biology), Vince Rinaldi and the staff of the Biomedical Research Facility (Western General Hospital) for expert technical assistance, and Norman Davidson, Tom McFetters, and Ted Pinner for assistance in preparing the illustrations. We also thank Jack Favor for kindly providing the Sey^{Neu} founder stock, and Nick Hastie, Duncan Davidson, Penny Rashbass, and Clare Everett for helpful comments on the manuscript. Figure 1 is based on an original diagram by Clare Everett. J.C.Q. is grateful to the Faculty of Medicine, University of Edinburgh, for a Ph.D. studentship, and J.D.W. is grateful to the Wellcome Trust for financial support (grant 036737).

The publication costs of this article were defrayed in part by payment of page charges. This article must therefore be hereby marked "advertisement" in accordance with 18 USC section 1734 solely to indicate this fact.

References

Breitman, M.L., S. Clapoff, J. Rossant, L.-C. Tsui, M. Glode, I.H. Maxwell, and A. Bernstein. 1987. Genetic ablation: Targeted expression of a toxin gene causes microphthalmia in transgenic mice. *Science* **238:** 1563–1565.

Chalepakis, G., J. Wijnholds, P. Giese, M. Schachner, and P. Gruss. 1994. Characterization of Pax-6 and Hox-1 binding to the promoter region of the neural cell-adhesion molecule L1. *DNA Cell Biol.* **13:** 891–900.

Chisholm, A. D. and H.R. Horvitz. 1995. Patterning of the *Caenorhabditis elegans* head region by the Pax-6 family member *vab-3*. *Nature* **377:** 52–55.

Coulombre, A.J. 1965. Experimental embryology of the vertebrate eye. *Invest. Ophthalmol.* **4:** 411–419.

Curtis, A.S.G. 1960. Area and volume measurements by random sampling methods. *Med. Biol. Illust.* **10:** 261–266.

Edelman, G.M. and F.S. Jones. 1992. Cytotactin—A morphoregulatory molecule and a target for regulation by homeobox gene-products. *Trends Biochem. Sci.* **17:** 228–232.

Everett, C.A. and J.D. West. 1996. The influence of ploidy on the distribution of cells in chimaeric mouse blastocysts. *Zygote* (in press).

Fujiwara, M., T. Uchida, N. Osumi-Yamashita, and K. Eto. 1994. Uchida rat (*rSey*): A new mutant with craniofacial abnormalities resembling those of the mouse *Sey* mutant. *Differentiation* **57:** 31–38.

Glaser, T., L. Jepeal, J.G. Edwards, S.R. Young, J. Favor, and R. Maas. 1994. PAX6 gene dosage effects in a family with congenital cataracts, aniridia, anophthalmia and central nervous system defects. *Nature Genet.* **7:** 463–471.

Goomer, R.S., B.D. Holst, I.C. Wood, G.M. Edelman, and F.S. Jones. 1994. Regulation in-vitro of an L-cam enhancer by homeobox genes Hoxd9 and HNF-1. *Proc. Natl. Acad. Sci.* **91:** 7985–7989.

Grainger, R.M. 1992. Embryonic lens induction: Shedding new light on vertebrate tissue determination. *Trends Genet.* **8:** 349–355.

Grindley, J.C., D.R. Davidson, and R.E. Hill. 1995. The role of Pax-6 in eye and nasal development. *Development* **121:** 1433–1442.

Gurdon, J.B., P. Lemaire, and K. Kato. 1993. Community effects and related phenomena in development. *Cell* **75:** 831–834.

Halder, G., P. Callaerts, and W.J. Gehring. 1995. Induction of ectopic eyes by targeted expression of the eyeless gene in *Drosophila*. *Science* **267:** 1788–1792.

Hanson, I.M., A. Seawright, K. Hardman, S. Hodgson, D. Zaletayev, G. Fekete, and V. van Heyningen. 1993. *PAX6* mutations in aniridia. *Hum. Molec. Genet.* **2:** 915–920.

Hanson, I.M., J.M. Fletcher, T. Jordan, A. Brown, D. Taylor, R.J. Adams, H. Punnett, and V. van Heyningen. 1994. Mutations at the PAX6 locus are found in heterogeneous anterior segment malformations including Peter's anomaly. *Nature Genet.* **6:** 168–173.

Harrington, L., G.K. Klintworth, T.E. Secor, and M.L. Breitman. 1991. Developmental analysis of ocular morphogenesis in αA-crystallin/diptheria toxin transgenic mice undergoing ablation of the lens. *Dev. Biol.* **148:** 508–516.

Hill, R.E. and D.R. Davidson. 1994. Comparative development, seeing eye to eye. *Curr. Biol.* **4:** 1155–1157.

Hill, R.E., J. Favor, B.L.M. Hogan, C.C.T. Ton, G.F. Saunders, I.M. Hanson, J. Prosser, T. Jordan, N.D. Hastie, and V. van Heyningen. 1991. Mouse *Small eye* results from mutations in a *paired*-like homeobox-containing gene. *Nature* **354:** 522–525.

Hogan, B.M., G. Horsburgh, J. Cohen, C.M. Hetherington, G. Fisher, and M.F. Lyon. 1986. *Small eyes* (*Sey*): A homozygous lethal mutation on chromosome 2 which affects the differentiation of both lens and nasal placodes in the mouse. *J. Embryol. Exp. Morphol.* **97:** 95–110.

Hogan, B.L.M., E.M.A. Hirst, G. Horsburgh, and C.M. Hetherington. 1988. *Small eye* (*Sey*): A mouse model for the genetic analysis of craniofacial abnormalities. *Development* (Suppl.) **103:** 115–119.

Holst, B.D., R.S. Goomer, I.C. Wood, G.M. Edelman, and F.S. Jones. 1994. Binding and activation of the promoter for the neural cell-adhesion molecule by Pax-8. *J. Biol. Chem.* **269:** 22245–22252.

Jacobson, A.G. and A.K. Slater. 1988. Features of embryonic induction. *Development* **104:** 341–359.

James, R.M., A.H.E.M. Klerkx, M. Keighren, J.H. Flockhart, and J.D. West. 1995. Restricted distribution of tetraploid cells in mouse tetraploid↔diploid chimaeras. *Dev. Biol.* **167:** 213–226.

Jones, F.S., B.D. Holst, O. Minowa, E.M. DeRobertis, and G.M. Edelman. 1993. Binding and transcriptional activation of the promoter for the neural cell-adhesion molecule by Hoxc6 (Hox-3.3). *Proc. Natl. Acad. Sci.* **90:** 6557–6561.

Jordan, T., I. Hanson, D. Zaletayev, S. Hodgson, J. Prosser, A. Seawright, N. Hastie, and V. van Heyningen. 1992. The human *PAX6* gene is mutated in two patients with aniridia. *Nature Genet.* **1:** 328–332.

Kaur, S., B. Key, J. Stock, J.D. McNeish, R. Akeson, and S.S. Potter. 1989. Targeted ablation of alpha-crystallin-synthesizing cells produces lens-deficient eyes in transgenic mice. *Development* **105:** 613–619.

Keighren, M. and J.D. West. 1993. Analysis of cell ploidy in histological sections of mouse tissues by DNA-DNA *in situ* hybridization with digoxygenin labelled probes. *Histochem. J.* **25:** 30–44.

———. 1994. Two new partially congenic transgenic strains. *Mouse Genome* **92:** 666.

Kozmik, Z., S. Wang, P. Dorfler, B. Adams, and M. Busslinger. 1992. The promoter of the CD19 gene is a target for the B-cell-specific transcription factor BSAP. *Mol. Cell. Biol.* **12:** 2662–2672.

Li, H.-S., J.-M. Yang, R.D. Jacobson, D. Pasko, and O. Sundin.

1994. Pax-6 is first expressed in a region of ectoderm anterior to the early neural plate: implications for stepwise determination in the lens. *Dev. Biol.* **162:** 181–194.

Lo, C. 1986. Localization of low abundance DNA sequences in tissue sections by in situ hybridization. *J. Cell Sci.* **81:** 143–162.

Lo, C.W., M. Coulling, and C. Kirby. 1987. Tracking of mouse cell lineage using microinjected DNA sequences: Analysis using genomic Southern blotting and tissue-section in situ hybridizations. *Differentiation* **35:** 37–44.

Matsuo, T., N. Osumi-Yamashita, S. Noji, H. Ohuchi, E. Koyama, F. Myokai, N. Matsuo, S. Taniguchi, H. Doi, S. Iseki, Y. Ninomiya, M. Fujiwara, T. Watanabe, and K. Eto. 1993. A mutation in the Pax-6 gene in rat *small eye* is associated with impaired migration of midbrain crest cells. *Nature Genet.* **3:** 299–304.

McLaren, A. and M. Buehr. 1990. Development of mouse germ cells in cultures of fetal gonads. *Cell Differ. Dev.* **31:** 185–195.

Palmer, S.J. and P.S. Burgoyne. 1991. The *Mus musculus domesticus Tdy* allele acts later than the *Mus musculus musculus Tdy* allele: A basis for XY sex reversal in C57BL/6-Y^{POS} mice. *Development* **113:** 709–714.

Quinn, P., C. Barros, and D.G. Whittingham. 1982. Preservation of hamster oocytes to assay the fertilizing capacity of human spermatozoa. *J. Repr. Fertil.* **66:** 161–168.

Quiring, R., U. Walldorf, U. Kloter, and W. Gehring. 1994. Homology of the *eyeless* gene of *Drosophila* to the *Small eye* gene in mice and *Aniridia* in humans. *Science* **265:** 785–789.

Roberts, R.C. 1967. Small eyes—A new dominant eye mutant in the mouse. *Genet. Res.* **9:** 121–122.

Saha, M.S., M. Servetnick, and R.M. Grainger. 1992. Vertebrate eye development. *Curr. Opin. Genet. Dev.* **2:** 582–588.

Saha, M.S., C.L. Spann, and R.M. Grainger. 1989. Embryonic lens induction: More than meets the optic vesicle. *Cell Differ. Dev.* **28:** 153–172.

Schmahl, W., M. Knoedlseder, J. Favor, and D. Davidson. 1993. Defects in neuronal migration and the pathogenesis of cortical malformations are associated with Small eye (Sey) in the mouse, a point mutation of the Pax-6-locus. *Acta Neuropathol.* **86:** 126–135.

Smelser, G.K. 1965. Embryology and morphology of the lens. *Invest. Ophthalmol.* **4:** 398–410.

Stuart, E.T., C. Kioussi, and P. Gruss. 1994. Mammalian Pax genes. *Annu. Rev. Genet.* **28:** 219–236.

Ton, C.C.T., H. Hirovenen, H. Miwa, M.W. Weil, A.P. Monaghan, T. Jordan, V. van Heyningen, N.D. Hastie, H. Meijers-Heijboer, M. Dreschler, B. Royer-Pokora, F. Collins, A. Swaroop, L.C. Strong, and G.F. Saunders. 1991. Positional cloning and characterization of a paired box and homeobox containing gene from the aniridia region. *Cell* **67:** 1059–1074.

Walther, C. and P. Gruss. 1991. *Pax-6*, a murine paired box gene, is expressed in the developing CNS. *Development* **113:** 1435–1449.

West, J.D., C.A. Everett, and M. Keighren. 1995. Corrections to transgenic nomenclature. *Mouse Genome* **93:** 145.

West, J.D. and J.H. Flockhart. 1994. Genotypically unbalanced diploid↔diploid foetal mouse chimaeras: Possible relevance to human confined mosaicism. *Genet. Res.* **63:** 87–99.

Zhang, Y.H. and S.W. Emmons. 1995. Specification of sense-organ identity by a *Caenorhabditis elegans* Pax-6 homolog. *Nature* **377:** 55–59.

Zwaan, J. and E.H. Webster. 1985. Localisation of keratin in the cells of the cornea in *aphakia* and normal mouse. *Exp. Eye Res.* **40:** 127–133.